A PROJECT REPORT

ON

"AERODYNAMIC DESIGN, ANALYSIS AND TESTING OF MEDICAL TRANSPORT UAV"

Submitted by

Chougle Muneeb Mohammed Arshad	**-**	**17ME14**
Khan Mohd Umar Raees Ahmed	**-**	**18DME19**
Mulla Mohamed Afaque Anis	**-**	**18DME27**
Latiwala Murtaza Zainuddin	**-**	**14ME30**

In partial fulfilment for the award of the Degree

Of

BACHELOR OF ENGINEERING

IN

MECHANICAL ENGINEERING

UNDER THE GUIDANCE

Of

Prof. Nawaz Motiwala

DEPARTMENT OF MECHANICAL ENGINEERING

ANJUMAN-I-ISLAM

KALSEKAR TECHNICAL CAMPUS NEW PANVEL,

NAVI MUMBAI – 410206

UNIVERSITY OF MUMBAI

ACADEMIC YEAR 2020-2021

ANJUMAN-I-ISLAM

KALSEKAR TECHNICAL CAMPUS NEW PANVEL

(Approved by AICTE, recg. By Maharashtra Govt. DTE,

Affiliated to Mumbai University)

PLOT #2&3, SECTOR 16, NEAR THANA NAKA, KHANDAGAON, NEW PANVEL,NAVI MUMBAI-410206, Tel.: +91 22 27481247/48 * Website: www.aiktc.org

CERTIFICATE

This is to certify that the project entitled

"AERODYNAMIC DESIGN, ANALYSIS AND TESTING OF MEDICAL TRANSPORT UAV"

Submitted by

Chougle Muneeb Mohammed Arshad	-	**17ME14**
Khan Mohd Umar Raees Ahmed	-	**18DME19**
Mulla Mohamed Afaque Anis	-	**18DME27**
Latiwala Murtaza Zainuddin	-	**14ME30**

To the Kalsekar Technical Campus, New Panvel is a record of bonafide work carried out by them under our supervision and guidance, for partial fulfillment of the requirements for the award of the Degree of Bachelor of Engineering in Mechanical Engineering as prescribed by **University of Mumbai**, is approved.

Prof. NAWAZ MOTIWALA
Project Guide

Prof. RAHUL THAVAI /
Prof. RIZWAN SHAIKH
Project Coordinator

Prof. ZAKIR ANSARI
HOD, Mechanical Department

Dr. ABDUL RAZAK HONNUTAGI
Director

ANJUMAN-I-ISLAM

KALSEKAR TECHNICAL CAMPUS NEW PANVEL

(Approved by AICTE, recg. By Maharashtra Govt. DTE,

Affiliated to Mumbai University)

PLOT #2&3, SECTOR 16, NEAR THANA NAKA, KHANDAGAON, NEW PANVEL,NAVI MUMBAI-410206, Tel.: +91 22 27481247/48 * Website: www.aiktc.org

APPROVAL OF DISSERTATION

This is to certify that the thesis entitled

"AERODYNAMIC DESIGN, ANALYSIS AND TESTING OF MEDICAL TRANSPORT UAV"

Submitted by

Chougle Muneeb Mohammed Arshad	-	**17ME14**
Khan Mohd Umar Raees Ahmed	-	**18DME19**
Mulla Mohamed Afaque Anis	-	**18DME27**
Latiwala Murtaza Zainuddin	-	**14ME30**

In partial fulfillment of the requirements for the award of the Degree of Bachelor of Engineering in Mechanical Engineering, as prescribed by University of Mumbai approved.

(Internal Examiner) **(External Examiner)**

_____ _____

Date: _____

ACKNOWLEDGEMENT

After the completion of this work, I would like to give our sincere thanks to all those who helped us to reach our goal. It's a great pleasure and moment of immense satisfaction for us to express my profound gratitude to our guide **Prof. Nawaz Motiwala,** whose constant encouragement enabled us to work enthusiastically. His perpetual motivation, patience and excellent expertise in discussion during progress of the project work have benefited us to an extent, which is beyond expression.

I would also like to give our sincere thanks to our Head of Department - **Prof. Zakir Ansari**, Project Coordinators - **Prof. Rahul Thavai and Prof. Rizwan Shaikh**, from Department of Mechanical Engineering, Kalsekar Technical Campus, New Panvel, for their guidance, encouragement and support during a project.

I take this opportunity to give sincere thanks to **Mr. Prashant and Arif Lambe,** from "Micro-tools and services" and **Vinod Karape,** from "Karape Enterprises" respectively, for all the help rendered during the course of this work and their support, motivation, guidance and appreciation.

I am thankful to Director, **Dr. Abdul Razak Honnutagi**, Kalsekar Technical Campus New Panvel, for providing an outstanding academic environment, also for providing the adequate facilities.

Last but not the least I would also like to thank all the staffs of Kalsekar Technical Campus (Mechanical Engineering Department) for their valuable guidance with their interest and valuable suggestions brightened us.

Chougle Muneeb Mohammed Arshad - 17ME14

Khan Mohd Umar Raees Ahmed - 18DME19

Mulla Mohamed Afaque Anis - 18DME27

Latiwala Murtaza Zainuddin - 14ME30

Declaration

I declare that this written submission represents my ideas in my own words and where others' ideas or words have been included, I have adequately cited and referenced the original sources. I also declare that I have adhered to all principles of academic honesty and integrity and have not misrepresented or fabricated or falsified any idea/data/fact/source in my submission. I understand that any violation of the above will be cause for disciplinary action by the Institute and can also evoke penal action from the sources which have thus not been properly cited or from whom proper permission has not been taken when needed.

Chougle Muneeb Mohammed Arshad - 17ME14

Khan Mohd Umar Raees Ahmed - 18DME19

Mulla Mohamed Afaque Anis - 18DME27

Latiwala Murtaza Zainuddin - 14ME30

Date:

Abstract

In order to minimize human contact, less work to be needed; energy saving and rapid delivery; air transport will address most, if not all, of the barriers faced by working with conventional methods of transporting organs and other key products.

This project aims to build a delivery drone for a greater cause with the concept of UAV and studies carried out on the construction of a VTOL-based drone in the opinions and statistical research carried out on the transport and handling of sensitive organs, blood for transfusion and other crucial medical equipment.

Technological progress in aspects of UAV has led to different opening up to concepts that could change the way traditional travel, art and distribution methods are used; etc.

The delicacy and demand for Cadaver Organs is huge, which has led to the high amount of investment of money and labour; let alone for the transportation. However, this project aims to cut down on such investment by the development of an Unmanned Aerial Vehicle. Which would not only help to cut down the cost of transportation but also delivering the supply in time of great urgency.

Given the current state of the world, it is critical to encourage activities that include less human interaction, and drones play a critical role in achieving this goal; to minimise human contact when delivering.

Contents

1. Introduction **1**

1.1 Background 1

1.1.1 Wright Flyer 2

1.2.1 Douglas Dc-3 3

1.2 Classification Of Aircrafts 5

1.3 Application Of Vtol Aircrafts 9

1.4 Components Of Vtol Aircrafts 13

1.5 Motivation 14

1.6 Aim And Objectives 14

1.7 Literature Review 15

1.7.1 Waapi 15

1.7.2 Lateral And Longitudinal Stability Analysis 16

1.7.3 Modelling And Analysis Of Aircraft Wing With And Without Winglet 18

1.8 Problem Definition 20

1.9 Scope 20

2. Conceptual Design **21**

2.1 Project Requirements 21

2.1.1 Problem Statement 21

2.2 Solution Requirements 30

2.2.1 Mission Profile 30

2.2.2 Uav Objectives 31

2.2 Concept Generation 31

3. Preliminary Design **32**

3.1 Vtol System Design 32

3.1.1 Power Systems 32

3.2 Fixed Wing Preliminary Design 35

3.2.1 Weight Estimation 36

3.2.2 Wing And Power Estimation 38

3.2.2.3 Maximum Speed 43

3.2.2.4 Take-off Run 44

3.2.2.5 Rate Of Climb 46

3.2.2.6 Ceiling 47

3.2.2.7 Matching Plot 48

4. Detailed Design **50**

4.1 Fixed Wing 50

4.1.1 Wing Design 50

4.1.2. Airfoil Selection 62

4.1.3 Wing Sizing 70

4.1.4 Lift Calculation And Drag Calculation 72

4.1.5 Wing Loading 75

4.2 Stability 76

4.2.1 Empennage Design 76

4.2.2 Control Surfaces 78

4.2.3 Static Stability 82

4.2.4 Dynamic Stability 82

4.3 Fuselage Design 83

4.4 Full Body Analysis 84

4.5 Aircraft Performance 87

4.5.1 Flight Envelope 87

4.5.2 Static Thrust 89

4.5.3 Vtol Performance 90

4.5.4 Dynamic Thrust And Power 91

5. Structural Design **93**

5.1 Structure Layout 93

5.2 Spar Design 94

5.2.1 Theoretical Calculations 97

5.2.2 Experimental Calculations 98

5.2.2.1 Simply Supported Beam Equations 99

5.2.2.2 Observed Calculations 99

5.3 Ribs 105

5.4 Total Wing Structure Weight Breakdown 108

5.5 Aluminum Hub 109

5.1.4.1 F.E.A Of The Aluminium Hub 109

5.6 Final Hub Design 112

5.7 Connectors 115

5.7.1 Load Calculation 116

5.8 Tilt Rotor Mechanism 119

5.9 Landing Gear 123

5.9.1 Functional Analysis And Design Requirements 125

5.9.2 Landing Gear Configuration 127

5.9.3 Comparison Between Fixed And Retractable Gear 131

5.9.4 Landing Gear Equation 131

5.9.5 Endurance Landing Gear 135

5.9.5.1 Landing Gear Calculations 135

5.9.5.2 Endurance Landing Gear Design 138

5.9.5.2.1 Main Gear Initial Design 138

5.9.5.2.1.1 F.E.A Of The Landing Gear 138

5.9.5.2.2 Main Gear Improved Design 140

5.9.5.2.2.1 F.E.A Of The New Design 142

5.9.5.2.2.2 Drag Force Calculation 144

5.9.5.2.3 Nose Gear 145

5.9.5.2.4 Tires 146

5.9.5.2.5 Net Weight Of Landing Gear 147

6. Electronics And Control Systems **148**

6.1 Thrust Motors 148

6.2 Esc 150

6.2.1 Brushless Esc (Yep-100a) 151

6.2.2 Aerostar Wifi 100a Brushless 152

6.3 Batteries 154

6.3.1 Gens Ace Li-po Battery 155

6.3.2 Tattu Lipo Battery 156

6.4 Servos 158

6.5 Gps 161

6.6 Buzzer 162

6.7 Autopilot 163

6.7.1 Pixhawk 164

6.8 Radiomaster 166

6.9 Dragon Link Transmitter 168

6.10 Schematics 169

6.10.1 Wiring Diagram Of Pixhawk 170

6.10.2 Full Body Wiring Diagram 171

7. Flight Test **173**

8. Cost Analysis **174**

9. Conclusion **177**

10. Appendices **178**

11. References **192**

List Of Figures

FIGURE NO.	CAPTION	PAGE NO.
1.1	Leonardo da Vinci's Flying Machine.	1
1.2	Wright Flyer 1903.	3
1.3	Douglas DC 3.	4
1.4	Runway Take off.	6
1.5	Helicopter (VTOL).	7
1.6	STOL.	7
1.7	STOVL.	8
1.8	UAV used for surveillance.	9
1.9	UAV used in delivery.	10
1.10	Military UAV.	11
1.11	UAV used for Aerial Photography.	12
1.12	Major Components of Endurance Aircraft.	14
1.13	WAAPI drone.	15
1.14	Four views of MAV.	17
1.15	Front view of MAV.	17
1.16	Total deformation (Static structural) without winglet.	19
1.17	Total Deformation with winglet at cant angle 18°.	19
1.18	Total Deformation with winglet at cant angle 45°.	19
2.1	Total number of utilized deceased organ donors (Global 2015).	22
2.2	Transplanted sum of vital organs (Global 2015).	22
2.3	Transplanted sum of vital organs (India 2000-21).	23
2.4	Population of Mumbai city.	23
2.5	Total Heart transplant done in India (2000-21).	24
2.6	Total Kidney transplant (deceased and living) done in India (2000-21).	24
2.7	Survey on the attitude towards Organ Donation in certain rural sectors of India.	26

2.8	Number of Heart Transplant centers in India (2015-21).	26
2.9	Procedure Time required of a particular vital organ transplant.	27
2.10	Green Corridor in India.	29
2.11	Mission profile for delivery purposes.	30
2.12	Endurance Aircraft Conceptual Design.	31
3.1	Thrust and Weight acting on aircraft.	32
3.2	Thrust, Weight and Drag acting on aircraft.	33
3.3	Drag and Climb rate.	34
3.4	Turnigy Sk3 5055-430kv and 17x8 APC style propeller.	35
3.5	Maximum Takeoff Weight.	36
3.6	Payload Prediction.	37
3.7	Sample Power loading and wing loading graph.	41
3.8	Stall Region.	42
3.9	Matching Plot.	48
4.1	Wing Design Procedure Flowchart.	50
4.2	Monoplanes (a), Biplanes (b), Triplane (c).	51
4.3	Monoplane Endurance Drone CAD Model.	51
4.4	Vertical Wing Locations.	52
4.5	C-5M Super Galaxy.	53
4.6	Smith Aerostar 600 N70VB.	54
4.7	Boeing 747.	55
4.8	Bakeng Duce ZU-CH8.	55
4.9	Aircraft Sweep.	57
4.10	(a) Dihedral angle (b) Anhedral angle.	57
4.11	Symmetrical (NACA 0009), High Lift (S1223) and Flat Bottom airfoils(Clark Y).	58
4.12	High aspect ratio (left) , Low aspect ratio (right).	59
4.13	(a) Straight wing , (b) Tapered wing (c) Delta wing.	60
4.14	Wing Incidence angle (iW).	61
4.15	Twisted wing.	61

4.16	Lift distribution of Twist wing.	61
4.17	Clark Y (purple) , NACA 3411 (red), NACA 2412 (green).	65
4.18	Graph of Coefficient of Lift (CL) versus Angle of Attack (α).	65
4.19	Graph of Coefficient of Lift (CL) versus Coefficient of Drag (CD).	66
4.20	Graph of Ratio of Coefficient of Lift to Coefficient of Drag (CL / CD) versus Angle of Attack (α).	66
4.21	Graph of Pitching Moment (CM) versus Angle of Attack (α).	67
4.22	Graph of Coefficient of Lift (CL) versus Angle of Attack (α) at Re = 600,000.	67
4.23	Graph of Coefficient of Lift (CL) versus Coefficient of Drag (CD) at Re = 600,000.	68
4.24	Graph of Ratio of Coefficient of Lift to Coefficient of Drag (CL / CD) versus Angle of Attack (α) at Re = 600,000.	68
4.25	Graph of Pitching Moment (CM) versus Angle of Attack (α) at Re = 600,000.	69
4.26	Wing dimensions.	70
4.27	Poly - Hexacore Mesh in ANSYS Fluent with Meshing Package.	72
4.28	Graph of Lift and Drag generated by XFLR5 and ANSYS.	73
4.29	CFD Post Processing.	74
4.30	Drag Plot from XFLR5.	74
4.31	Wing Loading Curve.	75
4.32	Empennage of an aircraft.	75
4.33	Conventional tail design.	76
4.34	T-Tail design.	76
4.35	Cruciform Tail design.	77
4.36	Twin tail design.	77
4.37	Example for control surfaces.	78
4.38	Short period response graph by XFLR5.	82
4.39	Phugoid response graph by XFLR5.	82
4.40 (a)	Fuselage side view.	83
4.40 (b)	Enclosure of half body.	84
4.41	Poly - Hexa Core mesh.	84

4.42	Full Body Pressure Contours.	85
4.43	Velocity Pathlines over Full body.	85
4.44	Vortex Generation Pathlines.	86
4.45	V-n Diagram.	87
4.46	Static Thrust Test Images.	88
4.47	VTOL flow simulation.	89
4.48	Extrapolated drag.	90
4.49	Figure 4.49 - Drag, Thrust, Power vs Velocity.	91
5.1	Spar.	93
5.2	Construction of spar.	95
5.3	The large rod at the top will be used as a main spar.	97
5.4	Loading Diagram.	98
5.5	S.F.D.	99
5.6	B.M.D.	100
5.7	Deflection Plot.	101
5.8	Slope Plot.	100
5.9	S.F.D	102
5.10	B.M.D.	102
5.11	Deflection.	103
5.12	Slope.	103
5.13	Components of Wings.	104
5.14	Arrangement of Balsa Wood for Laser Cutting.	105
5.15	Ribs being mounted on our spar.	106
5.16	Geometric dimensions of our ribs.	106
5.17	Al- 6062 hub.	108
5.18	The rods fixed at the end.	109
5.19	A load of 700N applied.	109
5.20	Von Mises Stress contour.	110
5.21	Displacement contour.	110
5.22	Final hub design.	111

5.23	Machining of carbon fibre using diamond.	112
5.24	Carbon fiber sheet wrapped around.	112
5.25	After Wrapping.	113
5.26	Main Body Testing.	113
5.27	Blueprint of our hub design.	114
5.28	Male connector.	116
5.29	Female connector.	116
5.30	Connector Assembly.	117
5.31	S.F.D and B.M.D.	117
5.32	Tilt rotor mechanism assembly blueprint.	118
5.33	Tilt rotor mount mechanism blueprint.	119
5.34	Tilt rotor assembly and mechanism.	121
5.35	Landing gear parameters.	123
5.36	Landing gear flowchart.	125
5.37	Landing gear types.	127
5.38	Landing gear height.	130
5.39	Fuselage clearance on take-off.	131
5.40	Wheelbase and track width.	132
5.41	Overturn angle (t).	133
5.42	Landing gear geometry.	135
5.43	Main gear.	137
5.44	Fixture and load.	138
5.45	Stress and Displacement from F.E.A.	138
5.46	F.O.S.	139
5.47	Main gear with improved design front view.	140
5.48	Main gear with improved design top view.	140
5.49	Stress and Displacement from F.E.A.	141
5.50	F.O.S of the Main Gear.	142
5.51	Main gear.	142
5.52	C.F.D of the main gear.	143

5.53	Landing gear drag graph.	144
5.54	Oleo Strut for Nose Gear.	144
5.55	Tires.	145
6.1	Placement of all Thrust Motors.	148
6.2	Turnigy Aerodrive SK3-5055.	149
6.3	Orthographic Representation for Turnigy Aerodrive SK3-5055.	149
6.4	Brushless ESC (YEP-100A).	151
6.5	AeroStar WiFi 100A Brushless ESC with 5A BEC.	152
6.6	Gens Ace 5600mAh Battery.	155
6.7	Tattu 3s battery.	156
6.8	Servo motor MG995 with Tilt rotor assembly.	157
6.9	Servo Motor MG995.	159
6.10	Orthographic representation of Servo motor MG995 with dimensions.	159
6.11	Radiolink SE100 GPS Module for PixHawk	161
6.12	Buzzer for Pixhawk PX4.	162
6.13	Mission Planner set Home at AIKTC campus.	162
6.14	Pixhawk.	163
6.15	Color Coding to understand Pixhawk.	164
6.16	Ports of Pixhawk.	164
6.17	Radiomaster TX16S.	167
6.18	DragonLink 433MHz.	168
6.19	Pixhawk Connection Diagram.	169
6.20	Full Body Wiring Diagram	171
7.1	Test Flight.	172
8.1	Cost Breakdown Pie Chart.	173

List of Tables

TABLE NO.	NAME	PAGE NO.
1.1	UAV WAPPI Specifications.	16
1.2	Variation of stress.	18
1.3	Variation of deformation.	18
2.1	Temperature preservation range of each vital organ and medicines.	28
2.2	List of Green Corridors in various Urban Cities of Maharashtra.	30
2.3	Objectives of UAV	31
3.1	Motor and propeller Selection	35
3.2	Comparison of Different UAV	37
4.1	Vertical Wing Location Trade Study	56
4.2	Airfoil Performance	69
4.3	Airfoil Selection Trade Study	70
4.4	Wing Dimensions	71
4.5	Lift generated in (N)	73
4.6	Drag generated in (N)	73
4.7	Lift and drag generated by full body.	85
4.8	Experimental Thrust Results.	89
4.9	Vtol Cfd Parameters and results.	
5.1	Comparison of carbon fiber and aluminium at the same weight.	95
5.2	Weight of wing structure.	107
5.3	Components of Tilt Rotor Mechanism's Aluminium frame.	120
5.4	Comparison between Fixed and retractable gear.	130
5.5	Net Weight of Landing Gear.	146
6.1	Specification of Turnigy Aerodrive SK3-5055.	147
6.2	Specification for Brushless ESC (YEP-100A).	150

6.3	Specifications for AeroStar WiFi 100A Brushless ESC with 5A BEC.	152
6.4	Difference between Lithium Ion and Lithium Polymer.	154
6.5	Li-po Batteries and their use.	154
6.6	Specifications of Gens Ace Li-po Battery.	155
6.7	Tattu Battery.	156
6.8	Specification for the Servo motor MG995.	158
6.9	Specification for Radiolink SE100 GPS Module for PixHawk.	160
6.10	Active Buzzer pattern.	161
6.11	Specifications for Radiomaster TX16S.	167
6.12	Specifications for DragonLink 433MHz.	168
8.1	Electronics Cost Breakdown.	173
8.2	Structural Cost Breakdown.	174
8.3	Tools Cost Breakdown.	174
8.4	Grand Total.	175

Notations and Abbreviations

1. DST – Douglas Sleeper Transport.
2. VTOL – Vertical Take-off and Landing.
3. CTOL – Conventional Take-off and Landing.
4. STOL – Short Take-off and Landing.
5. STOVL – Short Take-off and Vertical Landing.
6. UAV – Unmanned Aerial Vehicle.
7. WAAPI – Wild Area Aerial Protective Inspector.
8. MTOW – Maximum Take-off Weight.
9. MAV – Micro Air Vehicle.
10. AOA – Angle of Attack.
11. ROC – Rate of Climb.
12. CG – Centre of Gravity.
13. NACA - National Advisory Committee for Aeronautic.
14. MAC – Mean Aerodynamic Chord.
15. AR – Aspect Ratio.
16. CFD – Computational Fluid Dynamics.
17. CAD – Computer Aided Design.
18. CF – Carbo Fiber.
19. FEA – Finite Element Analysis.
20. ID – Internal Diameter.
21. OD – Outer Diameter.
22. SFD – Shear Force Diagram.
23. BMD – Bending Force Diagram.
24. CNC – Computerised Numerical Control.
25. CAE – Computer Aided Engineering.
26. FOS – Factor of Safety.
27. GPS – Global Positioning System.
28. ESC – Electronic Speed Control.
29. ASCF – Active Switch Continued Flow.
30. BEC – Battery Eliminator Circuit.
31. RF – Radio Frequency.

Chapter 01

Introduction

1.1 Background

Aviation is what we term an object or a system, when it takes a leap of predetermined flight in the air. The Flight could be driven by the help of certain aircraft propulsion or a set of motors working in synchronization, a fixed-wing aircraft that uses thrust from a piston engine, propeller, or rocket engine to propel it forward.

There are several different types, shapes, and wing configurations for aeroplanes. Recreation, movement of materials and persons, military, and science are only a few of the many applications for aeroplanes. At the initial stages of the development of aircrafts.

"The story of human flight began to take place over 230 years ago, in the 1780s, when people began to take to the skies in balloons. Later, Daredevil flyers launched themselves into the air in unpowered gliders, but they could not stay in the air for very long. The Invention of the gasoline engine made powered, controlled flight possible, and the first successful airplane flight took place in 1903. By the 1950s, jet airliners were carrying passengers swiftly and comfortably between continents and across vast oceans in a matter of hours." [1].

Leonardo da Vinci Flying Machine

The traces of aviation go even further back in time, dating upto 1490s; Leonardo da Vinci, an Italian polymath, drew his plans for a flying machine. The majority of Leonardo's aeronautical projects were ornithopters, which used flapping wings to produce lift and propel themselves. He drew those flying machines with the pilot prone, vertically upright, using arms and legs.

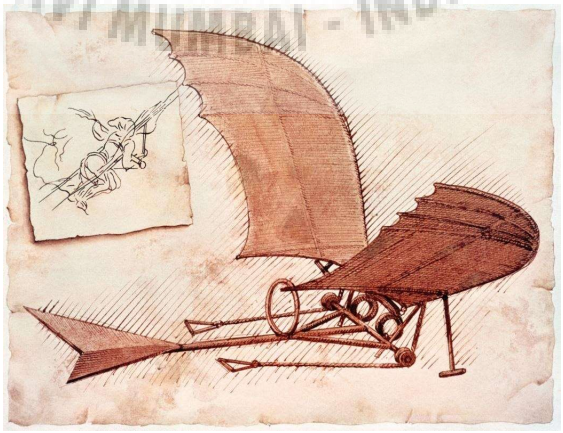

Figure 1.1 – Leonardo da Vinci's Flying Machine. [2]

He drew detailed diagrams of flapping wing structures and their control mechanisms. Emulating natural flight was an obvious place to start, given his close observation of nature and use of it as a basis for many of his ideas.

The detailed diagrams he drew of flapping wing structures and their control mechanisms were made considering the human muscle strength and psychology of birds. The underlying obstacle to an ornithopter, as imaginative as these prototypes were, is humans demonstrably reduced muscle strength and stamina when opposed to birds. He displays a basic understanding of the relationship between lift and a curved wing segment. He understands the idea of air as a fluid, which is fundamental to aerodynamics. Leonardo provides interesting remarks of birds gliding in flight and how they align themselves with their wings and tails.

He discusses the pilot's role in a future flying machine and how control could be accomplished by changing body weight, much as the early glider pioneers did in the late 1800s. He emphasises the importance of lightweight systems for aircraft. He also pointed to the force that would later be known as gravity by Newton.

"Among the many subjects Leonardo studied, the possibility of human mechanical flight held particular fascination. He produced more than 35,000 words and 500 sketches dealing with flying machines, the nature of air, and bird flight. These investigations of flight are scattered throughout the many da Vinci codices and manuscript collections, but he did produce one short codex almost entirely on the subject in 1505-1506, the *Codice sul volo degli uccelli* (Codex on the Flight of Birds). [3].

1.1.1 Wright Flyer

With the world's first successful flights by a powered heavier-than-air flying vehicle, the Wright brothers introduced the aerial era. Many of the fundamental tenets and methods of contemporary aeronautical engineering were invented by the Wrights, including the use of a wind tunnel and flight testing as modelling instruments.

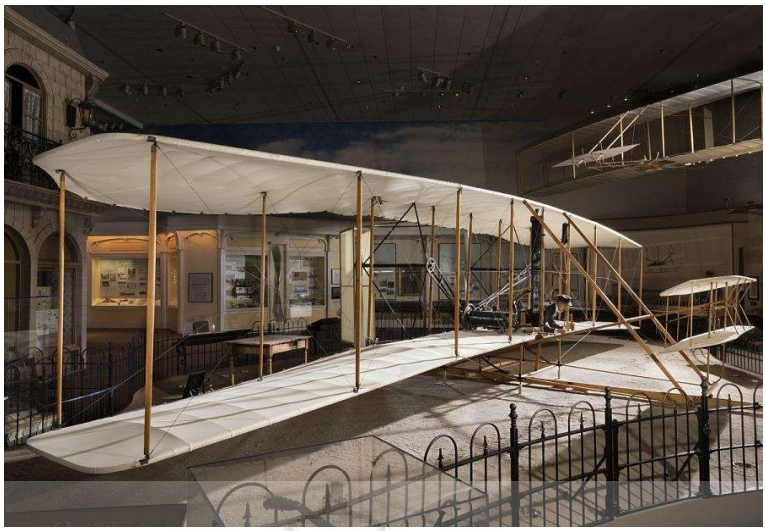

Figure 1.2 – Wright Flyer 1903. [4]

They not only took the first flight of an aircraft, but also the similarly significant achievement of laying the foundation for aeronautical engineering. The Wright Flyer I had a wooden frame made of spruce for the straight sections and ash for the curved parts. The twin propellers, which were both made by hand, were driven by a sprocket chain drive, which was inspired by bicycle technology.

The Wright brothers Flyer series of planes were the first to achieve powered heavier-than-air flight, but some of the technical methods they used to do so had little effect on the advancement of aviation as a whole, considering their theoretical accomplishments. The Flyer's configuration relied on wing-warping operated by a hip cradle beneath the pilot, as well as a foreplane or "canard" for pitch control, all of which were not scalable and resulted in a difficult-to-control aircraft.

By rotating the wings to adjust the wingtip angle in relation to the airstream, their imitators, such as Glenn Curtiss and Henri Farman, were able to make ailerons more functional. The Wright brothers' initial principle of synchronised coordinated roll and yaw control, which they conceived in 1902, refined in 1903–1905, and patented in 1906, represents the solution to powered flight and is found on almost every fixed-wing aircraft today.

1.1.2 Douglas DC-3

The Douglas DC-3 is a propeller-driven airliner that had a major impact on the airline industry, as well as World War II. It was a passenger aircraft, which first flew in 1935. In contrast to previous planes, the DC-3 had a range of distinctive characteristics. It was faster, had a longer range, was more dependable, and transported passengers with more comfort. It pioneered many air transport routes prior to World War II.

Figure 1.3 – Douglas DC 3. [2]

In the United States, the DC-3 popularised air travel. With three refuelling stops, eastbound transcontinental flights could reach the United States in around 15 hours, while westbound trips against the wind took 17-12 hours. Quick hops of slower and shorter-range aircraft during the day were combined with overnight rail travel just a few years ago.

There are quite a few minor operators flying DC-3s for revenue and freight. Passenger operation, aerial spraying, freight delivery, military transport, missionary travel, skydiver shuttling, and sightseeing are all existing uses for the DC-3. Because of the vast number of civil and military operators of the DC-3, it is impossible to list all of the airlines, air forces, and other existing operators. Although hundreds of DSTs and DC-3s ordered by airlines between 1941 and 1943 were forced into US military service while still on the production line, DST production ended in mid-1941 and civil DC-3 production ended in early 1943.

1.2 Classification of Aircrafts

Classification of aircraft can be done based on various factors as every aspect of aircraft building is equally important. Aircrafts are broadly classified in two types;

- Lighter than Air.
- Heavier than Air.

a) Lighter than Air –

It is the Aircraft that is held aloft by a lighter-than-air gas stored inside the plane. Also known as Aerostat. It includes;

- Airship.
- Free Balloon.
- Kite Balloon.

b) Heavier than Air –

It is an aircraft which is built by heavier elements, mostly metals. It is also known as Aerodynes. It includes;

- Gliders.
- Sailplane.
- Airplane.
- Rotary Wing Aircraft.
- Ornithopter.
- Drones.

Aircraft industry over the years has seen a lot of development throughout the years as in various aspects which includes the type of body, shape; use of fuel, etcetera. But most importantly progress was made in the aspect of Take-off and Landing as well.

Various methods for Aircraft Take-off and landing includes;

- CTOL.
- VTOL.
- STOL.
- STOVL.

a) CTOL –

Conventional take-off and landing or CTOL is also known as Horizontal take-off and landing HTOL, in this type of models, an aircraft needs a runway for its Take-off and Landing. A runway is a defined rectangular area, prepared for the take-off and landing of the aircraft. Aircraft will take off and land in a variety of ways. Traditional aeroplanes accelerate along the ground until enough lift is produced for take-off, then land by reversing the process. A short take-off is when an aircraft will take off at a low altitude.

During take-off, the aircraft accelerates down the runway while still on the ground, resting on its wheels, until it achieves take-off level, at which point the pilot manipulates the flight controls to allow the aircraft to pivot around the axis of its main landing gear while still on the ground, raising the lift from the wings and effecting take-off.

Figure 1.4 – Runway Take off. [5]

b) VTOL –

Vertical Take-off and Landing or VTOL is a method in which the aircraft can hover, take off, and land vertically. It does not require a runway. VTOL technology allows planes to potentially take off and land virtually anywhere, increasing their flexibility. They can also execute a range of movements that a conventional plane cannot; this is a major benefit for aircraft in battle scenarios.

A commercial passenger-carrying aircraft can arrive over the runway while still in flight speed during landings.

The final approach point, flare, touchdown, and roll-out phase make up the landing. Where feasible, they like to allow a rolling take-off from a runway because it needs less thrust.

Figure 1.5 – Helicopter. (VTOL) [6]

c) STOL –

Short take-off and landing or STOL aircraft need a short runway. Many STOL aircraft are often equipped with different provisions for use on rough runways. STOL aircraft have also been flown from STOL port airfields with short runways, including those used in scheduled passenger airline operations. A STOL aircraft would usually have a wide wing for its weight. Aerodynamic equipment such as flaps, slots, slats, and vortex generators are often used on these wings. First when designing an aircraft for excellent STOL performance, the maximum speed is typically reduced, but the payload lifting capacity is not.

Since many remote, disconnected populations rely on STOL aircraft as their only mode of transportation to the outside world for passengers or freight, the payload is important.

Figure 1.6 – STOL. [7]

d) STOVL –

Short take-off and vertical landing or STOL is a fixed-wing aircraft that can take off from a short runway or take off vertically if it doesn't have a large payload and land vertically. It is capable of overcoming a 15 m barrier and landing vertically within 450 m of beginning the take-off flight. In comparison to vertical take-off and landing (VTOL), STOVL allows aircraft to accommodate a greater payload while having only a small runway.

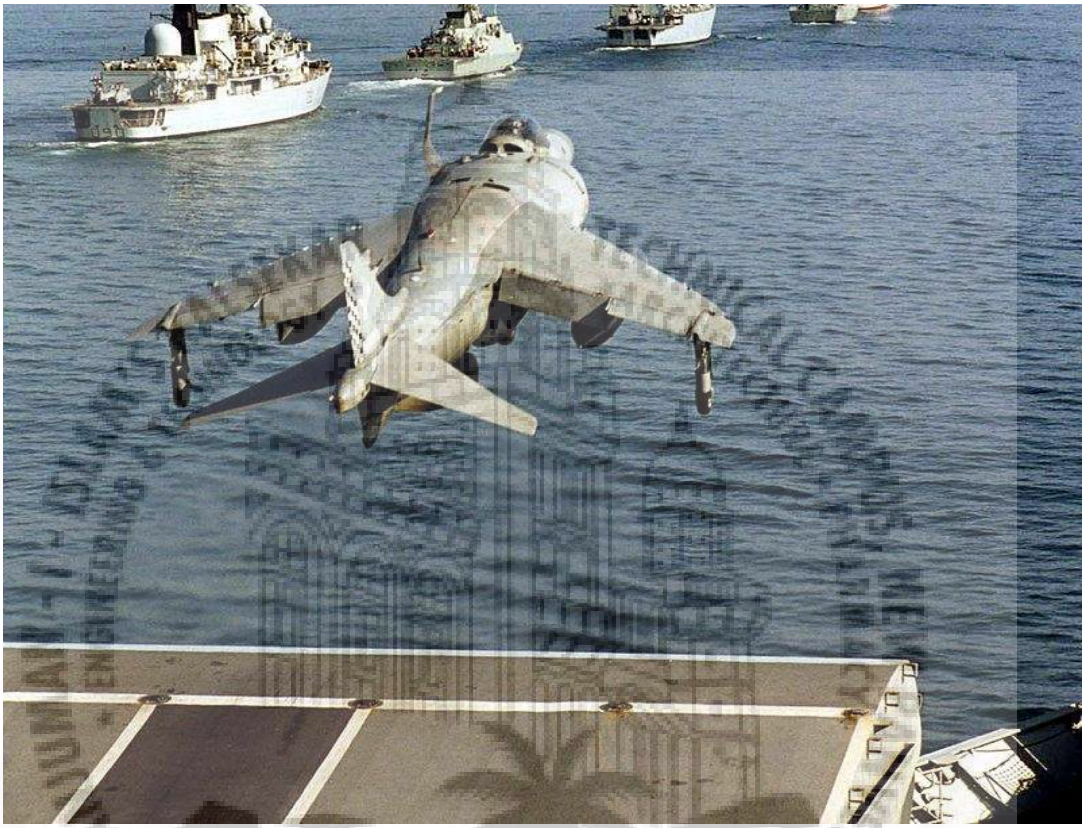

Figure 1.7 – STOVL. [8]

- Based on the classification, we decided to go further with the concept of the VTOL UAV, as it not only serves, but eliminates the danger of life of a pilot.

1.3 Application of VTOL Aircrafts

Unmanned Aerial Vehicle or UAV is a fairly new concept to the industries. Though it already has found its use in various aspects of life, which includes;

a) UAV used in Surveillance –

Use of UAVs in surveillance is common these days, as it provides a quick; effective and cost efficient method of survey which excludes the involvement of a pilot and the dangers it causes of life if any miscalculations occur.

Figure 1.8 – UAV used for surveillance. [9]

Present monitoring systems will be replaced by this system, which will be more convenient and reliable. It can be used for both peacekeeping and real-time surveillance of a location at any time of day. Unmanned surveillance drones collect still photographs, video files, or live video of targets such as humans, cars, or geographic locations.

Governments, militaries, law enforcement agencies, and commercial organisations can use them to gather data and information to improve decision-making.

Drone monitoring may provide access to locations that humans on foot or in land vehicles can find difficult or impossible to enter. Drones are usually quieter than manned aircraft, can fly at lower altitudes, and are less costly to maintain than manned aircraft. In potentially risky areas such as battlefields or crime scenes, using military and law enforcement monitoring drones will also help to avoid putting humans in danger.

b) UAV used in Deliveries –

Drones can carry medical supplies like blood, vaccines, and pharmaceuticals, as well as other supplies like pharmaceuticals and medical samples. Since drones can more quickly fly into and out of distant or otherwise inaccessible regions than vehicles or bikes, medical supplies have become one of the most common uses for drones.

When compared to conventional vehicle delivery, unmanned aerial vehicle delivery will save electricity and reduce greenhouse gas emissions, which is good for the atmosphere. Furthermore, UAVs will circumvent traffic limits, which are a major roadblock in parcel distribution.

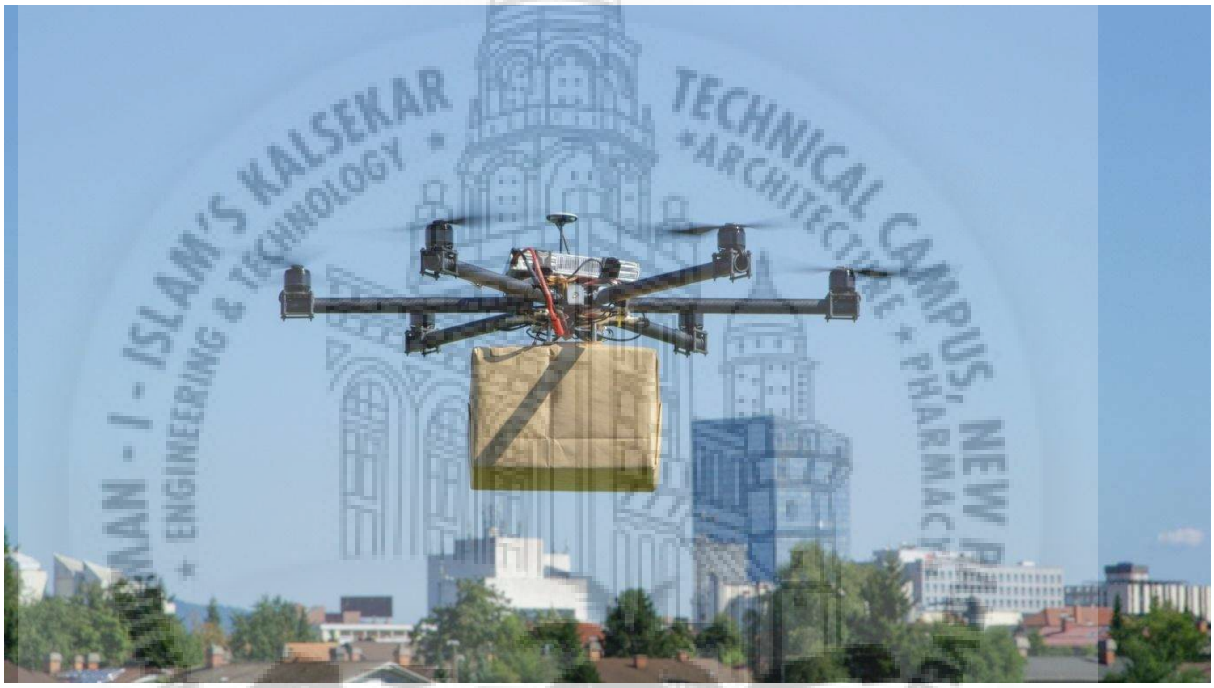

Figure 1.9 – UAV used in delivery. [10]

Due to their considerable cost and energy savings, unmanned aerial vehicles (UAVs) have emerged as one of the best options for optimising the “last-mile” supply of goods to customers, both economically and environmentally. UAV transport can complete deliveries that trucks can't or can only do at far higher prices, and it can still effectively save money and reduce CO2 emissions, which is good for the climate. UAV transmission saves more money and reduces CO2 emissions. Unmanned aerial vehicles that deliver cargo are currently in service in a variety of countries. The bulk of these UAVs were custom-built to suit the demands of the job or operation. There is a critical need for life-saving blood drugs in rural areas, but the country's road infrastructure is inadequate.

c) UAV used in Military purposes –

Military drones are used in a number of forms by the armed forces. It is a quickly evolving area of technology, and its global influence will almost definitely continue to expand. UAVs can fly autonomously using either pre-programmed flight plans or more advanced dynamic automation systems which are useful for the military.

It's crucial to consider the growing importance of unmanned aerial systems in settling such disputes. In addition, for some contemporary military planners, carrying out high-profile assaults is a crucial activity.

They are used for activities such as defence and traffic management over non-warring nations, in addition to fighting wars. They're also effective tools for battling forest fires. Drones are tracked using satellites by the drone pilots. The drone is operated by a ground-control station via a direct data link from take-off until it loses line of sight.

If the drone's contact link is broken, it is programmed to fly in circles or return to base before the link is restored.

Figure 1.10 – Military UAV. [11]

d) UAV used in Photography and Videography –

Drones are widely lauded for their ability to capture a new view on the world, exposing the wonders of our universe from afar. However, they are just the most recent breakthrough in aerial photography's long history. Airborne cameras have produced awe-inspiring photographs of our world, demonstrated the horrific magnitude of natural disasters, and tipped the scales in battle for hundreds of years.

Aerial photography's history, in some interesting respects, mirrors the last century of human history in general. Aerial photography with UAV was mainly limited to the military, devoted hobbyists, and individuals with access to full-size aircraft until just a few years ago. As for now people have forged a full-fledged carrier out of UAV Aerial Photography and Videography.

Drones purchased in shops today are comparatively cheap, provide high-quality images and video, and are easy to run. As a result of this combination, aerial photography has flourished, with uses ranging from commercial to artistic, such as real estate agents getting eye-catching images of houses they're trying to sell.

Since then, new hardware and applications such as stabilizers, autopilot, and crash detection technologies have given rise to drones sold in stores. In the 1980s, Israeli researchers built models with video cameras to track individuals of interest for hours at a time, resulting in the first modern-style drones.

Figure 1.11 – UAV used for Aerial Photography. [12]

e) Other UAV Applications –

- Food Deliveries in many Rural and deserted areas.
- Major Companies using UAV technology for fast and effective deliveries of good and other essential products.
- Nano Drones Technologies used in places where heavy aircrafts cannot be used.

1.4 Components of VTOL Aircrafts

There are five main components for building an Aircraft;

a) Fuselage –

With its long hollow frame, also known as the airplane's body, which carries passengers and luggage, the fuselage is one of the most significant aircraft components. The cockpit is located in this place, so the pilots are in the front of the fuselage. Despite the fact that fuselages come in a range of shapes and sizes, they all help to link the main components of an aircraft.

b) Wings –

Wings, also known as foils, are, unsurprisingly, aircraft parts that are essential for flight. The majority of the lifting force required for flight is produced by airflow over the wings. In addition to the wide wings that protrude from the centre of the fuselage, most aircraft have two smaller wings at the rear, known as the tail.

c) Empennage –

The empennage is the aircraft's tail end. It consists of two main components: the rudder and the elevator, which contribute to the plane's stability. The rudder assists in steering the aircraft from right to left, while the elevator aids in up and down travel.

d) Power Plant –

The engine and propeller are both part of an airplane's power plant or a motor and battery if it comes to it. The engine is a complex structure made up of several smaller components such as valves, fans, and pistons, whereas when the Aircraft is driven by motors; the system becomes simple. These aircraft components work together to produce an aircraft's strength or thrust.

e) Landing Gears –

It is impossible to get a stable plane without landing gear. Not only are these components needed for landing, but they also assist an aircraft in taking off and taxiing. The landing gear contains the plane's wheels as well as shock absorbers for a smooth landing and take-off.

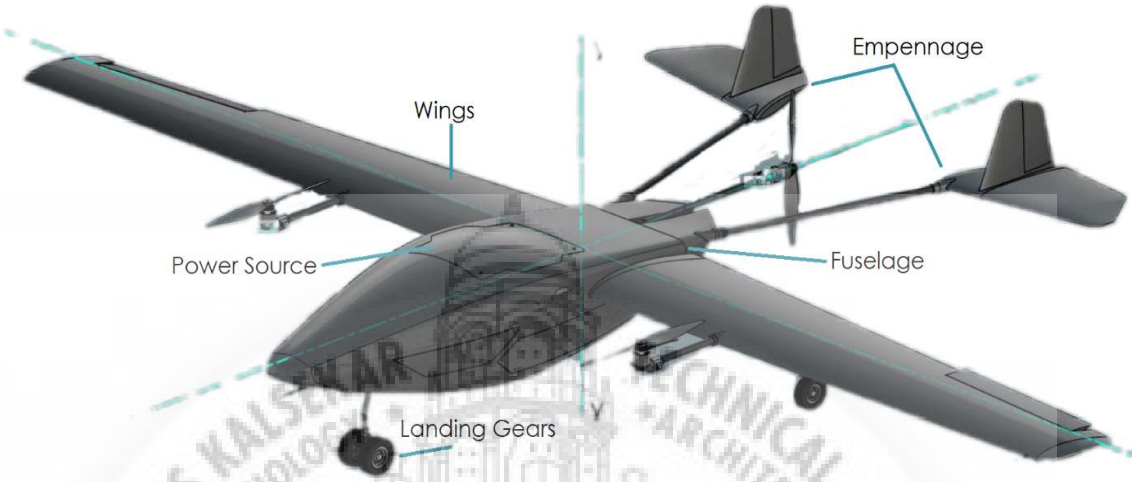

Figure 1.12 – Major Components of Endurance Aircraft.

1.5 Motivation

Observing the current state of the workflow for the transportation of Cadaver organs through roadways, and seeing all of these organs being lost or wasted due to late deliveries and manhandling. Encourages us to develop a better and more reliable method for delivering organs and other essential supplies that will help not only the wealthy, but also the vulnerable, due to its inherent cost-effectiveness. By focusing on a market where organ transplantation is in high demand, we will create a better solution if timely delivery of an organ is a contributing factor in saving an individual's life.

1.6 Aim and Objectives

This project aims to overcome the limitations of conventional medical transportation which includes medicines, vaccines, blood, organ transportation etc. By designing a drone which is faster, cost efficient and requires less human coordination and effort.

- **Objectives**

1. Speed upto 100 kmph.
2. Range above 50 Km.
3. Cost Efficient.
4. Payload range of 1.5 to 2.0 Kg.
5. Weather Resistant.
6. Autonomy.
7. Payload Temperature Regulation.
8. Portable and Quick Assembly.

1.7 Literature Review

Other professional work was examined to see how it matched the definition of the VTOL of our concern. These experiments aided us in comprehending the idea of different aerodynamic and structural designs used in previous drones. Basic calculations and simulations that are expected for the construction were beneficial. Listed down are some of the sample reports and papers that were referred in our knowledge:

1.7.1 WAAPI

WAAPI: Wild Area Aerial Protective Inspector is an unmanned Aerial System UAS, designed by Mina Khalilzadeh Fathi [13]; an Iranian Student. A drone was presented which was engine driven as it has a Linear Infrastructure range of 160.934 kilometres, payload of 2.25 kilograms; Endurance of about 10 hours. WAAPI also has an element of Interchangeability, which results in the drone remaining in service indefinitely but with all of the parts replaced whenever needed. It is also featured with Autonomous flight take-off and landing.

Figure 1.13 - WAAPI drone. [13]

One of the crucial missions for which WAAPI is designed has been linear infrastructure inspection and to take long flights Endurance and terrain modeling. Designing was also carried out in such a way where it can be mounted on the top of the car roof and to take-off from any surface available. The Autonomous take-off and landing makes it easier for WAAPI to map out its flight and work based upon the current environmental condition. WAAPI is also conditioned with portability of Ground Station which includes all the necessary components that will help in performing in the range of 100Km to 200Km.

Following a table represents the UAV specifications -

Table 1.1 : UAV WAAPI Specifications. [13]

Sr. No.	Parameters	Value
1.	MTOW	16.3293 kg
2.	Length	2.356104 m
3.	Wing Span	3.16992 m
4.	Take-off Method	Conventional takeoff, Car top launch
5.	Landing Method	Conventional landing, Parachute recovery
6.	Empty weight	13.040781 kg

1.7.2 Lateral And Longitudinal Stability Analysis

According to a Case Study performed by J. Jensin Joshua et al [15], on UAV Lateral and Longitudinal Stability Analysis Using XFLR5, the coefficient of lift is around 0.2 at an AOA of 2 degrees. Since the airfoil used is reflex cambered, the MAV has a stalling angle of around 25 degrees. The MAV's configuration allows it to achieve adequate lift at a speed of 15m/s, giving it a 30 percent margin before stalling at 25 degrees. Since the MAV is tailless, momentum varies in small intervals at high AOA.

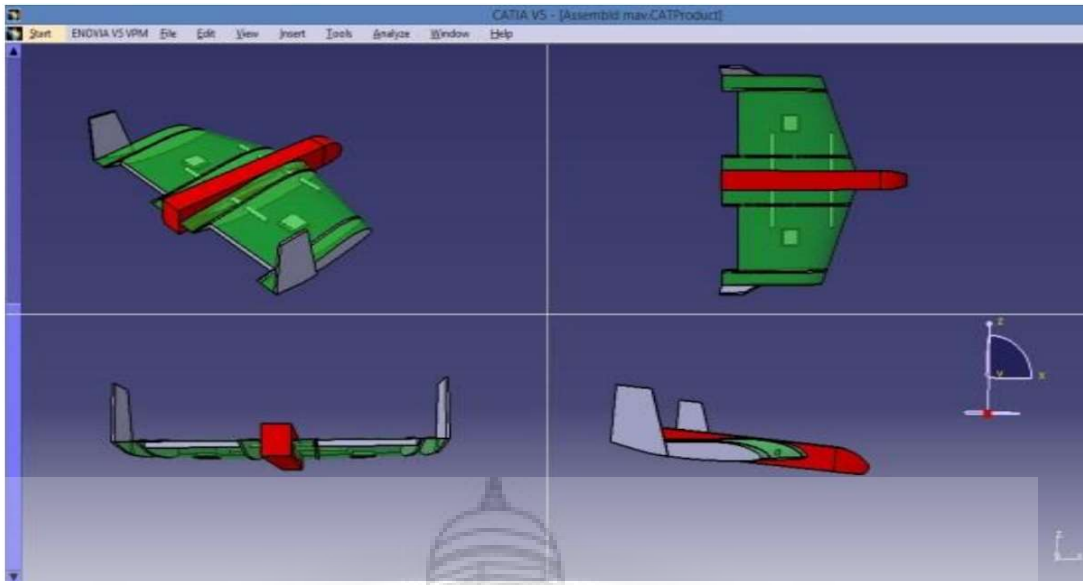

Figure 1.14 - Four views of MAV. [15]

The ability of an aircraft to return to its original location when displaced by a gust of wind or a rapid shift in the AOA is determined by its static longitudinal and lateral stability.

The MAV's high wings are located at the top of the fuselage.

The high wings provide more stability by guiding cross flow across the fuselage in a sideslip, changing the angle of attack at the wing root and wing tip, and resulting in a net lift portion that returns the MAV to a stable state.

Figure 1.15 Front view of MAV. [15]

Since the MAV has no tail, maintaining lateral stability is a difficult task. To accomplish this, the airfoil is used in such a manner that it can be returned to its original flight conditions. This generates an opposing reaction force, which keeps the MAV steady in flight.

As a result, a model capable of flying at low Reynolds numbers was developed, and the reliability of the model was investigated.

1.7.3 Modelling And Analysis Of Aircraft Wing With And Without Winglet

A case study was done by S P Venkatesan Sathyabama et al [16], on the aircraft wings concerning the analysis and results on the effects of winglets with the help of vibrational characteristics on the wings. This investigation makes use of an A300 aircraft wing with a NACA 64215 airfoil. The study was performed on the wing, with one end of the wing set fixed and the other end open. The total deformation and frequency of the wing without and with winglet at different angles is determined using workbench and finite element analysis methods in conjunction with structural analysis and model analysis.

Parameters were set regarding the angle and amount of stress to be applied following the modeling of a wing span using Catia v5. Following are the tables defining the Stress factor and the Angles of the Wings;

Table 1.2 - Variation of stress. [16]

Sr. No.	Aircraft Wing	Stress(MPa)
1.	Without Winglet	54.498
2.	With Winglet of 18°	94.291
3.	With Winglet of 45°	92.173

Table 1.3 - Variation of deformation. [16]

Sr. No.	Aircraft Wing	Deformation (mm)
1.	Without Winglet	6.1191
2.	With Winglet of 18°	19.35
3.	With Winglet of 45°	21.606

According to the study, skin must be at least 0.015 to 0.025 inches thick to withstand the friction applied to it when travelling across the atmosphere. The skin is moderately hard and strong, allowing it to withstand damage from the earth, such as stones and debris. As the wingspan was analysed at different vibrational frequencies i.e. 104.5 Hz, 256.24 Hz; 483.2 Hz, 580.7 Hz; etcetera.

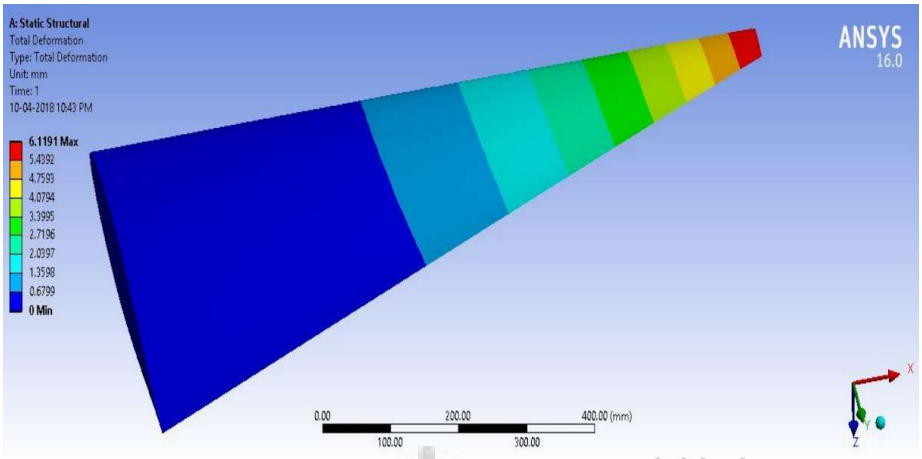

Figure 1.16 - Total deformation (Static structural) without winglet. [16]

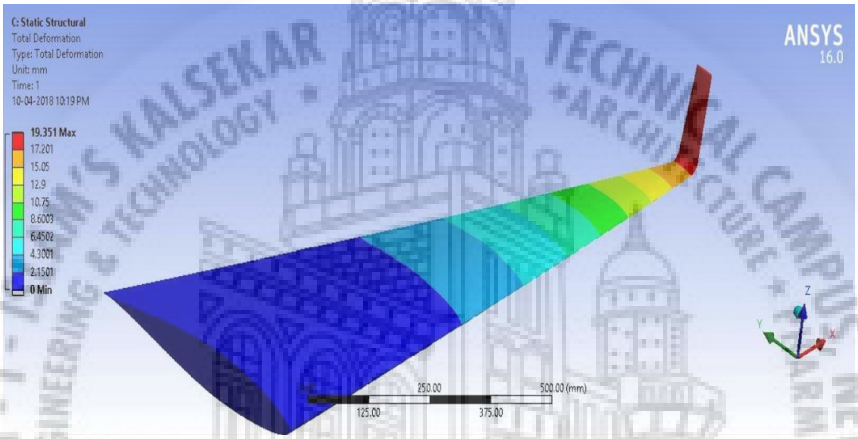

Figure 1.17 - Total Deformation with winglet at cant angle 18°. [16]

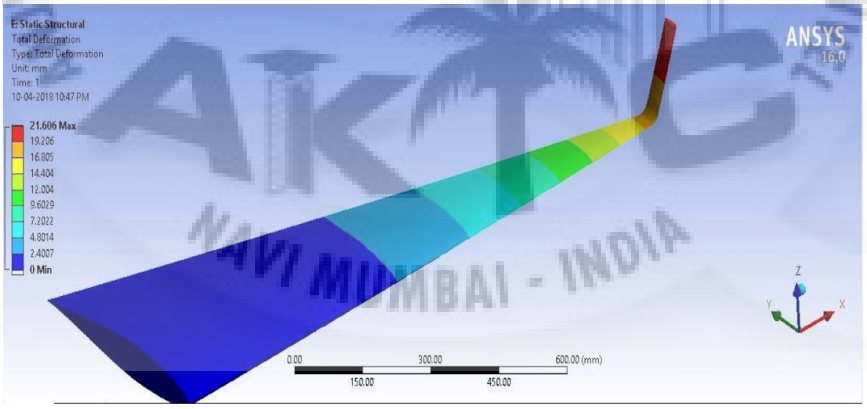

Figure 1.18 - Total Deformation with winglet at cant angle 45°. [16]

Which later on supported the conclusion of the case study with the winglet with an 18-degree cant angle is more optimised and can be used to increase wing stability. As the variations in deformation and natural and shear stresses clearly demonstrate that the winglet with an angle of 18 degrees produces the best performance, maintaining a strong structural wing.

1.8 Problem Definition

Throughout the developed and developing world, access to life-saving and critical health products is hampered by what is known as the last-mile problem, the inability to deliver the needed medicine/blood/organs within Cities and from a city to rural or remote locations because of inadequate transportation, communication or supply chain infrastructure.

1.9 Scope

The new project's reach contains the following:

a) Turning the drone into an Air Ambulance in its entirety.
b) Putting together a drone network to handle various deliveries.
c) Improving the drone's ability to deal with fire outbreaks.
d) Allowing a drone to be loaded with emergency relief supplies.

Chapter 02

Conceptual Design

2.1 Project Requirements

2.1.1 Problem Statement

Throughout the developed and developing world, access to life-saving and critical health products is hampered by what is known as the last-mile problem - the inability to deliver the needed medicine/blood/organs within Cities and from a city to rural or remote locations because of inadequate transportation, communication or supply chain infrastructure.

2.1.1.1 Overview of Organ and Medicine Transportation around the world

Organ transplantation is a critical procedure that is carried out all over the world. While organ transplantation is not a simple procedure, it is fraught with dangers, including the possibility of putting people's lives in jeopardy during the procedure. These activities are carried out in both developed and emerging nations, with one major contributing factor being the identification and finding of organ donors. Getting the donor is already a difficult task as finding the right volunteers for donating their organs with their consent is critical.

Organs such as the heart, lungs, liver, pancreas, cornea, intestine, and bone marrow (and certain varieties of medicines) are essential for human life. However, due to different medical problems, these organs can need to be removed and replaced in extreme cases. The most significant risk of organ transplant surgery is rejection of the transplanted organ. The body's immune system automatically removes what it recognises as foreign tissue, setting off a series of events. The aim is to match the blood and tissue types of the donor and recipient to reduce the chances of organ transplant rejection after surgery.

As a result, finding the best donor for the right beneficiary becomes critical.

Following are two graphs representing the number of utilized organs of the deceased people and a sum of vital organs transplanted around the world.

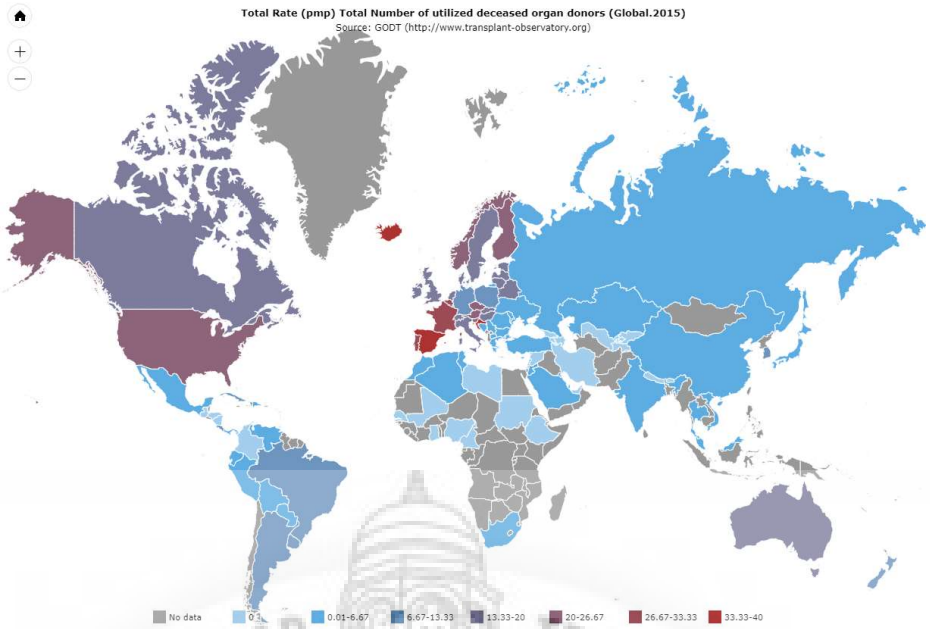

Figure 2.1 - Total number of utilized deceased organ donors. (Global 2015) [18]

2.1.1.2 Overview of Organ and Medicine transportation in Developing country (India)

One of the most important aspects of achieving a certain degree of growth for a country is providing a world-class hospital, medical facilities, and certified-experienced physicians. Despite having such a dense population, India has produced some of the world's best doctors and highly capable men. Transportation and traffic, which are exacerbated by India's dense population, are unquestionably a problem.

Following a graph represents data on transplant occurred in India in recent years;

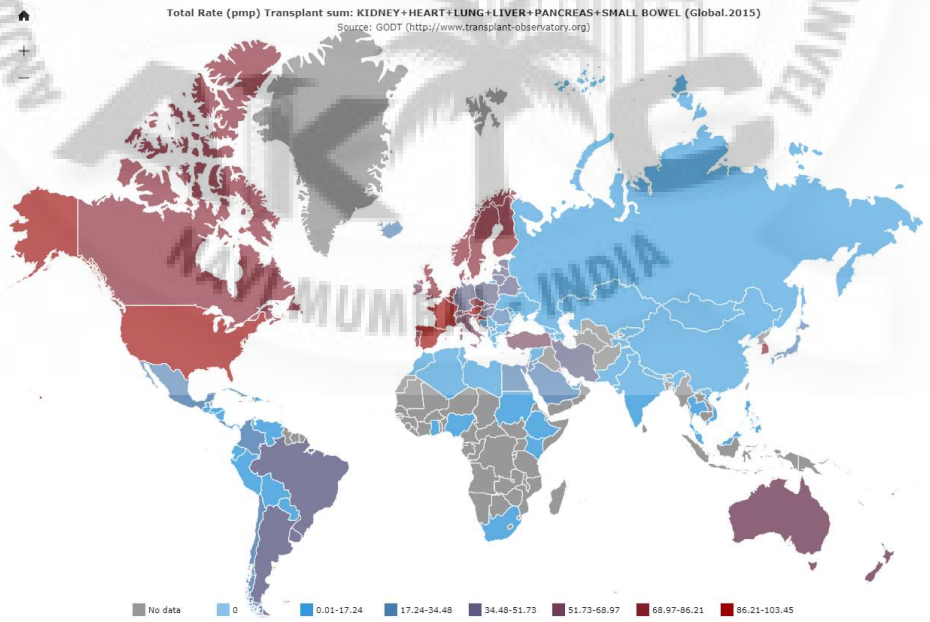

Figure 2.2 - Transplanted sum of vital organs. (Global 2015) [18]

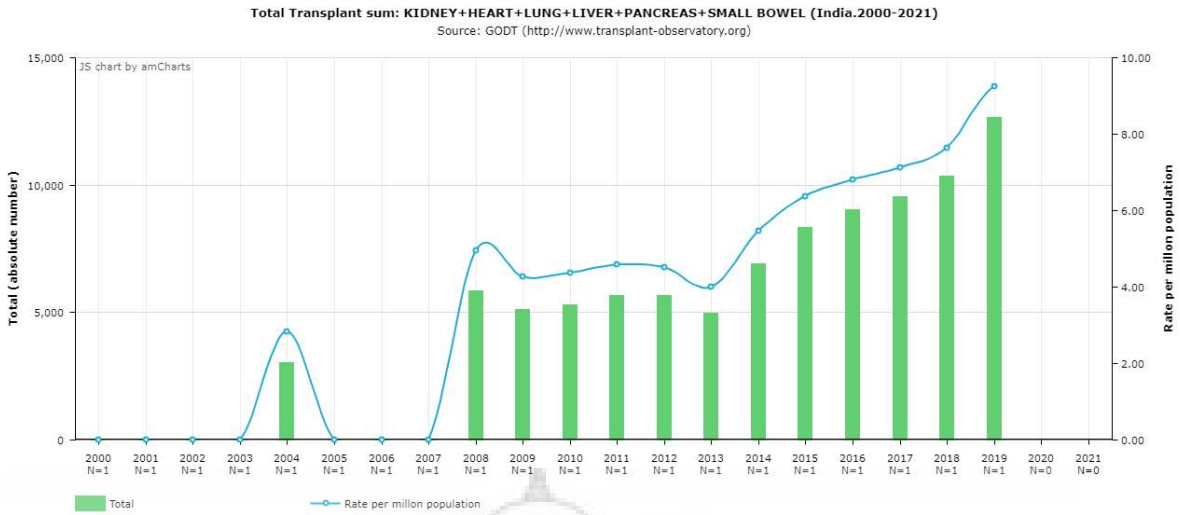

Figure 2.3 - Transplanted sum of vital organs. (India 2000-21) [18]

As these numbers are increasing due to one contributing factor of growth in the numbers of population, keeping up with the conventional means is lacking in various aspects compared to what it did in the previous decades.

2.1.1.3 Briefing about the Organ and Medicine Transport in the Urban sectors

One of India's major cities 'Mumbai', The total area of Mumbai is 603.4 km2. Mumbai's metro region population is expected to reach 20,667,656 in early 2021, 20,411,000 in 2020, up 1.12% from 2019. Mumbai's metro region population in 2019 was 20,185,000, up 1.03 percent from 2018. Mumbai's metro region population in 2018 was 19,980,000, up 1.13 percent from 2017.

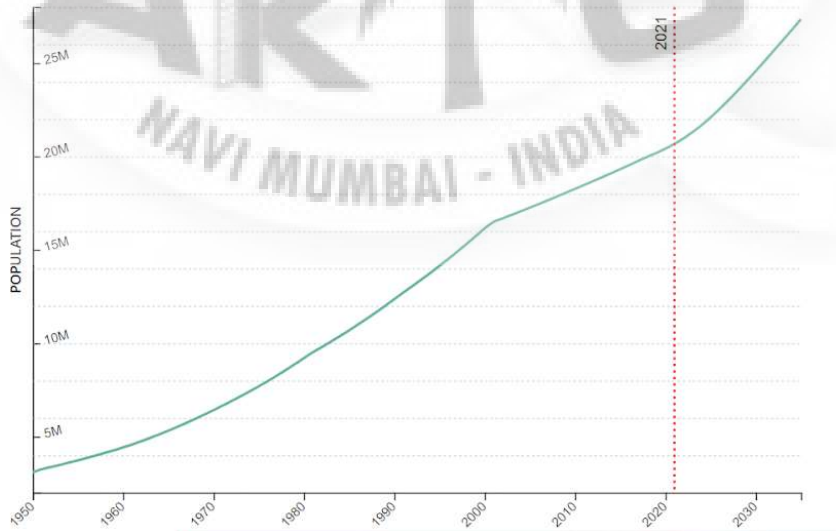

Figure 2.4 - Population of Mumbai city. [19]

After seeing these numbers for such a large population, it's easy to guess the number of treatment centres and clinics that would be needed to meet the city's medical needs. India, on the other hand, is capable of keeping up with these numbers at its own rate.

For major procedures such as organ transplants, blood transfusions, and so on. It's important that these organs get to the people who need them as soon as possible. In the last 24 years, only about 350 cardiac transplants have been performed in India, according to a news report published by "Times Now". The organs were not shipped on schedule, the transportation truck was caught in traffic, or the organ was mishandled when being delivered, which is why the percentages are so poor.

Following are two graphs representing the numbers of Heart and Kidney (two of the most common organ transplants in practice) Transplant occurred in various regions of India;

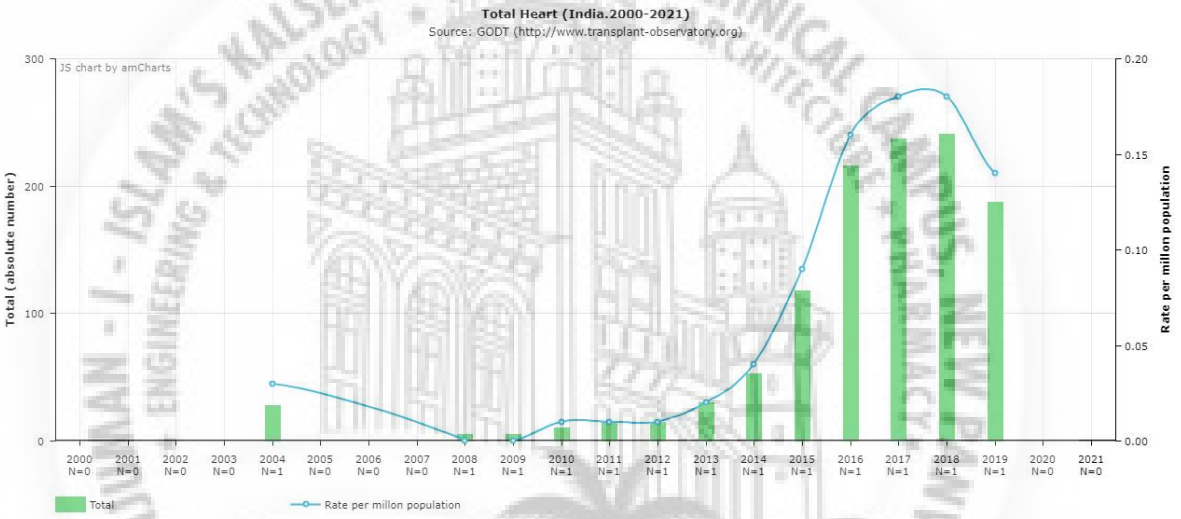

Figure 2.5 - Total Heart transplant done in India. (2000-21) [18]

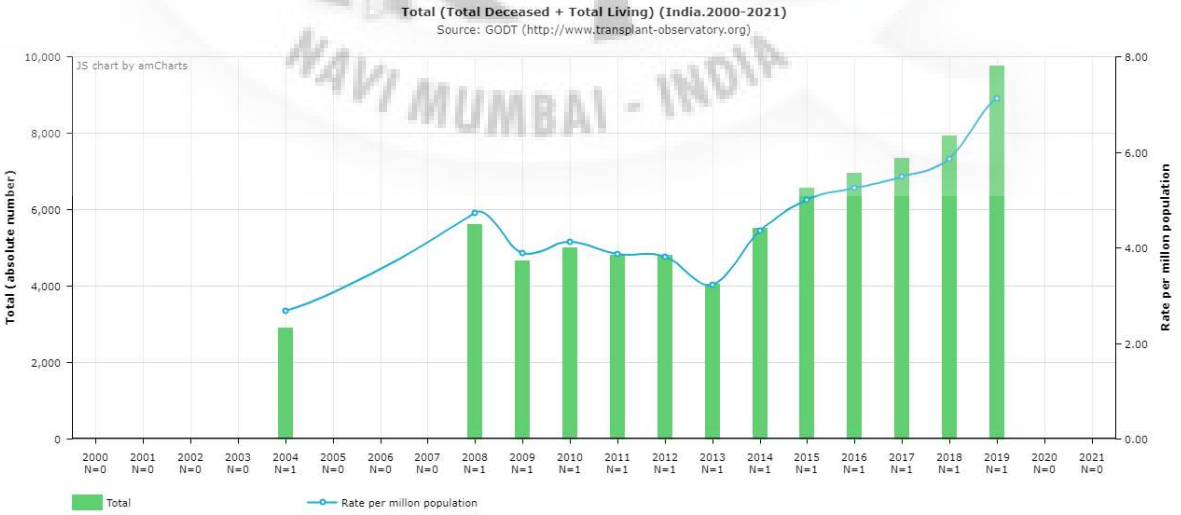

Figure 2.6 - Total Kidney transplant (deceased and living) done in India. (2000-21) [18]

In Urban cities of India, between 50,000 and a lakh patients are suffering from acute heart disease and will need a heart transplant at some stage in the future. A heart transplant in a private setting costs between Rs 15 and Rs 29 lakhs, including postoperative care; the expense of carrying the organ is calculated to be around Rs 85,000.

These are such a large number that an ordinary citizen doing a 9-5 job would not be able to afford these operations in an emergency. While India has its own traditional systems for transporting organs, they have not kept up with the system's disruption caused by the country's growing population. And the results are often the loss of a personal friend or relative.

2.1.1.4 Briefing about the Organ and Medicine Transport in the Rural sectors

The biggest obstacle confronting the world of organ transplantation today is organ scarcity. Especially in the Rural Sectors of India, families refused to donate the dead person's organs for a variety of reasons, including denial of brain loss, belief in magic, religious values, and fear of organ trafficking. The level of education has been shown to be directly related to organ donor awareness. The level of education has been shown to be directly related to organ donor awareness.

According to some research and surveys done in some rural sectors of Maharashtra and Tamil Nadu, places such as Lanja and Puducherry. The survey was carried out to see how awareness and attitudes about organ donation differed between urban and rural populations, and found that the rural population had less knowledge about organ donation than their urban counterparts. 400 students, middle-aged, and senior citizens were given a questionnaire containing demographic information, skills, and attitudes; 91.5 percent of the respondents were aware of organ donation. The most common sources of knowledge were television (55.2%) and newspapers (45.8%). A healthy human and a cardiac dead individual, respectively, were thought to be donors by 56.2 percent and 32.8 percent. [21]

In rural India, there is a high level of knowledge for both body and organ donation. The definition of brain death, on the other hand, is little understood. Aside from skin, kidney, and other organ and tissue donations, there is a need for more public awareness campaigns.

The graph below depicts the number of responses received as a result of the survey;

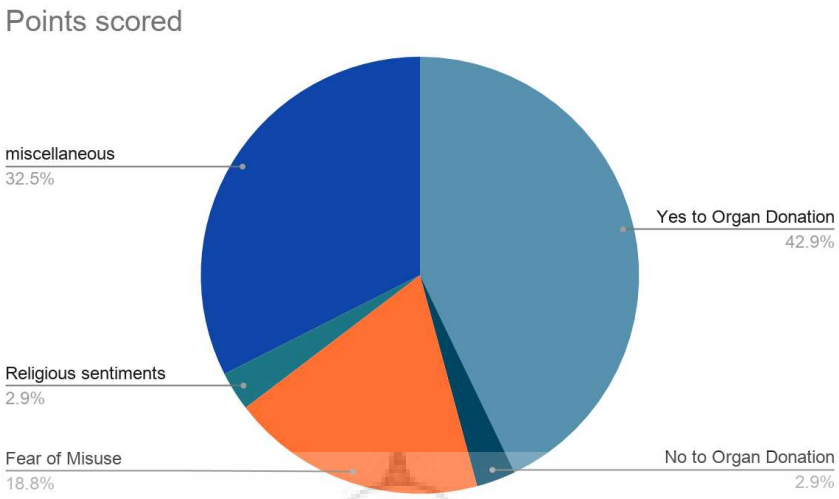

Figure 2.7 - Survey on the attitude towards Organ Donation in rural sectors of India. [21]

Based on the response it is safe to assume that a majority of the rural population is willing to participate in organ donation. Though they certainly lack behind in the aspect of right facilities and people to perform the operation. And they certainly lack the aspect of transparency in the system, which is the major cause which portrays a bad image of organ donation in the majority of the population. Thus even if an individual wants to get out of his or her comfort and come forth for organ donation they have to turn towards the urban sectors, if not then they would have to extract the organ at the nearest organ donation center and have it transfer to a better facilities in urban sectors for the better use of their donated organs.

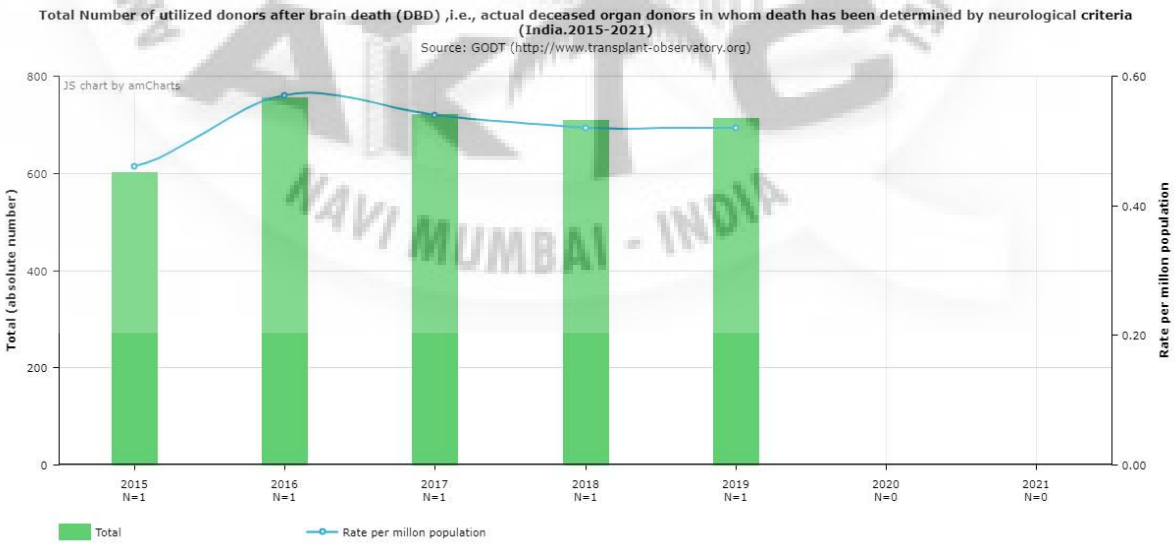

Figure 2.8 - Number of Heart Transplant centers in India (2015-21) [18]

Though as previously discussed, finding the right match is necessary. But finding the right donor is a rare occasion and when it is found, the replacement organ should be well preserved and transported to the needy in time; it is equally important alongside a successful surgery.

Following a graph represents the time for completing the procedure of an organ transplant;

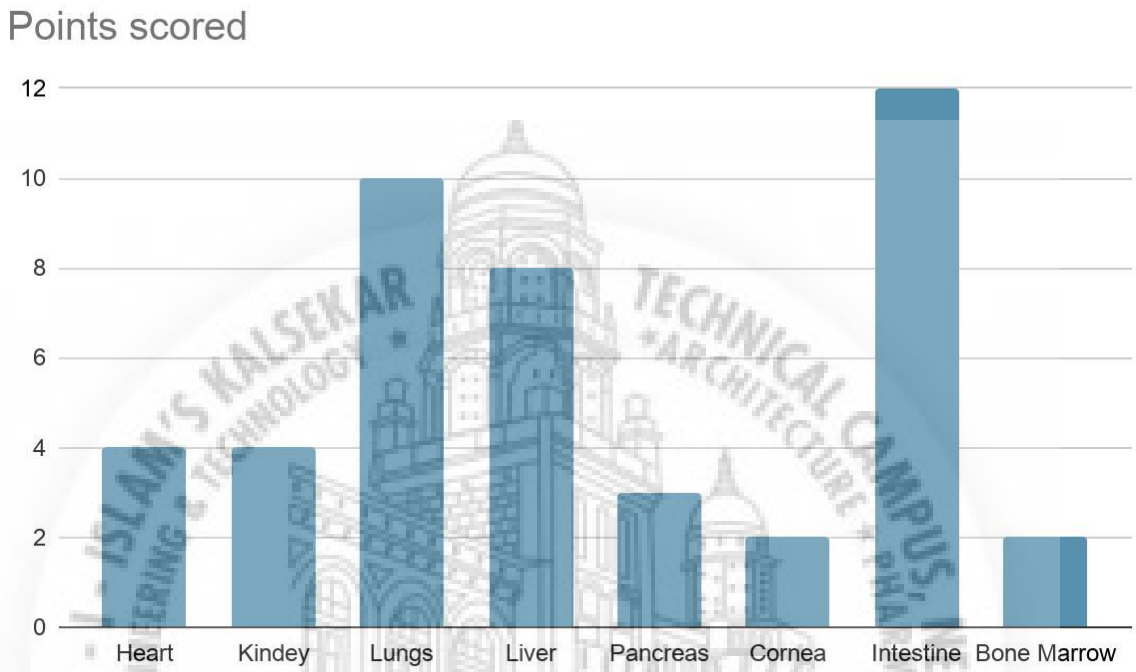

Figure 2.9 - Procedure Time required of a particular vital organ transplant.

As cadaver organs are delicate to handle, manhandling such delivery could lead to a great financial loss and leave many lives at stake. Which motivates us to find a better, more effective way of organ transport.

Owing to the brief lifetime of cadaver organs, transplantation can be performed within a few golden hours. After retrieval of the organ from a body, the heart is alive for only 6 hours; Liver and kidneys for 12 hours.

When removing an organ from a donor, each organ has a temperature range for storage in order to preserve it intact for the individual in need.

Following a table represent the Temperature range for the organ and other miscellaneous goods that needs to preserved at;

Table 2.1 - Temperature preservation range of each vital organ and medicines.

Sr. No.	Essential organs and other medical supports	Preservation Range in ℃
1.	Heart	4℃ - 8℃
2.	Lungs	4℃ - 8℃
3.	Liver	4℃ - 8℃
4.	Kidneys	4℃ - 8℃
5.	Pancreas	4℃ - 8℃
6.	Cornea	2℃ - 8℃
7.	Bone Marrow	2℃ - 8℃
8.	Intestine	5℃ or below
9.	Vaccines	2℃ - 8℃
10.	Medicines	2℃ - 8℃

Thus the urban and mostly the rural sector of India would have to rely upon the conventional method of organ transport.

2.1.1.5 Conventional Method of Organ transport in India

A "Green Corridor" is a special path that is designed so that all traffic signals between the hospital where an organ is removed and the hospital where it will be transplanted are green and manually operated. Although this system was originally designed to deal with medical emergencies, it is now commonly used to move donated organs.

Figure 2.10 - Green Corridor in India. [43]

Green corridor services were only recently launched in India, around 2014. However, the 25,000 rupee charge is just for organising one. To keep up with these numbers, a modern and more efficient infrastructure is needed to satisfy the medical and transportation needs.

A crucial aspect to look upon is that the cadaver organs as previously discussed have a short life span after extracting it from the donor, so the transplant should be done within a few golden hours; not considering the time it would also require to complete the procedure. Which certainly is not fulfilled because India lacks a robust system in organ transport systems.

It took 4 years to have at least more than 10 Green Corridor service in the major cities.

Following a table represents the number of green corridors introduced in the major cities of Maharashtra in recent years;

Table 2.2 - List of Green Corridors in various Urban Cities of Maharashtra. [17]

Sr. No.	Year	Mumbai	Pune	Aurangabad	Nagpur
1.	2015	0	7	0	0
2.	2016	4	8	0	0
3.	2017	24	0	0	0
4.	2018	18	35	17	11
5.	2019	11	21	3	3

2.2 Solution Requirements

2.2.1 Mission Profile

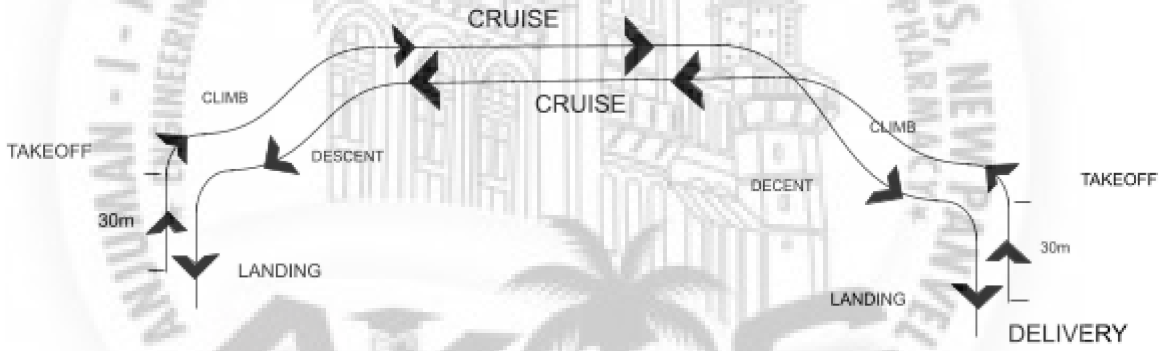

Figure 2.11 - Mission profile for delivery purpose.

The UAV mission profile for transport and delivery depicts that the aircraft takes-off vertically up to 30 meters of height from ground and makes transition to climb up to a desired cruising altitude and performs a second transition to climb down finally to land vertically at the delivery site. This first mission is performed from take-off site to the delivery site and a similar second mission is performed from the delivery site to the initial take-off site or site of origin.

2.2.2 UAV Objectives

Table 2.3 - Objectives of UAV.

Parameters	Description
Range	60km
Speed	Speed upto 100kmph
Payload	1.5kg to 2kg
VTOL	Can take off and land vertically hence, require less space for the task.
Weather Resistance	High operational capability almost in all weather.
Cost Efficient	In comparison with other options for the job like air ambulance and green corridors it is quite economic and cost efficient.
Quick Assembly	Can be assembled and dismantled within minutes.
Flight Time	1 hr

2.2 Concept Generation

Figure 2.12 - Endurance Aircraft Conceptual Design Render.

Chapter 03

Preliminary Design

3.1 VTOL System Design

As it is known that the main drawback of fixed wing aircraft systems is that they require a runway to take off and land, which limits their ability to be used in tight spaces. So in order to be able to operate in tight spaces without runways, like in cities and rural areas, we design a VTOL system for our aircraft which will enable them to take off vertically like a helicopter and fly like a fixed wing. This is the best of both worlds scenarios as Helicopters can operate virtually anywhere but consume more fuel and airplanes are fuel efficient but require runways to operate. Combining the best aspects of both gives us take off and landing capabilities vertically along with fuel efficient flight of a fixed wing aircraft.

3.1.1 Power Systems

The first step in designing a VTOL system is to estimate the weight to be lifted and Rate of climb desired.

3.1.1.1 Thrust Estimation

Consider a Vtol system in equilibrium, holding constant altitude in figure 3.1.

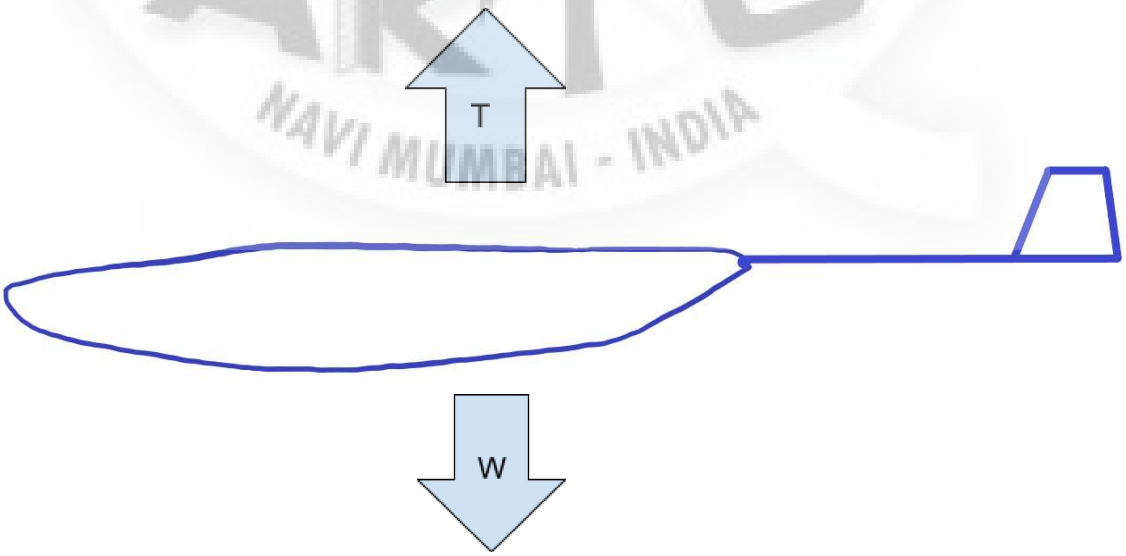

Figure 3.1 Thrust and Weight acting on aircraft.

When both the thrust (T) and weight (W) acting on the body remain the same the aircraft will hold altitude. But the condition for increasing altitude is given as:

$$T > W$$

As we have already determined the MTOW of the plane to be 117 Newton approximately, the required thrust (T_e) to hold altitude would be.

$$T_e = 117 \text{ N}$$

Consider a VTOL aircraft in a steady state climb. The forces acting on the aircraft will be:

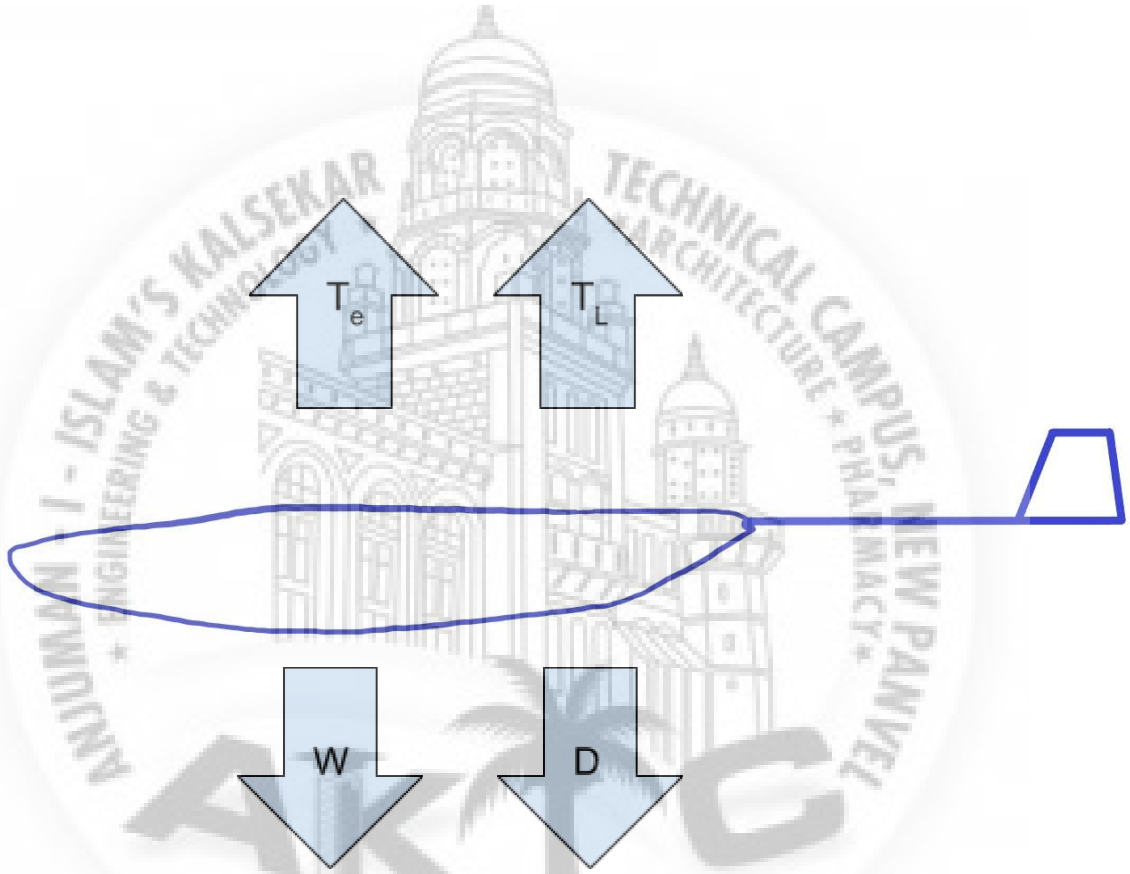

Figure 3.2 - Thrust, Weight and Drag acting on aircraft.

We know the forces T_e and W. The thrust required for climbing is given as T_L as shown in figure 3.2. The relationship between T_e and T_L is given as:

$$T_C = T_e + T_L \qquad \text{…(eq 3.1)}$$

where T_c is the Climb thrust. Drag (D) in the above figure 3.2 is the opposing force to the thrust force. We must first estimate the area normal to the drag. As we already have estimated the wing area to be 0.94 sq. meters, we can safely assume the area of fuselage and tail along with the wing will roughly be 2 sq. meters. The equation used used to calculate drag is given as:

$$D = \frac{1}{2} \cdot p \cdot A \cdot V^2 \cdot C_d \qquad \text{…(eq 3.2)}$$

where p is 1.225 at sea level, A is assumed to be 2 sq. meters, the desired velocity for climb is above 6 m/s and the coefficient of drag is assumed to be 1.14. Using the range of assumptions in the formula, the following graph is calculated:

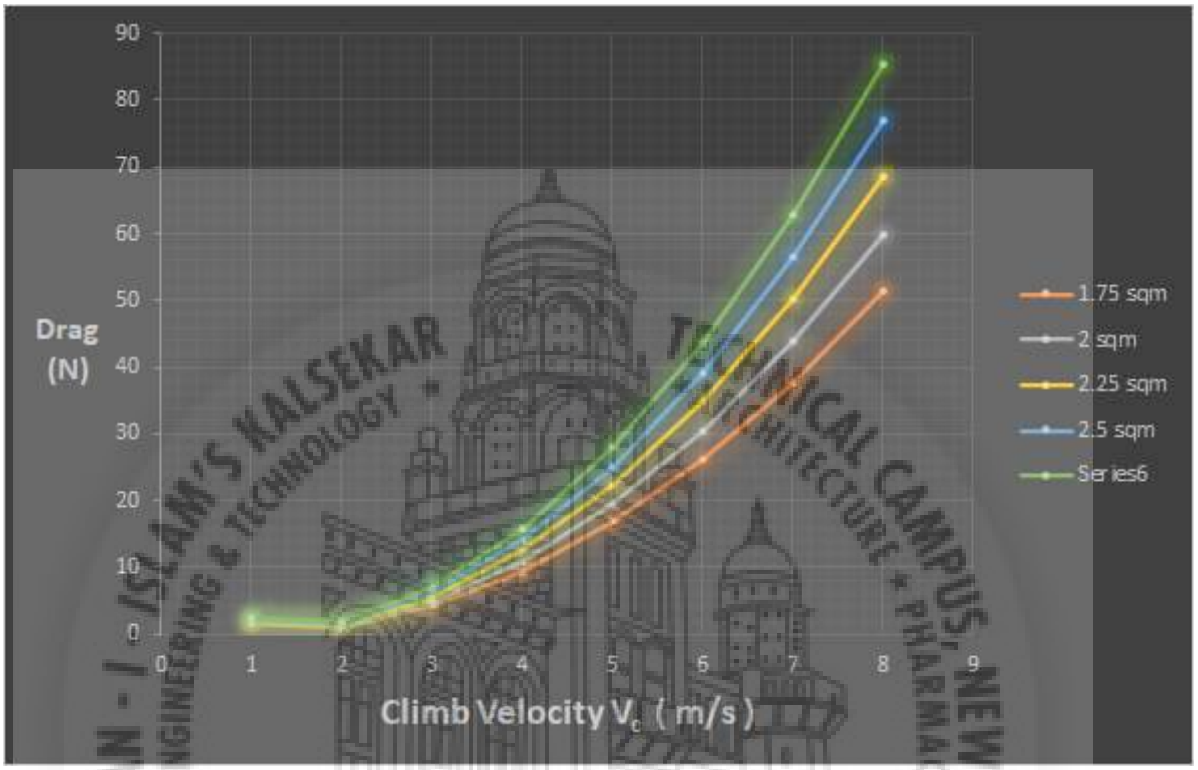

Figure 3.3 - Drag and Climb rate.

In figure 3.3 we can see the exponential increase in drag with respect to velocity. It can also be seen that higher area results in greater drag. At 6 m/s, the drag changes from 26N to 44 N with respect to change in area. We will assume the area of our aircraft to be 2 sq m. Resulting in the following climb velocity and drag:

$$V_c = 6 \text{ m/s} \quad \text{and} \quad D_{2sqm} = 34 \text{ N} \qquad \text{…(eq 3.3)}$$

Where the Value of Drag (D) is same as the value of Lift thrust (T_L)

Hence,

$$T_C = T_e + T_L = 117 + 34 = 151 \text{ N} \qquad \text{…(eq 3.4)}$$

3.1.1.2 Motor And Propeller Selection

As our drone is a tricopter, required thrust for vtol will be divided between 3 motors. The maximum climb thrust, T_C , as determined in equation 3.4 is 150 N approximately. Hence

each motor has to produce a maximum static thrust of 50N or more. After evaluation of many motor and propeller combinations, we settled on the Turnigy Sk3 5055-430kv motor with a 17x8 or 18x8 propeller.

Figure 3.4 - Turnigy Sk3 5055-430kv and 17x8 APC style propeller.

Table 3.1 - Motor and propeller Selection

Motor	Propeller	Estimated Thrust
Turnigy Sk3 5055-430kv	17 x 8 ACP	>5 Kgf thrust
Turnigy Sk3 5055-430kv	18 x 8	>6 Kgf thrust

3.2 Fixed Wing Preliminary Design

The preliminary design phase of an aircraft employs a calculation based approach to determine various parameters. These parameters are determined based on a decision-making process and selection technique. The parameters at this stage are not final but are essential and will directly influence the detailed design phase.

Three fundamental aircraft parameters determined during the preliminary design phase are: (i) aircraft maximum take-off weight (MTOW or WTO), (ii) wing reference area(SW or S ref or S), and (iii) engine thrust (TE or T) or engine power (PEorP). Hence, three primary aircraft parameters of WTO, S, and T (orP) form the output of the preliminary design phase. These three parameters will govern the aircraft size, the manufacturing cost, and the complexity of calculations.

3.2.1 Weight Estimation

The first step in the preliminary design phase generally is the estimation of MTOW (maximum take off weight) or AUW (All up weight). The design MTOW or W_{TO} is the total weight of an aircraft when it begins the mission for which it was designed.

The total aircraft weight (MTOW) is broken into several parts.

1. Payload weight (W_{pl}) - Payload weight is mostly known and is used to determine other weights
2. Empty weight (We) - Empty weight is the weight weight of the aircraft structure and components without the payload and battery weight.
3. battery weight (Wb) - Battery weight is determined as needed for required range and endurance.

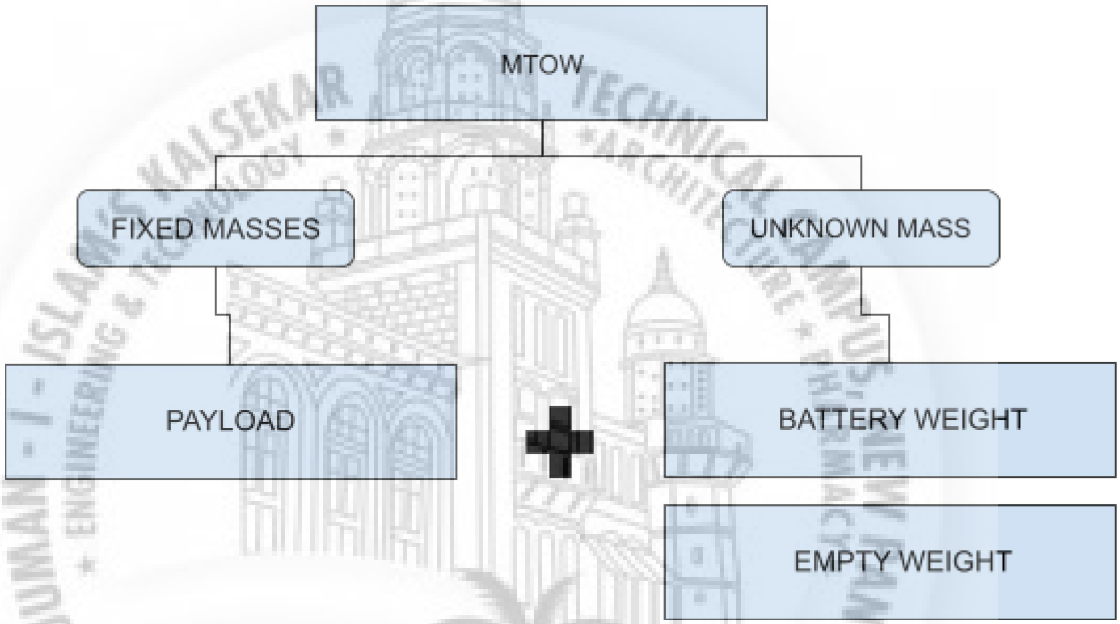

Figure 3.5 - Maximum Takeoff Weight.

$$W_{TO} = W_{PL} + W_E + W_B \quad \text{...(eq 3.5)}$$

As the payload of our aircraft is required to be in 2-3 Kg range,

$$W_{PL} = 2.5g \quad \text{...(eq 3.6)}$$

The estimation of MTOW will be determined using statistical data based on similar aircraft. We referred to three aircrafts namely, PD -1 from URKP Systems, YANGDA FW-250 and PLYMOUTH XV.

Table 3.2 - Comparison of Different UAV

Sr. No.	UAV	MTOW	PAYLOAD
1.	PD-1	40	10
2.	YANGDA FW-250	12	2.5
3.	PLYMOUT XV	16	4

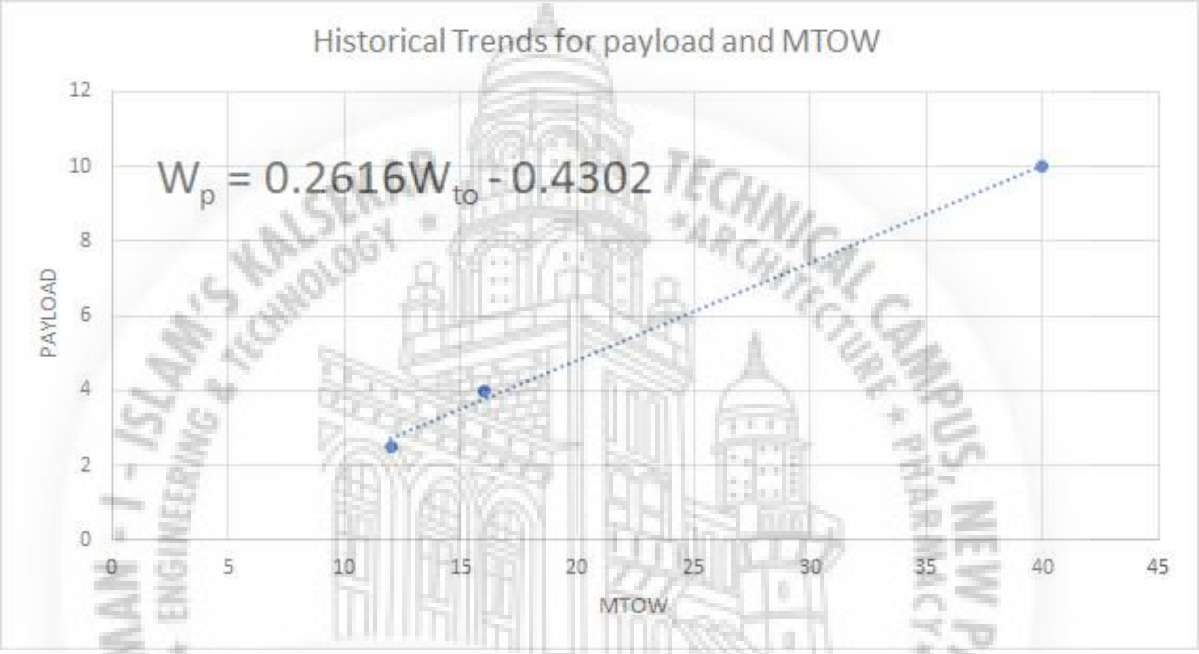

Figure 3.6 - Payload Prediction.

The graphical representation of table 3.2 is shown in figure 3.6. It can be seen that the payload and MTOW of each aircraft is plotted and a trendline is used to determine the MTOW of endurance for the given payload.

The trendline equation is given as:

$$W_{PL} = 0.2616W_{to} - 0.4302 \quad \text{...(eq 3.7)}$$

In terms of W_{TO}:

$$W_{To} = \frac{0.4302 + Wp_L}{0.2616} \quad \text{...(eq 3.8)}$$

Substitution of values from Eqn 3.7:

$$W_{To} = \frac{0.4302 + 2.5(9.81)}{0.2616} \quad \text{...(eq 3.9)}$$

$$W_{TO} = 11.2 \text{ KgF} \quad \text{...(eq 3.10)}$$

Estimating the Final MTOW to be 12 Kgs, that leaves us with We and Wb. Rewriting Eqn 3.9 in terms of We and WB:

$$W_E + W_B = W_{TO} - W_{PL} \quad \text{...(eq 3.11)}$$

$$W_E + W_B = 12 - 2.5 \quad \text{…(eq 3.12)}$$

$$W_E + W_B = 9.5 \text{ Kgf} \quad \text{…(eq 3.13)}$$

The battery weight is assumed to be 3.5 kgs which leaves us with an Empty weight of 6.5 Kgs.

3.2.2 Wing And Power Estimation

3.2.2.1 Technique Summary

The next Crucial step after weight determination is the wing area and engine power estimation. This is dependent upon aircraft performance requirements. Hence this is an analytical approach from Sadraey[42] which produces reliable results. The two main outputs of this design step are:

1. wing reference area (S or Sref);
2. engine thrust (T) or engine power (P).

The aircraft performance requirements utilized to size the aircraft in this step are:

•stall speed (V_s);

•maximum speed (V_{max});

•maximum rate of climb (ROC_{max});

•take-off run (S_{TO});

•ceiling (h_c);

•turn requirements (turn radius and turn rate).

In this section, three new parameters appear in almost all equations. So, we need to define them first:

1. Wing loading. The ratio between aircraft weight and wing area is referred to as wing loading and represented by W/S. This parameter indicates how much load (i.e., weight)is held by each unit area of the wing.
2. Thrust-to-weight ratio. The ratio between aircraft engine thrust and aircraft weight is referred to as thrust loading and is represented by T/W. This parameter indicates how heavy the aircraft is with respect to engine thrust. The term thrust-to-weight ratio is associated with jet aircraft (e.g., turbofan or turbojet engines). Although this designated name is convenient to use, it does not seem to fit very well with the concept related to thrust and weight. However,W/T seems to be a more convenient symbol to refer to as the thrust loading; which means how much weight is carried by each unit of thrust.

3. Power loading. The ratio between aircraft weight and engine power is referred to as power loading and is represented by W/P. This parameter indicates how heavy the aircraft is with respect to engine power. A better name for this parameter is weight-to-power ratio. This term is associated with propeller-driven aircraft (turboprop or piston engines).

In general, two desired parameters (S and T (or P)) are determined in steps. The Following are the steps to determine the wing area and engine power for a prop-driven aircraft.

1. Derive one equation for each aircraft performance requirement (e.g.,Vs, Vmax, ROC, STO, hc, Rturn, ωturn). If the aircraft is prop-driven, the equations are in the form of W/P as functions of W/S, as follows: [42]

$$\left(\frac{W}{P}\right)_{V_s} = f_1\left(\frac{W}{S}, V_s\right)$$

$$\left(\frac{W}{P}\right)_{V_{max}} = f_2\left(\frac{W}{S}, V_{max}\right)$$

$$\left(\frac{W}{P}\right)_{S_{TO}} = f_3\left(\frac{W}{S}, S_{TO}\right)$$

$$\left(\frac{W}{P}\right)_{ROC} = f_4\left(\frac{W}{S}, ROC\right)$$

$$\left(\frac{W}{P}\right)_{ceiling} = f_5\left(\frac{W}{S}, h_c\right)$$

$$\left(\frac{W}{P}\right)_{turn} = f_6\left(\frac{W}{S}, R_{turn}, \omega_{turn}\right)$$

…(eq 3.14 to 3.20)

2. Sketch all derived equations in one plot. The vertical axis is power loading (W/P) and the horizontal axis is wing loading (W/S). Thus, the plot illustrates the variations of power loading with respect to wing loading. These graphs will intersect each other at several points and may produce several regions.
3. Identify the acceptable region inside the regions that are produced by the axes and thegraphs. The acceptable region is the region that meets all aircraft performance require-ments. A typical diagram is shown in Figure 3.7. The acceptable region is recognized by the fact that as a performance variable (say V_{max}) is varied inside the permissible limits, the power loading must behave to confirm that trend. For instance, consider the graph of power loading versus wing loading for maximum speed. Assume that the power loading is inversely proportional to the maximum speed. Now, if the maximum speed is increased – which is inside the permissible limits – the power loading is decreased. So the reduction in power loading is acceptable. Hence, the lower region of this particular graph is acceptable.
4. Determine the design point (i.e., the optimum selection). The design point on the plotis only one point that yields the smallest engine in terms of power (i.e., the lowest cost).

5. From the design point, obtain two numbers: corresponding wing loading (W/S) and corresponding power loading (W/P). A typical graphical technique is illustrated in Figure 3.7 (for prop-driven aircraft).
6. Calculate the wing area and engine power from these two values, since the aircraft MTOW (W_{TO}) has been determined previously. The wing area is calculated by dividing the aircraft take-off weight by the wing loading. The engine power is also calculated by dividing the aircraft take-off weight by the power loading:

$$S = \frac{W_{TO}}{\left(\frac{W}{S}\right)}$$

$$P = \frac{W_{TO}}{\left(\frac{W}{P}\right)} \qquad \ldots(\text{eq } 3.21 \text{ \& } 3.22)$$

In this section. This graph that contains several performance charts is sometimes referred to as the matching plot, matching chart, or matching diagram.

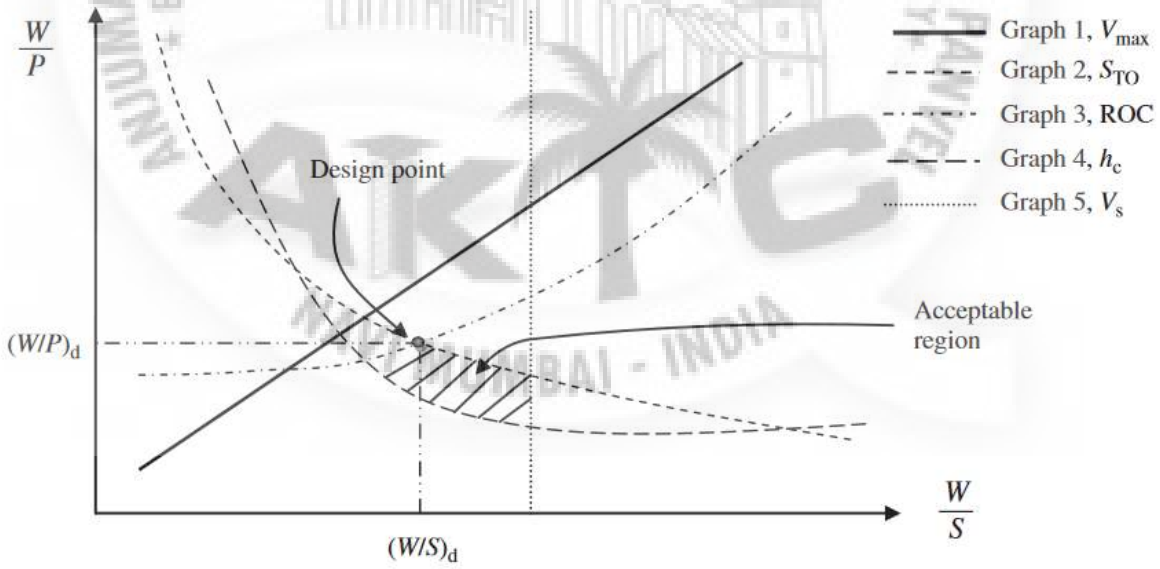

Figure 3.7 - Sample Power loading and wing loading graph.

3.2.2.2 Stall Speed

Stall speed is the speed below which the wing starts losing lift which will lead to loss of control of the aircraft. Thus it is an important design parameter. The level flight lift equation is given as:

$$L = \frac{1}{2} \cdot \rho \cdot V^2 \cdot S \cdot C_L$$

$$L = \frac{1}{2} \cdot \rho \cdot V^2 \cdot S \cdot C_{L_{max}} \quad \text{…(eq 3.23)}$$

where ρ denotes the air density at the specified altitude, and CL_{max} is the aircraft maximum lift coefficient . From Eqn we can drive wing loading with respect to stall speed:

$$\left(\frac{W}{S}\right)_{V_s} = \frac{1}{2} \cdot \rho \cdot V_s^2 \cdot C_{L_{max}} \quad \text{…(eq 3.24)}$$

$$\left(\frac{W}{S}\right)_{V_s} = \frac{1}{2} \cdot 1.225 \cdot 13^2 \cdot 1.2 = 124.215 \frac{N}{m^2} \quad \text{…(eq 3.25)}$$

This provides the first graph in the matching plot.

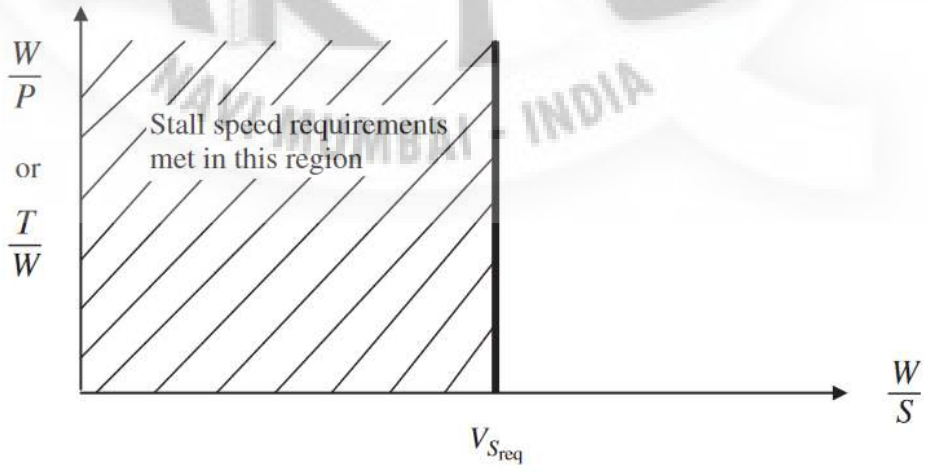

Figure 3.8 - Stall Region.

3.2.2.3 Maximum Speed

Another very important performance requirement, particularly for fighter aircraft, is the maximum speed. Two major contributors, other than aircraft weight, to the satisfaction of this requirement are the wing area and engine thrust (or power).

Consider a prop-driven aircraft flying at its maximum speed. The power required:

$$n_p P_{max} = T V_{max} \quad \text{...(eq 3.26)}$$

where engine thrust (T) must be equal to aircraft drag (D), and np is propeller efficiency.

The Coefficient of Drag equation is given as:

$$C_D = C_{Do} + C_{Di} = C_{Do} + K \times C_L^2 \quad \text{...(eq 3.27)}$$

Coefficient of Lift is given by:

$$C_L = \frac{2L}{\rho \cdot V^2_{max} \cdot S} \quad \text{...(eq 3.28)}$$

Substitution of values from eqn 3.26 and eqn 3.27 and eqn 3.28 yields:

$$n_p P = \frac{1}{2} \rho V^2_{max} S C_D \cdot V_{max} = \frac{1}{2} \rho V^3_{max} S C_D \quad \text{...(eq 3.29)}$$

$$n_p P = \frac{1}{2} \rho V^3_{max} S \left(C_{Do} + K \cdot \left(\frac{2W}{\rho V_{max} S} \right)^2 \right) \quad \text{...(eq 3.30)}$$

$$n_p P = \frac{1}{2} \rho V^3_{max} S C_{Do} + \frac{1}{2} \rho V^3_{max} S \cdot \frac{K(2W)^2}{\left(\rho V_{max} S \right)^2} \quad \text{...(eq 3.31)}$$

$$n_p P = \frac{1}{2} \rho V^3_{max} S C_{Do} + \frac{K 2W^2}{\rho V_{max} S} \quad \text{...(eq 3.32)}$$

Dividing both sides with aircraft weight (W):

$$n_p \frac{P}{W} = \frac{1}{2} \rho V^3_{max} \frac{S}{W} C_{Do} + \frac{K2W^2}{\rho V_{max} SW} \quad \text{...(eq 3.33)}$$

Inverting the equation:

$$\left(\frac{W}{P}\right)_{V_{max}} = \frac{n_p}{\frac{1}{2} \rho V^3_{max} \frac{1}{\left(\frac{W}{S}\right)} C_{Do} + \frac{K2}{\rho V_{max}} \cdot \left(\frac{W}{S}\right)} \quad \text{...(eq 3.34)}$$

Substituting Known parameters in the above equation:

$$\left(\frac{W}{P}\right)_{V_{max}} = \frac{0.7}{\frac{1}{2} \cdot 1.225 \cdot 26^3 \frac{1}{\left(\frac{W}{S}\right)} \cdot 0.03 + \frac{0.044 \cdot 2}{1.225 \cdot 26} \cdot \left(\frac{W}{S}\right)} \quad \text{...(eq 3.35)}$$

Power loading and wing loading equation for V_{max}:

$$\left(\frac{W}{P}\right)_{V_{max}} = \frac{0.7}{322.95 \cdot \frac{1}{\left(\frac{W}{S}\right)} + 2.762 \times 10^{-3} \cdot \left(\frac{W}{S}\right)} \quad \text{...(eq 3.36)}$$

3.2.2.4 Take-Off Run

The take - off run is another important parameter in aircraft performance and will be employed for plotting the matching chart.

The equation to estimate power loading and wing loading required for the take off run is sourced from Aircraft Design by Mohammed Sadrey. The equation is given as:

$$\left(\frac{W}{P}\right)_{S_{TO}} = \frac{1 - exp\left(0.6pgC_{D_G}S_{TO}\left(\frac{1}{\frac{W}{S}}\right)\right)}{\mu - \left(\mu + \frac{C_{D_G}}{C_{L_R}}\right)\left(exp\left(0.6pgC_{D_G}S_{TO}\left(\frac{1}{\frac{W}{S}}\right)\right)\right)} \cdot \frac{n_p}{V_{TO}} \quad \text{...(eq 3.37)}$$

The value for u is typically assumed to be 0.04 ,

$$V_{TO} = 1.1\ V_S = 1.1 \text{ x } 13 = 14.3 \text{ m/s} \quad \text{...(eq 3.38)}$$

The take off and drag coefficients are calculated as:

$$C_{L_{TO}} = C_{L_C} \quad \text{...(eq 3.39)}$$

where C_{LC} is assumed to be 0.3;

$$C_{LTO} = 0.3 \quad \text{...(eq 3.40)}$$

$$C_{DoLG} = 0.009 \quad \text{...(eq 3.41)}$$

$$C_{DoTo} = C_{Do} + K(C_{LTO})^2 = 0.039 + 0.044(0.3)^2 \quad \text{...(eq 3.42)}$$

$$C_{DoTo} = 0.0429$$

The take off rotation lift coefficient is:

$$C_{L_R} = \frac{C_{L_{max}}}{(1.1)^2} = \frac{1.2}{1.21} = 0.99 \quad \text{...(eq 3.43)}$$

The variable C_{DG} is:

$$C_{D_G} = C_{D_{TO}} - \mu \cdot C_{L_{TO}} = 0.0429 - 0.04 \cdot 0.3$$

$$C_{D_G} = 0.03096 \quad \text{...(eq 3.44)}$$

As the propeller used in this design will be fixed pitch, the typical value for propeller efficiency is 0.5. The distance for take off is set at 50 meters. Substitution of known values in equation 3.37 yields:

$$\left(\frac{W}{P}\right)_{S_{TO}} = \frac{1-exp\left(0.6\cdot 1.225\cdot 9.81\cdot 0.031\cdot 50\cdot\left(\frac{1}{\frac{W}{S}}\right)\right)}{0.04-\left(0.04+\frac{0.031}{0.99}\right)\cdot\left(exp\left(0.6\cdot 1.225\cdot 9.81\cdot 0.031\cdot 50\cdot\left(\frac{1}{\frac{W}{S}}\right)\right)\right)}\cdot\frac{0.5}{14.3}$$

…(eq 3.45)

Simplifying:

$$\left(\frac{W}{P}\right)_{S_{TO}} = \frac{1-exp\left(11.17\cdot\left(\frac{1}{\frac{W}{S}}\right)\right)}{0.04-(0.071)\cdot\left(exp\left(11.17\cdot\left(\frac{1}{\frac{W}{S}}\right)\right)\right)}\cdot 0.0349$$

…(eq 3.46)

3.2.2.5 Rate of Climb

Rate of Climb of an aircraft is a performance parameter which determines the change in aircraft altitude with respect to time. In other words it means how fast the aircraft can gain altitude. The equation for wing and power sizing based on ROC is sourced from Aircraft Design by Mohammed Sadrey. The ROC equation is given as:

$$\left(\frac{W}{P}\right)_{ROC} = \frac{1}{\frac{ROC}{n_p}+\sqrt{\frac{2}{p\cdot\sqrt{\frac{3C_{Do}}{K}}}\cdot\left(\frac{W}{S}\right)}\left(\frac{1.155}{\left(\frac{L}{D}\right)_{max}\cdot n_p}\right)}$$

…(eq 3.47)

The desired ROC is 10 m/s. The max L/D value is assumed to be 12. Substitution of known values in above equation yields:

$$\left(\frac{W}{P}\right)_{ROC} = \frac{1}{\frac{10}{0.7}+\sqrt{\frac{2}{1.225\cdot\sqrt{\frac{3\cdot 0.03}{0.044}}}\cdot\left(\frac{W}{S}\right)}\left(\frac{1.155}{(12)\cdot 0.7}\right)}$$

…(eq 3.48)

$$\left(\frac{W}{P}\right)_{ROC} = \frac{1}{14.28+\sqrt{1.141\cdot\left(\frac{W}{S}\right)}(0.1375)}$$

…(eq 3.49)

3.2.2.6 Ceiling

Another performance requirement that influences the wing and engine sizing is the ceiling.The ceiling is defined as the highest altitude that an aircraft can safely have a straight level flight. Another definition is the highest altitude that an aircraft can reach by its own engine and have sustained flight. Although our aircraft does not need to travel at high altitudes, we will include this for fun.

There are four types of Ceiling:

1. Absolute ceiling (hac). As the name implies, the absolute ceiling is the absolute max-imum altitude that an aircraft can ever maintain level flight. In other terms, the ceiling is the altitude at which the ROC is zero.
2. Service ceiling (hsc). The service ceiling is defined as the highest altitude at which the aircraft can climb with a rate of 100 ft/min (i.e., 0.5 m/s). The service ceiling is lower than the absolute ceiling.
3. Cruise ceiling (hcc). The cruise ceiling is defined as the altitude at which the aircraft can climb with a rate of 300 ft/min (i.e., 1.5 m/s). The cruise ceiling is lower than the service ceiling.
4. Combat ceiling (hcc). The combat ceiling is defined as the altitude at which a fighter can climb with a rate of 500 ft/min (i.e., 5 m/s). The combat ceiling is lower than the cruise ceiling. This ceiling is defined only for fighter aircraft.

The equation for service ceiling is sourced from Aircraft Design by Mohammed Saddrey and is given as:

$$\left(\frac{W}{P}\right)_C = \frac{\frac{p_c}{p_o}}{\frac{ROC_C}{n_p} + \sqrt{\frac{2}{p\sqrt{\frac{3 \cdot C_{Do}}{K}}}\left(\frac{W}{S}\right)\left(\frac{1.155}{\left(\frac{L}{D}\right)_{max} \cdot n_p}\right)}} \quad \ldots(\text{eq } 3.50)$$

The air density at 11000 meters is around 0.35 kg/m^3. Substituting known values in above equation yields:

$$\left(\frac{W}{P}\right)_C = \frac{\frac{0.35}{1.225}}{\frac{10}{0.7} + \sqrt{\frac{2}{0.35 \cdot \sqrt{\frac{3 \cdot 0.03}{0.044}}}\left(\frac{W}{S}\right)\left(\frac{1.155}{(12) \cdot 0.7}\right)}} \quad \ldots(\text{eq } 3.51)$$

$$\left(\frac{W}{P}\right)_C = \frac{0.2857}{0.71 + \sqrt{3.99 \cdot \left(\frac{W}{S}\right)}(0.1375)} \quad \ldots(\text{eq } 3.52)$$

3.2.2.7 Matching Plot

Now we have all the equations where power loading is defined as functions of wing loading. When we plot all of them in one graph we get the following result.

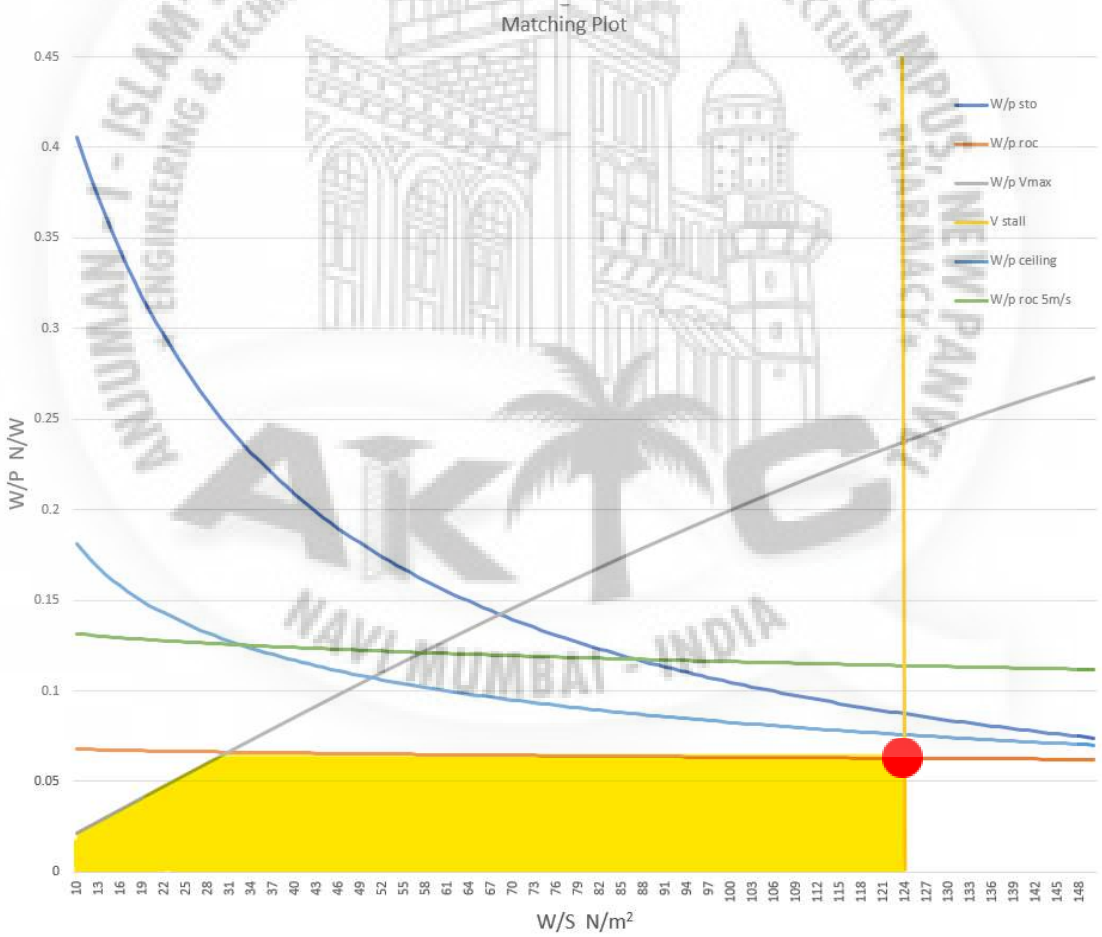

Figure 3.9 - Matching Plot.

The area below each graph is satisfying and the region above each graph is not satisfying. That leaves the area highlighted in yellow as the acceptable region. The Red dot at the

intersection between ROC and V stall graph is chosen as the design point, keeping in mind manufacturability constraints.

The power loading and wing loading extracted from the design point are given as:

$$W / P = 0.062 \ N/W \quad \text{...(eq 3.53)}$$

$$W / S = 124 \ N/m^2 \quad \text{...(eq 3.54)}$$

The wing are and engine power are calculated as:

$$S = \frac{W_{TO}}{\left(\frac{W}{S}\right)} = \frac{117}{124} = 0.94 \, m^2 \quad \text{...(eq 3.55)}$$

$$P = \frac{W_{TO}}{\left(\frac{W}{P}\right)} = \frac{117}{0.062} = 1887 \, W \quad \text{...(eq 3.56)}$$

Thus, the wing area and engine power will be 0.94 square meters and 1887 watts respectively.

Chapter 04

Detailed Design

4.1 Fixed Wing

4.1.1 Wing Design

The wing can be considered as the most important component of the aircraft. This is because a fixed wing aircraft cannot fly without a wing. The wing is also important as the wing geometry and sizing influences the other aircraft components. The main function of the wing is to generate sufficient Lift (L) of the aircraft to fly with minimum effort. In addition to Lift generation, the wing also produces two other forces which are Drag (D) and Pitching Moment (M). The wing is designed such that the generated lift should be maximum while keeping the drag and moment minimum. The lift that is produced by the wing is due to the shape of its cross section which is known as Airfoil. The airfoils are designed such that the air flowing over the airfoil shape moves faster than the air moving below the airfoil. This creates a pressure difference between the upper and lower part of the airfoil. This produces the upward force which is the lift. The following flow chart gives an overview of the procedure for wing design.

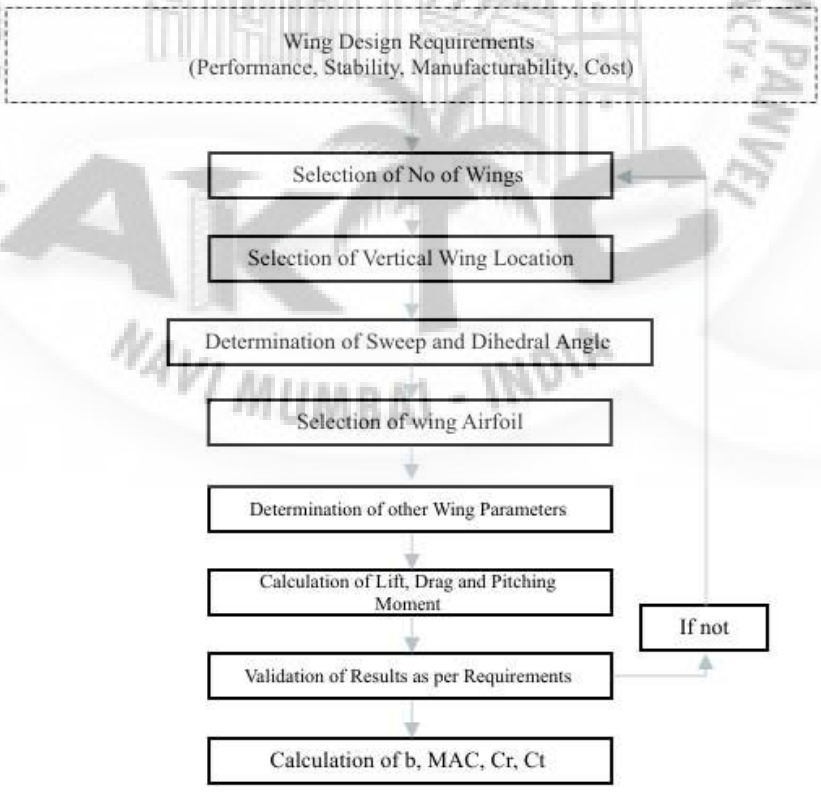

Figure 4.1 - Wing Design Procedure Flowchart.

4.1.1.1 Number of Wings

In an aircraft, more than one wing can be used. However, using more than three wings is not practical. Aircrafts with one wing are known as monoplanes and aircrafts with two wings are known as biplanes. In the modern era, most modern planes are monoplanes with few biplanes. The main advantage of employing a biplane is that it can reduce the wing span while keeping the effective wing area constant. In the previous generation, the aircraft manufacturers' challenge was to make this large wing structurally strong which was very difficult with the manufacturing technologies of that time. However in modern times, with the introduction of advanced materials like aluminium alloys and composites, making a wing with a large wing span has become possible.

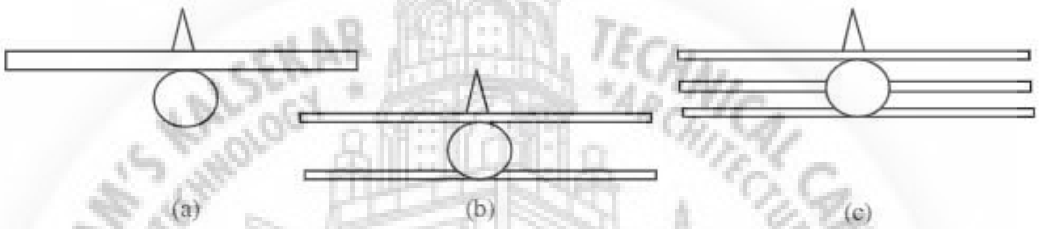

Figure 4.2 - Monoplanes (a), Biplanes (b), Triplane. (c)

Controlling an aircraft is often difficult. Hence controllability is the most important requirement in modern aircraft. Having a shorter wingspan provides a high roll rate. This will enable the aircraft to roll faster. On the other hand monoplanes have a larger wingspan, which is easy to control.

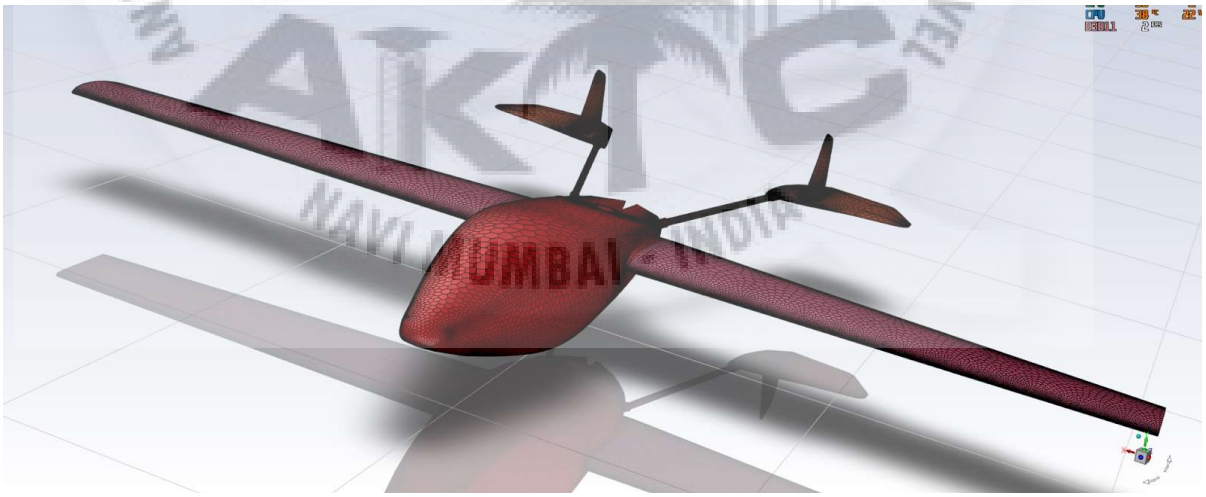

Fig 4.3 - Monoplane Endurance Drone CAD Model.

In the aircraft that is being designed, a single wing is selected as it is more stable compared to two or three wing aircraft. With the introduction of composite materials like Carbon Fiber,

high structural strength can be achieved. The other reason for selecting a single wing aircraft is that it reduces the weight significantly.

4.1.1.2 Vertical Wing Location

After selecting the number of wings that is to be employed, the next step is to determine the vertical location of the wing relative to the centre line of the fuselage. Wing vertical location influences the other design parameters of the aircraft. The main parameter affected by the vertical location of the wing is the Centre of Gravity (CG) of the aircraft. The design of the enpanage is also affected based on the vertical wing location.

There are four locations of the wing that are recognised and used in modern aircraft. They are High wing, Low wing, Mid-wing and Parasol wing. Figure 4.4 shows the schematic front view of the aircraft having different locations of the wings. In the figure (a) we can see that the wing is on the top of the fuselage. This wing configuration is known as High wing configuration. In figure (b) the wing is seen in the middle of the fuselage therefore this configuration is Mid-wing configuration. Figure (c) shows that the fuselage is on the top of the wing. such configuration is known as Low wing configuration. In the figure (d) the wing is placed well above the fuselage and connected to it by struts. This type of configuration is called Parasol wings. The wing configurations are selected based on the advantages and disadvantages of each configuration.

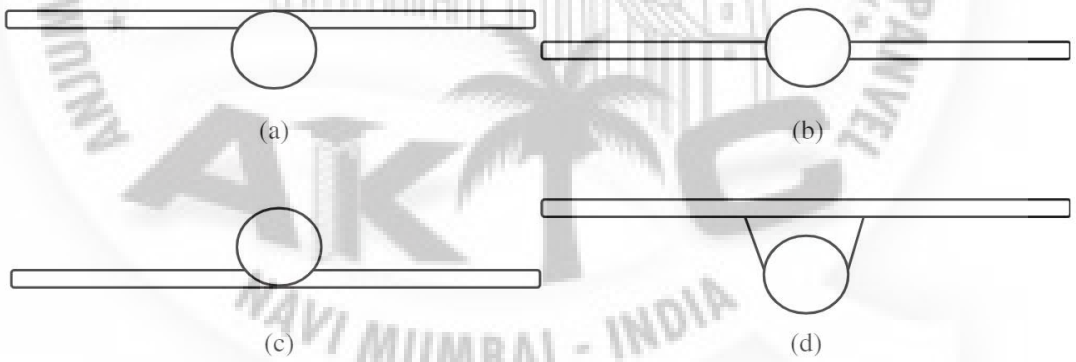

Figure 4.4 - Vertical Wing Locations.

4.1.1.2.1 High Wing

In high wing configuration the wing is situated on the top of the fuselage. It is connected to the fuselage. This wing configuration is employed in heavy cargo aircrafts. This is because High wing configuration generates more lift as compared to other configurations. On the other hand, a high wing tends to have a more frontal area which increases the total drag produced by the aircraft. Another reason for cargo aircrafts to employ high wing

configuration is that the loading and unloading can be carried out with ease. The main disadvantage of high wing configuration is that the overall weight of the wing is 20% higher than the weight of low wing configuration. High wing configuration enables larger wings to ground clearance. High wing configuration moves the landing gear location from the wings to the fuselage which decreases the space in the fuselage. High wing aircrafts can take off and land from the sea surface. The control of the high wing aircraft is easier as the location of the CG is lower than the wing. This wing configuration makes aircraft laterally more stable. This configuration tends to have lower ground effect therefore during takeoff the lift that will be generated will be lower as compared to low wing configuration which increases the takeoff length of the aircraft.

Figure 4.5 - C-5M Super Galaxy.[38]

4.1.1.2.2 Mid-Wing

In Mid-wing configuration the wing is located vertically in the middle of the fuselage. Mid wing configuration is said to have features of both high wing and low wing configuration. The main difference is that the main spar of the mid wing is cut in two half whereas in high wing configuration the spar is continuous. This decreases the structural strength of the wing. To compensate for the strength the wing is reinforced at the intersection on the fuselage. This adds to the overall weight of the wing. In some aircraft employing mid wing configuration, the spar is not cut and passes through the fuselage as a single part. This is to increase the strength without reinforcing the wing which creates and occupies space in the fuselage and decreases the effective space in the fuselage. Compared to high wing configuration, the drag produced in mid wing configuration is lower.

Figure 4.6 - Smith Aerostar 600 N70VB.[39]

4.1.1.2.3 Low Wing

In most commercial aircrafts the wings are located in the bottom of the fuselage. This type of wing configuration is known as Low wing configuration. The main reason to employ low wing configuration in commercial aircraft is that the overall performance of this configuration is better than other configurations. The takeoff performance is much better that of high wing configuration due to the ground effect. The landing gears are located inside the wings. This creates more space in the fuselage. The landing gear can be made shorter as the distance between the wing and the ground is shorter which decreases the weight of the aircraft. As the wing is situated below the fuselage, the wing is divided into two sections. This reduces the amount of lift generated by the wing. The stall speed in low wing configuration is increased because the lift that is generated is less. The induced drag in this configuration is less and compared to other configurations. Low wing configuration eliminated the use of struts to support the wing, decreasing the overall weight of the aircraft. The maneuverability of the aircraft increases in low wing configuration. Most of the passenger jets employ low wing configuration because of its high performance and less operational cost.

Figure 4.7 - Boeing 747.[40]

4.1.1.2.4 Parasol Wing

In Parasol wing configuration the wing is located vertically well above the fuselage. The wing is attached to the fuselage by struts which provide good structural strength. The configuration is similar to High wing configuration, but has a significantly high drag generation. This configuration was employed in previous generations of aircrafts. The main reason for using this configuration is that the complexity and manufacturability is much less when compared to other configurations. Aircrafts with parasol wing configuration are used in the modern era in agriculture sectors. Usually small aircrafts with single pilot capacity and sometimes two persons capacity use this configuration. Due to the advancements in aviation technology, more efficient aircrafts are built, limiting the use of aircrafts having Parason wing configuration.

Fig 4.8 - Bakeng Duce ZU-CH8. [41]

All the wing positions have their advantages and disadvantages. The correct configuration is selected based on the aircraft requirement and objectives. The different selection parameters for selecting the correct wing location configuration is given below in table 4.1 .

Table 4.1 - Vertical Wing Location Trade Study

Sr. No.	Parameters	Score	High Wing	Mid wing	Low Wing	Parasol WIng
1.	Stability	20	18	15	13	16
2.	Control	15	14	12	10	10
3.	Cost	10	10	7	6	7
4.	Manufacturability	10	10	7	6	6
5.	Operational requirements	40	35	30	28	29
6.	Other requirements	5	5	4	3	3
	Total	100	92	75	66	71

After observing various characteristics of different wing configurations, it can be concluded that high wing configuration is the most efficient and economical wing configuration. Therefore, High wing configuration is employed in the drone that is designed in this project.

4.1.1.3 Sweep and Dihedral Angles

4.1.1.3.1 Swept Wings

In the earlier generations, the aircraft wings were straight. However this limited the aircraft in racing at high cruise speeds. In the modern era to overcome this drawback of straight wings, the wings are more commonly angled towards the back of the aircraft and sometimes to the front of the aircraft. When the wings are angled, then the wings are known as Swept wings. The angle at which the wing is tilted is known as Sweep angle. In a straight wing the air flows over the wing in the direction parallel to the chord line of the wing, whereas in a swept wing the amount of air flowing parallel to the chord line is reduced and the remaining part flows perpendicular to the chord line. This flow which is perpendicular to the chord line is called Spanwise Flow. Due to this effect only the amount of air that is flowing parallel to the chord line is accelerated. Hence the aircraft can operate at higher speeds. For the drone being designed we selected an angle of 2^{o}.

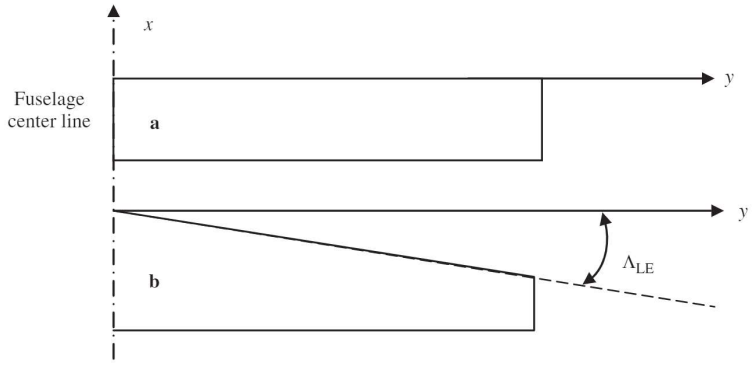

Fig 4.9 - Aircraft Sweep. [42]

4.1.1.3.2 Dihedral Angle

The angle between the chord line plane of a wing with the horizontal plane is known as a dihedral angle. If the wing tip is above the horizontal plane then the angle is known as a positive dihedral angle or simply dihedral angle. If the wing tip is below the horizontal plane then the angle is known as negative dihedral angle or anhedral angle. The main advantage of employing a dihedral angle is that it improves the lateral stability of the aircraft. The disadvantage of dihedral wings is manufacturability. It is hard to manufacture a dihedral wing. Therefore a wing with zero dihedral angle is employed in the drone being designed.

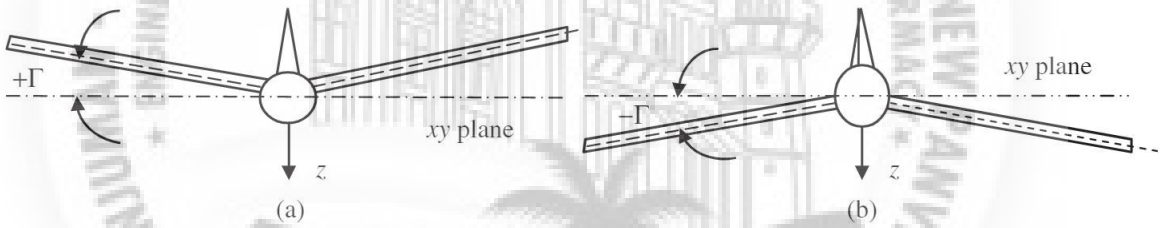

Figure 4.10 - (a) Dihedral angle (b) Anhedral angle. [42]

4.1.1.4 Wing Airfoil Selection

The primary function of the wing is to generate sufficient lift to fly the aircraft. For this purpose, a special cross-sectional shape is introduced in the wing which is known as Airfoil. The process of selection of airfoil is considered to be the second most important step after estimation of wing area. There are two main methods in selecting the suitable airfoil. The first method is to design the airfoil which can be suitable in the application. Designing a custom airfoil is very complex and time consuming. It also needs a higher level of knowledge as well as expertise in the fundamentals of aerodynamics. The other method is to select an existing airfoil. There are various types of airfoils available such as symmetrical airfoil, non-symmetrical airfoil, high lift airfoil, flat bottom airfoil, etc. All these airfoils

have unique features. Based on the application the suitable airfoil is selected from the list of available airfoils. The airfoil selected for this project is Clark y airfoil which is a flat bottom airfoil. Using this airfoil, the wing can be manufactured more easily than the other airfoils. The detailed analysis on airfoil is given in the further sections.

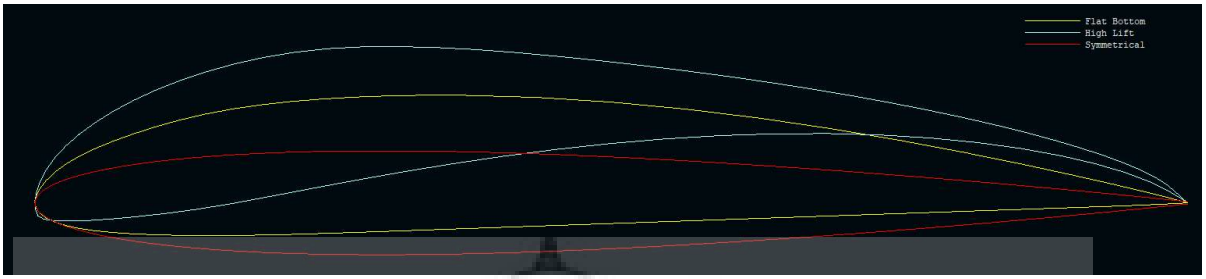

Fig 4.11 - Symmetrical (NACA 0009), High Lift (S1223) and Flat Bottom airfoils.(Clark Y)

4.1.1.5 Wing Parameters

After the suitable airfoil is selected, the next step is to determine the various wing parameters like Aspect Ratio (AR), Taper angle (λ), Wing incidence or Angle of Attack (i_W) and Wing Twist (α_t). All these parameters are very important in a stable wing design. These parameters are elaborated in the further sections.

4.1.1.5.1 Aspect Ratio (AR)

The wing has two major dimensions which are wingspan (s) and the mean aerodynamic chord or MAC (C bar). These dimensions derive the various wing parameters. The ratio of the wing span to the mean aerodynamic chord is known as the aspect ratio.

$$AR = \frac{b}{MAC} \qquad \text{… (eq 4.1)}$$

Aspect ratio is used to predict the aircraft aerodynamic performance and efficiency as the Lift-to-drag ratio increases with increase in AR. This improves the economy of the aircraft. The suitable aspect ratio of the wing is selected based on the purpose of the aircraft. Wings with high AR have a larger wingspan which increases the total lift generated by the wing. Having a higher AR also helps in improving the endurance of the aircraft. The downside is that the main spar of the wing should have a higher structural strength. High AR wings are employed in Gliders as they require longer endurance. Low AR wings have a shorter wingspan. It increases the maneuverability of the aircraft at the expense of lift generated. Low AR wings generated more drag as compared to wings with high AR. Generally fighter jets have a lower AR as they require more maneuverability. In passenger airlines, the aircraft have a medium AR to minimise the drag production and to have sufficient maneuverability.

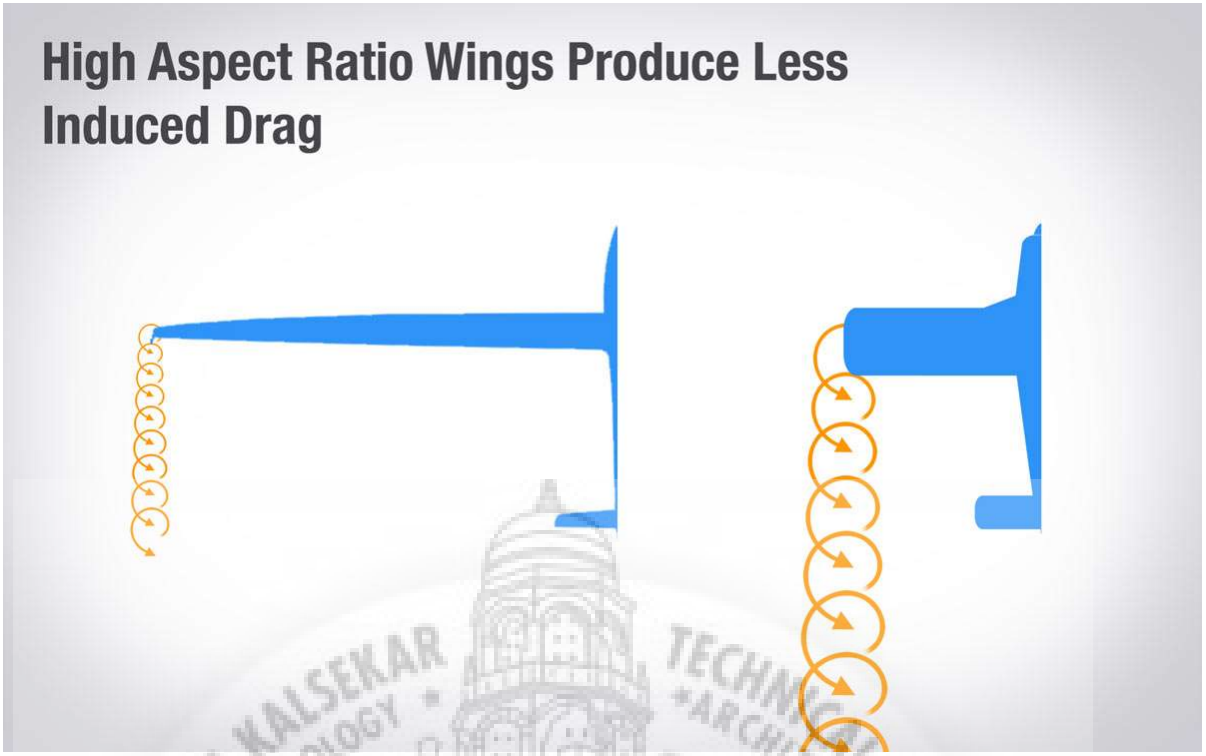

Fig 4.12 - High aspect ratio. (left) , Low aspect ratio. (right)

4.1.1.5.2 Taper Ratio (λ)

In the earlier generation aircrafts, wings were designed as straight wings. The main factor in implementing this type of design was the manufacturability of the wing. Straight wings are easy to manufacture. As these wings are straight, the root chord is equal to the tip chord. This causes a higher amount of drag to be generated by the wing, which in turn decreases the efficiency of the wing. In modern aircraft in order to reduce the drag generated by the wing, the tip chord is smaller than the root chord. Such wings are known as Taper wings. The ratio Tip Chord (C_T) to the Root Chord (C_R) is known as the Taper Ratio of the wing.

$$\lambda = \frac{C_T}{C_R} \quad \text{… (eq 4.2)}$$

The taper ratio ranges between zero to one.

$$0 < \lambda < 1$$

If the taper ratio (λ) is zero, it signifies that the wing is a straight wing. Rectangular wings are not aerodynamically efficient as the angle of downwash is larger at the tip than at the root. Due to this change in the downwash angle, the angle of attack at the tip of the wing decreases. This reduces the lift generated at the wing tip. Therefore the spanwise lift distribution is not elliptical. This also increases the induced drag. When the value of taper ratio (λ) lies between zero and one, the wing is known as tapered wing. The main advantage

of a tapered wing over the fixed wing is that it minimises the drag induced by the wing. Tapered wings tend to have a lower angle of attack of stall at the tip of the wing. This results in the wing tip stalling before the root. It affects the lateral stability of the aircraft. On the other hand, the spanwise lift distribution of the tapered wing is near to elliptical. If the taper ratio is one, the wing is said to be a Delta wing. This wing looks like a triangle with a large root chord and point at the tip. These wings are proven useful for high speed flights. The Delta wing improves the maneuverability of the aircraft.

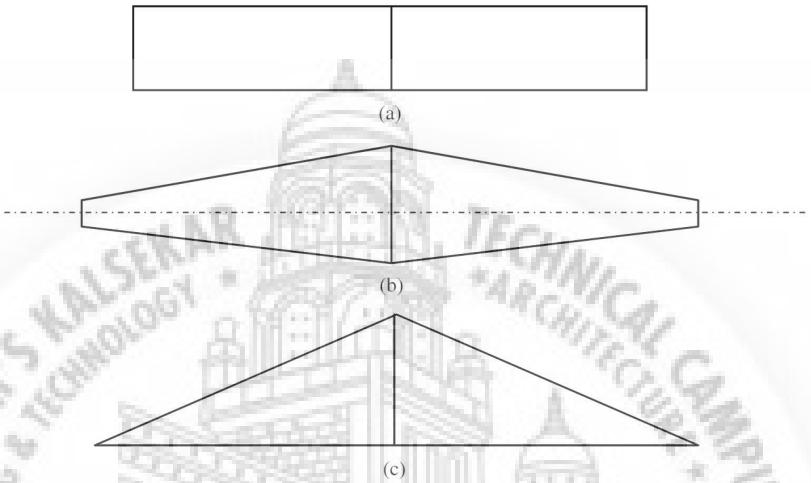

Fig 4.13 - (a) Straight wing. (b) Tapered wing. (c) Delta wing. [42]

4.1.1.5.3 Wing Incidence (i_W) or Angle of Attack

The angle between the fuselage centre line and the chord line of the wing is known as the Wing Incidence or Angle of Attack (AOA). If this angle is set to zero, due to the aerodynamic structure of the wing, some amount of lift will be generated. If the lift generated is not sufficient, the angle is increased. On increasing the incidence angle, the lift is increased significantly. However, at a certain incidence angle, the lift will start to decrease and drag increases. This point is known as a stall point. The angle at which the aircraft stalls is known as the Critical Angle of Attack. Therefore, the value of AOA is selected lower than the critical angle. The critical angle can be estimated by plotting a graph of Coefficient of Lift (C_L) versus Angle of Attack (α). For the drone designed in this project, the zero incidence angle has been selected. It was selected on the basis of lift calculation and also considering the manufacturability of the wing.

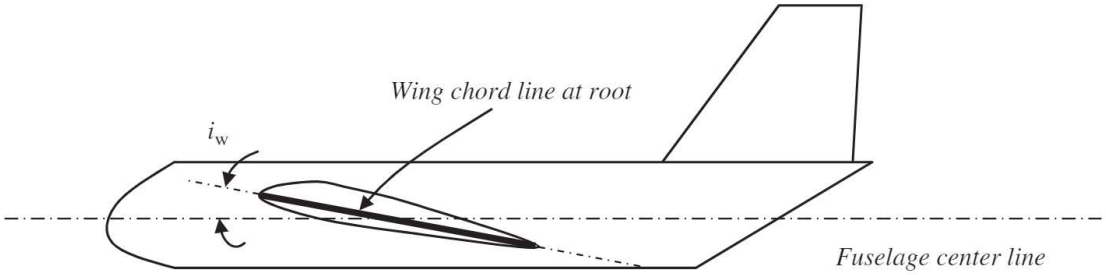

Fig 4.14 - Wing Incidence angle. (i_W) [42]

4.1.1.5.4 Wing Twist Angle

When the angle of incidence of the wing tip varies from the angle of incidence of the wing root, then the wing is known as a twist wing. If the angle of incidence at the wing tip is lower than the angle of incidence at the root, then the wing is set to have a negative twist or twist. Whereas if the angle of incidence at the root is smaller than the angle of incidence at the wing tip then the wing is considered to have a positive twist or wash-in. Generally a washout type of wing is used in most aircrafts. In negative twist wings the angle of attack decreases along the wing span. This reduces the amount of lift generated along the wing span. Hence, it helps in making the lift distribution along the wing span more elliptical. This helps in increasing the stability of the aircraft. The major disadvantage of twist wing aircraft is manufacturability. Therefore, for the drone being designed, a wing with zero twist angle is employed. The wing is designed to have a taper ratio to compensate for the spanwise lift distribution.

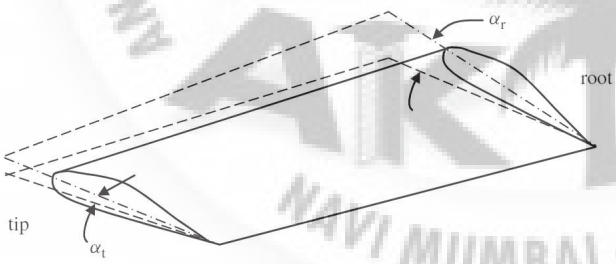

Fig 4.15 - Twisted wing. [42]

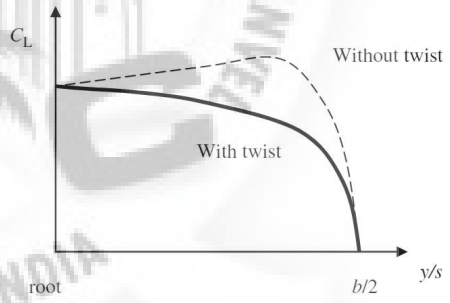

Fig 4.16 - Lift distribution of Twist wing. [42]

4.1.1.6 Lift Drag and Pitching Moment Calculation

Calculation of Lift (L), Drag (D) and Pitching Moment (M) are the most fundamental and important calculations for designing an efficient and stable wing. Lift (L) can be defined as the total upward force that is generated by the wing when the air flows over it. This force is produced as a result of the pressure difference generated by the aerodynamic structure of the airfoil. Drag (D) is the force generated by the wing in the horizontal plane along the direction of the air flow. It is produced due to the vortex generation by the wing. For an efficient wing

Lift (L) should be maximum while Drag (D) should be minimum. Pitching Moment (M) is the moment of the wing about the quarter of the chord. Pitching moment helps in determining the stability of the aircraft.

The formulas for Lift (L), Drag (D) and Pitching moment (M) are given below.

Lift (L)

$$L = C_L \times \frac{\rho \times V^2}{2} \times S \quad \text{... (eq 4.3)}$$

Drag (D)

$$D = C_D \times \frac{\rho \times V^2}{2} \times S \quad \text{....(eq 4.4)}$$

Pitching Moment (M)

$$M = C_M \times q \times S \quad \text{...(eq 4.5)}$$

where,

C_L - Coefficient of Lift

C_D - Coefficient of Drag

C_M - Coefficient of Moment

ρ - Air Density

V - Air Velocity

S - Wing Surface Area

q - Dynamic Pressure

4.1.2. Airfoil Selection

For instance, subsonic flight design requirements are very much different from supersonic flight design objectives. In contrast, flight in the transonic region requires a special airfoil that meets Mach divergence requirements. The designer must also consider other requirements such as airworthiness,structural, manufacturability, and cost requirements. In general, the following are the criteria to select an airfoil for a wing with a collection of design requirements:

1. The airfoil with the highest maximum lift coefficient (Clmax).
2. The airfoil with the proper ideal or design lift coefficient (CldorCli).
3. The airfoil with the lowest minimum drag coefficient (Cdmin).
4. The airfoil with the highest lift-to-drag ratio ((Cl/Cd)max).
5. The airfoil with the highest lift curve slope (Clαmax).

6. The airfoil with the lowest (closest to zero; negative or positive) pitching moment coefficient (Cm).
7. The proper stall quality in the stall region (the variation must be gentle, not sharp).
8. The airfoil must be structurally reinforceable. The airfoil should not be so thin that spars cannot be placed inside.
9. The airfoil must be such that the cross-section is manufacturable.
10. The cost requirements must be considered.
11. Other design requirements must be considered. For instance, if the fuel tank has been designated to be placed inside the wing inboard section, the airfoil must allow sufficient space for this purpose.

The practical steps that are followed in selection of the airfoil is given in the following

Calculation of ideal cruise lift coefficient (C_{LC}).

$$C_{L_C} = \frac{2 \times W_{TO}}{\rho \times V_C^2 \times S} \quad \ldots \text{(eq 4.6)}$$

where, W_{TO} = Take Off Weight

ρ = Density of air

V_C^2 = Cruise velocity

S = Projected Surface area

Substituting the variables in above equation we get,

$$C_{L_C} = \frac{2 \times 12 \times 9.81}{1.225 \times 26^2 \times 0.94} = 0.3024 \quad \ldots \text{(eq 4.7)}$$

Calculation of wing cruise lift coefficient (C_{LCW})

$$C_{L_{C_W}} = \frac{C_{L_C}}{0.95} = \frac{0.3024}{0.95} = 0.3183 \quad \ldots \text{(eq - 4.8)}$$

Calculation of wing airfoil ideal lift coefficient (C_{Li})

$$C_{Li} = \frac{C_{L_{C_W}}}{0.9} = \frac{0.3183}{0.9} = 0.3536 \quad \ldots \text{(eq 4.9)}$$

Calculation of aircraft maximum lift coefficient (C_{Lmax})

$$C_{L\,max} = \frac{2 \times W_{TO}}{\rho \times V_S{}^2 \times S} \quad \text{... (eq 4.10)}$$

Where, V_s = Stall speed

Substituting the variables in above equation we get,

$$C_{L\,max} = \frac{2 \times 12 \times 9.81}{1.442 \times 13^2 \times 0.94} = 1.2098 \quad \text{... (eq 4.11)}$$

Calculation of wing maximum lift coefficient ($C_{L\,max\_w}$)

$$C_{L\,max_w} = \frac{C_{L\,max}}{0.95} = \frac{1.2098}{0.95} = 1.2734 \quad \text{... (eq 4.12)}$$

Calculation of wing airfoil gross maximum lift coefficient ($C_{l\,max\_gross}$)

$$C_{L\,max_{gross}} = \frac{C_{L\,max_w}}{0.9} = \frac{1.2734}{0.9} = 1.4148 \quad \text{...(eq 4.13)}$$

Calculation of wing airfoil net maximum lift coefficient ($C_{l\,max}$)

$$C_{l\,max} = C_{L\,max_{gross}} - \Delta C_{L_{HLD}} \quad \text{... (eq 4.14)}$$

Where, $C_{L\,HLD}$ = Coefficient of lift of High Lift Devices

As there are no High Lift Devices employed in the drone, we can assume $C_{L\,HLD}$ as zero. Therefore substituting the same in above equation, we can conclude that

$$C_{l\,max} = C_{L\,max_{gross}} = 1.4148 \quad \text{....(eq 4.15)}$$

After observing the above calculations, we can conclude that, for a stable and efficient fight we will have to select an airfoil which should have $C_{L\,i}$ equal to or approximately 0.3536 and $C_{l\,max}$ equal to or approximately 1.4148. Based on the conclusion three airfoils are selected which are Clark Y, NACA 3411 and NACA 2412. A detailed performance comparison of these airfoils is done in the further section.

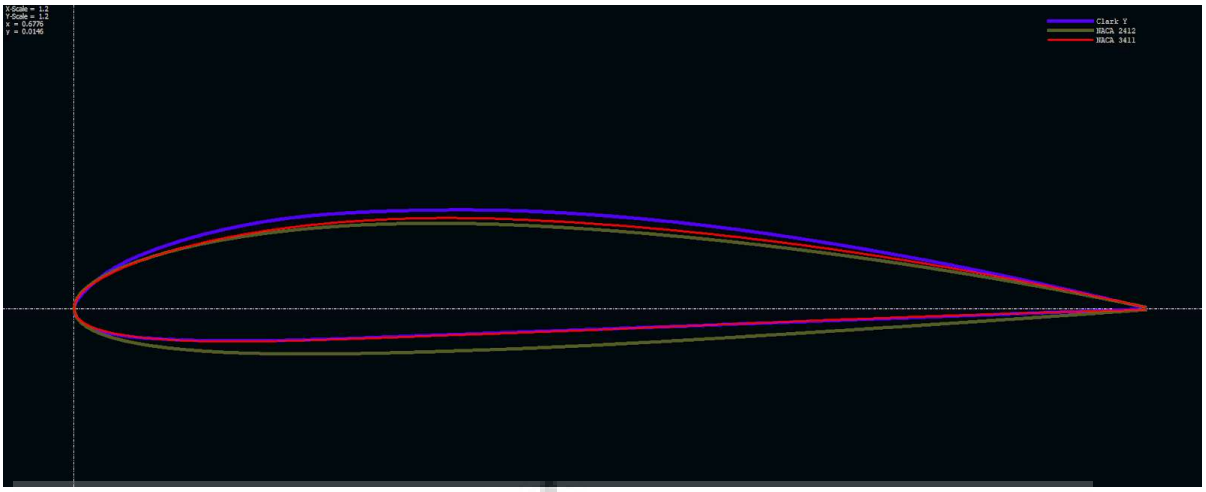

Fig 4.17 - Clark Y. (purple) , NACA 3411. (red), NACA 2412. (green)

Comparison between Clark Y, NACA 3411 and NACA 2412

Reynolds Number Range - Re_{min} = 10,000 Re_{max} = 900,000

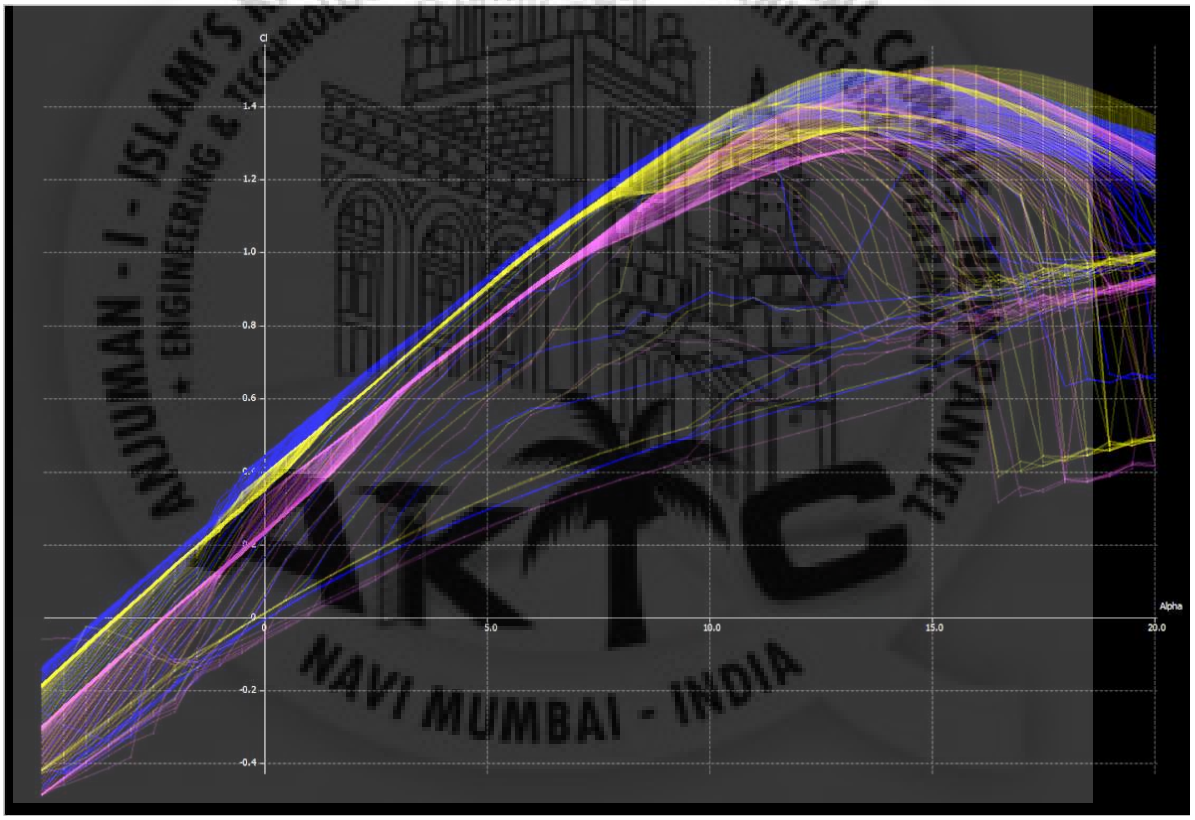

Fig 4.18 - Graph of Coefficient of Lift (C_L) versus Angle of Attack. (α)

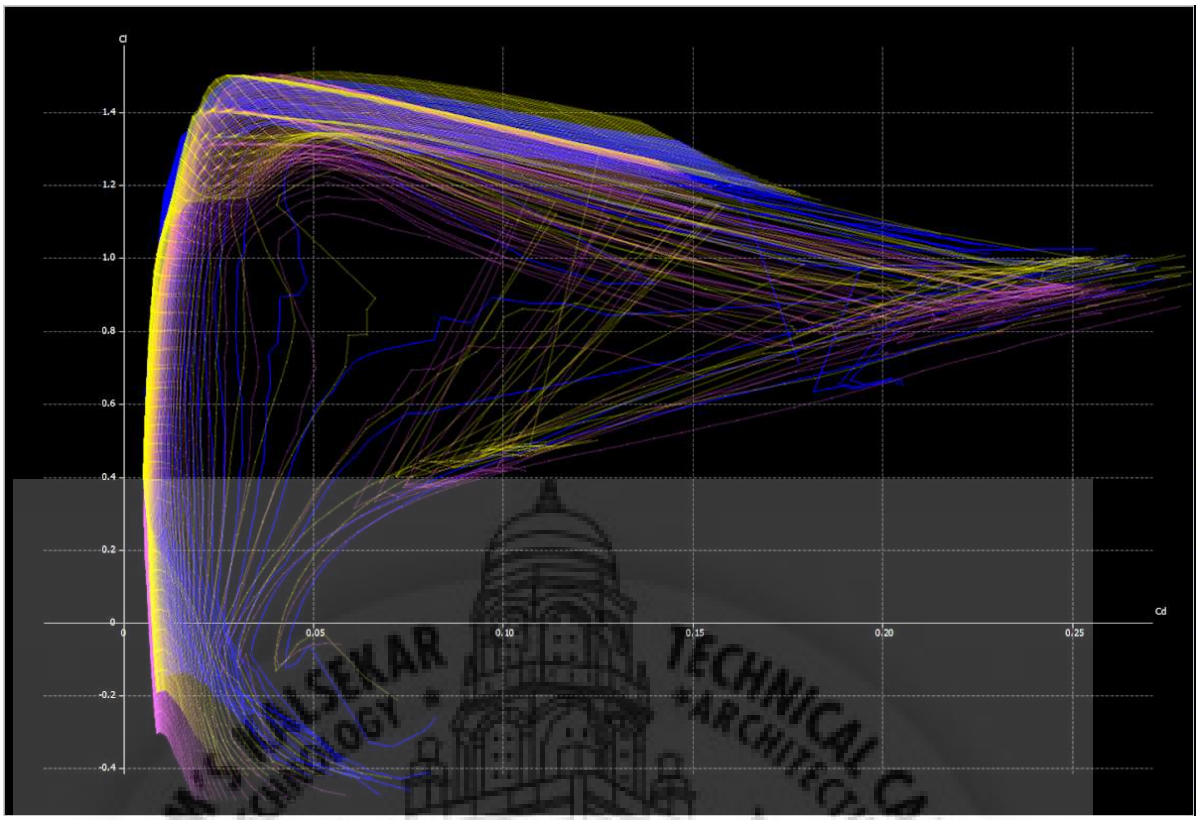

Fig 4.19 - Graph of Coefficient of Lift (C_L) versus Coefficient of Drag. (C_D)

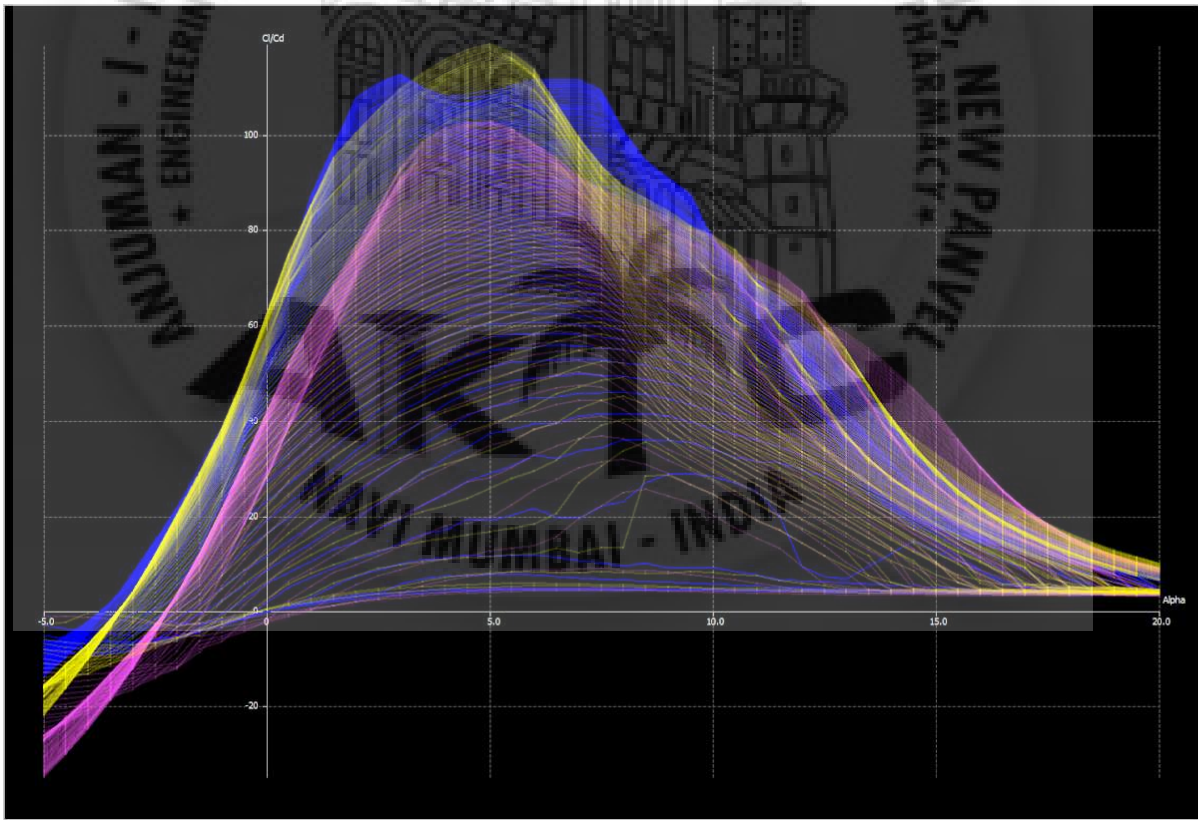

Fig 4.20- Graph of Ratio of Coefficient of Lift to Coefficient of Drag (C_L / C_D) versus Angle of Attack. (α)

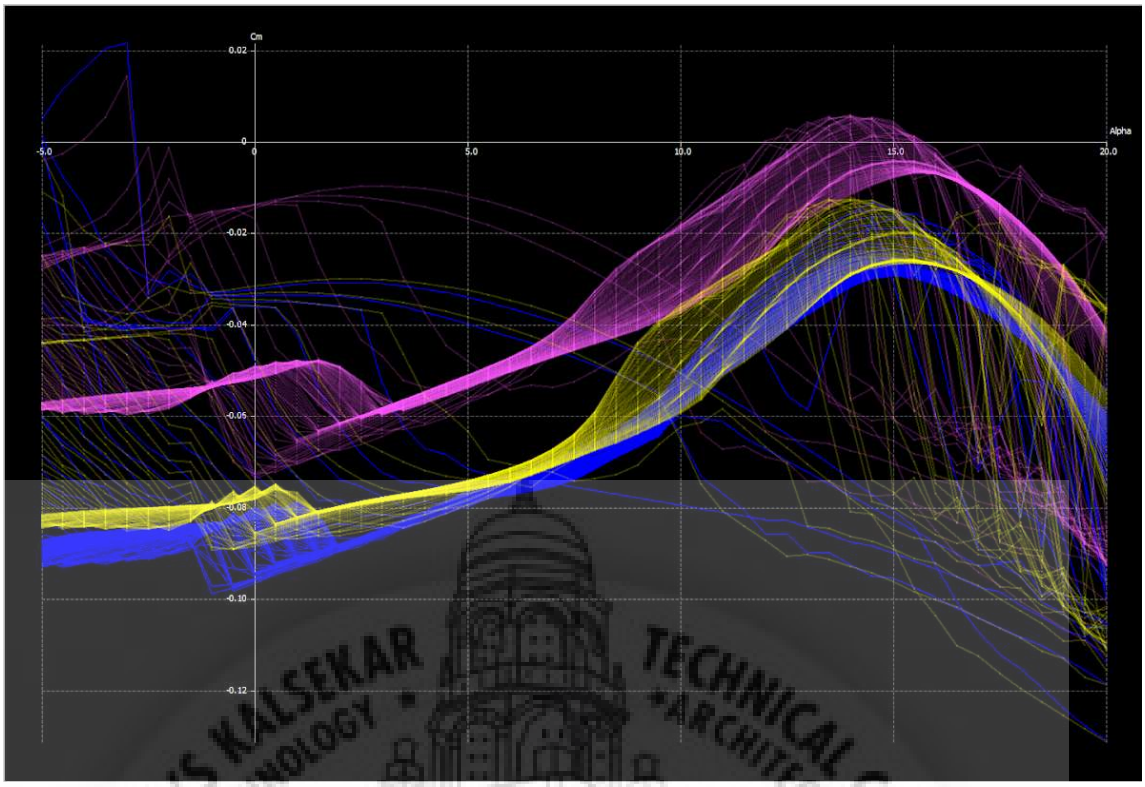

Fig 4.21 - Graph of Pitching Moment (C_M) versus Angle of Attack. (α)

By analysing the mission profile, it is observed that the drone will be operating in Cruise Fight. Hence, the Reynolds Number at Cruise speed (V_C) is calculated which is approximately 600,000. Therefore, the performance characteristics during cruise flight are shown in the following graphs.

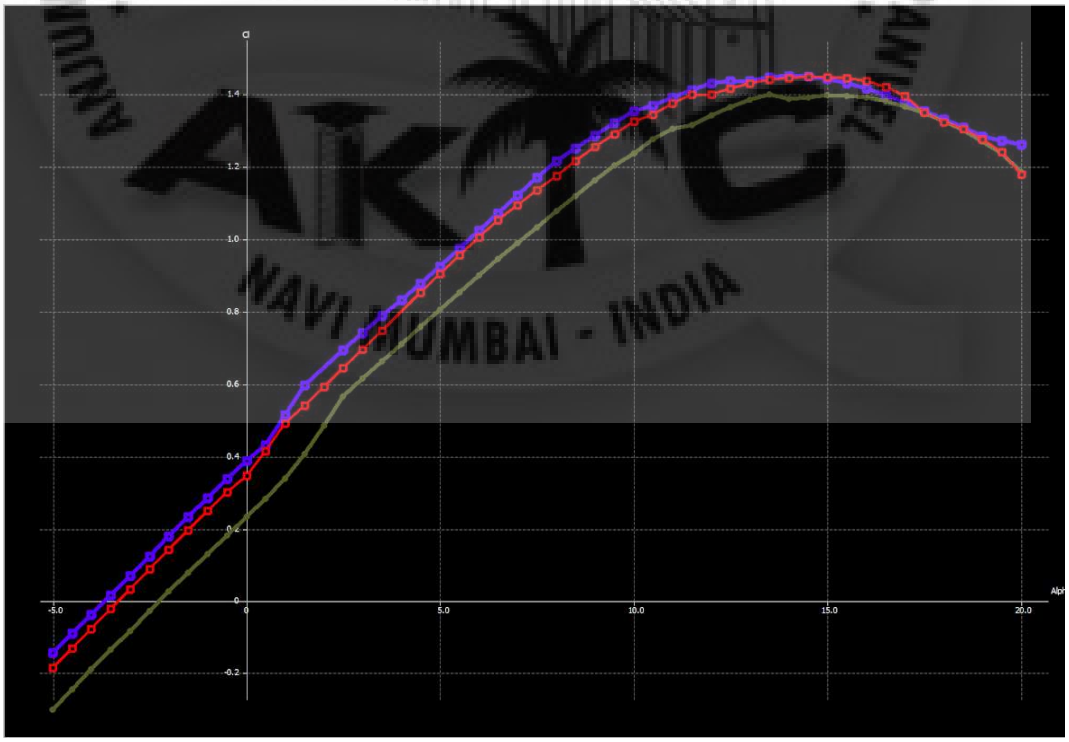

Fig 4.22 - Graph of Coefficient of Lift (C_L) versus Angle of Attack (α) at Re = 600,000

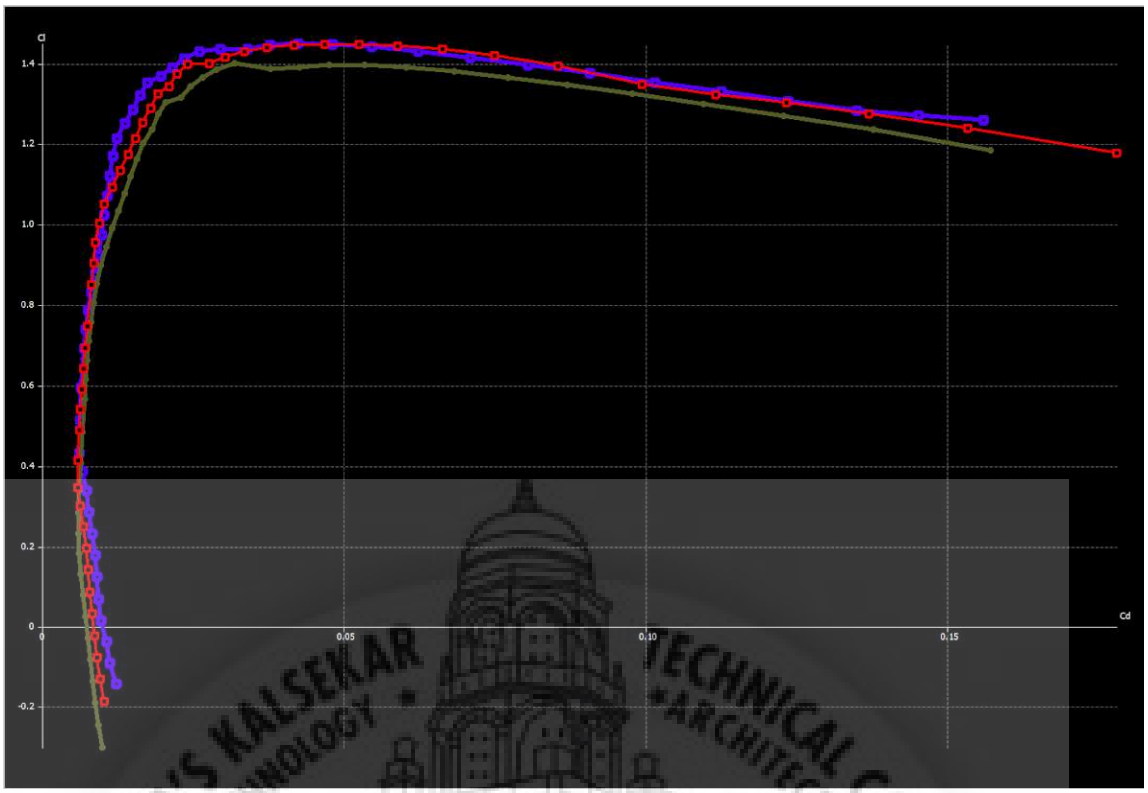

Fig 4.23 - Graph of Coefficient of Lift (C_L) versus Coefficient of Drag (C_D) at Re = 600,000

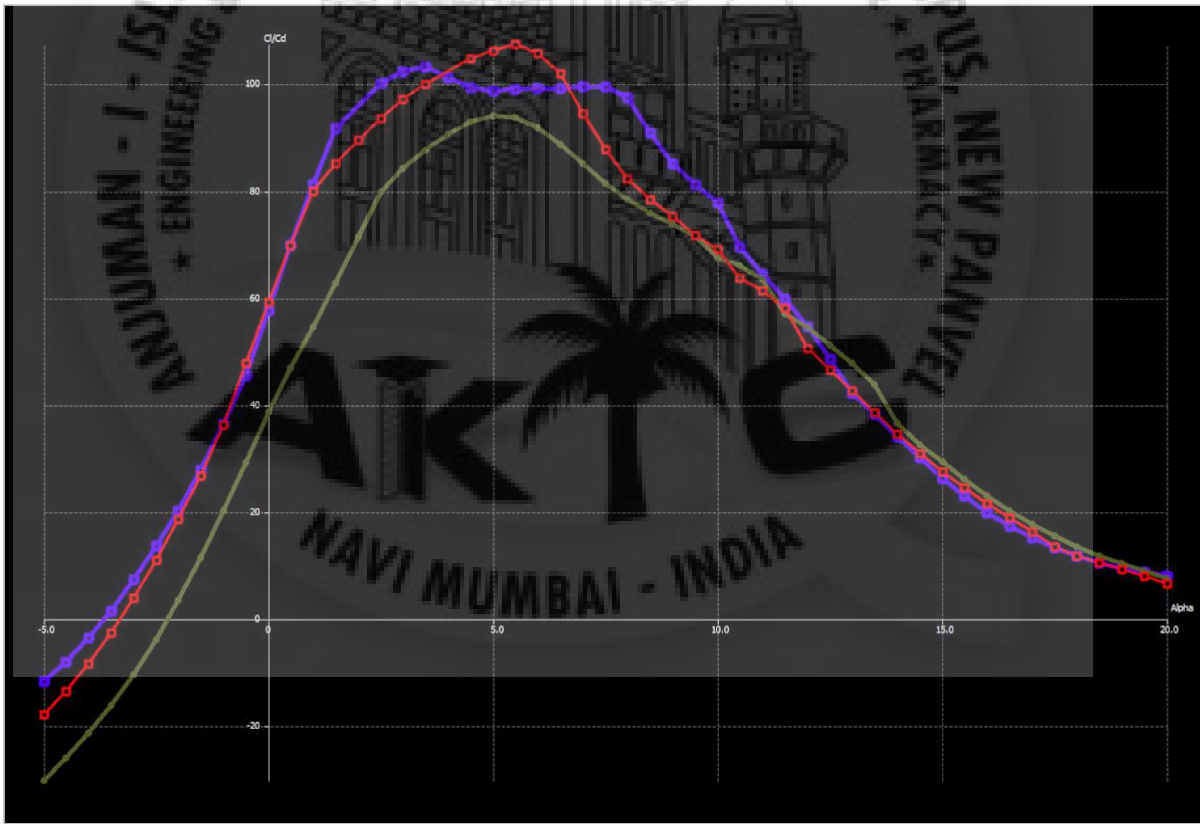

Fig 4.24 - Graph of Ratio of Coefficient of Lift to Coefficient of Drag (C_L / C_D) versus Angle of Attack (α) at Re = 600,000

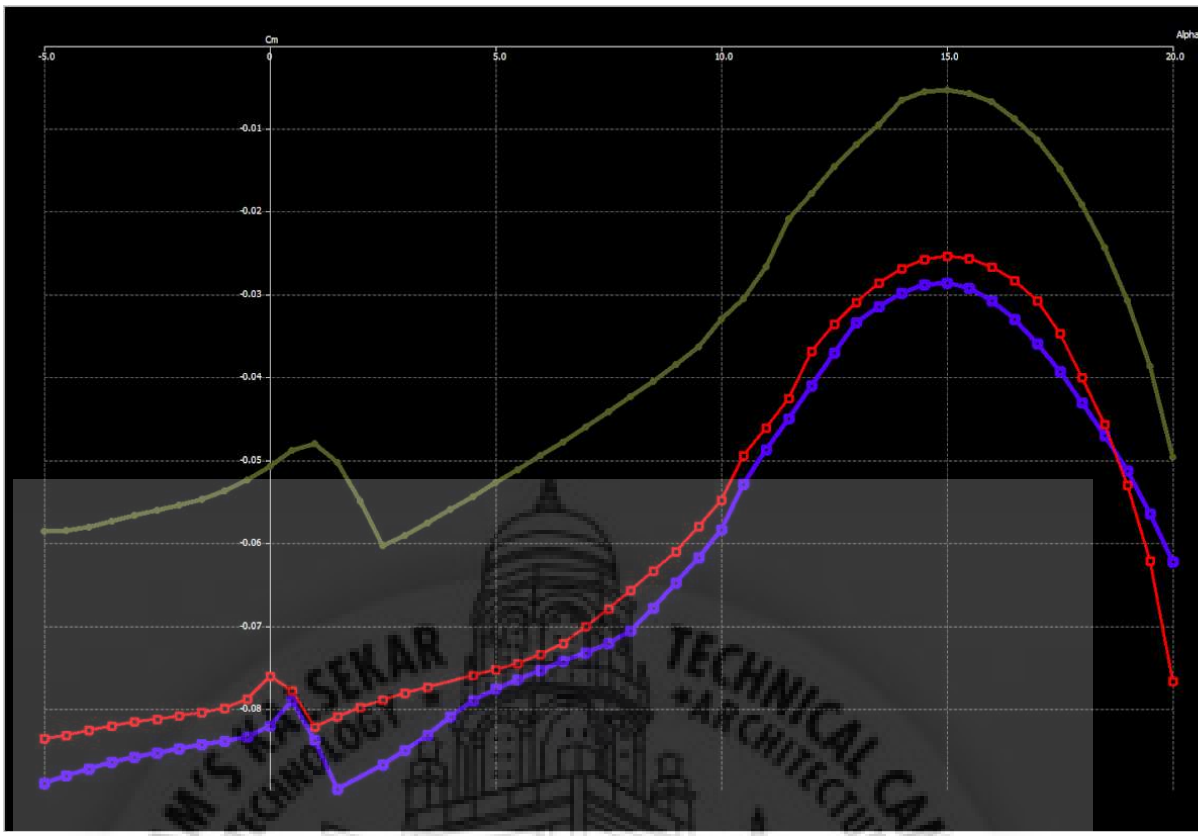

Fig 4.25 - Graph of Pitching Moment (C_M) versus Angle of Attack (α) at Re = 600,000

The following table is prepared based on the performance characteristics obtained from the graphs and calculations.

Table 4.2 - Airfoil Performance

Sr. No	Airfoil	$C_{l\,max}$	$C_{d\,min}$	C_d at C_l=0.3	α_s	C_{mo}	C_l/C_d max	Stall quality	Manufacturability
1.	Clark Y	1.45	0.0063	0.0077	7.48	-0.089	103.23	Docile	High
2.	3411	1.44	0.0058	0.0063	5.49	-0.082	107.41	Sharp	Medium
3.	2412	1.4	0.006	0.006	5.5	-0.06	93.899	Moderate	Low

A trade study is conducted for selecting the appropriate airfoil from the selected airfoils. The trade study is given in the below.

Table 4.3 - Airfoil Selection Trade Study

Sr.No	Parameters	Score	Clark Y	NACA 3411	NACA 2412
1.	Cl max	20	20	18	15
2.	Cd min	5	3	4	5
3.	Cd at Cl = 0.3	5	3	4	5
4.	Alpha s	5	5	3	3
5.	Cmo	5	2	4	5
6.	Cl/Cd max	20	4	5	2
7.	Stall quality	20	20	15	10
8.	Manufacturability	20	20	15	5
	Total	100	11	68	50

From the trade study we can conclude that Clark Y is the appropriate airfoil for the drone that is designed. Clark Y airfoil has a docile stall quality. The main advantage of Clark Y is manufacturability as it is a flat bottom airfoil

4.1.3 Wing Sizing

4.1.3.1 Wing Planform Area

Wing Planform area is the area of the wing when viewed from the top. Wing planform is the most important variable that is to be determined. For the drone being designed we have selected a root chord C_R as 400 mm and tip chord C_T as 250 mm. As the tip chord is smaller than the root chord, the wing is a trapezoidal wing. Therefore calculating the area of trapezoid is given in equation 4.15

$$S = \frac{1}{2} \times \left(C_T + C_R \right) \times 2b = \frac{1}{2} \times (0.25 + 0.4) \times 2 \times 1.4 = 0.91\ m^2 \quad \text{...(eq 4.16)}$$

The following figure (4.26) shows the basic dimensions of the wing.

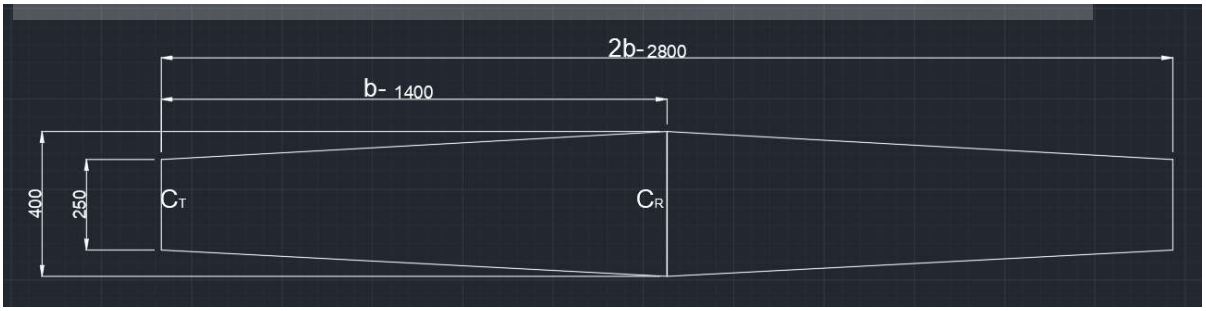

Fig 4.26 - Wing dimensions.

4.1.3.2 Taper Ratio (λ)

From figure 4.26 we can identify the root chord C_R as 0.4 m and tip chord C_T as 0.25 m. Hence we can calculate the taper ratio of the wing by

$$\lambda = \frac{C_T}{C_R} = \frac{0.25}{0.4} = 0.625 \qquad \text{...(eq 4.17)}$$

As the taper ratio is less than 1 we can say that the wing is a tapered wing.

4.1.3.3 Aspect Ratio (AR)

Figure 4.26 shows the principal dimensions of the wing. From the figure we can observe that the root chord C_R is 0.4 m and tp chord C_T is 0.25 m. Therefore we can find the Mean Aerodynamic Chord (MAC) by

$$MAC = C_R \times \frac{2}{3} \times \left(\frac{1+\lambda+\lambda^2}{1+\lambda} \right) = 0.4 \times \frac{2}{3} \times \frac{1+0.625+0.625^2}{1+0.625} = 0.3307\ m \qquad \text{...(eq 4.18)}$$

After calculating the Mean Aerodynamic Chord (MAC) we can calculate the Aspect Ratio (AR) by using the formula for Aspect Ratio. The wing span (2b) of the aircraft is 2.8 m

$$AR = \frac{2b}{MAC} = \frac{2 \times 1.4}{0.3307} = 8.46 \qquad \text{...(eq 4.19)}$$

4.1.3.4 Wing Dimensions

Table 4.4 - Wing Dimensions

	Parameters	Values
1.	Root Chord (C_R)	0.4 m
2.	Tip Chord (C_T)	0.25 m
3.	Wing span (2b)	2.8 m
4.	Taper ratio (λ)	0.625
5.	Wing planform Area (S)	0.91 m^2
6.	Mean Aerodynamic Chord (MAC)	0.3307 m
7.	Aspect ratio (AR)	8.46
8.	Wing twist angle (αt)	0^o

4.1.4 Lift Calculation and Drag Calculation

The lift and drag generated by the wing was calculated using XFLR5 and ANSYS. The output of XFLR5 gives theoretical results. On the other hand ANSYS can give results which are closer to practical results. A fair amount of analysis was conducted to find the approximate values of lift and drag that is produced by the wing. All the results are combined in figure 4.28 and then observed.

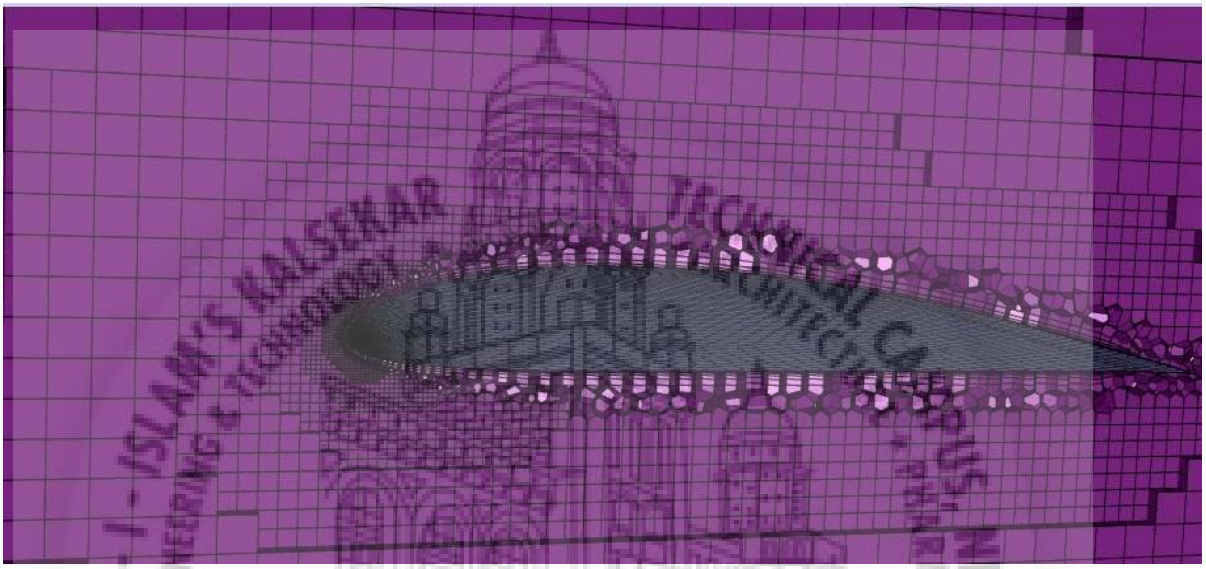

Figure 4.27 - Poly - Hexa Core Mesh in ANSYS Fluent with Meshing Package.

A 3D CAD model of the wing was constructed in Solidworks and Fusion 360. This CAD model was then imported into ANSYS Space claim to create an enclosure and named sections. An enclosure was constructed with the appropriate size. All the necessary named selections were added in Space claim. This Spaceclaim file was then imported into ANSYS 'Fluent with meshing' package. A mesh was generated of the enclosure in Fluent meshing. The type of mesh selected is Poly-Hexa Core mesh. An image of the mesh is shown in figure 4.27. All the boundary conditions like Inlet velocity of 26 m/s which is cruise speed of the aircraft and outlet pressure of 1 bar were set. The analysis was then conducted with the mathematical model as K - Omega SST. The result of the analysis was then plotted on a graph in figure 4.28.

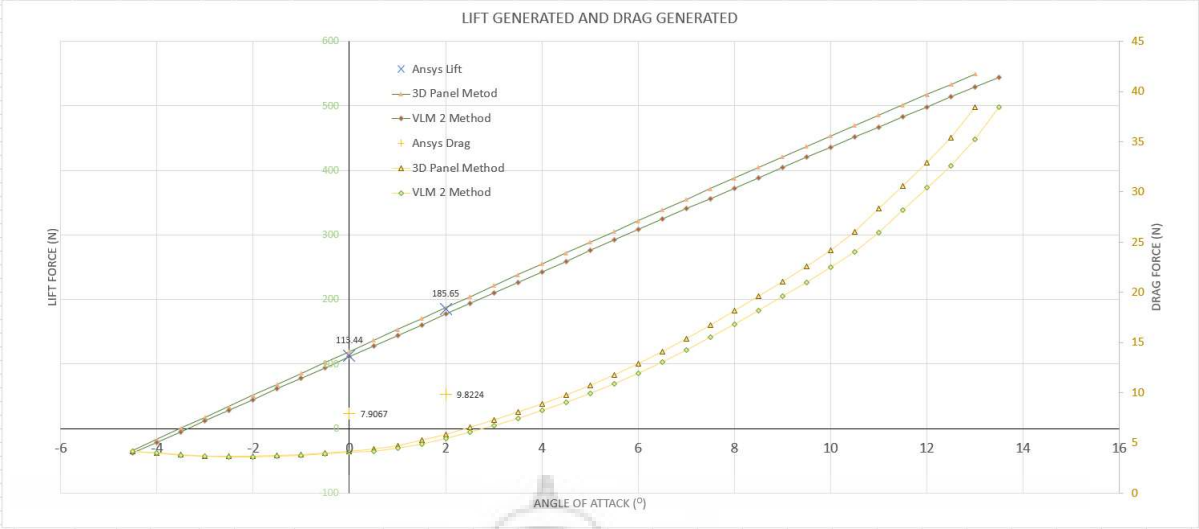

Figure 4.28 - Graph of Lift and Drag generated by XFLR5 and ANSYS.

In figure 4.28, 3D Panel Method and VLM 2 Methods are solved in XFLR5. We can consider the values generated by XFLR5 as theoretical values. The "X" marked values are the values of lift generated and '+' marked values are the values of the drag generated by ANSYS. We can conclude that the values obtained from ANSYS are acceptable as they are close to the theoretical values. The values of lift and drag we obtained are given below in table 4.5 and table 4.6

Table 4.5 - Lift generated in (N)

Angle of Attack (α)	VLM 2 Method	3D Panel Method	ANSYS
0	111.2487	119.6952	113.4404
2	117.3381	187.6386	185.6502

Table 4.6 - Drag generated in (N)

Angle of Attack (α)	VLM 2 Method	3D Panel Method	ANSYS
0	4.0461	4.1896	7.9067
2	5.4464	5.8533	9.8224

The results from ANSYS Fluent are then passed to CFD Post Processing. CFD Post Processing helps in visualizing the flow characteristics of fluid. Figure 4.29 is a display of CFD Post Processing. From the figure 4.29 we can observe the flow of air over the wing. As the wing has an airfoil cross section, the velocity of air flowing above the wing surface is greater than the velocity of air flowing below the wing. This creates a high pressure region below the wing and a low pressure region above the wing. This pressure difference generates a force in the direction perpendicular to the airflow which is known as lift. This pressure difference can be observed from the pressure contour over the wing surface. The difference

in velocity can be seen by observing the pathlines depicting the airflow over the wing. The direction of incident air on the wing and the direction of air leaving the trailing edge is different. This phenomenon is known as a downwash effect. This can be seen by pathlines. We can also observe a vortex generation at the tip of the wing. This vortex generation is a main contributor in the Drag (D) generation.

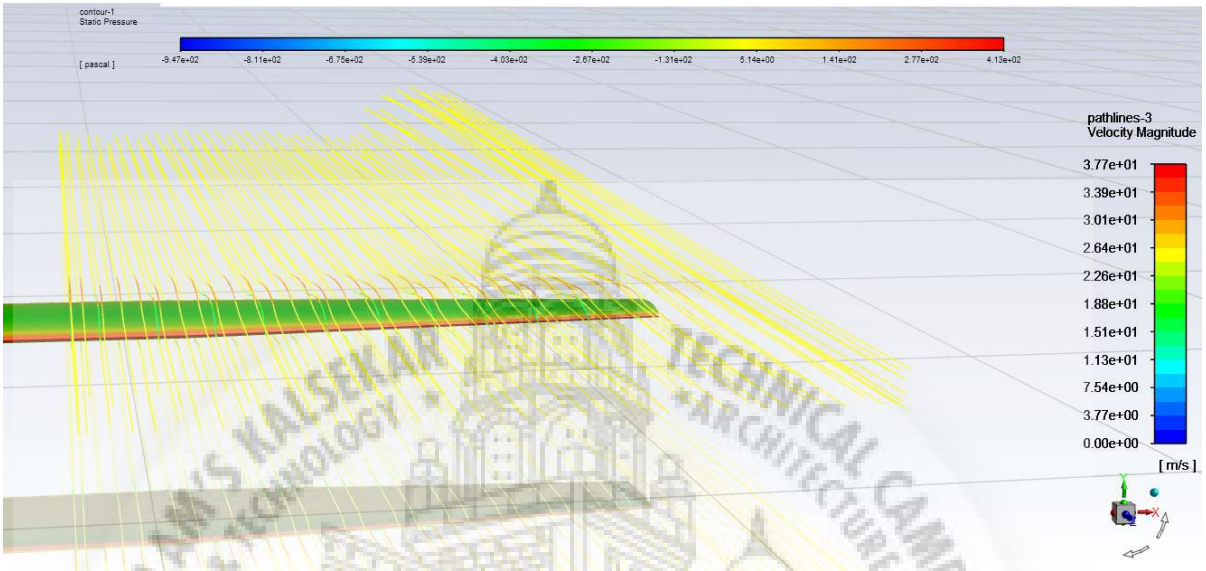

Figure 4.29 - CFD Post Processing.

The same method is used to estimate the Drag force (D) generated by the wing. The estimation of Drag force (D) is also necessary as it is very important in determining the power required by the aircraft. The drag force is increased by the vortex created at the wing tips. From the analysis conducted, the observed values of drag force are given in figure 4.28. From table 4.6 we can observe that the drag values obtained from ANSYS differ from the ones generated by XFLR5. This is because XFLR5 tends to underestimate the drag which is produced by the wing. A pictorial depiction of drag force is shown in figure 4.30.

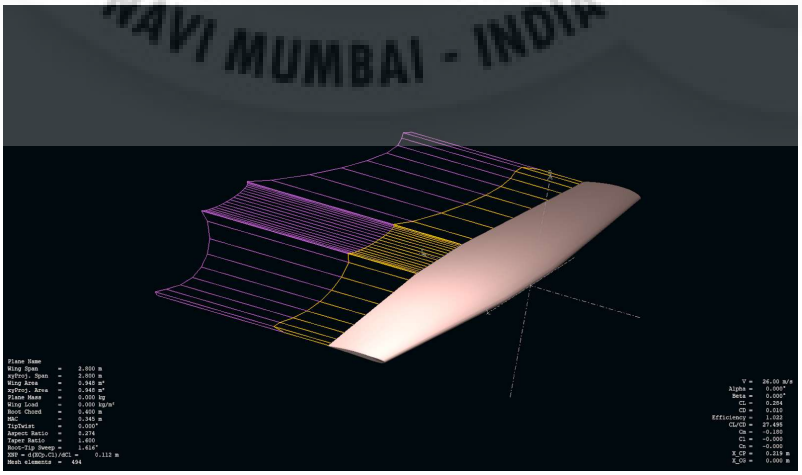

Figure 4.30 - Drag Plot from XFLR5.

4.1.5 Wing Loading

The estimation of wing loading is a very essential part of wing design. The type and dimensions of spar to be used depends on the nature of the wing loading curve. After the analysis of the wing was conducted in XFLR5, a wing loading curve was generated. The wing loading curve is shown in figure 4.31.

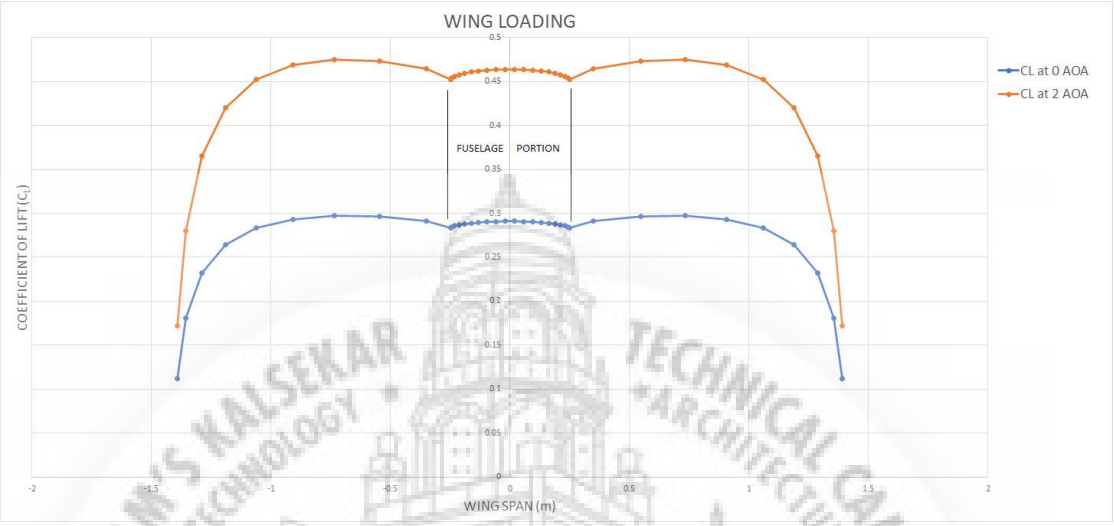

Figure 4.31 - Wing Loading Curve.

From figure 4.31 we can conclude that the lift force that is generated tends to decrease along the span of the wing. This is because of the tapered geometry of the wing. This nature of lift curve is known as an elliptical lift curve. An elliptical lift curve is important from a structural point of view. If the lift curve is not made elliptical it will increase the stresses induced in the spar of the wing.

4.2 Stability

4.2.1 Empennage Design

The empennage is the whole tail unit at the extreme rear of the fuselage and it provides the stability and directional control of the aircraft. Structurally, the empennage consists of the entire tail assembly, including the vertical stabiliser, horizontal stabilisers, rudder and elevators attached to fuselage at the rear section shown in fig 4.32.

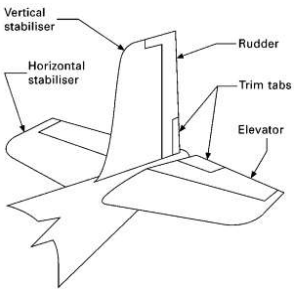

Figure 4.32 - Empennage of an aircraft.

To meet the dual requirement of stability and control there are many different forms of aircraft tail. Most tail designs have a horizontal wing like structure and one or more vertical or near-vertical structures. These structures are identified as the horizontal and vertical stabilizers.

4.2.1.1 Conventional Tail Design

The conventional tail design is the most common form. It has one vertical stabilizer placed at the tapered tail section of the fuselage and one horizontal stabilizer divided into two parts, one on each side of the vertical stabilizer. For many airplanes, the conventional arrangement provides adequate stability and control with the lowest structural weight.

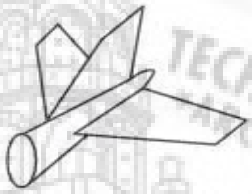

Figure 4.33 - Conventional tail design.

4.2.1.2 The T-Tail Design

In the T-tail design, a common variation of the conventional tail, the horizontal stabilizer is positioned at the top of the vertical stabilizer. The horizontal stabilizer is then above the propeller flow, or prop wash, and the wing wake. Because the horizontal stabilizer is more efficient, it can therefore be made both smaller and lighter. The placement of the horizontal stabilizer on top of the vertical stabilizer can also make the vertical stabilizer more aerodynamically efficient.

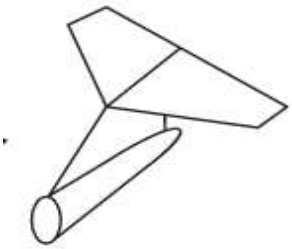

Figure 4.34 - T-Tail design.

4.2.1.3 Cruciform-Tail Design

The cruciform tail is an obvious compromise between the conventional and T-tail designs. In the cruciform design, the horizontal stabilizer is moved part of the way up the vertical stabilizer. In this position, the horizontal stabilizer is moved up and away from the jet exhaust and wing wake. The lifting of the horizontal stabilizer also exposes the lower part of the vertical stabilizer, as well as the rudder, to undisturbed airflow.

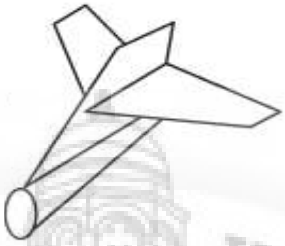

Figure 4.35 - Cruciform Tail design.

4.2.1.4 Twin-Tail Design

A twin tail is an aircraft with a set of two stabilizers mounted vertically on the tail assembly. Aircraft with this configuration are more stable and easier to control. The twin tail design was especially popular during the Second World War and continues to be used in the production of a number of aircraft today, including both small and large planes. One advantage to the twin tail is the ability to control the plane even if one tail becomes compromised. Hence we chose this tail design for our aircraft with split tail as its modification.

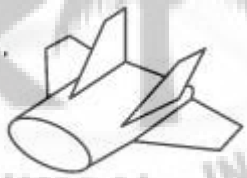

Figure 4.36 - Twin tail design.

The tail in a conventional aircraft has two components, horizontal tail and vertical tail, and carries two primary functions:

1. Trim (longitudinal and directional).

2. Stability (longitudinal and directional).

Since two conventional control surfaces (i.e., elevator and rudder) are indeed parts of the tail to implement control, it is proper to add the following item as the third function of a tail:

3. Control (longitudinal and directional)

4.2.2 Control Surfaces

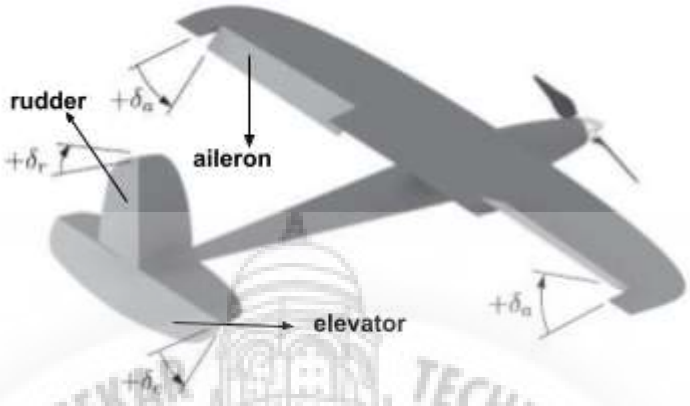

Figure 4.37 - Example for control surfaces.

As the name suggests, control surfaces are surfaces of aircraft which are responsible for the stability control of an aircraft. There are primarily three control surfaces;

i) Aileron which governs the aircraft rolling moment;

ii) Elevator which governs the aircraft pitching moment;

iii) Rudder which governs the aircraft yawing moment.

4.2.2.1 Ailerons

Ailerons control the roll of an aircraft along with directional control. Lateral control is governed by roll rate (P). Ailerons are the structural part of the wing and have two pieces each located at the trailing edge of the outer portion of the wing left and right section. As both the ailerons perform similar functions they are identical in dimensions and geometries.

Mainly four parameters are need to be determined for design of an aileron;

i) aileron planform area (S_a);

ii) aileron chord/span (Ca/ba);

iii) maximum aileron up and down deflection (±δAmax);

iv) location of inner edge of the aileron (b_a).

Design calculations are as follows,

The aileron rolling moment coefficient derivative ($C_{l\delta\alpha}$) is calculated employing equation

$$C_{l_{\delta_a}} = \frac{c_{l_{\delta_a}} C_R}{Sb}\left[\left(b_2^2 - b_1^2\right) + \frac{4(\lambda - 1)}{3b}\left(b_2^3 - b_1^3\right)\right] \quad \text{... (eq 4.20)}$$

where,

Cr = wing root chord = 0.4 m

c_{lda} = wing lift curve slope = 10.950

S = planform area of lifting = 1.175 m^2

b = wing span = 3.5 m

λ = taper ratio = 0.625

b1 = start edge distance of aileron = 1.5 m

b2 = = end edge distance of aileron = 0.839 m

After calculations,

$$C_{l\delta a} = 1.2032 \text{ / rad} \quad \text{...(eq 4.21)}$$

Roll damping calculation,

$$C_{l_p} = -\frac{\left(c_{l_\alpha} + c_{d_o}\right) \cdot C_R b}{24S}\left[1 + 3\lambda\right] \quad \text{...(eq 4.22)}$$

where,

$C_{l\alpha}$ = lift curve slope = 10.950

C_{do} = section drag coefficient = 0.020

Cr = wing root chord = 0.4 m

b = wing span = 3.5 m

S = planform area of lifting = 1.175 m^2

λ = taper ratio = 0.625

After calculations,

$$C_{lp} = -1.6048 \text{ rad/}^o \quad \text{...(eq 4.23)}$$

Now, calculating the steady state roll rate which is given by the equation,

$$p = -\frac{C_{l_{\delta_a}}}{C_{l_p}}\delta_a\left(\frac{2V}{b}\right)$$

…(eq 4.24)

where,

$C_{l\delta a,}$& C_{lp} are taken from equation (4.2.2.2) & (4.2.2.4),

$\delta_a = 15^o$

V = 12m/s

hence, after calculations we get steady-state roll rate as,

$$p = 77.1170\ ^o/s$$

...(eq 4.25)

Geometry of ailerons,

Aileron span = b_a = 1.5-0.839 = 0.67 ≃ 0.7 m

Aileron chord = $C_a = 0.2C_w = 0.2x0.341 = 0.068$ m

Overall planform area of both right and left ailerons is,

$S_A = 2b_AC_A = 2x0.7x0.068 = 0.0952\ m^2$

4.2.2.2 Rudder

Rudders provide the yawing moment to the aircraft. In our design, we have two split tails therefore, we have two rudders incorporated with the two similar elevators. Rudders are moving part of the vertical tail.

Length of vertical tail = 2x0.210 m

Rudder length is calculated as,

Rudder length = 90% of vertical tail length = 0.9x0.210 m= 0.189 m

Calculating surface area of vertical tail which is given by vertical tail volume coefficient,

$$\overline{V}_v = \frac{l_v S_v}{bS}$$

...(eq 4.26)

where,

V_v = Typical value of vertical tail volume coefficient = 0.07

l_v = distance between the vertical tail aerodynamic center (acv) and the wing/fuselage aerodynamic center = 1.0115 m

b = wing span = 3.5 m

S = wing planform area = 1.1375 m^2

After calculation we get vertical tail surface area as,

S_v = 0.2755

4.2.2.3 Elevators

Elevators provide the pitching moment to the aircraft. For complete stability and design easiness we have kept all moving elevators.

Horizontal tail span = 1.306 m

Horizontal tail area = 0.2615 m^2

4.2.3 Static Stability

Stability and Control are two important aspects for safe flight of any aircraft. Stability is basically the tendency of an aircraft to stabilize itself and resist the disturbances caused by gust or turbulence and return to its normal steady-state condition. Stability is divided into sub parts:

The aircraft flight motion has 6 degrees of freedom (6DOF) about three axes x,y,z, hence stability is measured about three axes:

Lateral stability;Longitudinal stability;Directional stability.

Longitudinal stability deals with a motion in pitch and dynamic variation of the pitching moment with respect to angle of attack (α) hence, Cmα is the derivative which determines the longitudinal stability and Cmq influences the longitudinal stability.[4]The derivative Cmα is the rate of change of the pitching moment coefficient (Cm) with respect to change in the angle of attack (α). The derivative Cmq is the rate of change of pitching moment coefficient (Cm) with respect to the change in pitch rate (q).

$$C_{m_\alpha} = \frac{\partial C_m}{\partial \alpha}$$
$$C_{m_q} = \frac{\partial C_m}{\partial q}$$

…(eq 4.25 & 4.26)

4.2.4 Dynamic Stability

Dynamic stability is the tendency of an aircraft to return to its steady-state trim conditions after disturbances disturb the trim values.

The directional stability is mainly concerned with motion in yaw, so the pertinent dynamic characteristic is the variation of the yawing moment with respect to the sideslip angle (β).

The primary stability[4] derivative that determines the static directional stability is Cnβ. Moreover, the primary stability derivative that influences the dynamic directional stability is Cnr. The derivative Cnβ is the rate of change of yawing moment coefficient (Cn) with respect to change in the sideslip angle (β). The derivative Cnr is the rate of change of yawing moment coefficient (Cn) with respect to change in the yaw rate (r):

$$C_{n_\beta} = \frac{\partial C_n}{\partial \beta}$$
$$C_{n_r} = \frac{\partial C_n}{\partial r}$$

…(eq 4.27 & 4.28)

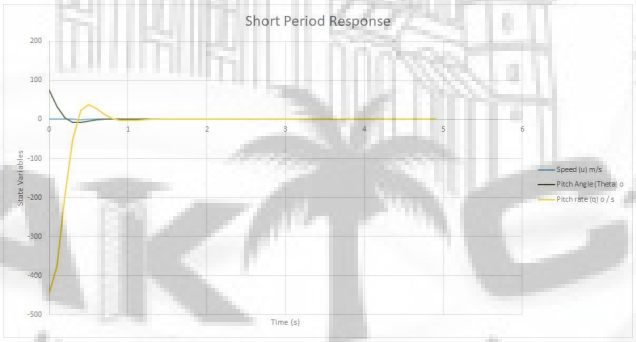

Figure 4.38 - Short period response graph by XFLR5.

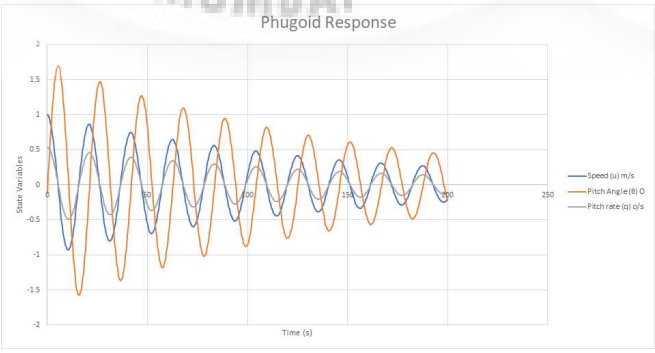

Figure 4.39 - Phugoid response graph by XFLR5.

From the above graphs in figures, indicates the response of the UAV in Short period and Phugoid response. In short term response we can observe that the UAV stabilizes in less then two seconds.

4.3 Fuselage Design

Fuselage is the main body of the drone. All the electronics and payload are incorporated in the fuselage. A side view of the fuselage is shown in the figure 4.40. The fuselage contains a section which contains the peltier box. The payload which are blood packets, medicines or organs are kept in the peltier box which keeps them at desired temperature. Fuselage also contains a pocket where all the electronics are mounted. The fuselage is made as an aerodynamic shape to decrease the drag produced by it and also to produce lift. Fuselage houses the batteries that are used to power the aircraft.

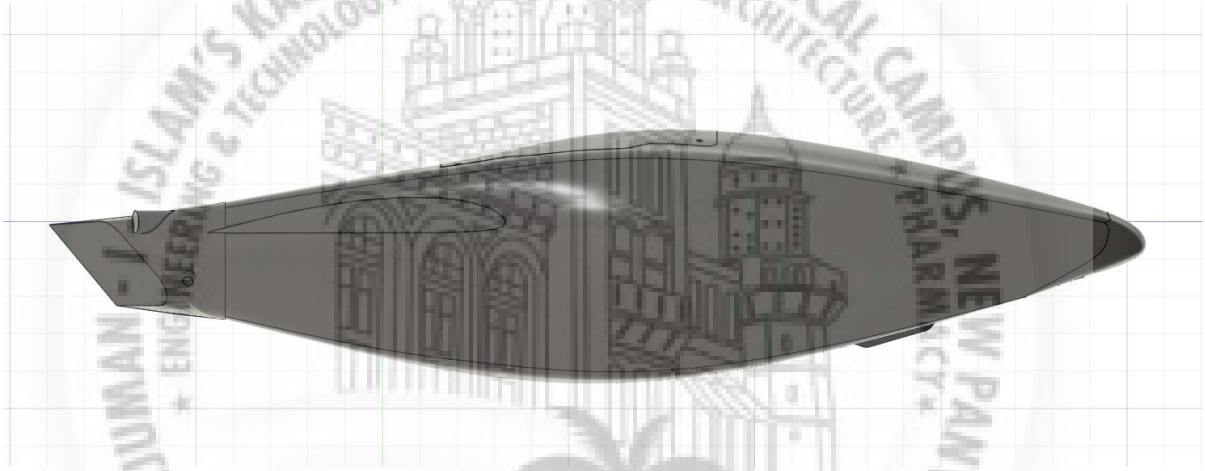

Figure 4.40(a) - Fuselage side view.

4.4 Full Body Analysis

Conducting a full body analysis is very important to visualize the flow pattern around the body of the aircraft. It also helps in determining the variations in the lift and drag of the aircraft. After designing all the dimensions of the drone, a 3D CAD model was created in Fusion 360. This model was then imported in ANSYS Fluent for further analysis. All the steps used for analysis were the same as the steps used in analysis of the wing. To cut down on computation time we made an enclosure for only one half of the aircraft as the aircraft is symmetrical.

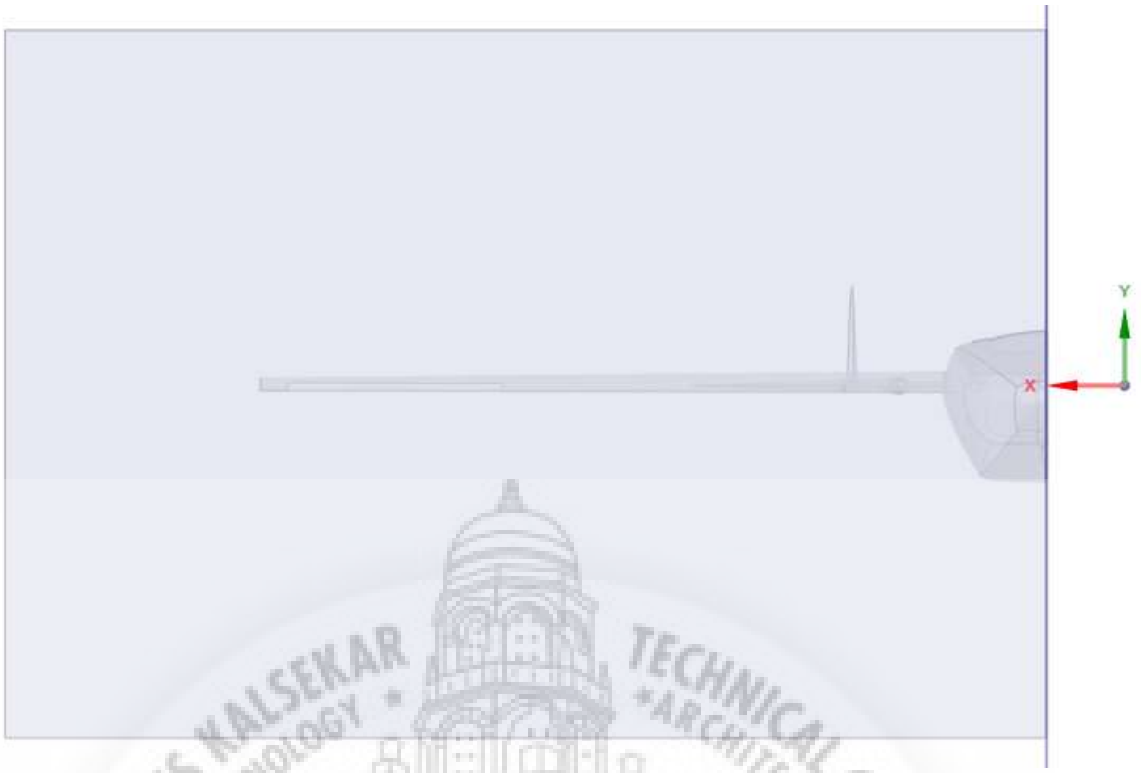

Figure 4.40(b) - Enclosure of half body.

A fine mesh was created to increase the fidelity of the results. The type of mesh used was Poly - Hexa Core mesh. The figure 4.41 shows the full body mesh.

Figure 4.41 - Poly - Hexa Core mesh.

After completing the mesh, the analysis was carried by taking the boundary conditions of the aircraft in cruise flight. The airspeed was taken as 26 m/s at the inlet and the outlet pressure was taken as 1 bar. On completion of the analysis the results were noted. The results are shown in the table 4.7.

Table 4.7 - Lift and drag generated by full body

Airspeed	Angle of Attack	Lift force	Drag force
26 m/s	0^{O}	141.4636 N	13.3712 N

We can observe an increase in the lift and drag force on the whole aircraft as compared to only the wing. This is because of the addition of fuselage and tail. Fuselage contributes to the generation of lift and also increases the drag on the aircraft.

Figure 4.42 - Full Body Pressure Contours.

The figure 4.42 is taken from CFD post processing. In this figure we can observe all the high pressure and low pressure regions that are generated all around the aircraft. There is a low pressure region that is created on the top of the aircraft and a high pressure region created below the aircraft. This contributes to the lift that is generated by the aircraft.

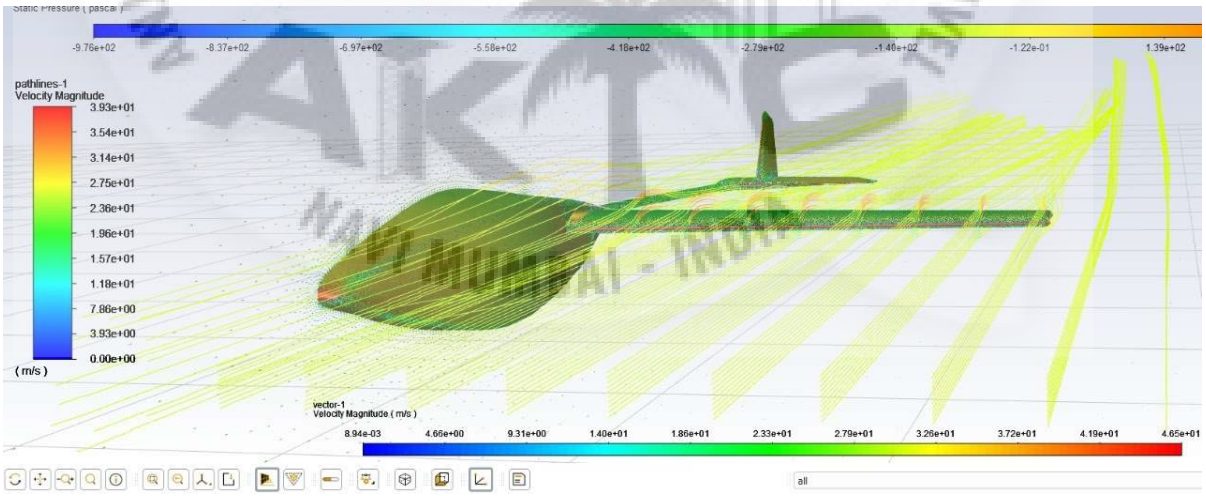

Figure 4.43 - Velocity Pathlines over Full body.

The figure 4.43 shows the flow of air over the drone body in the form of pathlines. As the flow over the fuselage is streamline, there is minimum drag that is created by the fuselage .

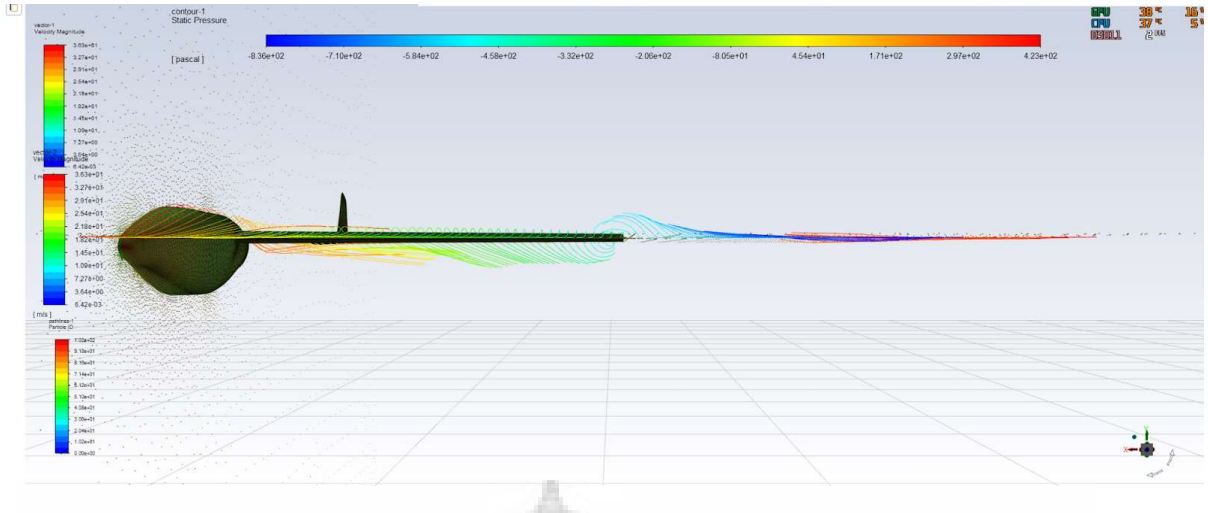

Figure 4.44 - Vortex Generation Pathlines.

The intensity and location of the vortex can be visualized in figure 4.44. The vortex generation at the tip of the wing is also made as low as possible to decrease the drag produced. We can also observe the downwash of the stream created by the wing.

4.5 Aircraft Performance

In this section we will analyze various factors that affect performance of the aircraft. The aircraft needs to perform within set constraints and achieve the desired performance goals. Various parameters such as flight envelope, Vtol Climb rate, Static and dynamic thrust, etc will be estimated.

4.5.1 Flight Envelope

One of the most important diagrams for the flight mission profile, which defines aircraft loads is the Flight Envelope (V-n) diagram. This diagram defines the limits in which aircraft can safely operate and exceeding these limits can result in either loss of aircraft control or failure of aircraft structure. The V in (V-n) stands for indicated velocity and n in (V-n) stands for load factor.

The load factor is basically the ratio of the lift to the weight of the aircraft ie. L/W and it is expressed as a factor of acceleration due to gravity ‘g’.

The positive and negative stall curves represent the limiting stall with respect to speed, Crossing this limit will result in stall.

The stall speed V_S is given as

$$V_S = \sqrt{\frac{2W}{p \cdot C_{Lmax} \cdot S}} \qquad \text{…(eq 4.29)}$$

where, W is aircraft weight in newtons, in our case, around 117 N. p is air density and C_{Lmax} for our aircraft is 1.2 and S is the surface area, which is 0.92 m^2 for our aircraft. Hence,

$$V_S = 13 \text{ m/s}$$

The negative stall speed utilizes the same formula but with a negative C_{Lmax} , in our case, around -0.5.

The stall curve can be plotted using the formula:

$$V_n = V_s (V_n)^{½} \qquad \text{…(eq 4.30)}$$

The maneuvering speed, V_a is at the intersection of caution limit and stall curve.

The positive and negative load limits are based on the design requirements and directly influences the strength of the structural components and in turn also the weight of the aircraft. The positive load factor n is chosen to be 4g and the negative load value is typically -0.5 times positive load factor, hence -n is determined to be -2.

The cruise speed is determined by the designer on the basis of given requirements, in our case target V_C is approximately 26 m/s.

V_d or dive speed typically must be more than 1.4 times V_C , Hence a rough estimated value of 41 m/s is chosen.

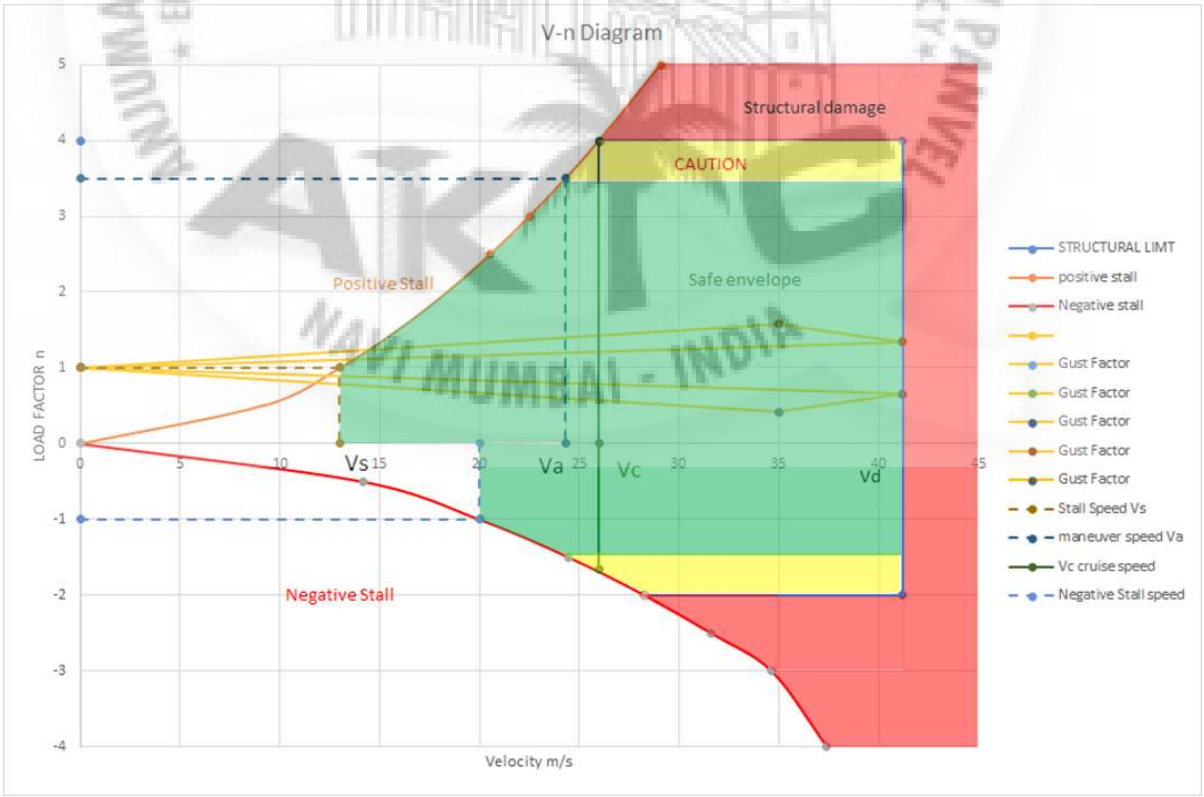

Figure 4.45 - V-n Diagram.

In the above figure 4.45, the stall speeds, both negative and positive, have been plotted along with positive and negative load limits. The red area marks the structural damage region, while yellow marks the caution region and green is the safe operation area.

4.5.2 Static Thrust

In preliminary design we selected the motor and propeller combination that satisfies our requirements. In the below figure, our test setup can be seen. It consists of a simple pivoted cantilever beam with the motor on the other end. The motor end is supported by a rod which transfers the thrust generated directly to the weighing machine. Despite being simple this method is adequately accurate.

Figure 4.46 - Static Thrust Test Images.

Table 4.8 - Experimental Thrust Results.

Motor	Propeller	RPM	Thrust	Power
Turnigy Sk3 5055-430kv	17 x 8 ACP	6700	5.2 Kgf	1380 w
Turnigy Sk3 5055-430kv	18 x 8	6200	6 Kgf	1495 w

The analytical method to calculate static thrust and dynamic thrust will be explored in section 4.5.4.

4.5.3 Vtol Performance

In this section we will use computational fluid dynamics to determine the vtol performance of aircraft. The chosen Climb velocity is 6 m/s which is the max desired speed. the operational standard velocity will be less than 6 m/s .

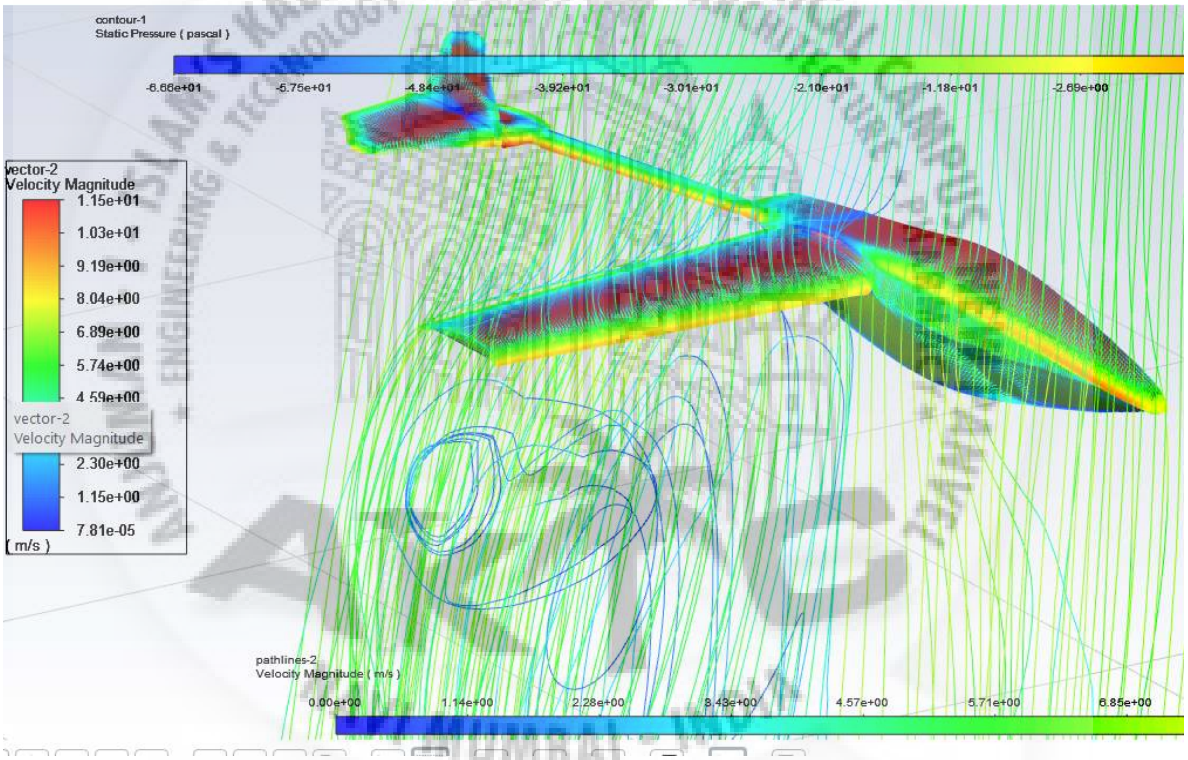

Figure 4.47 - VTOL flow simulation.

Table 4.9 - Vtol Cfd Parameters and results.

V_C , Climb Speed	Surface Area	Cd	Drag force
6 m/s	1.54 m^2	1.158	39.34 N

As it can be seen in the table above, the Drag force at steady 6 m/s climb is 39.34 Newtons. Which is a satisfactory result. The thrust required to achieve a V_C of 6 m/s will require a

force of 39.34 N plus the Aircraft weight ie. 117 N, which would equal roughly 156 N. Furthermore we can extrapolate the Ansys data to find drag at various velocities of climb,

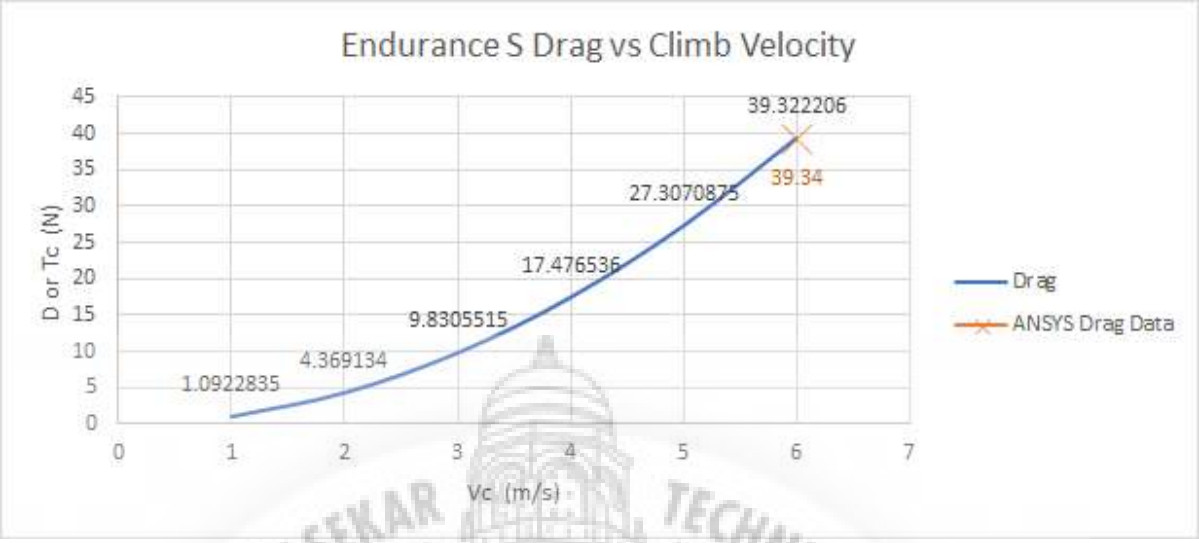

Figure 4.48 - Extrapolated drag.

While climb velocity of 6 m/s is highest, the standard climb velocity will be around 4 m/s. This is so in order to maximise the range of the aircraft as it is a more economical climb speed.

4.5.4 Dynamic Thrust and power

Dynamic thrust is the change in thrust with respect to airspeed, as airspeed increases the thrust drops as effective angle of attack of the propeller decreases resulting in loss of lift and hence loss of thrust. The Calculation of Dynamic thrust is very difficult and involves various interdependent variables which are non linear.

We will be Calculating Drag values with respect to thrust using analytical formulas along with CFD results. Then we will use the Drive Calculator by Helmut Schenk [49] to derive power, thrust, and with respect to speed at different rpms. All this data is overlaid alongside the drag and velocity chart as shown in Figure - 4.49. The data can be matched to obtain values at certain velocity and rpms. We will also require the motor data for this but that data is currently not analysed as the project is not yet complete due to COVID-19.

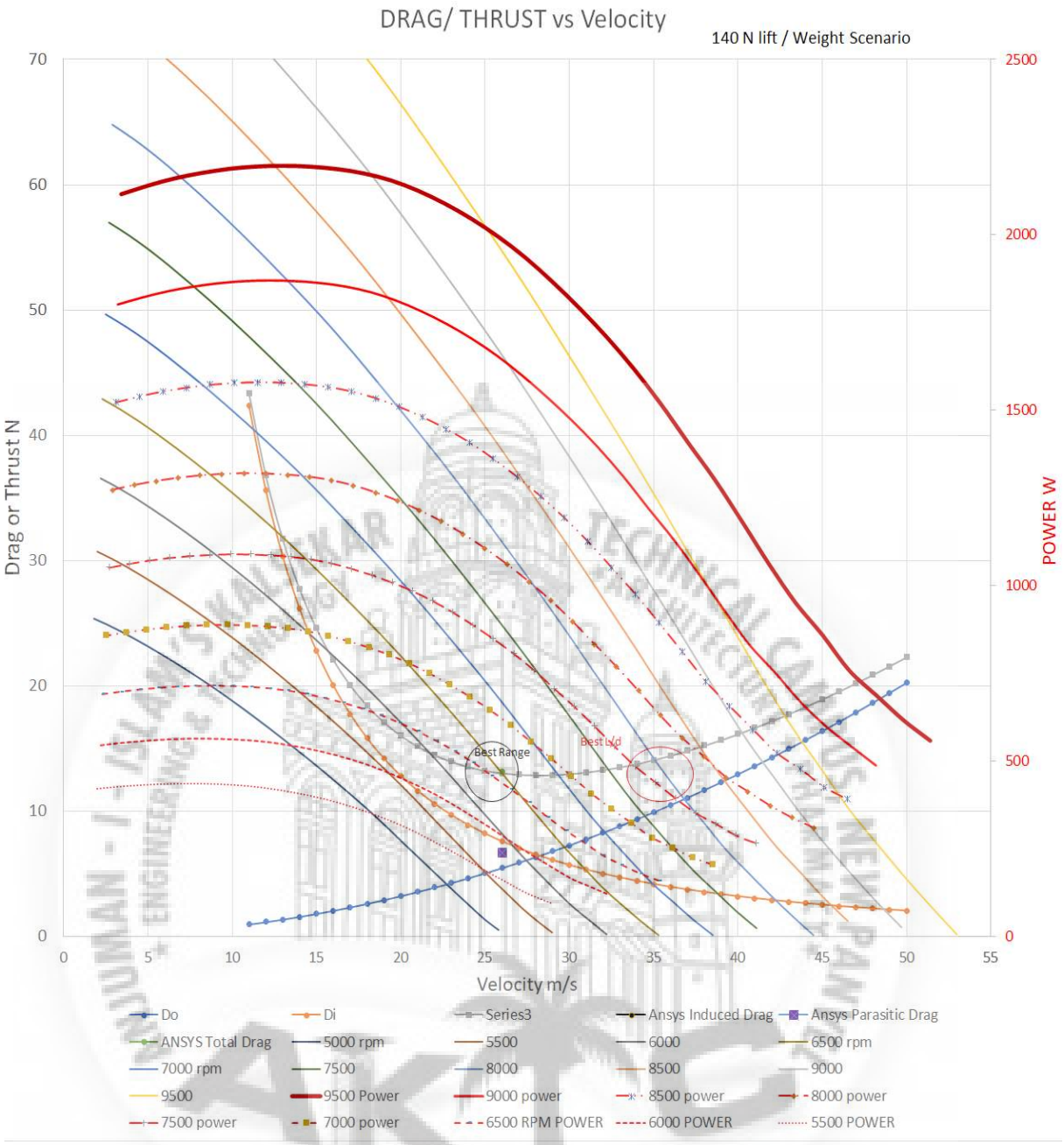

Figure 4.49 - Drag, Thrust, Power vs Velocity.

Chapter 05

Structural Design

5.1 Structure Layout

This Chapter will contain a detailed study of the structural aspects of Endurance aircraft. The structure of the endurance aircraft was made with special emphasis on weight saving and high strength to weight ratio. The more efficient we are with these two parameters, the better we get in terms of payload.

A good structure design incorporates all the factors initiated during the preliminary stage. At the very beginning the designer writes a set of specifications which is required to be fulfilled by his design. However, it should be known that it is not always possible to fulfill all the requirements completely. Sometimes the requirements might be unattainable. The designer has to make compromises sometimes, the judgement and the experience of the designer is crucial in this. It must be noted that a good design satisfies its requirement the most and has the least amount of compromises.

The most crucial aspect of structural design is integration of different components with each other.

Our wings will be connected to the fuselage by carbon fibre rods. For this a design had to be thought out to integrate these two. After multiple designs, a design was finalized which fulfilled our criteria the most.

In this chapter we will discuss the various aspects of aircraft structural design, literature study, design and analysis of the aluminium hub, wing structure i.e. spar and ribs, connectors, tilt motor mechanism and landing gear. We will also discuss the challenges faced and how we were able to overcome those.

5.2 Spar Design

Figure 5.1 - Spar.

Spars are structural members of the wing running from the root of the fuselage to the tip of the wings. Spars support many substructures on the wings. The spar is connected to the fuselage as a cantilever and supports the weight of the wing. Along with the weight it is subjected to dynamic load as well. Spar is considered the skeleton of the aircraft.

Along with the weight of the structure the spar commonly carries critical components that are used to control the flight. Very commonly propulsion systems are also mounted on the wings, the load of which has to be supported by the spar.

A safe spar design is one of the basic requirements of an aircraft design. As the spar is a structural support and the skeleton of the aircraft, the design of the spar should be such that it outlasts every other component in the aircraft. The designer has to be very careful in considering the loading of the spar and it naturally requires a high safety factor. The wings are in fact designed to carry about 2.5 times the weight of the aircraft.

Some of the forces that the spar is subjected to are: -

1. Downward bending force generated by the weight of the components in the wings when the aircraft is stationary. As we know the engine which is quite heavy is

supported by the spar. The bending moment generated is a significant value and is one of the key factors in determining the dimensions of the spar.

2. Upward bending force generated by the lift force while flying. Some amount of this force is countered by downward bending force generated by the weight of the wing structure.
3. Drag force again generated while flying. It is the force that acts opposite to the direction of the aircraft while flying. It increases with speed.
4. Inertia force due to moving aircraft.
5. Twisting force generated while flying. This force arises due to aerodynamics and moves along the chord of the airfoil. Its magnitude changes depending on the airspeed, thrust generated and the angle of attack.

The way the combination of spar and ribs are designed, they distribute the load effectively at different points and ensure that there is no concentration of load at any part of the structure.

Due to the various combinations of loads acting on the wing, the material selection for the design of spar becomes very important here. We want the whole wing structure to support 2.5 times the weight of the aircraft but at the same time we have to ensure that the weight is not too high to fly.

By now it is clear that the spar requires high quality high strength materials. Historically, a range of materials from wood to alloys have been used. But since its invention aluminium spars have been used predominantly due to its lightweight, durability, corrosion resistance and most importantly high strength to weight ratio. But now since the invention of composites carbon fibre is increasingly being used and replacing aluminium.

For our endurance craft aluminium and carbon fibre were shortlisted for the construction of our spar but due to our preliminary focus on weight saving and high strength to weight ratio, aluminium was quickly eliminated.

Table 5.1 - Comparison of carbon fiber and aluminium at the same weight.

Sr. No.	Measurement	Carbon Fiber	Aluminum	Carbon/Aluminum Comparison
1.	**Modulus of elasticity (E) GPa**	70	68.9	100%
2.	**Tensile strength (σ) MPa**	1035	450	230%
3.	**Density (ρ) g/cm3**	1.6	2.7	59%
4.	**Specific stiffness (E/ρ)**	43.8	25.6	171%
5.	**Specific tensile strength (σ /ρ)**	647	166	389%

The table 5.1 shows that carbon fibre has a specific tensile strength 3.9 times that of aluminium, 1.7 times the specific stiffness all that at 41% reduction in weight.

Depending on the design fundamental spars can be classified as: -

1. Monospar: - In this type one longitudinal member is added throughout the span of the wing to support the structure.
2. Multispar : - In multispar setup more than one longitudinal member is used to support the cantilever structure.
3. Box beam: - The box beam type structure incorporates multiple stringers and webs in a box shape along with the spar to distribute the load.

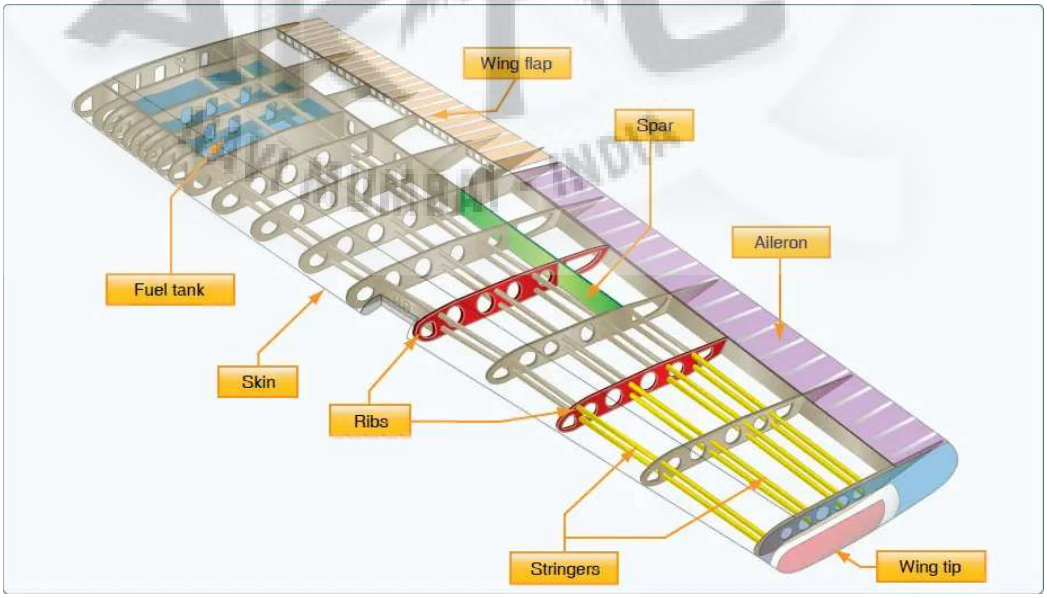

Figure 5.2 - Construction of spar.

Apart from this numerous modifications of this basic design is used across the manufacturers.

After confirming the material to be used we now have to design the shape of the spar. The shape of the spar is greatly varied across different designs. Some of the common shapes of spars taken are - L-shaped, I-beam, rectangular solid, rectangular box, part hollow, tubular etc. Since the top and bottom section of the beam are typically the most heavily loaded I-beam structure is very popular. Even though I beams are fairly popular, no shape is considered perfect and it's left up to the aircraft designer to decide which profile suits his wing structure the best.

So for our spar design we go with the multispar design and shape of the structure of the spar would be either rectangular or tubular. Finally we decided to go for the round tube although working with square tube would have been easier for us, round tubes have higher resistance to flex and torsional twisting at the same weight.

So the dimensions of our carbon fibre tube are going to be dictated by bending forces generated by the weight of the net wing structure.

5.2.1 Theoretical calculations

Equation of bending is given by: -

$$\sigma b = M * y/I \qquad \ldots(\text{eq } 5.1)$$

where , σb = Bending stress

M = Bending Moment

y = radius

I = moment of inertia of the section.

For a hollow cylinder,

$$I = \pi/64\ (D^4 - d^4) \qquad \ldots(\text{eq } 5.2)$$

Taking $\sigma = 215\ Mpa$ and O.D as 30 mm and I.D as 27 mm and replacing in the above equation we get,

$$M = 195.99 * 10^3\ N - mm \simeq 19.98\ kg - m$$

The total weight of our endurance aircraft is 14 kg with payload, so a bending moment generated of 14 kg-m is safe.

The problem with carbon fibre though is the great deal of variability they come with. Different manufacturing techniques and variable quality due to defects, make it such that every carbon fiber is different. Therefore an experimental test was required to confirm our findings with analysis done above.

5.2.2 Experimental Calculations

So our ordered specimen of carbon fibre has an O.D of 30.2 mm, I.D of 27 mm and a length of 1600mm.

Figure 5.3 - The large rod at the top will be used as a main spar.

So for our test we decided to fix the beam at two ends to calculate the bending stress generated. So an equivalent force had to be applied to generate a bending moment of 14 kg-m.

5.2.2.1 Simply Supported Beam Equations

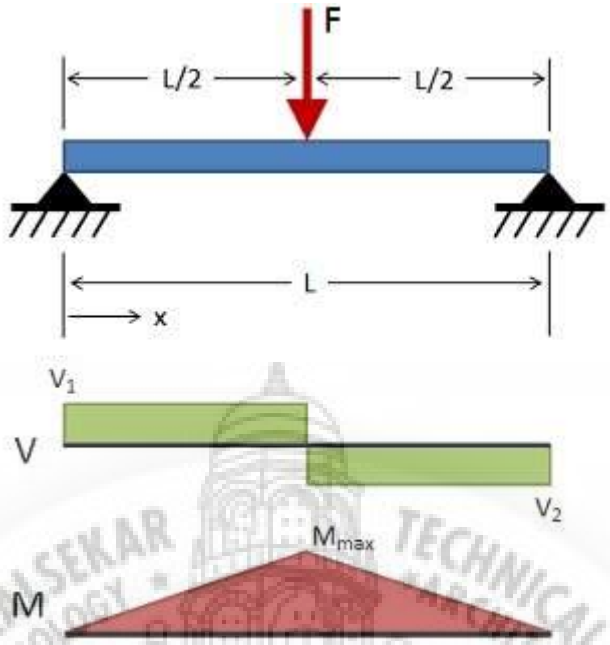

Figure 5.4 - Loading Diagram.

Deflection:

$$\delta max = F * L^3/(48 * E * I) \quad \text{...(eq 5.3)}$$

Slope:

$$\theta = F * L^2/(16 * E * I) \quad \text{...(eq 5.4)}$$

Shear:

$$V1 = +F/2 \ (0 \le x \le L/2) \quad \text{...(eq 5.5)}$$

$$V2 = -F/2 \ (L/2 \le x \le L) \quad \text{...(eq 5.6)}$$

Moment:

$$Mmax = (F * L)/4 \quad @\ L/2 \quad \text{...(eq 5.7)}$$

5.2.2.2 Observed Calculations

The beam was held at two ends, the distance between them being 1000 mm. So a load had to be applied at 500 mm for maximum deflection.

Therefore,

L = 1000 mm,

M = 15 Kg-m (our requirement)

From eq- 5.7 we get,

$$15*9.81*1000 = (F*1000)/4$$

$$F = 588.6\ N \Rightarrow m = 60\ kg$$

Therefore a mass load of 60 kg needs to be applied at the centre to satisfy our requirements in this setup.

So a person weighing 60 kg was told to stand at the centre of the beam. We observed no deformation.

The bending stresses generated here can be calculated by eq 5.2 :

$$\sigma b = (60 * 9.81 * 1000 * 30 * 64)/(8 * \pi * (30^4 - 27^4))$$

$$\sigma b = 161.426\ Mpa$$

Transverse Shear force from eq 5.5 can be calculated as:

$$V x = F/2 = 294.3\ N$$

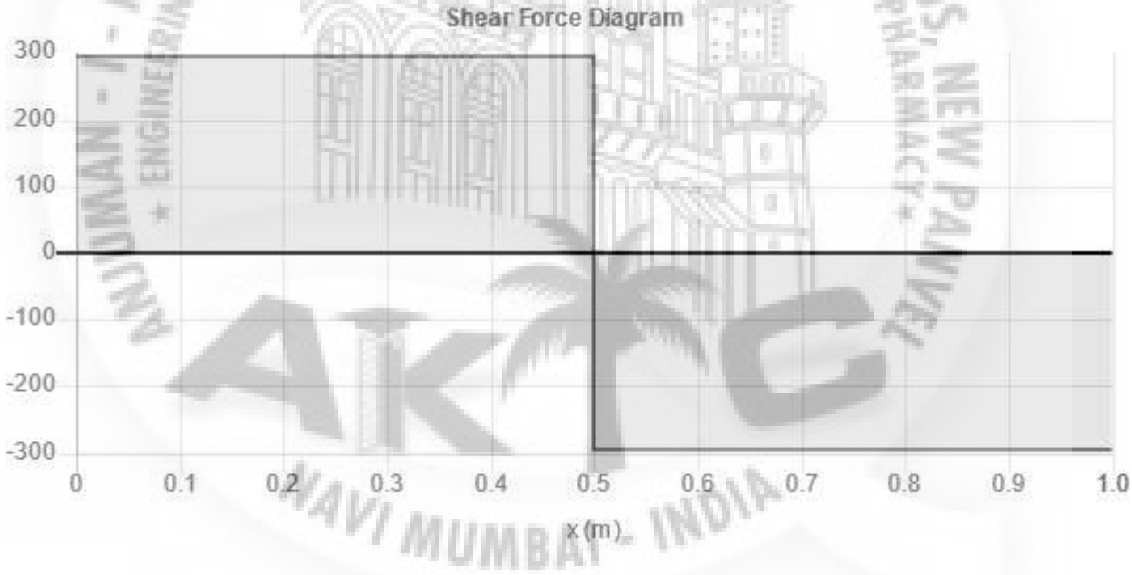

Figure 5.5 - S.F.D.

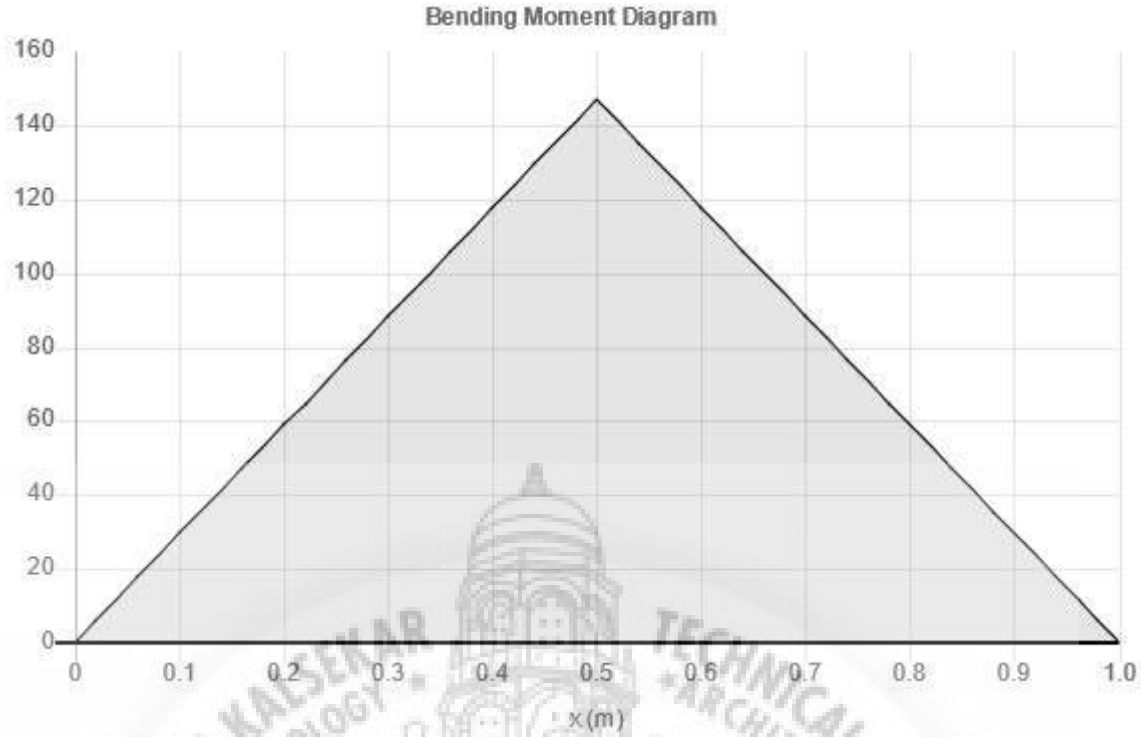

Figure 5.6 - B.M.D.

The deflection measured at beam being held at a distance of 950 mm apart with the same load as 20 mm.

Therefore from eq - 5.3,

$$E = (60 * 9.81 * (950^3) * 64)/(48 * 20 * \pi * (30^4 - 27^4))$$

E = 38.44 Gpa

Maximum slope from eq - 5.4,

Maximum Slope $[\theta_{max}] = 3.619$

Stiffness of the beam is,

E.I = 525.7 N-m^2

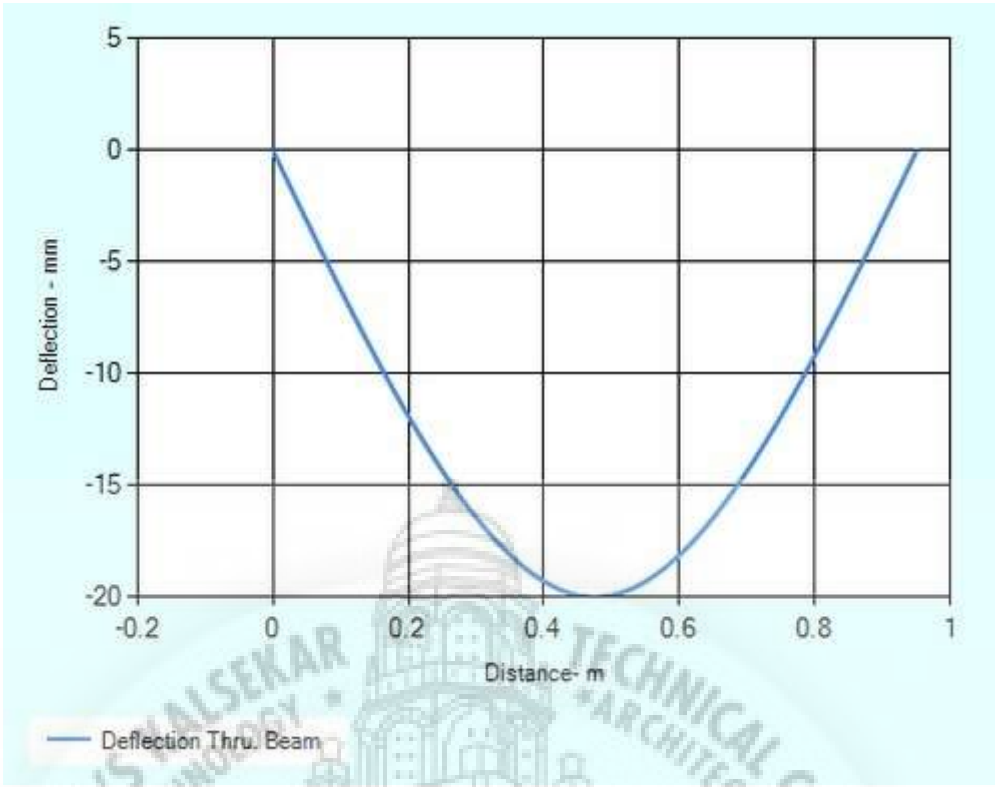

Figure 5.7 - Deflection Plot.

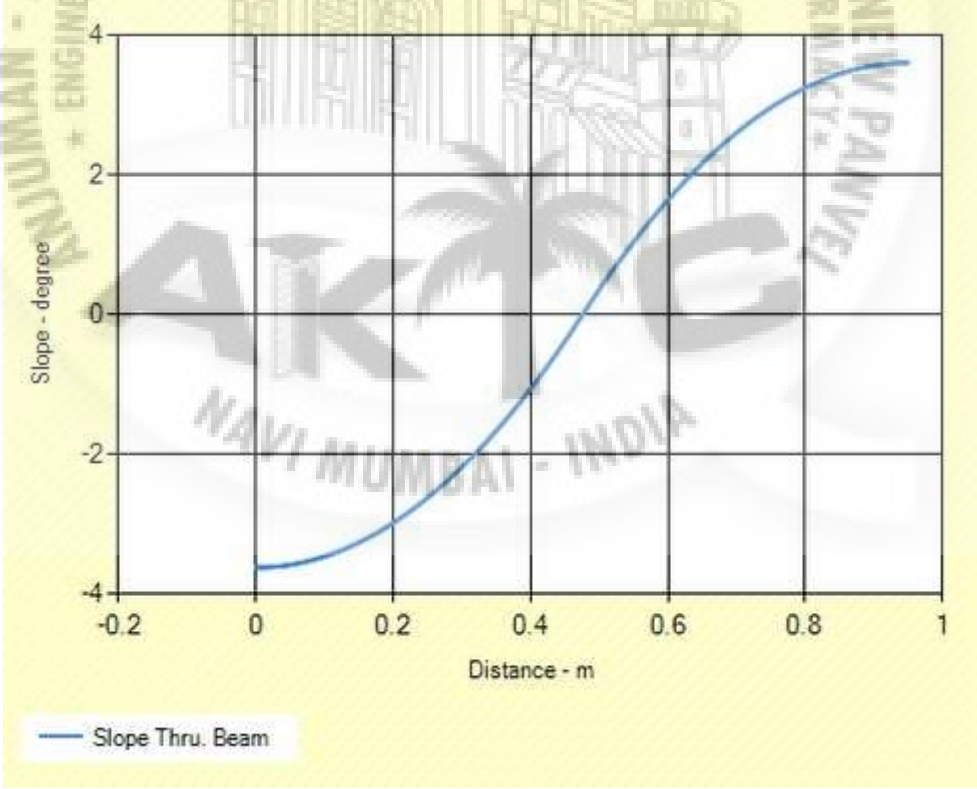

Figure 5.8 - Slope Plot.

This time the load was increased to 70 kg with all other parameters being the same. Thereby generating a moment of 17.5 kg-m.

$$\sigma b = 188.33\ MPa$$

$$Vx = 343.35\ N$$

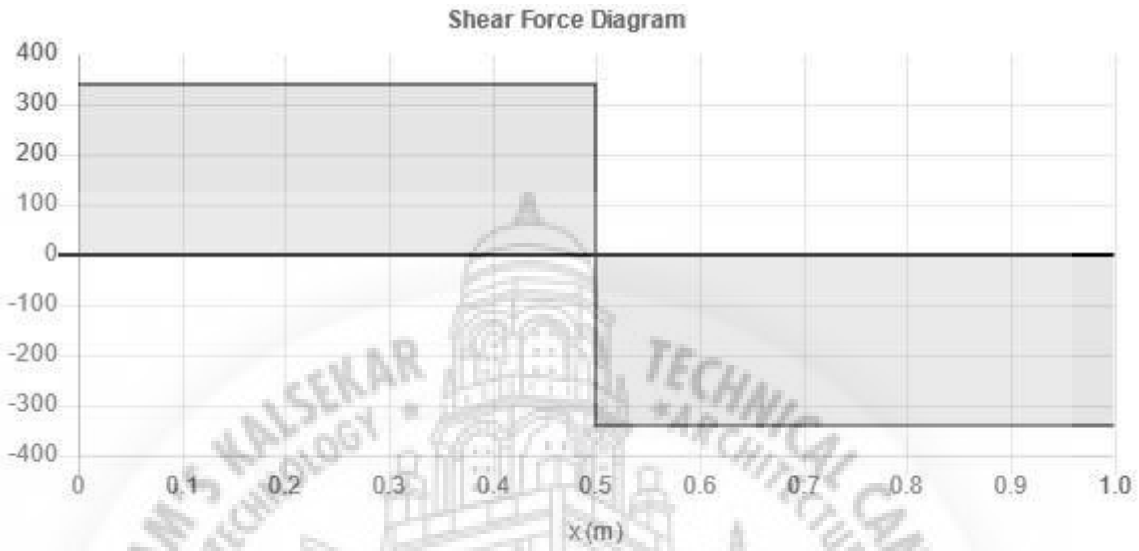

Figure 5.9 - S.F.D.

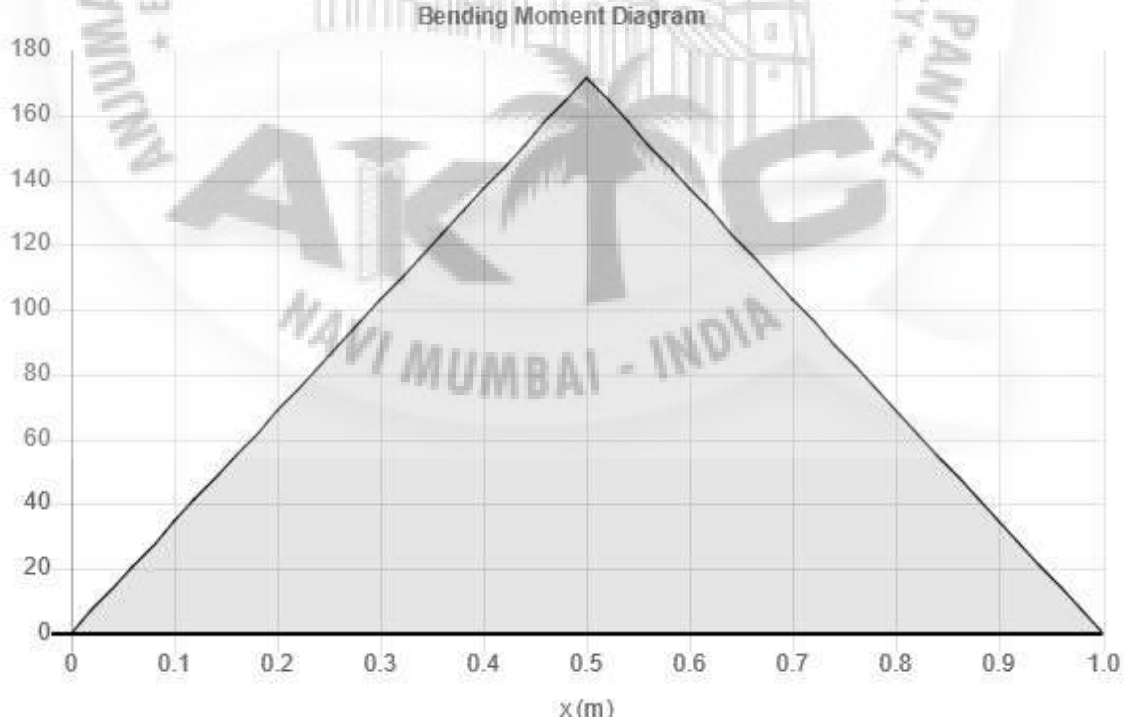

Figure 5.10 - B.M.D.

ymax = -27.214

$\theta = 4.678^{\circ}$

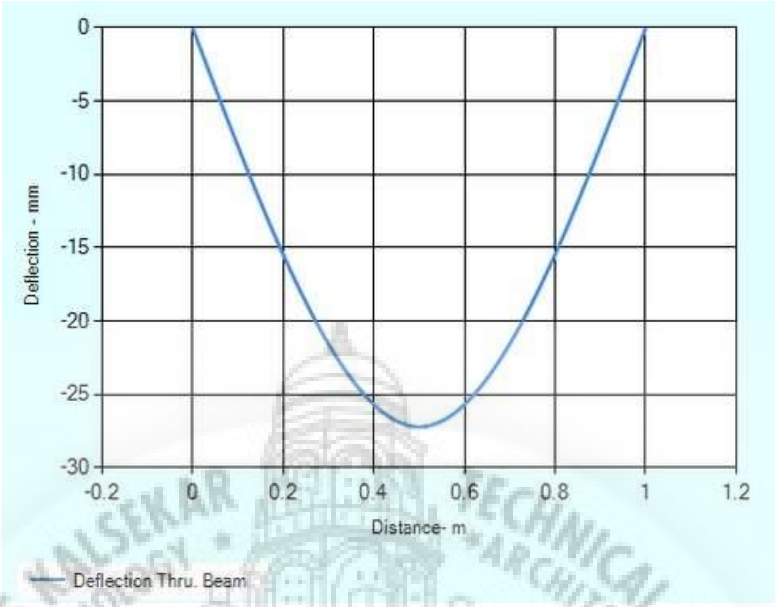

Figure 5.11 - Deflection.

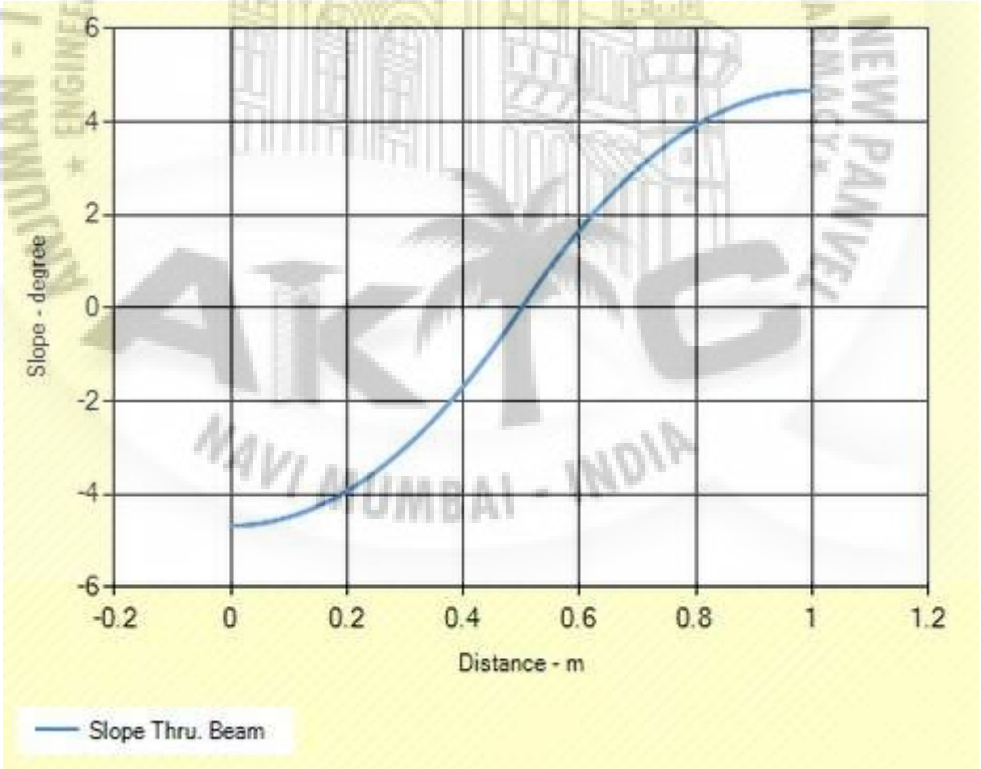

Figure 5.12 - Slope.

5.3 Ribs

1.3 COMPONENTS OF WING:

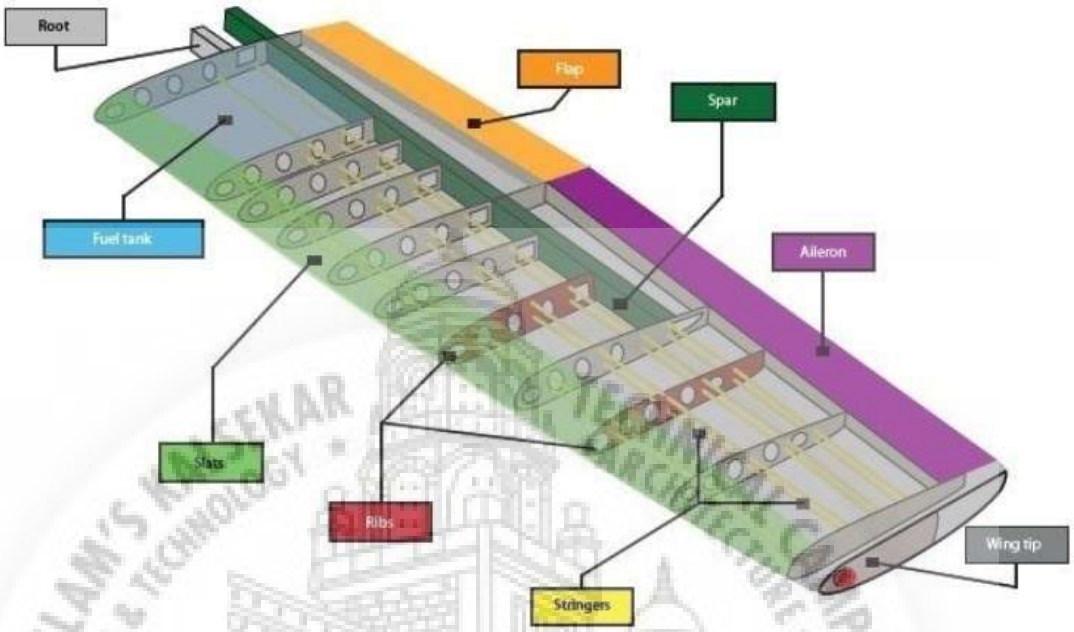

Main structural parts of wing:

1. Spar
2. Stringer
3. Ribs

Figure 5.13 - Components of Wings.

In an aircraft, ribs are forming elements of the structure of swing, especially in traditional construction. By analogy with the anatomical definition of "rib", the ribs attach to the mainspar, and by being repeated at frequent intervals, form a skeletal shape for the wing. Usually ribs incorporate the airfoil shape of the wing, and the skin adopts this shape when stretched over the ribs. There are several types of ribs. Form-ribs, plate-type ribs, truss ribs, closed-ribs, forged ribs and milled ribs, where form-ribs are used for light to medium loading and milled ribs are as strong as they can get. Form-ribs are made from a sheet of metal bent into shape, such as a U-profile. This profile is placed on the skin, just like a stringer, but then in the other direction. Plate-type ribs consist of sheet-metal, which

has upturned edges and weight-saving holes cut into it. Truss ribs are built up out of profiles that are joined together. These joints require great attention during design and manufacture. The ribs may be light or heavy in design, which makes them suitable for a wide range of loads. Closed-ribs are constructed from profiles and sheet metal and are suitable for closing off sections of the wing. Here too, particular care must be taken with the joints and this type of rib is also suitable for application in a variety of loading conditions.Forged ribs are manufactured using heavy press-machinery. The result is fairly rough; for more refined parts, high-pressure presses are required, which are very expensive.

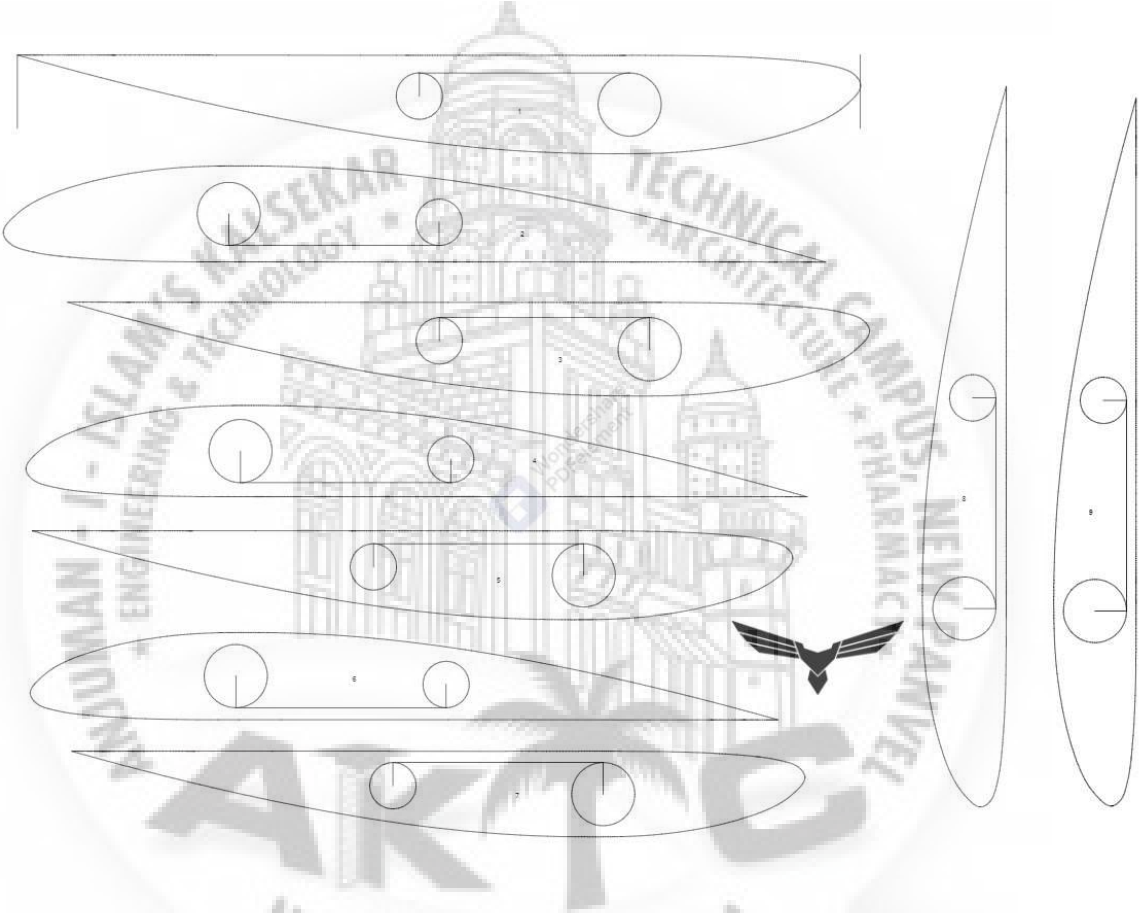

Figure 5.14 - Arrangement of Balsa Wood for Laser Cutting.

The ribs would be directly attached to our carbon fibre rods. The main function of the ribs would be to provide sufficient rigidity to our wing. For this the material chosen was balsa wood as it has a high strength to weight ratio. The fibre glass sheet would then be wrapped around the balsa structure. So the shape of our airfoil would also be provided by the ribs. The dimensions of the ribs continue to decrease as we move away from the fuselage. A total of 8 ribs on each side of the wing would help in providing sufficient rigidity. A poor cut on balsa could be detrimental to the performance of our UAV. A poor cut may result in different attack angles at different parts of the wing, this may cause stability issues in our aircraft . So the decision was made to cut balsa by water jet machining.

We were satisfied with the quality of the cut on our ribs. The tolerance in water jet machining is at an acceptable limit.

Figure 5.15 - Ribs being mounted on the spar.

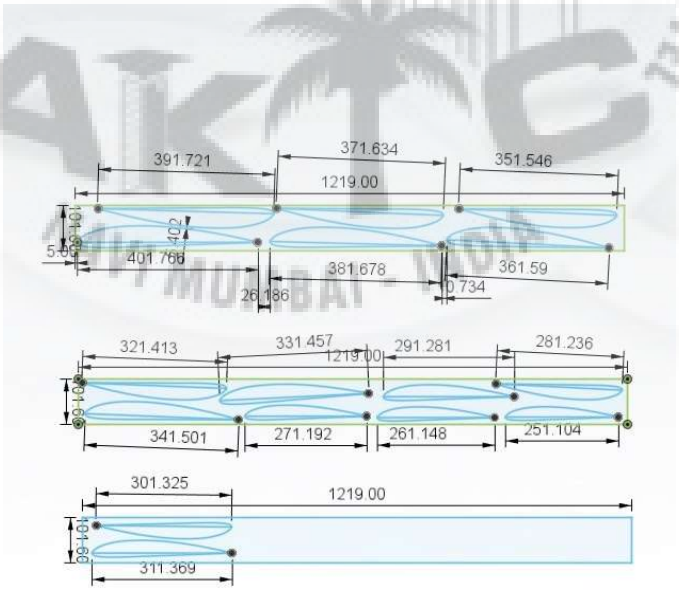

Figure 5.16 - Geometric dimensions of our ribs.

5.4 Total Wing Structure Weight Breakdown

Table 5.2 Weight of wing structure.

Part	Volume (mm3)	Density (kg/m3)	Mass (g)
BALSA RIB 1	35731.675	230	8.21828525
BALSA RIB 2	33757	230	7.76411
BALSA RIB 3	31836	230	7.32228
BALSA RIB 4	29955	230	6.88965
BALSA RIB 5	29956	230	6.88988
BALSA RIB 6	28136	230	6.47128
BALSA RIB 7	26873	230	6.18079
BALSA RIB 8	24104	230	5.54392
BALSA RIB 9	21484	230	4.94132
BALSA RIB 10	18991	230	4.36793
BALSA RIB 11	16648	230	3.82904
BALSA RIB 12	15108	230	3.47484
BALSA RIB 13	13730	230	3.1579
CF rod main	87297.00586	1250	109.1212573
Cf rod extended	82938.04605	1200	99.52565527
CF rod secondary	29845.13021	1200	35.81415625
SKIN COMPOSITE	200178	700	140.1246
SKIN SECONDARY	3002670	45	135.12015
BALSA EXTRA 1	18991	230	4.36793
BALSA EXTRA 2	29956	230	6.88988

Total weight = 1.347 kg

5.5 Aluminum Hub

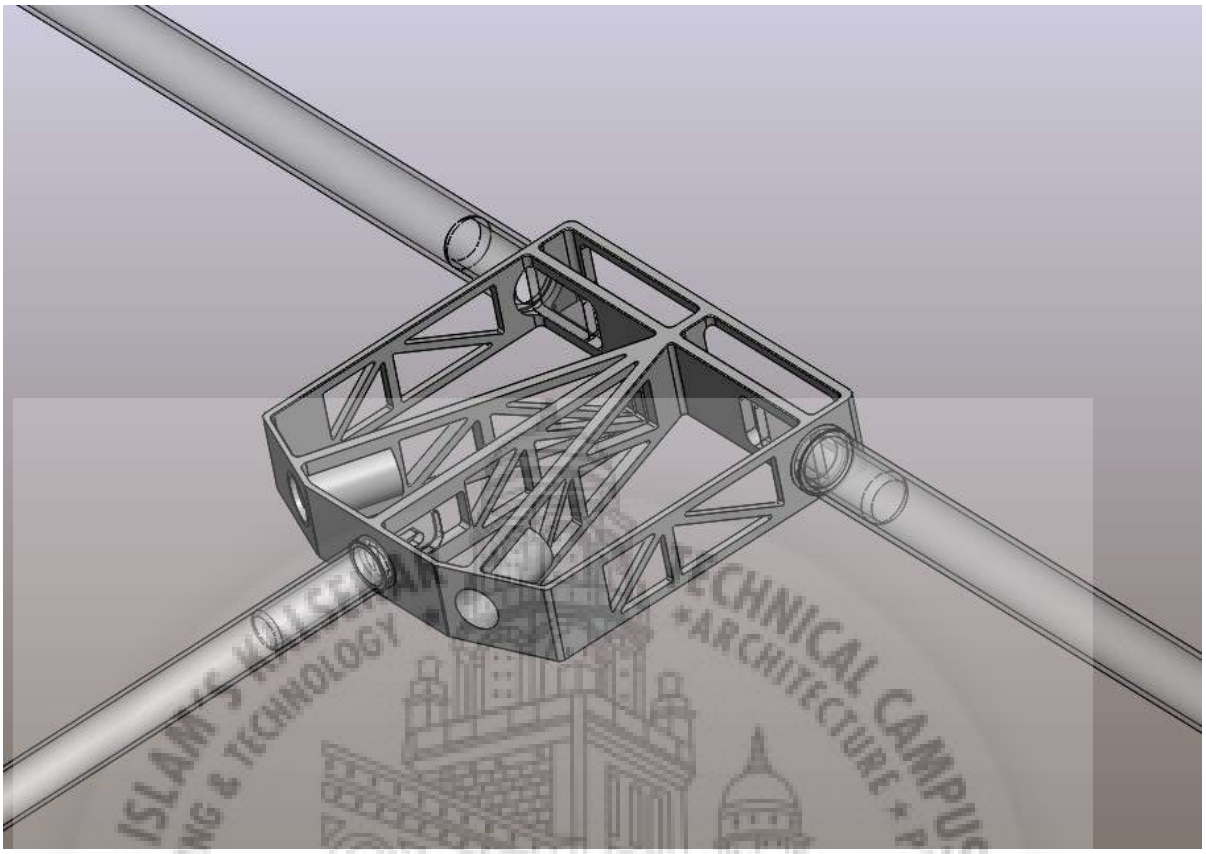

Figure 5.17 - Al- 6062 hub.

Our modified fuselage design consisted of an aluminium block right at the centre which would hold our carbon fibre rods of the wings by the help of extension rods.. The block dimensions were 200*200mm, it was hollowed down on sections where material was considered excess. The resultant weight of the aluminium block turned out to be 500g.

5.1.4.1 F.E.A Of The Aluminium Hub

In the FEA of our aluminium hub all the rods were fixed and a force of 700 N was applied around the C.G. This was considered as a reasonable approximation of our loading conditions.

⊟ Loads

⊟ Remote Force1

Type	Remote Force
Magnitude	700 N
X Value	0 N
Y Value	-700 N
Z Value	0 N
Position X	0 mm
Position Y	35 mm
Position Z	-54.53 mm

Figure 5.18 - The rods fixed at the end.

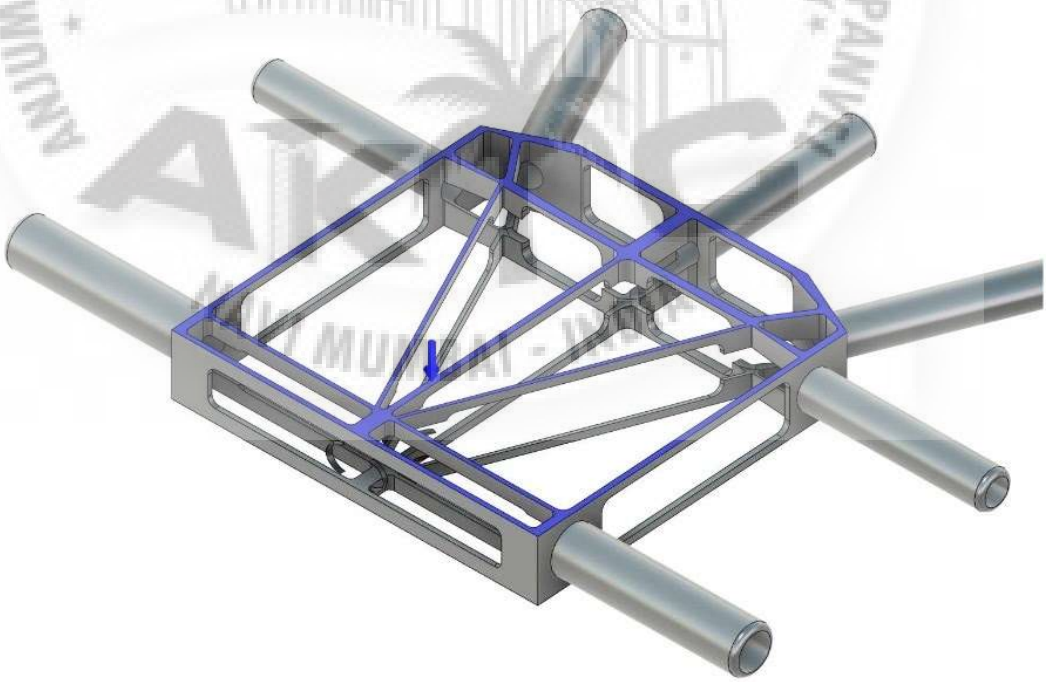

Figure 5.19 - A load of 700N applied.

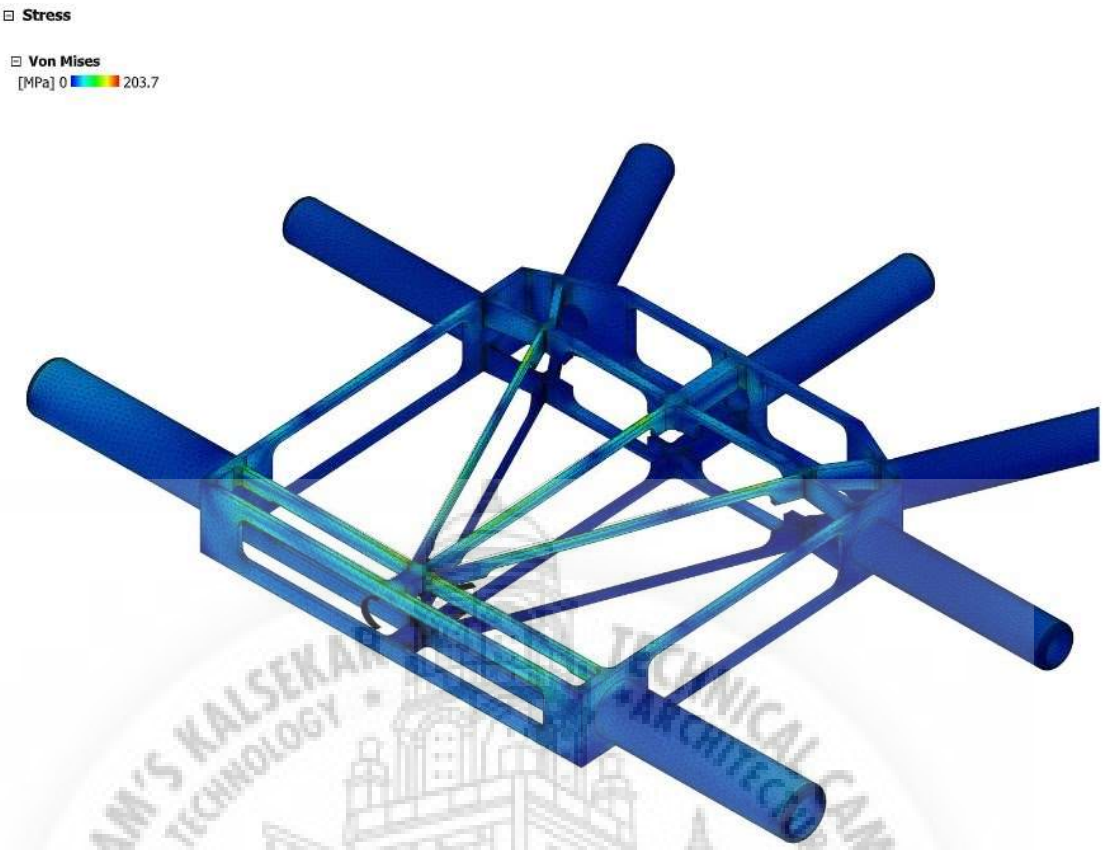

Figure 5.20 - Von Mises Stress contour.

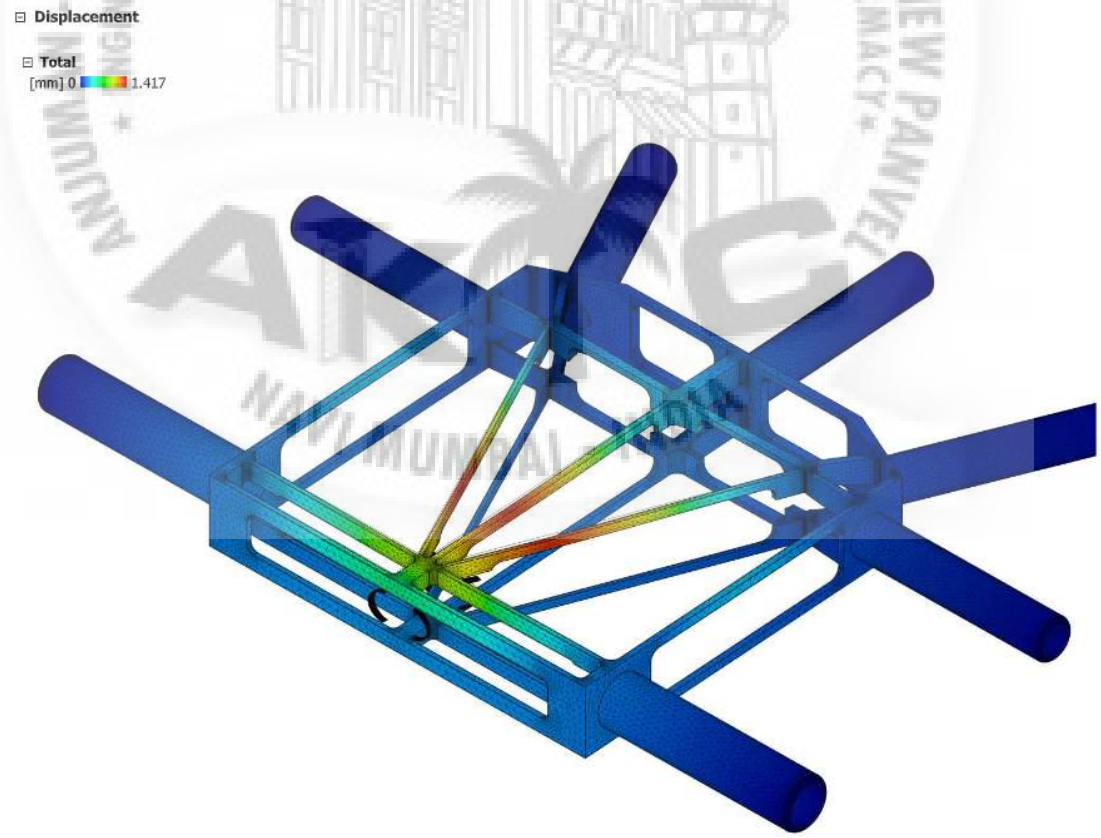

Figure 5.21 - Displacement contour.

A peak stress at around 207 MPa, well below Al-6062 limit of 275 Mpa and deflection less than 2mm, the design was considered adequate. However, weight of around 0.5 Kg, low strength to weight ratio and wastage of material resulted in scrapping of this design.

5.6 Final Hub Design

The design was then reconsidered to reduce the weight and increase the strength to weight ratio. Here we came up with a design, where we directly connect the carbon fibre rods with the help of epoxy resins and carbon fibre cloth. The inspiration of this design came from the manufacturing of carbon fibre bicycles.

For this we started with the cutting of the carbon fibre rod in designed dimensions then we cut the edges of tilt rotor rods and horizontal stabilizer rods using the diamond cutter so we got the respective contours which perfectly matched the outer body surface of the main spar.Next step was to align all the rods accurately for this we made use of our CAD model. Printout of the CAD 2D design of the junction area was taken with 1:1 scale then the rodsw were aligned as per the design using the tool holders.Then it was super glued and ribs were also attached for additional strength. After this Carbon fibre cloth was wrapped on it to make it concrete.

Figure 5.22 - Final hub design.

.

Figure 5.23 - Machining of carbon fibre using diamond.

Figure 5.24 - Carbon fiber sheet wrapped around.

Carbon Fibre cloth of 200gsm was used to wrap the junction of all the rods. It was done using the resin and harder in the proportion of 50gms of resin to 5gms of hardener. Then compressive load was applied using the C-clamps and 50kg anvil. Thermocol was placed between the flat bar and the structure. It was then kept in the same state for curing for 3 days and our main body of the aircraft was ready.

Figure 5.25 - After Wrapping.

Figure 5.26 - Main Body Testing.

After adequate curing the body was tested under a static load of 7kgs at each end point. The results were satisfactory.

This structure that we developed has an excellent strength. Everything was integrated very neatly with the help of resin and hardener mixture. Initially it was thought it would be trickier to work with composites. But for us working on carbon fibre turned out to be quite interesting and we learned an amazing skill.

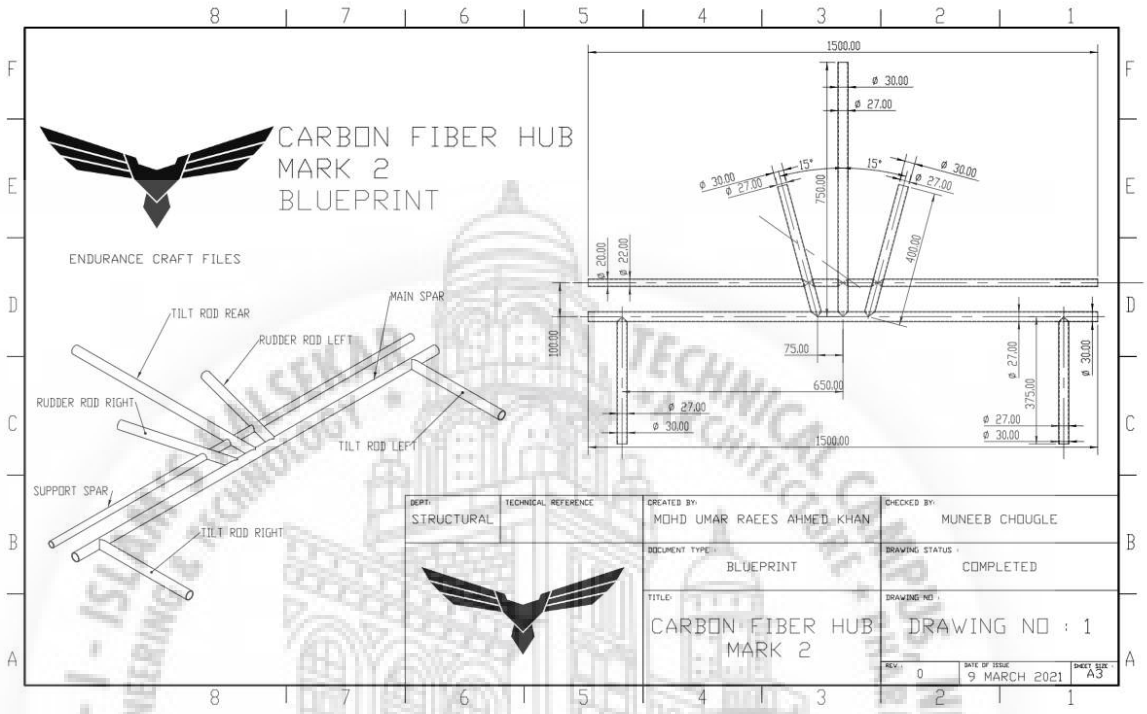

Figure 5.27 - Blueprint of our hub design.

5.7 Connectors

The connectors are the components used for attaching the extended wing and horizontal stabilizers or elevators of the aircraft. These are simple yet very important parts for an extended wing aircraft. Connectors are designed to bear tensile loading, bending moment and shear. In geometrical aspects a connector is a cylindrical piece with centrally drilled through hole and a hole which is perpendicular to the longitudinal axis for lock pin arrangement. Material requirements for such components are good machinability, optimum flexibility, optimum tensile strength. Aluminium 6012 has all the required properties for the job and hence it is used for making connectors. In total there are 4 pairs of the connectors out of which 2 pairs are for the extended wings and 2 pairs are used for extended rods of horizontal stabilizers.

These connectors are forced into the carbon fibre rods of the main frame to have an interference fit and then aluminium connectors and the CFR is locked via lock pin assembly. This process is the same for both i.e. extended wings and horizontal stabilizers. Dimensions of CFR for wings is 30mm OD and 27mm ID. Dimensions of CFR for horizontal stabilizer are 22mm OD and 19mm ID. As we want an interference fit ODs of both the aluminium connectors are 27mm and 19mm for wings and horizontal stabilizers respectively. For determining the IDs which are to be drilled centrally to reduce the weight bending stress calculations are done.

5.7.1 Load Calculation

As bending stress is maximum in our loading condition, the connector is designed on the basis of the bending stress criteria. Relation used for determining the IDs of connectors and the diameter of lock pin is

$$(M/I)=(\sigma_b/y) \qquad \text{...(eq 5.8)}$$

$$\therefore M = (\sigma_b/y)\times I$$

Where,

M = Bending Moment acting on connectors = 8.5 kg-m = 85000 Nmm.

I = Moment of Inertia of hollow cylinder = $(\pi/64)\times(D^4-d^4)$ kg-m^2.

where,

D = OD of aluminium connector in mm.

d = ID of aluminium connector in mm.

σ_b = Designed bending stress in MPa(N/mm^2).

y = Distance of outermost fibre from neutral axis in mm = D/2.

Now, the equation becomes

$$M = \sigma_b\times[(\pi/32)\times(D^4-d^4)\times D^{-1}]$$

Material properties of Aluminium 6012 used for designing are as follows:

σ_{ut}= 276 MPa, considering FOS=2, σ_b= $(1.2\times\sigma_{ut}/2)$ = 160 MPa.

Calculation for ID of aluminium connector for extended wings,

$$85000 = 160 \times [(\pi/32)\times(27^4-d^4)\times 27^{-1}]$$

$$d = 25mm$$

To maintain machining standard 20mm through hole is made in the connector therefore the ID for extended wing connector is 20mm.

Calculation for ID of aluminium connector for horizontal stabilizers or elevators,

Here, the bending moment acting on the connector is calculated by following calculations, in order to increase the factor of safety σ_b = 100 MPa and considering the loading dimensions of CFR.

$$\therefore M = 160 \times [(\pi/32)\times(22^4-19^4)\times22^{-1}]$$

$$M = 45000\ Nmm$$

ID of the aluminium connector,

$$85000 = 160 \times [(\pi/32)\times(19^4-d^4)\times19^{-1}]$$

$$d = 17mm$$

To maintain machining standard 14mm through hole is made in the connector therefore the ID for horizontal stabilizers or elevators connector is 14mm.

Length for both the connectors is 150mm.

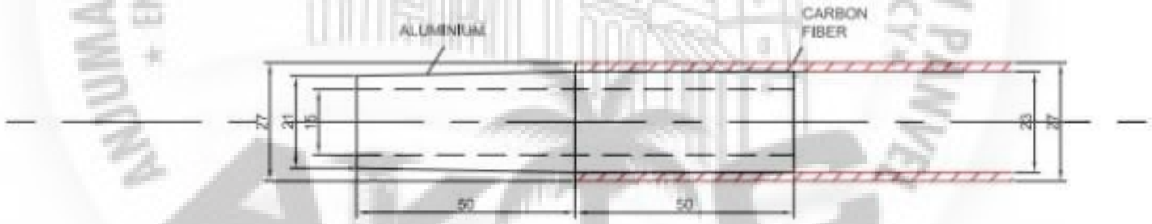

Figure 5.28 - Male connector.

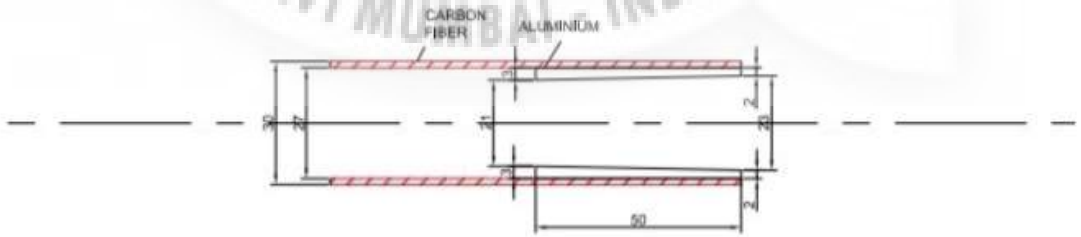

Figure 5.29 - Female connector.

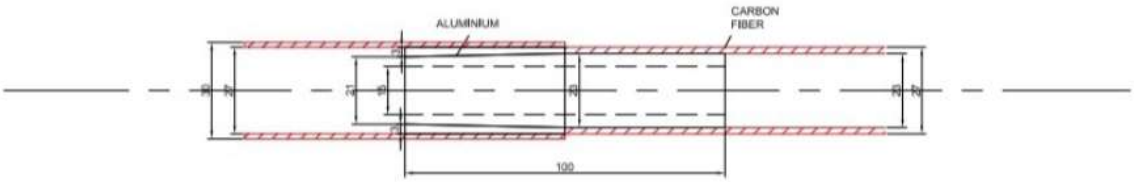

Figure 5.30 - Connector Assembly.

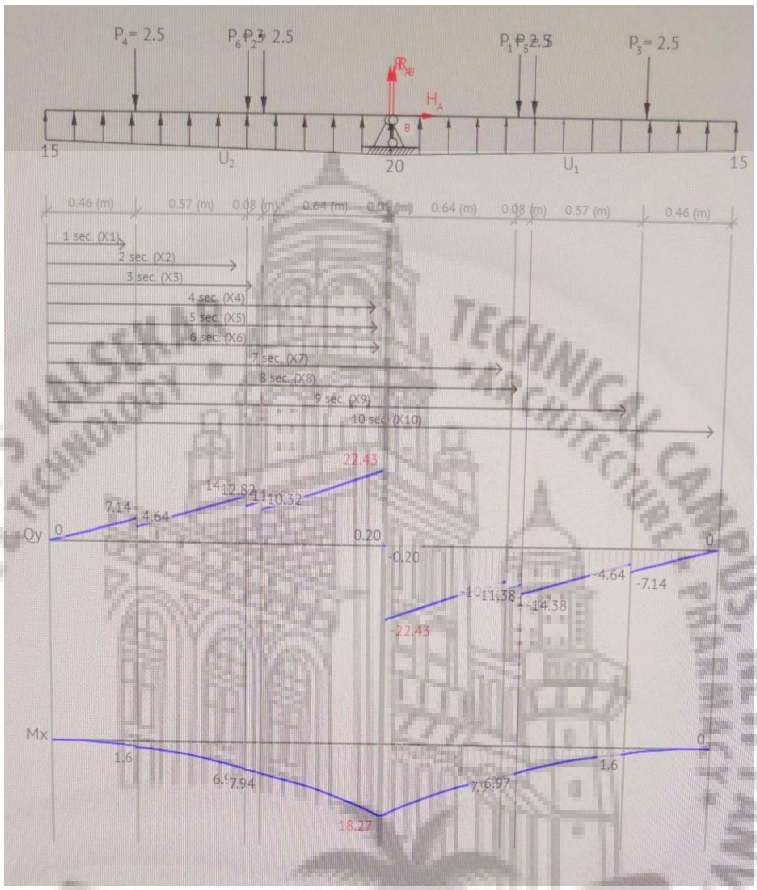

Figure 5.31 - S.F.D and B.M.D.

5.8 Tilt Rotor Mechanism

Endurance Craft MK II is designed for VTOL (Vertical Take Off & Landing) and STOL (Short Take Off & Landing). VTOL is accomplished without using any secondary thrust motors. In turn, it is achieved by tilting the main thrust motors using metal gear servos. For this it is mandatory for the mechanism to be robust and flawless because while in VTOL aircraft have vertical speed and zero ground speed then after a certain safe height tilting starts and the aircraft moves forward as per the vector forces acting on it.

For such a dynamic and crucial activity an indigenously designed mechanism is manufactured, which is very unique in every aspect. Three such tilt rotor mechanisms were fabricated using CNC and manufactured / assembled, two are used for front propellers tilting and one is used for the rear one. Following are the design sheets of the tilt rotor mechanism.

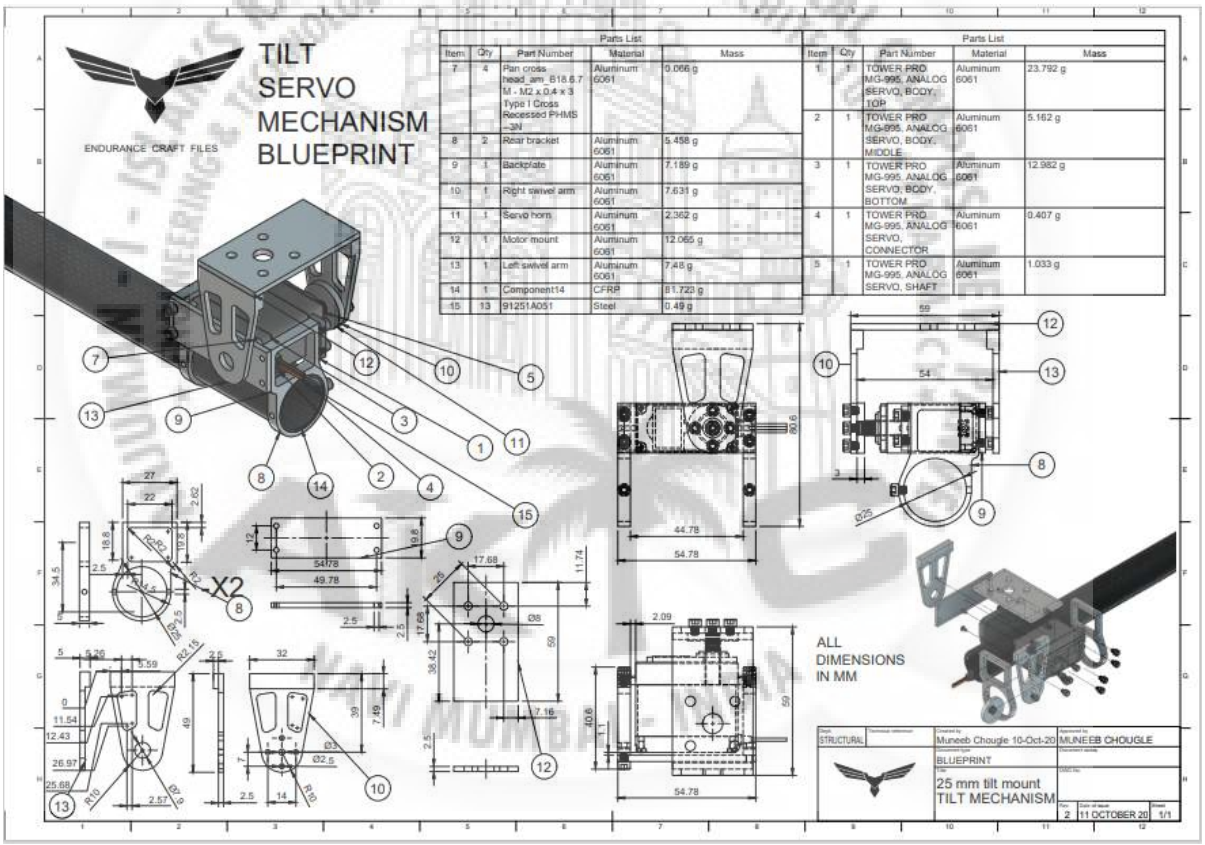

Figure 5.32 - Tilt rotor mechanism assembly blueprint.

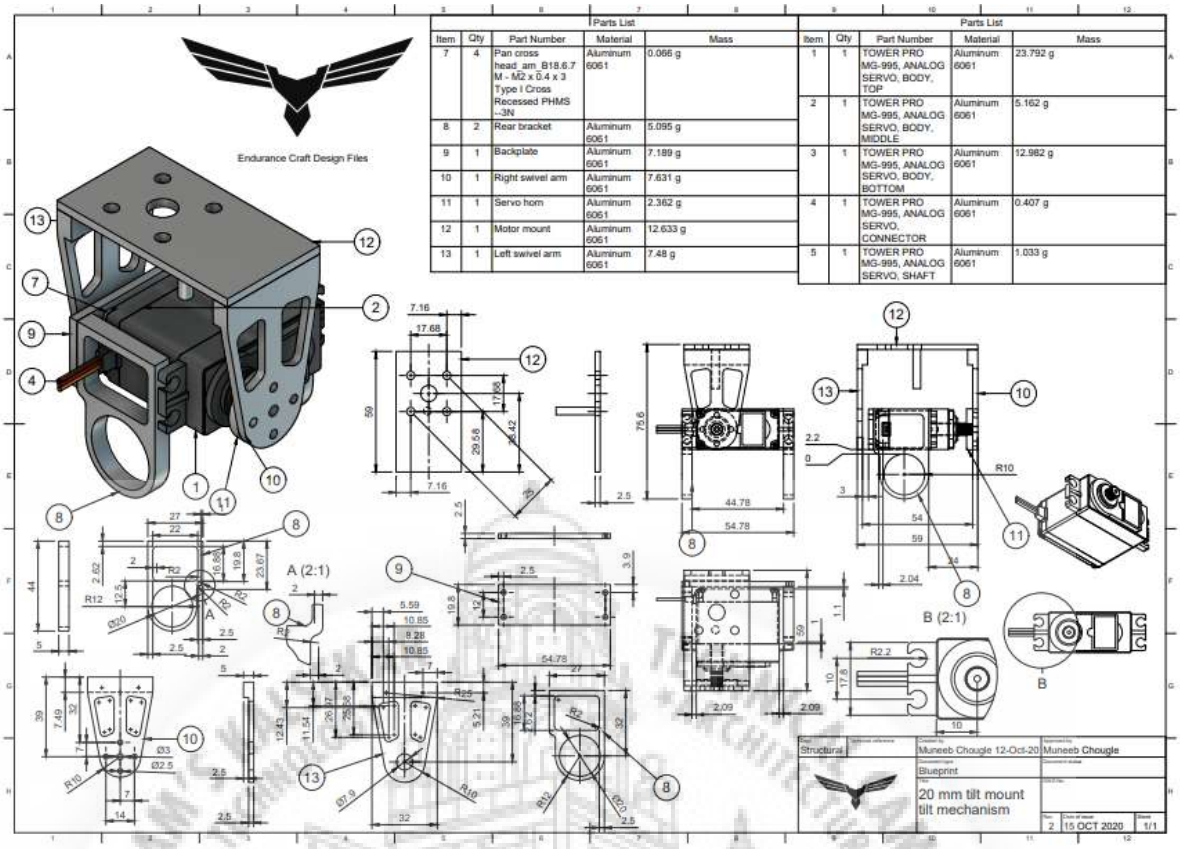

Figure 5.33 - Tilt rotor mount mechanism blueprint.

Tilt rotor mechanism contains a metallic frame and a servo motor, the motion of the servo motor is transferred to the metallic frame via flywheel(servo horn) mounted at the metal gear of the servo motor. This whole assembly is mounted on the CFR and the thrust motor is mounted on the motor mount of the metallic frame. In turn, the propeller is mounted on the thrust motor. Material used for making the metallic frame is Aluminium 6061 as it has high strength to weight ratio and offers right tensile strength and flexibility for the job on top of it, it has good machinability. Servo motor used is Towerpro MG995 High Torque Metal Gear Analog Servo with torque of 10kg-cm.

Components of Tilt Rotor Mechanism's Aluminium frame are as follows : -

Table 5.3 - Components of Tilt Rotor Mechanism's Aluminium frame.

Sr. No.	Part Name	Quantity	Material	Mass (grams)
1.	Rear bracket	2	Aluminium 6061	5.458
2.	Back plate	1	Aluminium 6061	7.189
3.	Right swivel arm	1	Aluminium 6061	7.631
4.	Left swivel arm	1	Aluminium 6061	7.48
5.	Servo horn	1	Aluminium 6061	2.362
6.	Motor mount	1	Aluminium 6061	12.065
7.	91251A051 (Allen bolt 3mm)	13	Steel	0.49

All the components of this tilt rotor assembly require high accuracy and precise machining therefore all the components are manufactured using CNC machining and by using standard components which are easily available in the market to maintain interchangeability. All the components are then assembled and mounted on the CFR. Design also included weight saving aspects like slots and grooves with consideration of load bearing areas using CAE tool ANSYS.

Working of the tilt rotor mechanism : -

The entire assembly is mounted on the CFR then the electrical connections are made in this case the servos are connected to pixhawk input channels. In turn pixhawk is linked to the Radiomaster TX16S radio controller via the Dragon Link Transmitter Receiver module. Pixhawk needs to be calibrated in various aspects along with the Radiomaster for giving appropriate command and receiving the correct data, those will be elaborate in respective sections.

Once all the calibration part is done keys need to be assigned on Radiomaster for respective actions and tilting of the motor and after this propellers will tilt as per command given.

Figure 5.34 - Tilt rotor assembly and mechanism.

5.9 Landing Gear

Landing gear supports aircraft while it is taxiing on ground, while takeoff or landing.

The key functions to be performed by a landing gear are as follows:

1.To ensure the stability of the aircraft on the ground, during loading, unloading, taxi and cross winds.

2.To steer the aircraft effectively on the ground.

3.To provide sufficient clearance between other aircraft components such as wing,fuselage and propellers while the aircraft is on the ground position to prevent any damage by the ground contact

Retractable landing gear is used to reduce drag. Aircraft landing gear include wheels along with a shock absorber. In a retractable gear system the space where Wheels stowed is called wheel wells. Extra wheels are added to support the weight of a larger aircraft. The landing position gear will depend on design, type and load of aircraft. Some landing gears are mounted on the wing and some under the fuselage. Most of them are mounted on wings.

Followings are the landing gear parameters :

1. Type (e.g. nose gear (tricycle), tail gear, bicycle)
2. Fixed, retractable, partially retractable
3. Height
4. Wheel base
5. Wheel track
6. the space between main gear and aircraft cg
7. Strut diameter
8. Tire sizing (diameter, width)
9. Landing gear compartment if retracted
10. Load on each strut

The descriptions of primary parameters are as follows. Landing gear height is the distance between the rock bottom point of the undercarriage (i.e. bottom of the tire) and therefore the attachment point to the aircraft. Since, undercarriage could also be attached to

the fuselage or to the wing; the term height may have different meaning. Furthermore, the undercarriage height may be a function of shock and therefore the undercarriage deflection. The height is typically measured when the aircraft is on the ground; it's maximum take-off weight; and undercarriage has the utmost deflection(i.e. lowest height). Thus, the undercarriage when it's the utmost extension remains height, but is a smaller amount important and application. The distance between rock bottom point of the undercarriage to the aircraft cg is additionally of serious importance and used to determine the Main gear, Wheel track (T), Height (H)cg, Height (H)strut wheel Wheel base (B)

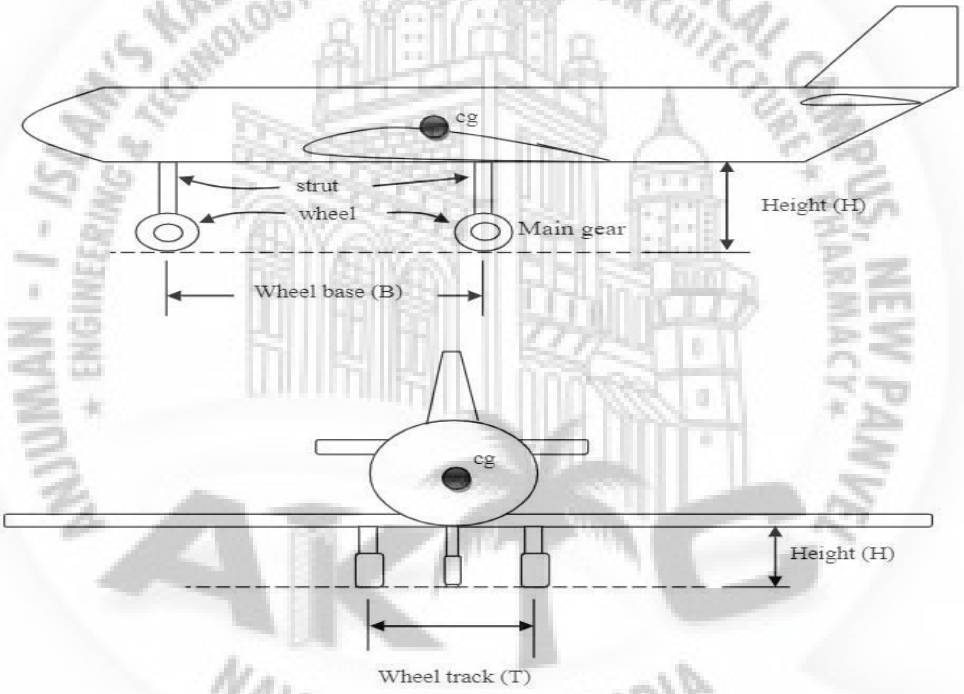

Figure 5.35 - Landing gear parameters.

Wheelbase is the distance between main gear and other gear (from side view) whereas Wheel track is the distance between two main gears (left and right) from front view.

The undercarriage is split into two sections:

1. Main gear or main whee1,

2. Secondary gear or secondary wheel.

Main gear is the gear which is closer to the aircraft center of gravity (cg). The main gear is placed at a distance away from the c.g such that it supports around 80-90% of the aircraft weight. During the landing operation, the main gear touches first and for a longer duration. Furthermore, during the take-off operation, the main gear leaves the ground last. That is why design of the main gear is one of the most crucial aspects of aircraft design. Since the main gear carries a great portion of the aircraft load on the ground .If a gear is predicted to hold high load, it's going to have more than one wheel.

5.9.1 Functional Analysis and Design Requirements

Landing gear is one of the last major aircraft components to be designed. It is preferred that other major components like fuselage, wing, tail, propulsion system etc. be designed prior to the landing gear. Also it is important to know the most aft center of gravity (cg) and the most forward cg of the aircraft for the landing gear to be designed. Sometimes, the design of the landing gear may influence the aircraft designer to modify the aircraft configuration slightly to landing gear design requirements. However under most circumstances it is such that the landing gear is adjusted to comply with the design and satisfy its own requirements.

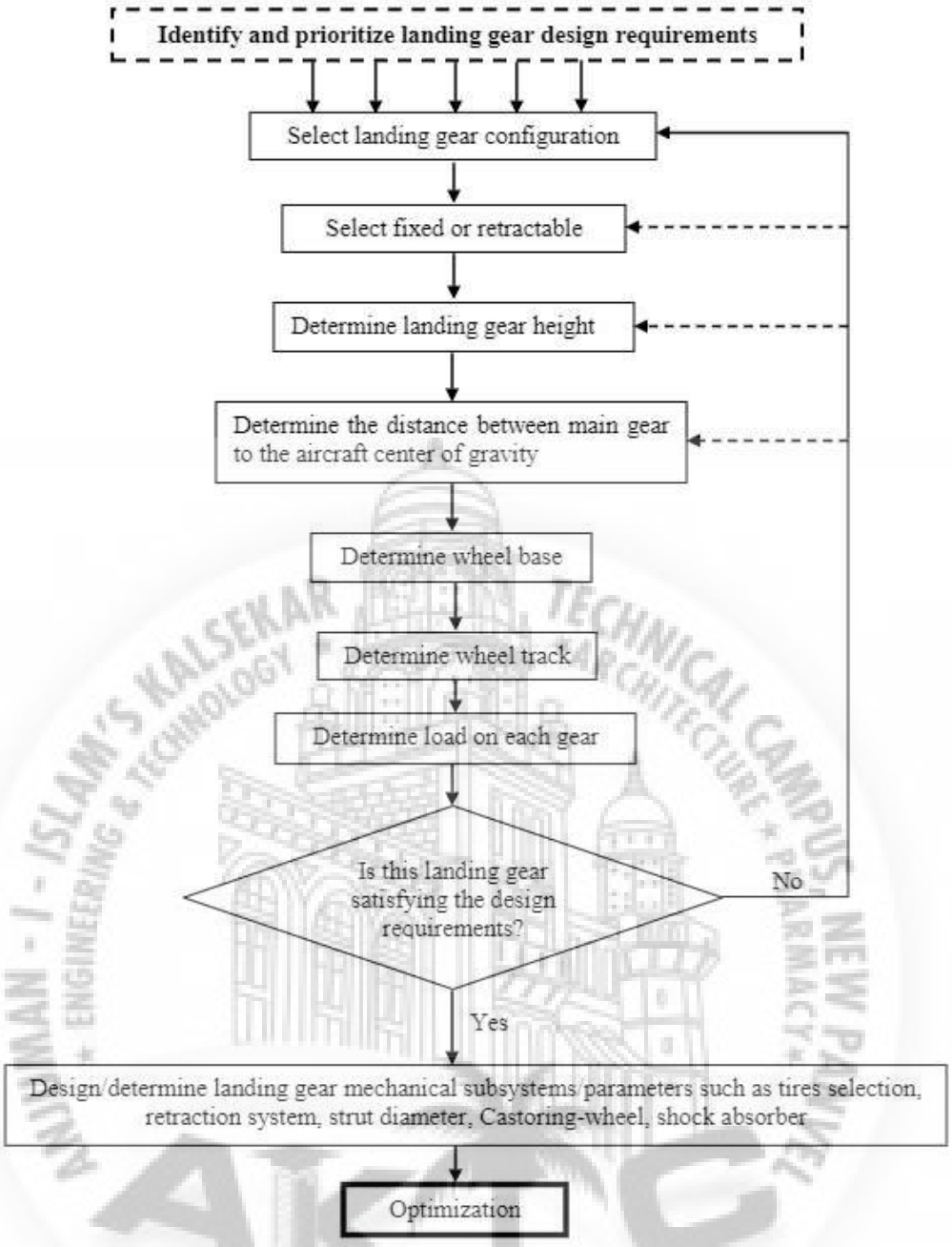

Figure 5.36 - Landing gear flowchart.

In order to permit for a undercarriage to function effectively, the subsequent design requirements are established:

1.Ground clearance requirement

2.Steering requirement

3.Take-off rotation requirement

4.Tip back prevention requirement

5.Overturn prevention requirement

6.Touch-down requirement

7.Landing requirement

8.Static and dynamic load requirement

9.Aircraft structural integrity

10.Ground lateral stability

11.Low cost

12.Low weight

13.Maintainability

14.Manufacturability

5.9.2 Landing Gear Configuration

The very first thing the landing gear designer has to figure out is what configuration of the gear suits his aircraft the best. The same function of the landing gear can be performed by different configurations. However the type of configuration to choose will depend on other factors such as design of the aircraft, weight of the aircraft, aircraft performance, location of the cg, the change of cg on loading and unloading conditions, type of surface to land or takeoff, landing or takeoff distance, steering requirements on ground, cost of the gear, weight of the gear and maintenance and the ease of replaceability of the gear.

Following are the common configurations of the landing gear: -

1.Single main

2.Bicycle

3.Tail-gear

4.Tricycle or nose-gear

5.Quadricycle

6.Multi-bogey

7.Releasable rail

8.Skid

9.Seaplane landing device

10.Human leg

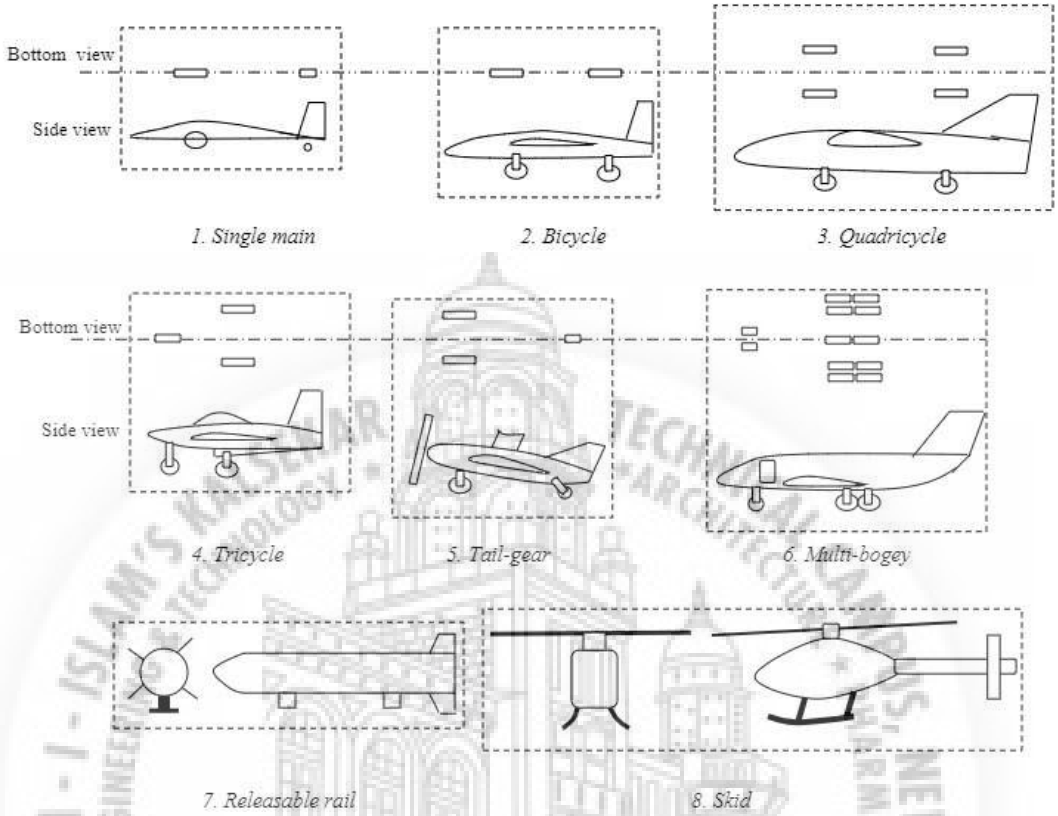

Figure 5.37 - Landing gear types.

1. Single Main

It is one of the simplest configurations of landing gear. It includes one large main gear that carries a large portion of the aircraft weight and load; plus s very small gear under the tail. In terms of size, the main gear is much larger than the secondary one. This type of configuration is popular in sailplanes. The single main landing gear is mostly of fixed type and it is very short in height. This type of gear has stability issues on the ground as the aircraft has a tendency to tip over the wings. It may require an operator to hold the wings prior to takeoff.

Main advantage of this arrangement are

1 The design simplicity

2 and Low weight.

Disadvantage of this configuration are

1. Ground instability

2. The longer take-off run, since the take-off rotation is limited.

2. Bicycle

The bicycle landing gear is an extension to the single main. Bicycle landing gear, has two main gears, one aft and one forward of aircraft cg; and both wheels have a similar size and are spaced at an equal distance from the cg, thus, both gears are carrying a similar load. To negate sideways tipping, two auxiliary small wheels are employed on the wings. This landing gear is employed for aircraft with narrow fuselage and high wing configuration. It shares its advantages and disadvantages with single main.

3. Quadricycle

As the name implies a quadricycle landing gear utilizes four gears; similar to a conventional car wheel system with two wheels in front of aircraft cg and other two aft of cg. If the aft and forward wheels have the same distance to cg, they will carry the same load. In this configuration, it becomes difficult to rotate the aircraft during take-off and landing. This makes the take-off run longer as compared to the tricycle configuration. The advantage of this type of setup is that the aircraft is very stable on the ground and during taxiing.

4. Tricycle

Tricycle is the most commonly used landing gear configuration. The wheels aft of the aircraft cg is very close to it and carry much of the aircraft weight and load; thus is referred to as the main wheel. Two main gears are in the same distance from the cg in the x-axis and the same distances in y-axis (left and right sides); thus both carry the same load. The main gear supports about 80 to 90 percent of the total load, so the nose gear is carrying about 10 to 20 percent. Both the gears have the same height, so the aircraft is level on the ground. This configuration of aircraft is directionally stable on the ground as well as during taxiing. The reason being if the aircraft yaws slightly while taxiing, the rolling and skidding resistance of the main gear, acting behind the cg, tends to straighten the aircraft out. This enables the aircraft to have a fairly large side-slip angle during cross wind landing.

5. Tail-gear

Tail-gear landing gear has two main at the front of the aircraft cg and a small wheel under the tail. The wheels in front of the aircraft are closer to the cg and carry much of the aircraft weight and load, thus it is referred to as the main wheel. The tail wheel is far

away from cg and carries a minimal load. The main gear carries about 80 to 90 percent of the total load.

This is the landing gear of the conventional type. In tail daggers a flat plate is used to reduce drag. On the ground the aircraft stands at an angle due to the main gear being much larger than the tail gear. Due to the high angle of attack during ground roll, the tail will be lifted up during take-off operation. This makes the take-off run longer compared with a tricycle landing gear. Since the aircraft has three wheels, the aircraft is stable on the ground. However, it is inherently directionally unstable during ground maneuver (turn). The reason being when an aircraft with a tail gear starts to turn on the ground around main gear, the cg behind main gear generates a centrifugal force. If the aircraft ground speed is high ,the moment of the centrifugal force will be larger than the moment of the friction force on tail gear; so it causes the aircraft to yaw around the main gear.

6. Skid

V-TOL aircraft and helicopters do not need to taxi on the ground, so they are equipped with a beam-type structure called skids instead of a regular landing gear. The configuration of skids mainly comprises three or four fixed cantilever beams which are deflected outward when a load is applied. The deflection of skid on impact plays the role of a shock absorber during landing operations. However, they are not as efficient as oleo shock absorbers. It is much easier to design a skid. The beam deflection and bending stress equation will help us to design the skid. It is also a good thing to take into account the fatigue loading and fatigue life to predict the skid endurance.

5.9.3 Comparison Between Fixed And Retractable Gear

Table 5.4 - Comparison between Fixed and retractable gear.

Sr. No.	Parameters	Fixed	Retractable
1.	Cost	Cheaper.	Expensive.
2.	Weight	Light.	Heavy.
3.	Design	Simple.	Complex.
4.	Drag	More drag.	Less drag.
5.	Aircraft Structure	Easier to integrate as it does not interfere with the structure of the aircraft.	Requires structural accommodation.
6.	Retraction	No retraction.	Requires retraction mechanism.
7.	Volume occupies	Low	High

From the above table it can be concluded that retractable landing gear is only suitable when the drag force generated by a fixed type gear is very significant. Therefore, it is much more common to see retractable type gear in large and fast airliners. As the drag force generated is very high and causes high fuel consumption even offsetting its self weight disadvantage. Speed is also a factor considered.

5.9.4 Landing Gear Equation

1. Take-off Rotation and Ground Clearance Requirement

An aircraft is usually rotating about the main gear in order to increase the lift to prepare for take-off. In an aircraft the height of the landing gear must be set so that the tail or rear fuselage does not strike the ground during the take-off rotation or landing with a high angle of attack.

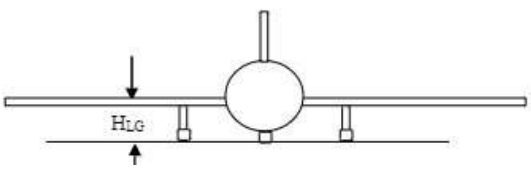

Figure 5.38 - Landing gear height.

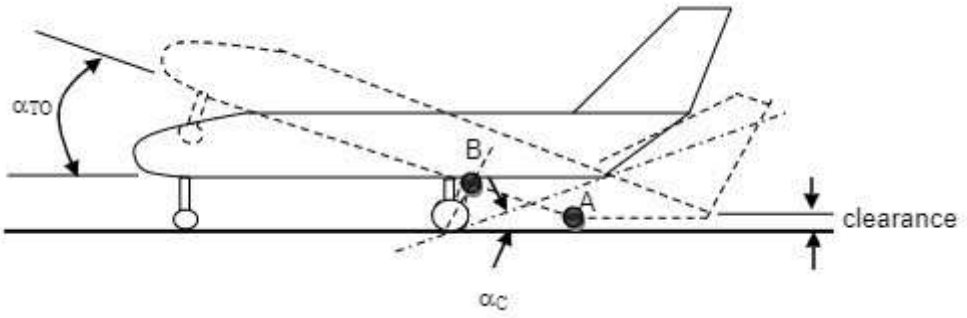

Figure 5.39 - Fuselage clearance on take-off.

Tail-strike can be prevented through an increase in the landing gear height. Another common solution to this problem is to cut the rear fuselage by an upsweep angle. The occurrence of the hit is examined by looking at the angle between ground and the line passing from the main gear contact with ground) to the beginning of upsweep angle at the fuselage (i.e. αc). The take-off rotation ground clearance requirement to prevent a fuselage hit is as follows:

$\alpha c \geq \alpha To$

where the clearance angle is:

$$\alpha c = tan^{-1}(H/AB) \quad \text{…(eq 5.9)}$$

H = Distance between the fuselage and the runway

If the clearance angle (αc) is less than the aircraft rotation angle (αTo) during take-off, the fuselage will strike the ground.

2. Wheel Base

Wheel base(B) has an important role to play on the load distribution between primary (i.e. main) gear and secondary (e.g. nose, or tail) gear. Wheel base influences the ground controllability and ground stability. Therefore, the wheel base must be carefully determined and an optimum value needs to be calculated to ensure it meets all relevant design requirements.

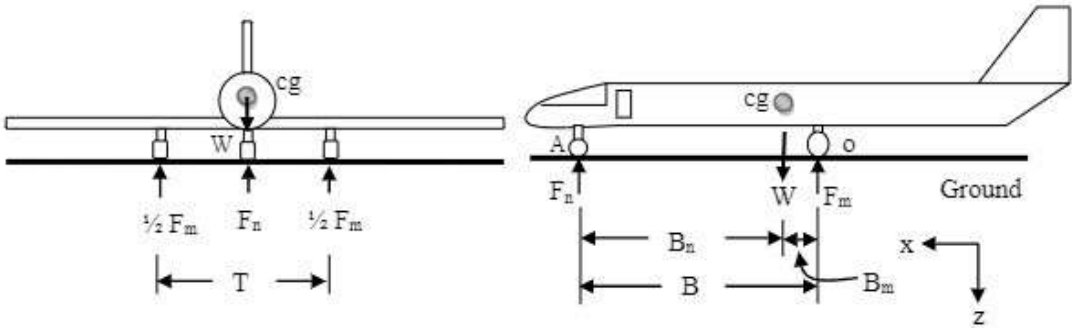

Figure 5.40 - Wheelbase and track width.

The aircraft weight (W) is carried by two main gears and one nose gear. Due to the steering requirement, typically the nose gear must not carry less than about 5 percent of the total load and also must not carry more than about 20percentof the total load (e.g. aircraft weight). Thus, main gear carries about 80%to 95%of the aircraft load. The loads on main and nose gears are denoted by Fm and Fn respectively.

Calculation of the static loads is performed by employing equilibrium equations:

$$Fx = 0,\ Fn + Fm = W \qquad \ldots(\text{eq } 5.10)$$

$$Mo = 0,\ Fn.B - W.Bm = 0 \qquad \ldots(\text{eq } 5.11)$$

The load on the main gear must be divided equally between left and right gear, so each wheel will carry one half of the main gear load.

Apart from the static load landing gear experiences dynamic loading due to aircraft acceleration and deceleration during take-off and landing. The nose gear will experience a dynamic loading during the landing operation when the aircraft is braking. The equation for breaking can be given as:

$$\sum Mo = 0 \Rightarrow Fn.B - W.Bm - (W|\alpha l|Hcg)/g \qquad \ldots(\text{eq } 5.12)$$

where αl = *Breaking deceleration*

For dynamic loading: -

$$F = (|\alpha l|.W.Hcg)/gB \qquad \ldots(\text{eq } 5.13)$$

The above equations help us in determining the position of the landing gear.

3. Wheel Track

Wheel track (T) is the distance between the most left and the most right gears.

The value of wheel track depends on the following requirements; -

1. Ground lateral control,

2. Ground lateral stability

3. Structural integrity.

Wheel track should be sufficient to ensure that the aircraft does not roll over during cross winds and taxiing.

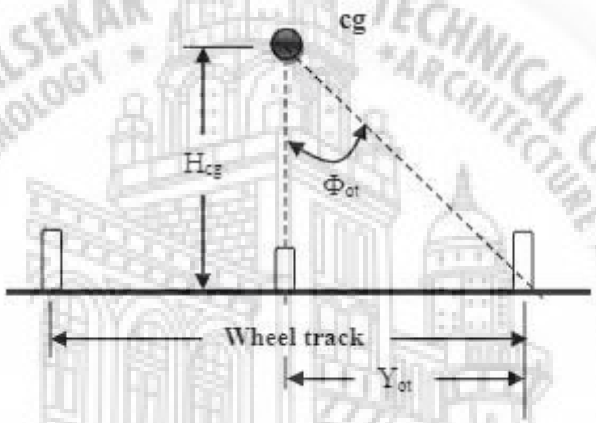

Figure 5.41 - Overturn angle (φt).

The overturn angle (φt) will be influenced by the forces which will be able to tip over the plane such as:

1. Centripetal force on turning
2. Cross wind force

$$Fc = mv^2/R \qquad \text{...(eq 5.14)}$$

where, v = aircraft ground speed

R = radius of the turn

$$Yot = Hcg.Fc/mg \qquad \text{...(eq 5.15)}$$

Therefore,

$$T \geq 2\,Hcg.Fc/mg \qquad \text{...(eq 5.16)}$$

$$\tan(\varphi t) = Yot / Hcg \quad \text{...(eq 5.17)}$$

Cross wind force on aircraft is

$$Fw = \rho.As.Cds.Vw^2/2 \quad \text{...(eq 5.18)}$$

where , Vw = Wind speed

Cds = aircraft side drag coefficient

$$Yot = Fw.Hcg/W \quad \text{...(eq 5.19)}$$

3. Tip Back Angles Requirement and Tip Forward Angles Requirement

Tipback is the maximum nose up angle.

$$\alpha tb = tan^{-1}(xmg/hcg) \quad \text{...(eq 5.20)}$$

$$\alpha tb \geq \alpha to + 5^{\circ} \quad \text{...(eq 5.21)}$$

where, αtb is the Tip back angle

αto is the Take-off angle

The tip forward angle is the angle between the vertical and the line passing through the aircraft's most forward cg and the contact point between tire and the ground.

$$\alpha tf \geq \alpha ti + 5^{\circ} \quad \text{...(eq 5.12)}$$

where, αti is the inclination angle

5.9.5 Endurance Landing Gear

Based on the literature study done above, fixed gear of tri-cycle configuration was chosen for our aircraft. A leaf spring structure will be used for shock absorbing.

5.9.5.1 Landing Gear Calculations

1. Clearance Height and Maximum Takeoff Angle: -

The critical component for determining the clearance height is the 21" propeller of our V-TOL motors which is at a distance of 650 mm from the cg.

Taking $\alpha c = 15^{\circ}$ i.e clearance angle,

and distance of main gear from cg as 210 mm

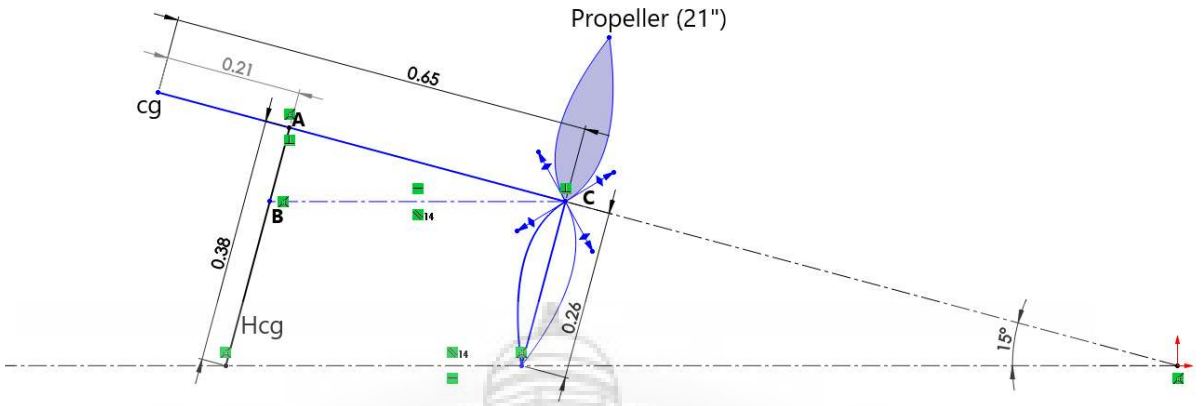

Figure 5.42 - Landing gear geometry.

In Right Δ ABC,

AC = 0.65 - 0.21 = 0.44

Angle BCA = 15°

$$sin(\alpha c) = AB/AC$$

$$AB = 0.11388 \text{ m}$$

Therefore,

$$Hcg = 0.3738 \text{ m} \approx 380\ mm$$

Therefore to prevent propeller strike we need to ensure a takeoff angle of less than 15°

$$\alpha c\ (15^{\circ}) \geq \alpha to$$

2. Wheelbase: -

   For effective steering weight of the nose gear should be around 5-20% , refer figure 5.40.

   Taking 80:20 distribution on main gear and nose gear respectively,

   M = 14 kg (mass of endurance aircraft)

   W = 14*9.81 = 137.34 N

Fm = 0.8*W = 109.72 N

Fn = 0.2*W = 27.468 N

Bm = 0.21 m (from above)

Taking moment about cg,

$$\sum Mo = 0 \ (Moment\ about\ cg),$$

$$Fn * Bn = Fm * Bm$$

$$Bn = 0.8391\text{m} \approx 839.1\ mm$$

Therefore total wheelbase,

$$B = Bn + Bm$$

$$B = 1.0491\ mm$$

3. Minimum Track Width: -

Mass of Endurance craft = 14 kg

Velocity of endurance craft turn 2m/s

Radius of the turn = 1m

$$Fc = M * V^2/R$$

$$Fc = 14 * 2^2/1$$

$$Fc = 56\ \text{N}$$

$$\varphi ot = tan^{-1}(Fc/(m * g))$$

$$\varphi ot \approx 23°$$

$$T = 2* Fc*Hcg/(m*g)$$

$$T = 0.31\ \text{m}$$

T is the minimum track width required to perform the turn at overturn angle 23°

5.9.5.2 Endurance Landing Gear Design

5.9.5.2.1 Main Gear Initial design

Leaf Spring Design was chosen for our main gear and the dimensions were made to satisfy the above calculations.

The material shortlisted for the design were Al 7075 and Carbon fibre.

Al-7075 was eliminated due to high weight, cost and unavailability.

Carbon Fibre of 5mm thickness was to be used.

The weight of the leaf spring was calculated to be 275g.

Figure 5.43 - Main gear.

5.9.5.2.1.1 F.E.A Of The Landing Gear

A good approximation of the real scenario was to fix the upper base on which the aircraft would rest and to apply loads at the ends where the wheel would be.

A force of 450 N on each wheel would satisfy our 3g load test.

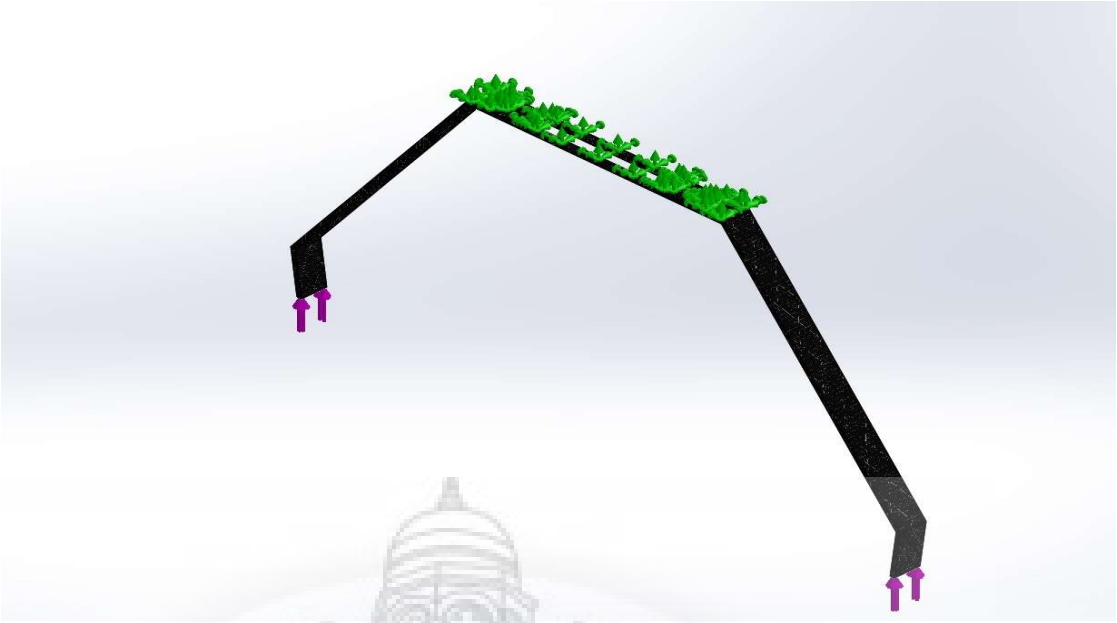

Figure 5.44 - Fixture and load.

Study Results

Name	Type	Min	Max
Stress	VON: von Mises Stress	1.026e-07N/mm^2 (MPa) Node: 15420	5.712e+02N/mm^2 (MPa) Node: 61405

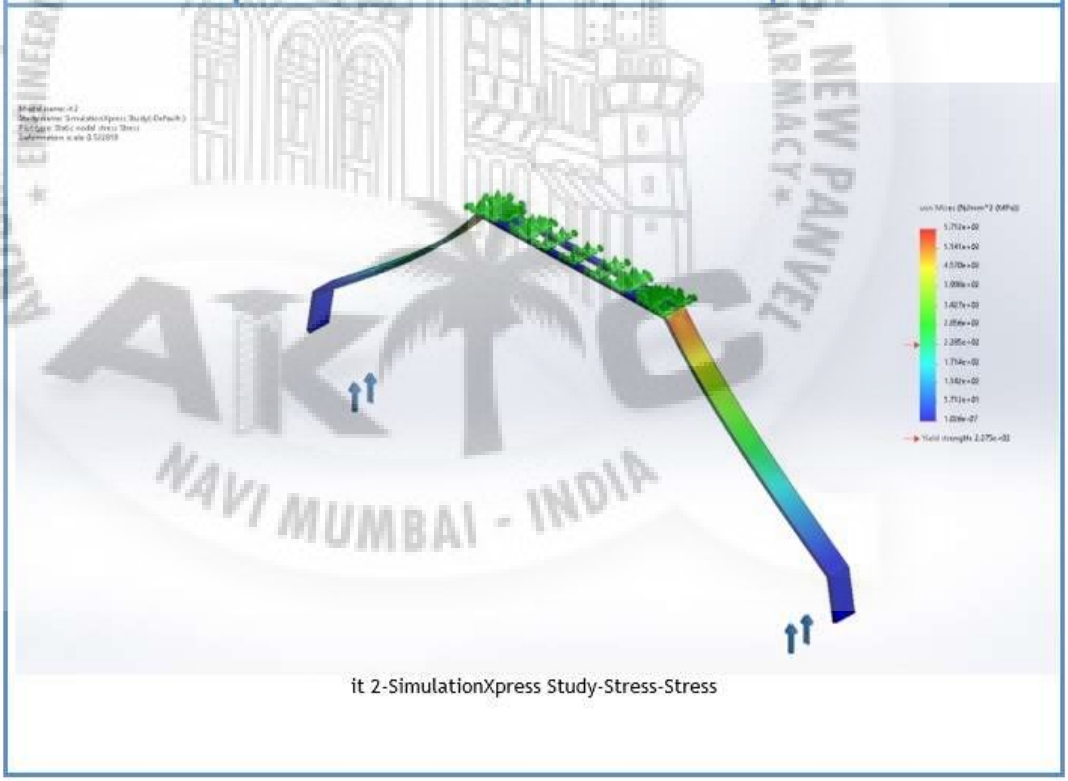

it 2-SimulationXpress Study-Stress-Stress

Name	Type	Min	Max
Displacement	URES: Resultant Displacement	0.000e+00mm Node: 8	1.552e+02mm Node: 2734

Figure 5.45 - Stress and Displacement from F.E.A.

The results obtained were overwhelming, a peak stress of 571MPa showed that our design had some serious design flaws and needed a complete remodel.

The stresses particularly around the bends were very high and the thickness of the material of 5mm was too low to contain the stress.

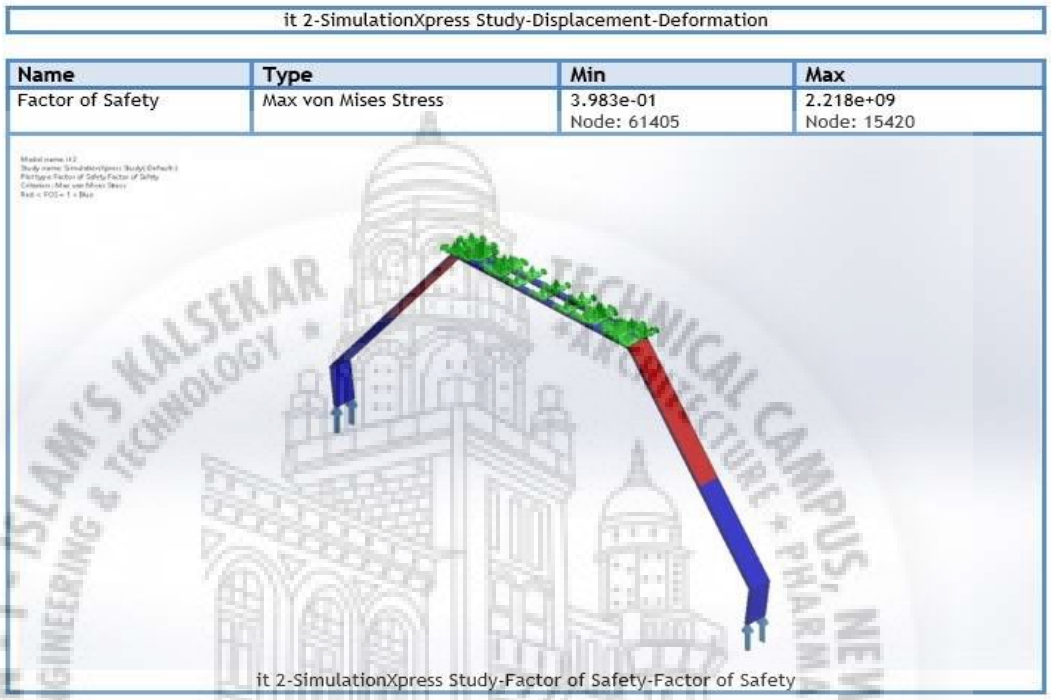

Figure 5.46 - F.O.S.

5.9.5.2.2 Main Gear Improved Design

On further analysis it was found out that the shape of the initial design was causing accumulation of stresses at bends and the rib thickness was too low.

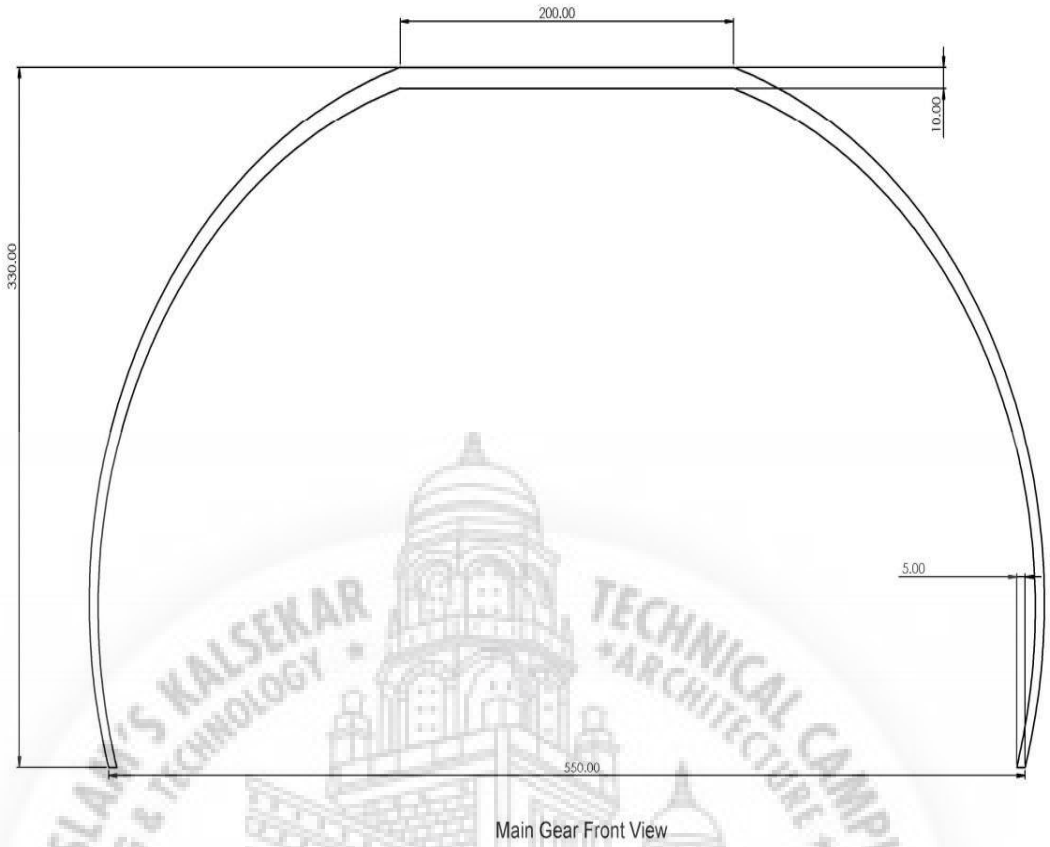

Figure 5.47 - Main gear with improved design front view.

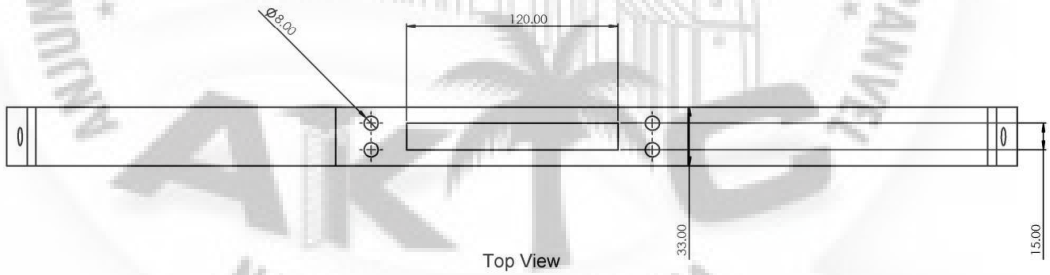

Figure 5.48 - Main gear with improved design top view.

The design changes included: -

1. A circular design was found to distribute the stresses more effectively.
2. Maximum thickness was increased from 5mm to 10mm.
3. As the weight increased significantly, variable thickness design was chosen.

4. The thickness changes from 5mm at the end where less material is required to 10mm at the highly loaded region.
5. Cut outs were provided to reduce the weight.

5.9.5.2.2.1 F.E.A of the new design

Study Results

Name	Type	Min	Max
Stress	VON: von Mises Stress	1.344e-03N/mm^2 (MPa) Node: 67776	1.886e+02N/mm^2 (MPa) Node: 90478

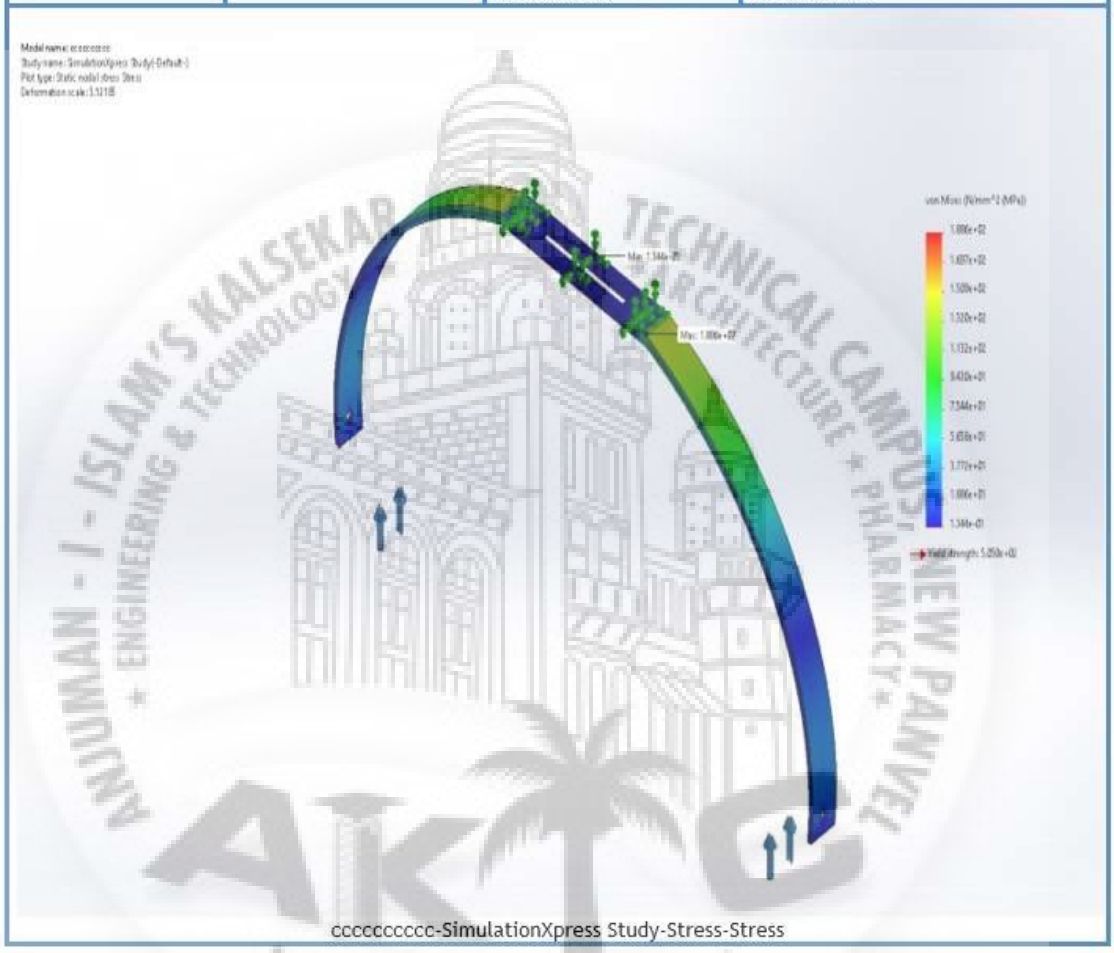

Name	Type	Min	Max
Displacement	URES: Resultant Displacement	0.000e+00mm Node: 62	1.969e+01mm Node: 341

Figure 5.49 - Stress and Displacement from F.E.A.

With a peak stress of around 186MPa the newer design changes ensure moderate stress levels at 3g loading. The landing gear displaces by around 19.7 mm at this loading.

The weight of the leaf spring is around 415 grams.

Figure 5.50 -. F.O.S of the Main Gear.

Figure 5.51 - Main gear.

5.9.5.2.2.2 Drag Force Calculation

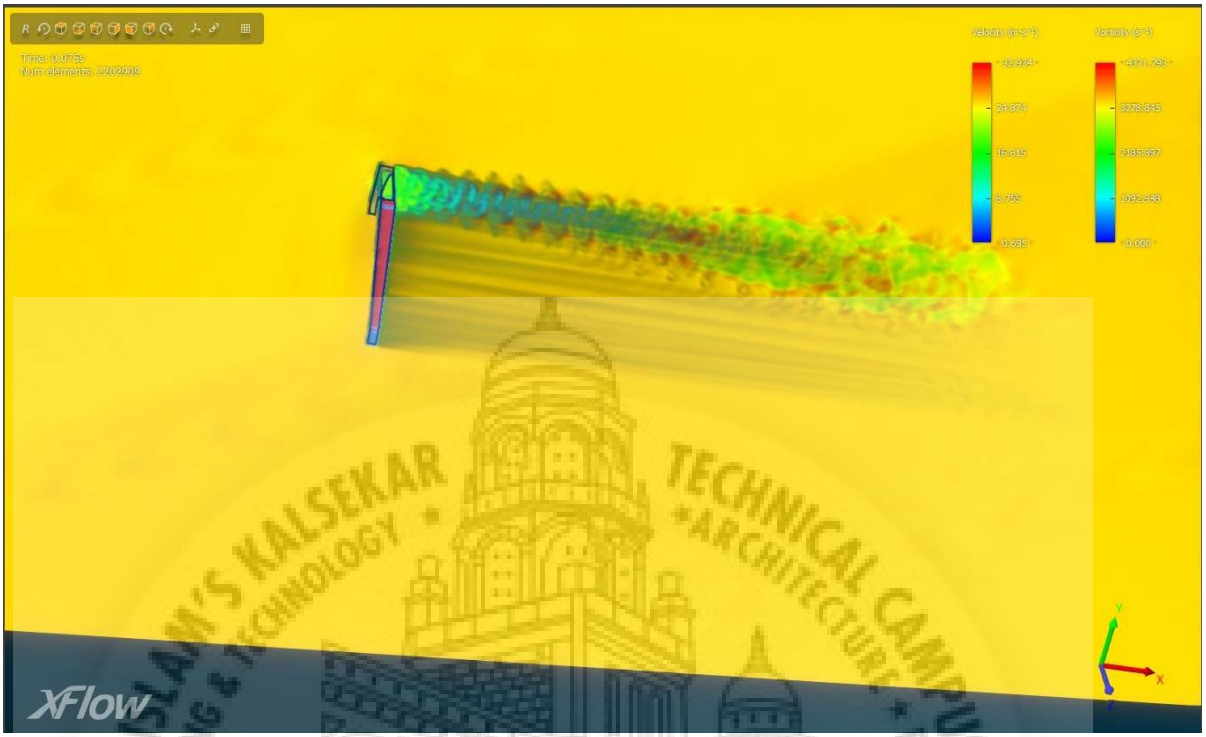

Figure 5.52 - C.F.D of the main gear.

Finally C.F.D was done to calculate the drag force generated by the landing gear. The analysis was done at cruising speeds of our endurance aircraft i.e at 26 m/s and at 0 AoA.

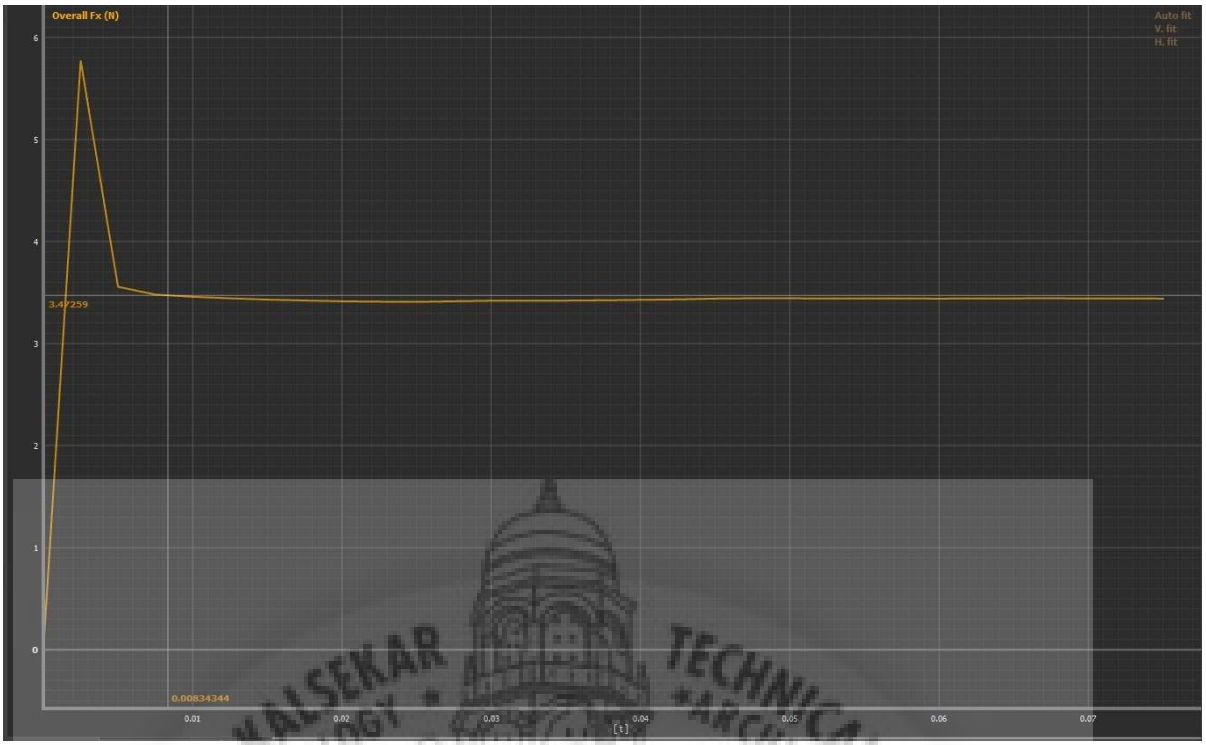

Figure 5.53 - Landing gear drag graph.

The results obtained confirmed that the aircraft does not need a retractable system as the drag force generated is very insignificant at just 2 N .

The complexity and the weight of a retractable is a bigger disadvantage to us than the drag force generated by the fixed gear.

5.9.5.2.3 Nose Gear

Figure 5.54 - Oleo Strut for Nose Gear.

For the nose gear offset oleo struts of 280mm were chosen. These struts have been used reliably for aircraft of our size. The load they are expected to carry is 20% of the drone weight i.e 2.8 kilos. The weight of the nose gear is 154 grams

5.9.5.2.4 Tires

Figure 5.55 - Tires.

Rubber tires of 4” inch were chosen from hobbyking. These tyres provide extra cushion and dampen some force making the work of landing gear easier. All three gears will use the same set of tyres. They weigh around 90 grams each.

5.9.5.2.5 Net Weight Of Landing Gear

Table 5.5 - Net Weight of Landing Gear.

Sr. No.	Component	Weight
1.	Main Gear Leaf spring	415 g
2.	Nose Gear	154 g
3.	Tires	90*3 g

$$Total\ weight\ =\ 839\ g\ =\ 0.839\ kg$$

Percentage of Landing gear weight to the aircraft body

$$(0.839/12) * 100\ =\ 6.992\%$$

Which satisfies the criteria of the weight of landing gear accounting for 5 to 10% weight of the aircraft.

Chapter 06

Electronics And Control Systems

The electronic components used in the development of this project were chosen with care, since each component used meets the project's specifications. Thrust Motors, Servo Motors, ESCs, Connectors, Batteries, Pixhawk, GPS, Buzzer, and other electronic components are used in Endurance Craft.

6.1 Thrust Motors

Thrust is generated when a high-powered motor is used to produce an output. It may be used for a variety of ships and motors, including vessels, motorboats, propellers, and piston engines. Thrust motors are important for the drone's lifting.

The thrust motor used for the drone is Turnigy Aerodrive SK3-5055.In order to produce the lift, three Thrust motors would be used. They are arranged in such a way as to have optimum longitudinal and lateral stability. The following is a list of requirements that correspond to the needs of the drone's lift and propulsion.

Table 6.1 - Specification of Turnigy Aerodrive SK3-5055. [23]

Sr. No.	Parameter	Value
1.	Turns	18T
2.	Voltage	6 - 10S Lipoly
3.	RPM/V	280KV
4.	Internal Resistance	0.031 Ohm
5.	Max Loading	60A
6.	Max Power	1510W
7.	Shaft Dia	6mm
8.	Bolt Holes	25mm
9.	Bolt Thread	M4
10.	Weight	369g
11.	Motor Plug	4mm Bullet Connector

Placement of motors for any drone is crucial. As it determines the aesthetics and ergonomics of the drone in visual aspect and the amount of thrust it would generate on each motor ends in order to obtain maximum stability during takeoff, landing and while the flight is in the air.

Following is orthographic representation of the placement of the Thrust motors determined for this purpose ;

Figure 6.1 - Placement of all Thrust Motors.

During takeoff, the front two motors are in charge of lifting and balancing the entire drone. The propulsion of the drone is handled by a single rotor at the rear of the drone. With the aid of a structural and electronic integrity (Tilt rotor mechanism), these high-power motors may also make a vertical take-off and landing, allowing the maximum capacity of these thrust motors to operate in a specific state.

Following a figure represents an actual Thrust Motor used in the drone;

Figure 6.2 - Turnigy Aerodrive SK3-5055. [23]

Below is an Orthographic representation with dimensions for the Thrust motor Turnigy Aerodrive SK3-5055;

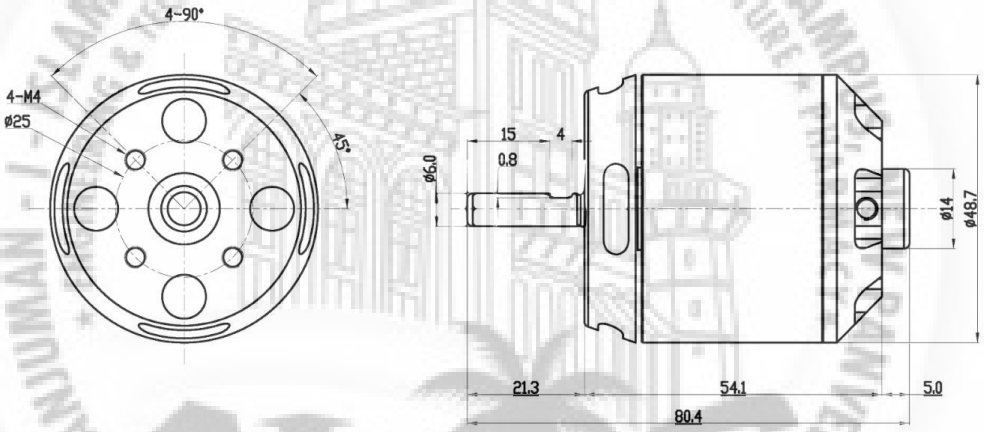

Figure 6.3 - Orthographic Representation for Turnigy Aerodrive SK3-5055.

6.2 ESC

Electronic Speed Controller or ESC is a circuit that regulates and monitors the rotational speed of an electric motor. It could also be capable of engine reversal and dynamic braking. In electrically operated radio controlled versions, miniature electronic speed sensors are used. The speed of the drive motors in full-size electric vehicles is also regulated by systems.

A few safety measures are normally included in ESCs built for radio-controlled aircrafts. If the battery capacity is inadequate to keep the electric motor operating, the ESC will limit or shut off power to the motor while allowing the use of the ailerons, rudder, and elevator

functions to continue. This encourages the pilot to keep hold of the plane and glide or fly to safety on low fuel.

ESCs are an important part of modern quadcopters and other multirotors because they provide high-speed, high-frequency, high-resolution 3-phase AC power to a motor in a very small Package. The variable speed motors that drive the propellers are completely reliant on these craft. This wide range of motor/prop speed variance and fine RPM modulation provides much of the control required for a quadcopter to operate. In the development of the project, two forms of ECS were used.

6.2.1 Brushless ESC (YEP-100A)

The YEP ESC series features a super smooth linear throttle response, making them ideal for fixed-wing applications. This ESC is in a class by itself, thanks to its super smooth soft start and ultra high resolution throttle response. It can be programmed using either the optional programming card or the transmitter stick inputs. It has high anti-interference capability and automatically adjustable low voltage cut-off safety.

It also has a protected power-on feature that prevents the motor from starting before the throttle is returned to the lowest position. Anti-sparking circuitry is also used in the ESC, which eliminates connection sparks.

Following a table represents specification for Brushless ESC (YEP-100A).

Table 6.2 - Specification for Brushless ESC (YEP-100A). [25]

Sr. No.	Parameters	Value
1.	Max Cont Current	100A
2.	Max Burst Current	120A for 10 seconds
3.	Input Voltage	2-6 cells li-XX
4.	BEC	5.5V/6A Switching
5.	PWM	8~16 KHz
6.	Max RPM	240,000rpm for 2 Poles Brushless Motor
7.	PCB size	50x30mm
8.	Weight	81g (including wires)

Following is a figure representing the Brushless ESC (YEP-100A).

Figure 6.4 - Brushless ESC (YEP-100A). [25]

6.2.2 AeroStar WiFi 100A Brushless

Brushless electronic speed controls (ESCs) from Aerostar are designed for RC fixed-wing aircraft but can also be used in helicopters and quadcopters; multirotors. They have a super smooth initialization, a linear throttle response, and a variety of safety features. This device is equipped with an efficient microprocessor with excellent anti-interference capabilities.

It has an adjustable startup mode for planes or helicopters, as well as safety measures that stop the motor if the throttle is set too fast on power up. This also has Active Switch Continued Flow or ASCF technology, which is more efficient and reduces heat generation significantly. It is supported with Propeller Brakes.

Following a table represents specifications of AeroStar WiFi 100A Brushless ESC with 5A BEC.

Table 6.3 - Specifications for AeroStar WiFi 100A Brushless ESC with 5A BEC. [26]

Sr. No.	Parameters	Value
1.	Input Voltage	2~6S lipo battery
2.	Continuous Current	100A
3.	Burst Current	120A
4.	BEC Output	8.4V/7.4V/6V/5V, 5A
5.	Programmable	Yes
6.	Dimensions	82.5x39.5x23.5mm
7.	Weight	125g
8.	Rx Connector	JR type (white, red, black)
9.	Wifi Connect wire	JR type (orange, red, brown)
10.	Reverse wire	Single Orange wire

Following a figure represents AeroStar WiFi 100A Brushless ESC with 5A BEC.

Figure 6.5 - AeroStar WiFi 100A Brushless ESC with 5A BEC. [26]

6.3 Batteries

A battery is a power source for electrical devices that consists of one or more electrochemical cells with external connections.

The negative terminal is the source of electrons that will pass to the positive terminal from an external electric circuit. A redox reaction occurs when a battery is attached to an external electric load, converting high-energy reactants to lower-energy components, and the free-energy difference is transmitted to the external circuit as electrical energy.

Batteries come in a variety of shapes and sizes, ranging from tiny cells that power hearing aids and wristwatches to slim, lightweight cells that power smartphones, to large lead acid or lithium-ion batteries in cars, and, at the most extreme, massive battery banks the size of rooms that provide standby or emergency power for telephone exchanges and electronic data centres.

The two classified forms of batteries are primary and secondary form; where primary batteries are intended to be used until they are fully depleted of energy before being discarded. They can't be recharged and their chemical reactions aren't usually reversible. As the battery's stock of reactants runs out, it ceases supplying current and becomes useless. While the secondary batteries can be recharged, which means that by adding electric current to the battery, the chemical reactions in the cell can be reversed. This regenerates the initial chemical reactants, allowing them to be reused, recharged, and reused.

Any main batteries, such as those used in telegraph circuits, were resurrected by replacing the electrodes. Owing to dissipation of active materials, electrolyte degradation, and internal corrosion, secondary batteries cannot be recharged indefinitely.

The Two basic types of common use batteries are Lithium ion batteries and Lithium polymer batteries. Following a table explains a brief difference between two batteries.

Table 6.4 - Difference between Lithium Ion and Lithium Polymer.

Sr. No.	Parameters	Lithium ion	Lithium Polymer
1.	Ageing	Loses actual Charging capacity over time	Retains Charging capacity better than Li-ion
2.	Energy Density	High Energy Density	Low as compared to Li-ion
3.	Conversion Rate	85%-95%	75%-85%
4.	Safety	More Volatile	Less chance of explosion
5.	Cost	Cheaper	Slightly expensive (+30%)
6.	Weight	Heavier	Light Weight
7.	Charging Duration	Longer Charge duration	Comparatively Shorter charge duration

Based on the requirements of the project i.e. Light weight, Less volatile; Less charging duration, and availability in different shapes. Lithium Polymer batteries were selected for the further progress of the project.

Two Li-po batteries were selected for their particular purposes.

Table 6.5 - Li-po Batteries and their use.

Sr. No.	Li-po Battery	mAh	Purpose
1.	Gens Ace	5600	Main Source
2.	Tattu	2200	Auxiliary Source

6.3.1 Gens Ace Li-po Battery

Gens Ace Lithium Polymer battery is the main source of power. This battery is highly suitable for RC helicopters in general. This battery has a sole purpose to power all the main

electronic components which are responsible for the flight to take-off, landing and flight propulsion. This unit single handedly powers three Thrust Motors, Servo motors via respective ECS which are allotted to each pair of motors.

Table 6.6 - Specifications of Gens Ace Li-po Battery. [31]

Sr. No.	Parameters	Value
1.	Capacity	5600mAh
2.	Voltage	22.2V
3.	Max Continuous Discharge	80C
4.	Weight	800gms
5.	Dimensions	149*50*56
6.	Balance Plug	JST-XHR
7.	Discharge Plug	EC5
8.	Charge Rate	1-3

Figure 6.6 - Gens Ace 5600mAh Battery. [31]

6.3.2 Tattu Lipo Battery

Tattu Li-po Battery is the Auxiliary Battery. This battery also serves as an emergency backup to the Main Battery, if it runs out of juice or ends up getting faulty. Tattu Battery also serves as the source of powering other accessories included in the drone. It also keeps the RAC unit working and intact.

Table 6.7 - Tattu Battery. [32]

Sr. No.	Parameters	Value
1.	Capacity	2200mAh
2.	Voltage	11.1V
3.	Max Continuous Discharge	35C
4.	Max Burst Discharge	70C
5.	Weight	195g
6.	Dimensions	108*33*25 mm
7.	Balance Plug	JST-XH
8.	Discharge Plug	Dean/T-plug
9.	Charge Rate	1-3C General; 5C Max

Figure 6.7 - Tattu 3s battery. [33]

6.4 Servos

A servomotor is a rotary or linear actuator that allows for precise angular or linear position, velocity, and acceleration control. It consists of an appropriate motor coupled with a position feedback sensor. It also necessitates a sophisticated controller, which is usually a dedicated module designed especially for servomotors.

This motor's output shaft can be shifted to a certain angle, location, and velocity that a normal motor cannot. A normal motor is used in the Servo Motor, which is coupled with a sensor for spatial feedback. The controller is the most crucial component of the Servo Motor, which was engineered and built especially for this use.

The servo motor is a closed-loop control system that uses positional feedback to control rotational or linear speed and direction. An electric signal, either analogue or digital, controls the engine, determining the amount of acceleration that indicates the shaft's final command location. Encoders are a form of sensor that provides speed and location input. This circuitry is housed inside the motor housing, which is normally equipped with a gear mechanism.

For our project, we chose MG995 servo motors with 180° rotational independence. It comes with a three-pack for this particular drone, so as to fit in each of the Tilt rotor mechanisms.

The drone will now allow the higher potentials of autonomous flight with the aid of the servo-tilt rotor mechanism. To improve the flight profile's stability.

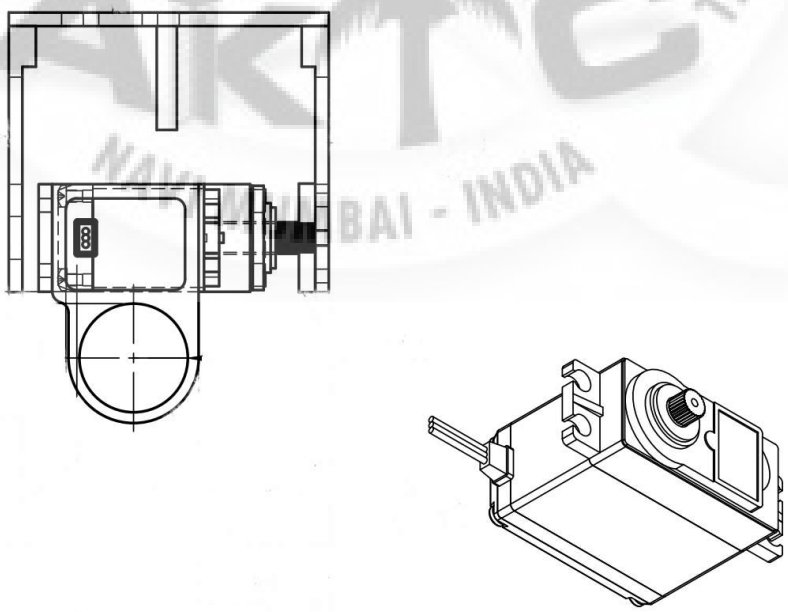

Figure 6.8 - Servo motor MG995 with Tilt rotor assembly.

Following is a table presenting the specification list of Servo motor MG995.

Table 6.8 - Specification for the Servo motor MG995. [24]

Sr. No.	Parameters	Value
1.	Weight(gm)	55gm
2.	Operating Voltage	4.3 - 7.2 V
3.	Operating Speed	4.8V20sec/60°
4.	Operating Speed	6.6V16sec/60°
5.	Stall Torque	4.8V10 kg-cm
6.	Stall Torque	6.6V12 kg-cm
7.	Operating Temperature (°C)	30 °C- 60 °C
8.	Dead Band Width	1 µs
9.	Gear Type	Metal
10.	Rotational Degree	180 deg
11.	Cable Length	30mm
12.	Length	40.5mm
13.	Width	20mm
14.	Height	44mm
15.	Shipment Dimensions	9*8*3cm

Figure 6.9 - Servo Motor MG995. [24]

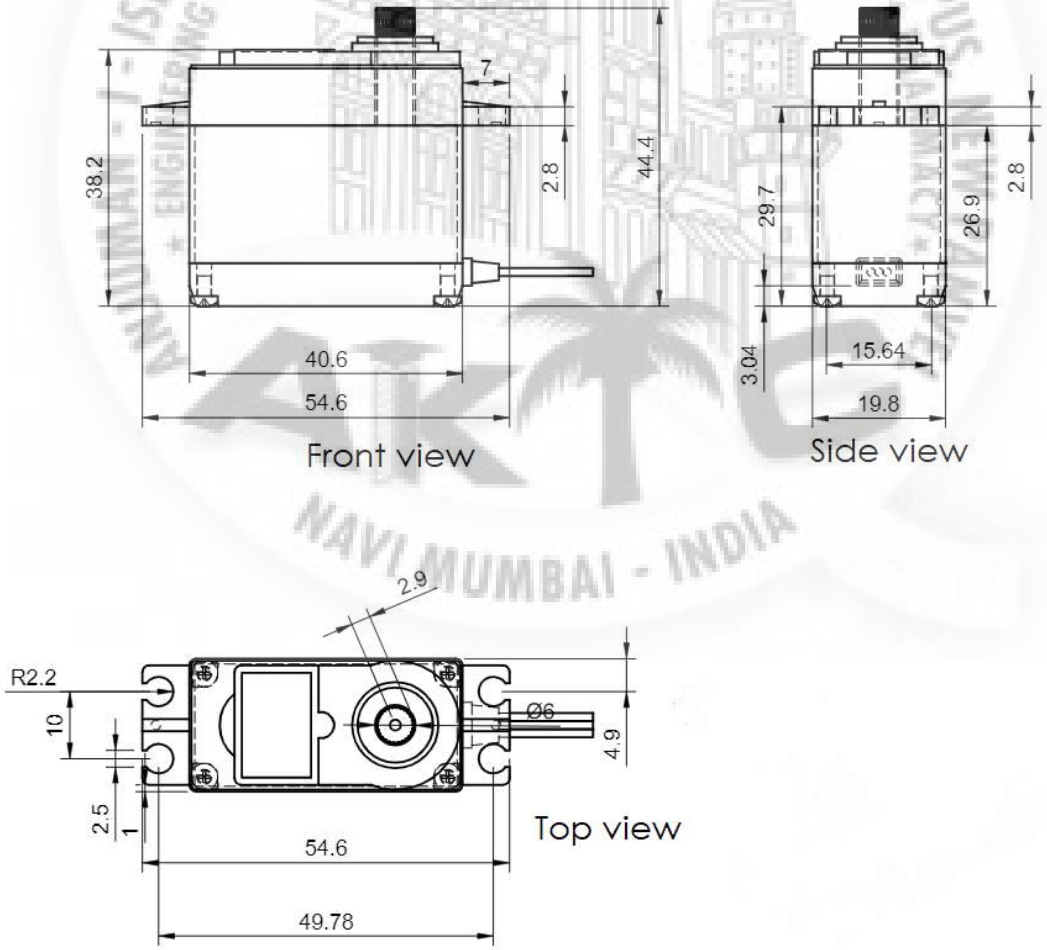

Figure 6.10 - Orthographic representation of Servo motor MG995 with dimensions.

6.5 GPS

The Global Positioning System (GPS) is an important device that aids in the tracking of aircraft during flight. Its use isn't limited to monitoring, though. It's also a crucial component of achieving Autonomy. With the installation of a GPS device, it is simple to position the flight on autopilot mode with additional intelligence, allowing it to take off without the need for human intervention. The GPS unt selected for this particular project is the Radiolink SE100 GPS module for Pixhawk.

Table 6.9 - Specification for Radiolink SE100 GPS Module for PixHawk. [27]

Sr. No.	Parameters	Value
1.	Positional Accuracy	1m - concurrent GNSS 2.5m - single GNSS
2.	Velocity Precision	0.1m/s
3.	Max height	50000m
4.	Max speed	515m/s
5.	Max Acceleration	4G
6.	Max update rate	upto 18Hz
7.	Sensitivity Tracking and Na	-167dBm; Reacquisition-163dBm; Cold Start-151dBm; Hot start-159dBm
8.	Time to first fix	Cold Start-26s; Hot Start-1s
9.	Power supply	voltage 3.3 VDC + -5%, current 50~55mA

Figure 6.11 - Radiolink SE100 GPS Module for PixHawk. [27]

6.6 Buzzer

The buzzer is a device that aids in determining the state of the Communication unit of the aircraft. It can be used to alert the driver to changes in the vehicle's status. This may be an active device, only requiring voltage added to generate a single frequency tone; or a passive piezo device powered by PWM capable of generating variable tones, depending on board capabilities.

Following a table explains different types of active buzzer patterns.

Table 6.10 - Active Buzzer pattern. [29]

Sr. No.	Status	Pattern
1.	Arming	3 Sec Long Beep
2.	Arming Failure	Single Beep
3.	Disarmed	Single Beep
4.	Battery Failsafe	Single Beep repeating after every 3 sec
5.	EKF Failure	Beeeep-Beeep-Beep-Beep
6.	Lost Vehicle	Beep-Beep repeating every 3 sec

Figure 6.12 - Buzzer for Pixhawk PX4. [27]

6.7 Autopilot

Mission planner is used to calibrate and monitor the Pixhawk. ArduPilot is a multi-copter, conventional helicopter, fixed-wing aeroplanes, rovers, submarines, and antenna tracker autopilot system. ArduPilot Autopilot Software Suite that can fly multirotor drones, fixed-wing and VTOL planes, helicopters, ground rovers, boats, submarines, and antenna trackers. The ArduPilot software suite includes ground station controlling software such as Mission Planner, APM Planner, QGroundControl, MavProxy, Tower, and others, as well as navigation software that is usually referred to as firmware when it is compiled to binary form for microcontroller hardware targets operating on the vehicle (Copter, Plane, Rover, AntennaTracker, or Sub).

By using the mission planner which is also an open source software, the tracking of the drone and its various flight factors such as pitch, roll; altitude, etcetera can be tracked.

Figure 6.13 - Mission Planner set Home at AIKTC campus.

To pair this software to drone hardware, a unit is used known as pixhawk.

6.7.1 Pixhawk

Pixhawk is an integral part of the drone. It could also be called the brains of the drone. As the pixhawk is directly responsible for all the static and dynamic motions of the drone. Such as in certain cases where the flight is in the air, it would require stability with the propulsion provided from the rear end. So in order to achieve that, pixhawk would simply send a signal of increasing speed to one end of the wing span where the gust effect is enough to destabilize the drone and would reduce the speed of the rotor in the other side of the wing, and this would continue till the drone is stabilized.

While in other conditions such as getting the vertical take-off and landing, pixhawk would simply send signals to all the servo motors to just face upwards vertical for the front two rotors and to face downwards vertical to the rear rotor, and in conditions of destabilize drone it would again provide high power through ESC to the lacking side till it is stabilized again.

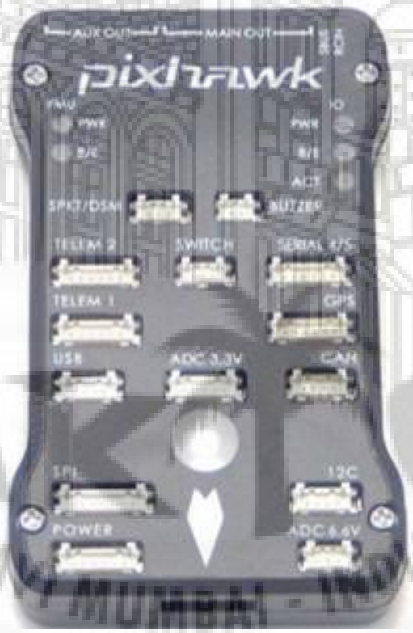

Figure 6.14 - Pixhawk. [35]

Pixhawk, being the brains of the drone, has many important components connected to it such as radiolink, GPS, buzzer, Safety Switch, etc. Completes in achieving full Autonomous mode and Manual mode just to switch in between.

Following is a Figure 6.15, Representing color coding which pixhawk uses for communicating while in the preparation stage.

Figure 6.15 - Color Coding to understand Pixhawk. [36]

Pixhawk is a versatile electronic component and its use goes beyond the scope of Aircraft development. Thus it is loaded with many ports of applications and memory expansion for professional use. Some ports such as Telemetry port 1, USB, GPS port, Safety Switch port, LED indicator, Power to name a few were used in the course of this project.

Following is a Figure 6.16, defining each and every port available in the Pixhawk.

Figure 6.16 - Ports of Pixhawk. [37]

6.8 Radiomaster

Radiomaster is one of the most advanced drone controllers with an Internal multi-protocol RF system. And is it compatible with OpenTX. Radiomaster has 16 model memories which are also expandable, which opens enough ways for the research and development of the controlling of the drone; manual and autonomous. Radiomaster can also accept JR/Frsky style modules. With its Outdoor readable capabilities, it expands the usability of the drone at certain terrain locations with ease.

Following is a table for specification for Radiomaster TX16S.

Table 6.11 - Specifications for Radiomaster TX16S. [30]

Sr. No.	Parameter	Value
1.	Type	TX16S w/Hall Sensor Gimbals 16ch Multi-Protocol OpenTx Transmitter
2.	Frequency	2.4GHz
3.	No of Channels	16
4.	Modes	Modes 1~2
5.	Model Memories	16 (expandable with SD card)
6.	RF	Internal multi-protocol system
7.	Compatibility	OpenTX
8.	Screen	4.3" color, daylight readable
9.	Gimbal	Non-contact 3D vector Hall effect
10.	Functions	Voice and vibration reminder
11.	Telemetry	Supported (protocol and receiver dependent)
12.	Status	3 color LED display
13.	UART Ports	2
14.	SD Card	Micro SD card slot included
15.	Input Voltage	7~8.4V DC
16.	Working Current	400mAh (excluding external module)
17.	Battery Compartment	97x52x25mm
18.	Dimensions	183x212x66mm
19.	Weight	736g (excluding batteries)

Figure 6.17 - Radiomaster TX16S. [30]

6.9 Dragon Link Transmitter

Dragonlink transmitter is a special electronic unit used to increase the range of the ground controls and other communications. Due to which the range at which the drone could accelerate and cover the distance would increase significantly.

The transmitter unit selected for the very purpose of increasing the range at minimum frequency is DRAGONLINK 433 MHz.

The Dragon Link Advanced 433 MHZ WiFi is built with the highest-performing, highest-quality components, as well as the most up-to-date and advanced hardware available. The built-in long-range Radio Modem will provide you with any alternative for displaying complete telemetry on laptops, tablets, phones, and other ground station gadgets.

There are no extra measures once the Dragon Link scheme is set up; simply switch on your RC transmitter and ride. This electronic unit is highly compatible and can be used with almost every open software available.

The following table presents the specifications for DragonLink 433MHz.

Table 6.12 - Specifications for DragonLink 433MHz. [34]

Sr. No.	Parameters	Value
1.	Transmitter Module Voltage	5 - 8 Volts
2.	Frequency	433 MHz
3.	Typical Range	40km using supplied Antennas

Figure 6.18 - DragonLink 433MHz. [34]

6.10 Schematics

Wiring Schematics are also an integral section of study, this study deals with all the electrical connections responsible for the complete communication between the structure of the drone and the electronic components, i.e. thrust motors, servo motors; ESCs, batteries; etc. A simplified visual depiction of an electrical system or circuit's actual connections and architecture. It depicts the interconnection of electrical cables as well as where fixtures and components may be attached to the system.

With all the color coding and the minimalism it deals with. it becomes easier to understand and differentiate between all the essential wirings responsible for the functioning of the drone in its desired condition.

6.10.1 Wiring Diagram of Pixhawk

As the Pixhawk being the brain of the drone and responsible for the main functions of the drone; namely switching between the manual and autonomous mode of its working. Thus having a clear map of its construction is equally crucial in the development phase.

The main components attached to the pixhawk are defined in the Figure 6.19, representing all the necessary connections built in the circuit board. These include Safety Switch, Buzzer; Radiolink SE 100, DragonLink; etc.

For the Safety Switch, it is connected to the pixhawk in the switch port. Next to the buzzer allotted port. As for the Dragon link Advance, it is connected to the pixhawk in the Telemetry port 1, which enables the drone to have a wide working range for delivery. A GPS unit is also allotted to the Pixhawk Circuit diagram, where it has a dedicated port for ease of use. due to which the tracking of the drone becomes easy.

All of these configurations with the pixhawk circuit enables the drone to communicate with the drone pilot and complete a certain feedback loop. As all these units convey any errors faced or any success in the steps occurred easily, which in return helps in understanding the drone configuration even better, for the customers and the manufacturers.

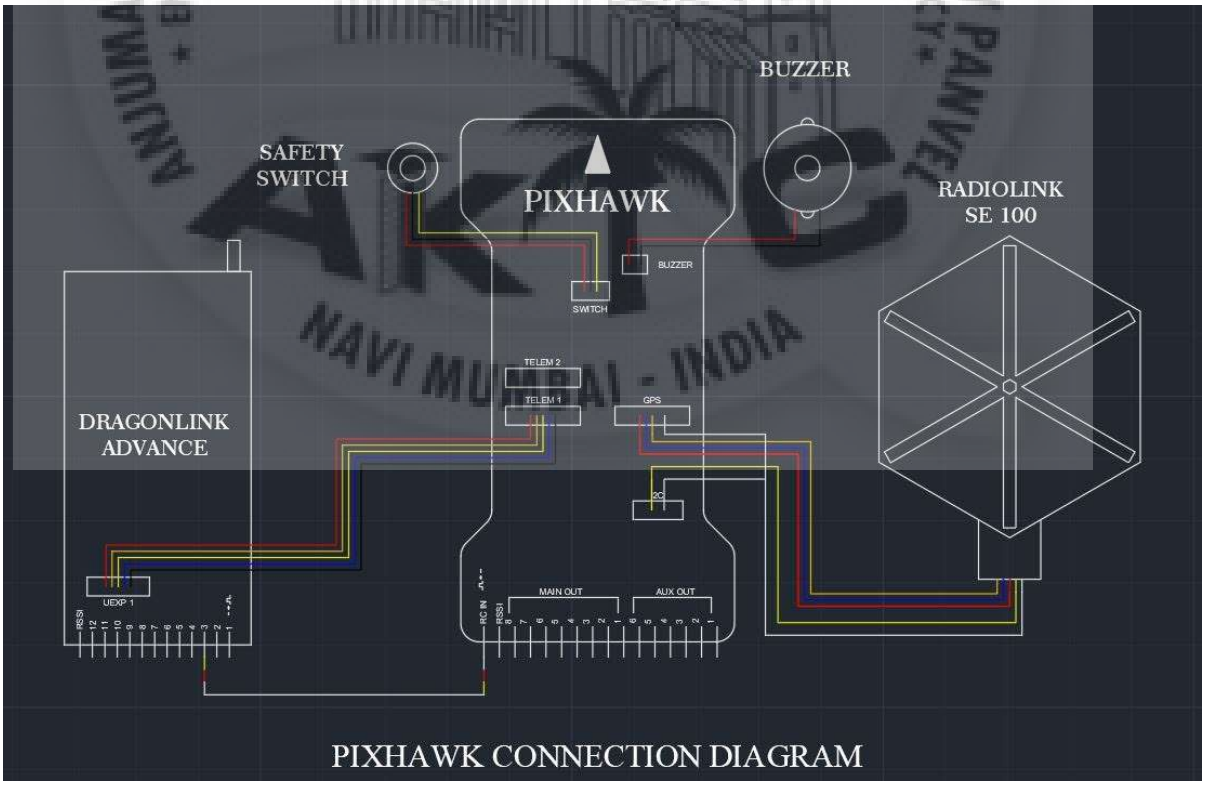

Figure 6.19 - Pixhawk Connection Diagram.

6.10.2 Full Body Wiring Diagram

Following the pixhawk connection diagram, which is the brain circuit of the drone. A full body circuiting is equally important for the functioning of the drone. Full body connection schematics is shown in figure 6.20. The commands taken from the pixhawk will determine the dynamic and static motions of the drone.

This circuit includes the entire pixhawk circuit unit along with the connections to the Thrust Motors, Servo motors; ESCs, XT 90; and the Batteries.

Batteries which are selected in order to power the thrust motors to generate lift are connected to the circuit via pixhawk. As the pixhawk would determine the amount of volts to supply in an individual thrust motor. In order to carry out this action safely, another unit called ESC is used in between the Thrust Motor and the Pixhawk. To achieve stability while in flight, increasing speed in one motor and reducing in other or vice versa, an ESC unit is important to be added. Pixhawk is also responsible for the propulsion of the drone, as Servo motors which determines the angle at which the thrust motors faces are controlled by pixhawk.

As during the propulsion phase, the pixhawk circuit unit would give the signal to the rare servo motor to move at a certain degree which would result in the forward motion of the drone whilst the front two servo motors would work in synchronisation with the mounted thrust motors to maintain the stability of the flight throughout the course of flight.

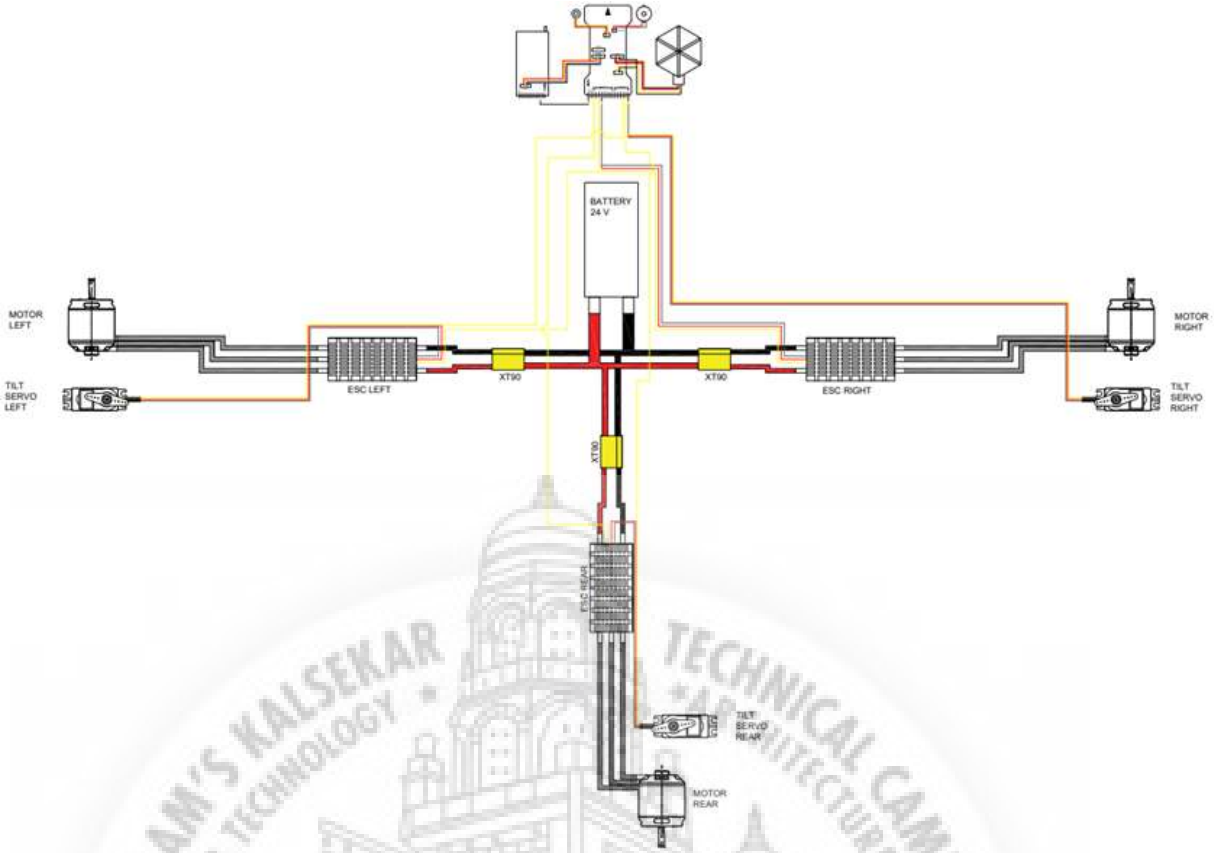

Fig 6.20 - Full Body Wiring Diagram.

Chapter 07

Flight Test

After successfully manufacturing the frame of the Endurance Craft MK2 we took it for a test in the backyard of our college. We set up the ground station where we monitored crucial data with the help of Mission Planner software which controlled the autopilot of our plane. We conducted preflight checks and were ready to fly. Initially it was unable to balance itself then we switched to Q-stabilize mode and after a few attempts it took off vertically with an unexpectedly high rate of climb. Our idea was not to take it much higher but rather keep it close to ground and monitor its stabilizing function. As you can see in Figure - 7.1 the aircraft was stable. But unfortunately it shot up way higher than our expectation so, take off was great but landing was not as per our plan. We quickly throttled down which was not a very wise idea and Unfortunately the aircraft made a very heavy landing. We had mounted the PVC safety structure for absorbing landing loads from 1 meter drop but the drop was from 2.5 m height and the impact load was very high and resulted in the failure of the frame.

Figure 7.1 - Test Flight.

Chapter 08

Cost Analysis

A brief overview of the expenditure of the project is displayed in the pie chart in figure 8.1given below.

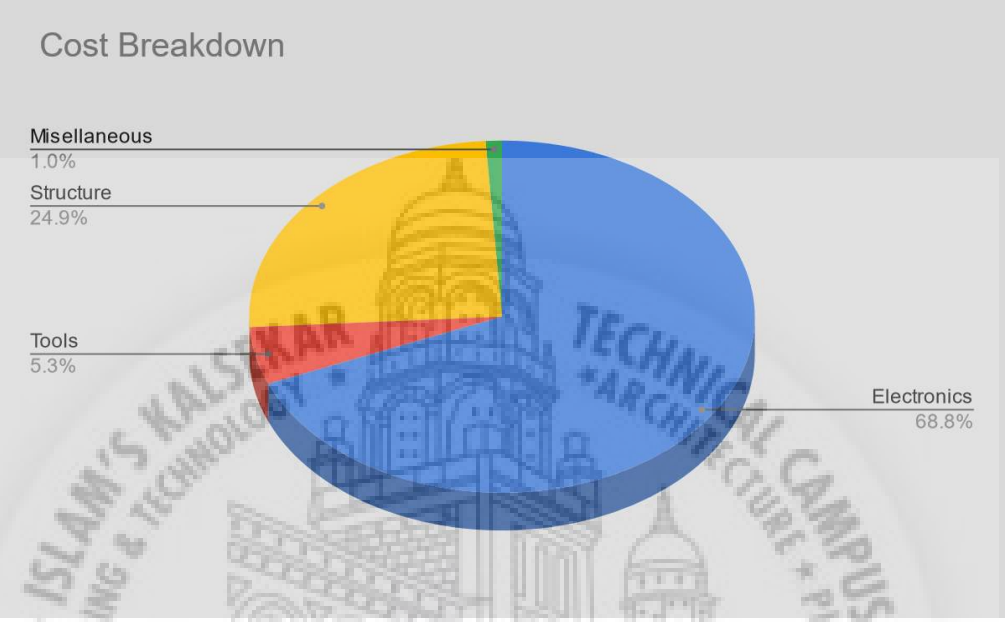

Figure 8.1 - Cost Breakdown Pie Chart.

The following tables show the break up of the expenditure of the project.

Table 8.1 -Electronics Cost Breakdown.

Sr. No	Particulars	Quantity	Cost (₹)
1	SK3 Turnigy Motor	3	15,000/-
2	Aerostar 100A ESC	3	12,000/-
3	Gens Ace 5600 - battery	2	12,000/-
4	Radio-Link Pixhawk	1	12,000/-
5	Yep ESC	1	7,782/-
6	Tattu Lipo	1	2,176/-
7	LG-HG 2 Li-ion	6	2,600/-
8	Radiomaster	1	15,500/-
9	Servo MG995	3	1,356/-
10	Transmitter and Receiver	1	15,000/-
	Total	22	95,414/-

Table 8.2 - Structural Cost Breakdown.

Sr. No	Particulars	Quantity	Cost (₹)
1	Carbon Fiber Rods	5	8060/-
2	Carbon Fiber Cloth	2	3700/-
3	Aluminium Rods	2	1010/-
4	Aluminium Block	1	1850/-
5	Balsa Wood	2	3750/-
6	PVC Frame	1	1542/-
7	Fiberglass	1	655/-
8	CNC Machining	2	8800/-
9	Wattmeter	1	1188/-
10	Balsa Laser Cutting	2	1000/-
	Total	19	31,555/-

Table 8.3 - Tools Cost Breakdown.

Sr. No	Particulars	Quantity	Cost (₹)
1	Drill set	4	400/-
2	Super Glue	6	330/-
3	Stationary	8	750/-
4	Hole Saw Cutter Set	1	180/-
5	Laser Guide	1	600/-
6	Bolts and Nuts	50	750/-
7	Diamond cutter	3	1000/-
8	Wires	10	1320/-
	Total	83	5330/-

Table 8.4 - Grand Total.

Sr. No	Particulars	Cost (₹)
1	Electronics	95,414/-
2	Structural	31,555/-
3	Tools	5,330/-
4	Miscellaneous	5.584/-
	Total	1,37,883/-

Chapter 09

Conclusion

This thesis explores our vision of designing and manufacturing an unmanned aerial vehicle which would not only serve as an educational stepping stone but also be a great help to society. The main goal of this project is to design and construct an aerial platform which will be able to transport medical supplies within cities and also from cities to rural areas. We conducted extensive research of the problem faced by the current medical transport solutions and brainstormed on possible solutions. We concluded that the payload capacity of approximately 2.5 kg and a range of about 100 km is good for most scenarios regarding medicine and organ delivery. We decided to proceed with a VTOL solution as it can take off and land vertically in tight city spaces and fly efficiently like a fixed wing aircraft. The configuration chosen was a tricopter with tilt mechanism for transition from vertical to forward flight. Then the aircraft is preliminarily sized. The specifications based on our initial calculations are a wingspan of 2.8 metres, Wing area of 0.92 square meters and stall velocity of 13 m/s. Then numerical analysis and computational fluid dynamic tools were used to analyse the performance of our drone. The drone can theoretically cruise at a velocity of 26 m/s with 14 kg of total weight , drag of 13 newtons and power consumption of 464 watts. The projected endurance at 26 m/s speed with a battery capacity of 30000 mAh is more than 1 hour. We used Carbon fibre as the main load bearing structural element. We performed analytical calculations as well as experiments and determined that the structure was sound for our application. We conducted our first flight test when all the necessary components for VTOL were assembled i.e. approximately 50 percent of total manufacturing. The VTOL system was calibrated and prepared for the first flight with makeshift landing gears. Unfortunately during the testing the aircraft shot up too fast as no limits were defined in the autopilot.The plan was to hover at 1 meter above ground and the plane rose to 2.5 meters above ground which resulted in a panic throttle down response which led to a very fast decent which resulted in the destruction of the frame. All the electronics were safe. We then improved upon the existing frame with a new frame. This concludes the current work done. COVID-19 greatly hindered our progress but we remain determined to see this project to fruition.

Chapter 10

Appendices

Propeller Thrust Velocity etc at given Rpm. Generated using prop Calc Software.

5000	RPM						
J	CT	CP	eta	Thr [N]	P [W]	v [m/s]	Re 0.7
0.05	0.1052	0.0366	0.14	25.397	318.3	1.8	137521
0.07	0.1032	0.037	0.2	24.912	321.4	2.6	137560
0.09	0.101	0.0373	0.26	24.374	324.1	3.4	137612
0.12	0.0985	0.0376	0.31	23.791	326.2	4.2	137679
0.14	0.096	0.0377	0.35	23.184	327.9	5	137760
0.16	0.0934	0.0379	0.4	22.553	328.9	5.8	137854
0.18	0.0907	0.0379	0.44	21.897	329.3	6.6	137963
0.21	0.0879	0.0379	0.48	21.215	329.1	7.4	138085
0.23	0.085	0.0378	0.51	20.511	328.2	8.2	138221
0.25	0.0819	0.0376	0.54	19.781	326.7	9	138372
0.27	0.0788	0.0373	0.57	19.031	324.4	9.8	138536
0.29	0.0756	0.037	0.6	18.253	321.1	10.6	138713
0.32	0.0723	0.0365	0.63	17.452	316.8	11.4	138905
0.34	0.0689	0.0359	0.65	16.634	311.6	12.2	139110
0.36	0.0654	0.0352	0.67	15.798	305.5	13	139328
0.38	0.0619	0.0344	0.69	14.955	298.7	13.8	139560
0.41	0.0584	0.0335	0.71	14.095	290.9	14.6	139806
0.43	0.0547	0.0324	0.72	13.212	281.6	15.4	140065
0.45	0.051	0.0312	0.74	12.304	271.1	16.2	140337

0.47	0.0472	0.0299	0.75	11.385	259.7	17	140622
0.49	0.0433	0.0285	0.75	10.445	247.3	17.8	140920
0.52	0.0392	0.0269	0.75	9.471	233.4	18.6	141232
0.54	0.035	0.0251	0.75	8.458	217.8	19.4	141557
0.56	0.0307	0.0231	0.75	7.409	200.4	20.2	141894
0.58	0.0265	0.0211	0.73	6.396	183.3	21	142244
0.61	0.0223	0.019	0.71	5.372	165	21.8	142607
0.63	0.018	0.0168	0.67	4.345	146	22.6	142982
0.65	0.0138	0.0146	0.61	3.321	126.9	23.4	143370
0.67	0.0097	0.0125	0.52	2.332	108.3	24.2	143771
0.69	0.0056	0.0102	0.38	1.348	88.8	25	144183
0.72	0.0022	0.0087	0.18	0.538	75.2	25.8	144608
5500	RPM						
J	CT	CP	eta	Thr [N]	P [W]	v [m/s]	Re 0.7
0.05	0.1052	0.0365	0.14	30.722	421.6	2	151273
0.07	0.1031	0.0368	0.2	30.123	425.9	2.9	151317
0.1	0.1009	0.0371	0.26	29.462	429.5	3.8	151376
0.12	0.0984	0.0374	0.31	28.741	432.3	4.7	151452
0.14	0.0958	0.0376	0.36	27.988	434.5	5.6	151544
0.16	0.0931	0.0377	0.4	27.205	435.8	6.5	151652
0.19	0.0903	0.0377	0.45	26.391	436.3	7.4	151776
0.21	0.0875	0.0377	0.49	25.546	435.9	8.3	151916
0.23	0.0845	0.0376	0.52	24.673	434.6	9.2	152073
0.25	0.0814	0.0374	0.55	23.77	432.4	10.1	152244
0.28	0.0782	0.0371	0.58	22.839	429	11	152432
0.3	0.0749	0.0367	0.61	21.87	424.1	11.9	152636
0.32	0.0715	0.0361	0.64	20.876	417.9	12.8	152855

0.35	0.068	0.0355	0.66	19.861	410.4	13.7	153090
0.37	0.0645	0.0348	0.68	18.828	401.9	14.6	153341
0.39	0.0609	0.0339	0.7	17.783	392.1	15.5	153607
0.41	0.0572	0.0329	0.72	16.709	380.6	16.4	153888
0.44	0.0534	0.0318	0.73	15.601	367.2	17.3	154185
0.46	0.0495	0.0305	0.75	14.465	352.3	18.2	154497
0.48	0.0456	0.0291	0.76	13.314	336	19.1	154824
0.5	0.0415	0.0275	0.76	12.13	318.1	20	155167
0.53	0.0373	0.0258	0.76	10.905	298.1	20.9	155524
0.55	0.0329	0.0238	0.76	9.622	275.3	21.8	155896
0.57	0.0287	0.0218	0.75	8.37	252.6	22.7	156283
0.6	0.0244	0.0198	0.73	7.117	228.7	23.6	156684
0.62	0.0201	0.0176	0.7	5.865	203.8	24.5	157101
0.64	0.0158	0.0154	0.66	4.623	178.4	25.4	157531
0.66	0.0118	0.0134	0.58	3.458	155.5	26.3	157976
0.69	0.0078	0.0113	0.48	2.291	131.1	27.2	158435
0.71	0.0043	0.0097	0.32	1.265	111.8	28.1	158908
0.73	0.0011	0.0082	0.1	0.327	95	29	159395
6000	Rpm						
J	CT	CP	eta	Thr [N]	P [W]	v [m/s]	Re 0.7
0.05	0.1051	0.0363	0.14	36.553	545.1	2.2	165025
0.07	0.1031	0.0367	0.21	35.831	550.7	3.2	165074
0.1	0.1008	0.037	0.26	35.031	555.5	4.2	165141
0.12	0.0983	0.0372	0.32	34.159	559.1	5.2	165226
0.14	0.0956	0.0374	0.36	33.244	561.9	6.2	165329
0.17	0.0929	0.0375	0.41	32.294	563.6	7.2	165451
0.19	0.09	0.0376	0.45	31.304	564.2	8.2	165590

0.21	0.0871	0.0375	0.49	30.279	563.5	9.2	165748
0.24	0.0841	0.0374	0.53	29.221	561.6	10.2	165924
0.26	0.0809	0.0372	0.56	28.13	558.6	11.2	166118
0.28	0.0777	0.0369	0.59	26.997	553.8	12.2	166330
0.3	0.0743	0.0364	0.62	25.817	546.9	13.2	166559
0.33	0.0708	0.0359	0.65	24.608	538.3	14.2	166806
0.35	0.0672	0.0352	0.67	23.378	528.1	15.2	167072
0.37	0.0636	0.0344	0.69	22.125	516.3	16.2	167354
0.4	0.06	0.0335	0.71	20.848	502.6	17.2	167654
0.42	0.0562	0.0324	0.73	19.53	486.5	18.2	167972
0.44	0.0523	0.0312	0.74	18.164	467.8	19.2	168307
0.47	0.0483	0.0298	0.76	16.779	447.4	20.2	168659
0.49	0.0442	0.0283	0.76	15.373	425.2	21.2	169029
0.51	0.0401	0.0267	0.77	13.924	400.5	22.2	169415
0.54	0.0357	0.0248	0.77	12.422	372.7	23.2	169818
0.56	0.0313	0.0228	0.77	10.891	342.9	24.2	170238
0.58	0.027	0.0208	0.76	9.383	312.6	25.2	170675
0.61	0.0227	0.0187	0.73	7.88	280.7	26.2	171128
0.63	0.0184	0.0166	0.7	6.396	248.4	27.2	171598
0.65	0.0144	0.0146	0.64	5.005	219.1	28.2	172084
0.68	0.0105	0.0126	0.56	3.645	189.7	29.2	172586
0.7	0.0068	0.0108	0.44	2.353	161.8	30.2	173104
0.72	0.0036	0.0094	0.27	1.25	141.7	31.2	173638
0.74	0.0004	0.0081	0.04	0.155	120.9	32.2	174187
6500	RPM						
J	CT	CP	eta	Thr [N]	P [W]	v [m/s]	Re 0.7
0.05	0.1051	0.0362	0.15	42.881	690.2	2.3	178777

0.07	0.103	0.0365	0.21	42.027	697.5	3.4	178831
0.1	0.1007	0.0369	0.26	41.078	703.7	4.5	178905
0.12	0.0981	0.0371	0.32	40.041	708.3	5.6	178999
0.14	0.0955	0.0373	0.37	38.949	711.9	6.7	179114
0.17	0.0927	0.0374	0.42	37.814	714	7.8	179249
0.19	0.0898	0.0374	0.46	36.633	714.6	8.9	179405
0.21	0.0868	0.0374	0.5	35.411	713.6	10	179580
0.24	0.0837	0.0373	0.53	34.15	711.2	11.1	179776
0.26	0.0805	0.037	0.57	32.85	707	12.2	179992
0.29	0.0772	0.0367	0.6	31.498	700.5	13.3	180227
0.31	0.0737	0.0362	0.63	30.08	691.1	14.4	180483
0.33	0.0702	0.0356	0.65	28.632	679.4	15.5	180759
0.36	0.0666	0.0349	0.68	27.158	665.7	16.6	181054
0.38	0.0629	0.034	0.7	25.658	649.7	17.7	181369
0.4	0.0591	0.0331	0.72	24.126	631.2	18.8	181703
0.43	0.0552	0.0319	0.74	22.538	609.4	19.9	182057
0.45	0.0512	0.0306	0.75	20.9	584.6	21	182431
0.47	0.0472	0.0292	0.76	19.245	557.5	22.1	182823
0.5	0.0431	0.0277	0.77	17.57	528.3	23.2	183235
0.52	0.0388	0.026	0.78	15.834	495.4	24.3	183665
0.54	0.0344	0.024	0.78	14.026	458.1	25.4	184115
0.57	0.03	0.022	0.77	12.242	420.7	26.5	184583
0.59	0.0256	0.02	0.76	10.45	381.1	27.6	185070
0.61	0.0213	0.0178	0.73	8.688	340.4	28.7	185575
0.64	0.0171	0.0158	0.69	6.995	301	29.8	186098
0.66	0.0133	0.014	0.63	5.443	267	30.9	186640
0.68	0.0095	0.0121	0.54	3.886	230.3	32	187199

0.71	0.0063	0.0107	0.42	2.557	204	33.1	187776
0.73	0.0032	0.0094	0.25	1.285	178.9	34.2	188371
0.76	0.0003	0.0083	0.02	0.11	158.7	35.3	188983
7000	RPM						
J	CT	CP	eta	Thr [N]	P [W]	v [m/s]	Re 0.7
0.05	0.105	0.036	0.15	49.691	858.6	2.5	192529
0.07	0.1029	0.0364	0.21	48.704	867.9	3.7	192588
0.1	0.1006	0.0367	0.27	47.597	875.9	4.9	192669
0.12	0.098	0.037	0.32	46.382	881.8	6.1	192773
0.15	0.0953	0.0372	0.37	45.099	886.2	7.3	192899
0.17	0.0925	0.0373	0.42	43.764	888.8	8.5	193048
0.19	0.0896	0.0373	0.46	42.374	889.5	9.7	193219
0.22	0.0865	0.0373	0.5	40.94	888.1	10.9	193412
0.24	0.0834	0.0371	0.54	39.461	885	12.1	193628
0.26	0.0802	0.0369	0.57	37.934	879.4	13.3	193866
0.29	0.0768	0.0365	0.61	36.345	870.9	14.5	194126
0.31	0.0733	0.036	0.63	34.667	858.4	15.7	194407
0.34	0.0696	0.0354	0.66	32.957	843.1	16.9	194711
0.36	0.066	0.0346	0.69	31.218	825	18.1	195037
0.38	0.0622	0.0337	0.71	29.454	804.1	19.3	195384
0.41	0.0584	0.0327	0.73	27.636	779.6	20.5	195753
0.43	0.0544	0.0315	0.74	25.755	751	21.7	196144
0.45	0.0504	0.0302	0.76	23.827	719.1	22.9	196555
0.48	0.0462	0.0287	0.77	21.879	684.1	24.1	196988
0.5	0.0421	0.0271	0.78	19.899	646.1	25.3	197442
0.53	0.0377	0.0253	0.78	17.852	603.3	26.5	197917
0.55	0.0333	0.0233	0.78	15.747	556.4	27.7	198413

0.57	0.0289	0.0214	0.78	13.664	509	28.9	198929
0.6	0.0245	0.0192	0.76	11.58	458.8	30.1	199466
0.62	0.0202	0.0171	0.73	9.559	408.5	31.3	200023
0.65	0.0163	0.0153	0.69	7.715	364.6	32.5	200600
0.67	0.0126	0.0136	0.62	5.958	323.4	33.7	201198
0.69	0.009	0.0119	0.53	4.256	282.5	34.9	201815
0.72	0.006	0.0107	0.4	2.827	255.1	36.1	202451
0.74	0.0029	0.0095	0.23	1.389	225.7	37.3	203107
0.76	0.0003	0.0086	0.02	0.119	205.9	38.5	203782
7500	RPM						
J	CT	CP	eta	Thr [N]	P [W]	v [m/s]	Re 0.7
0.05	0.1049	0.0359	0.15	57.002	1052.1	2.7	206281
0.07	0.103	0.0363	0.21	55.966	1063.2	3.9	206339
0.09	0.1009	0.0366	0.26	54.801	1072.6	5.1	206418
0.12	0.0985	0.0368	0.31	53.52	1079.8	6.3	206518
0.14	0.096	0.037	0.36	52.165	1085.3	7.5	206639
0.16	0.0934	0.0371	0.41	50.753	1089	8.7	206781
0.18	0.0907	0.0372	0.45	49.288	1090.6	9.9	206944
0.21	0.0879	0.0372	0.49	47.771	1090.1	11.1	207128
0.23	0.0851	0.0371	0.52	46.215	1087.5	12.3	207332
0.25	0.0821	0.0369	0.56	44.619	1083.2	13.5	207557
0.27	0.0791	0.0367	0.59	42.966	1075.5	14.7	207803
0.29	0.0759	0.0363	0.62	41.233	1064.4	15.9	208070
0.32	0.0726	0.0358	0.64	39.424	1049.1	17.1	208357
0.34	0.0692	0.0352	0.67	37.583	1030.8	18.3	208664
0.36	0.0658	0.0344	0.69	35.718	1009.6	19.5	208992
0.38	0.0623	0.0336	0.71	33.824	985.2	20.7	209340

0.41	0.0587	0.0326	0.73	31.877	957	21.9	209709
0.43	0.055	0.0315	0.75	29.861	924.4	23.1	210097
0.45	0.0512	0.0303	0.76	27.805	888.4	24.3	210505
0.47	0.0474	0.029	0.77	25.729	849.2	25.5	210933
0.49	0.0435	0.0275	0.78	23.633	807	26.7	211381
0.52	0.0395	0.0259	0.79	21.473	760	27.9	211848
0.54	0.0354	0.0241	0.79	19.239	707.5	29.1	212335
0.56	0.0314	0.0224	0.79	17.041	655.5	30.3	212841
0.58	0.0273	0.0205	0.78	14.808	599.7	31.5	213366
0.61	0.0232	0.0185	0.76	12.605	541.9	32.7	213910
0.63	0.0193	0.0166	0.73	10.506	486.3	33.9	214473
0.65	0.0159	0.015	0.69	8.627	440.6	35.1	215055
0.67	0.0125	0.0134	0.62	6.782	394.3	36.3	215656
0.69	0.0093	0.012	0.54	5.049	352.3	37.5	216275
0.72	0.0065	0.011	0.42	3.53	321.5	38.7	216912
0.74	0.0037	0.0098	0.28	1.998	288	39.9	217567
0.76	0.0012	0.0091	0.1	0.642	265.9	41.1	218240
8000	RPM						
J	CT	CP	eta	Thr [N]	P [W]	v [m/s]	Re 0.7
0.05	0.1049	0.0358	0.15	64.817	1272.8	2.9	220034
0.07	0.103	0.0362	0.21	63.633	1286.5	4.2	220096
0.1	0.1008	0.0365	0.26	62.295	1298.3	5.5	220183
0.12	0.0984	0.0367	0.32	60.82	1307.2	6.8	220292
0.14	0.0959	0.0369	0.36	59.255	1313.9	8.1	220424
0.16	0.0932	0.037	0.41	57.618	1318.3	9.4	220579
0.19	0.0905	0.0371	0.45	55.921	1320.1	10.7	220758
0.21	0.0876	0.0371	0.49	54.166	1319.2	12	220959

0.23	0.0847	0.037	0.53	52.366	1315.9	13.3	221183
0.25	0.0817	0.0368	0.56	50.515	1310	14.6	221430
0.28	0.0786	0.0365	0.59	48.597	1300	15.9	221700
0.3	0.0754	0.0361	0.62	46.578	1285.3	17.2	221992
0.32	0.072	0.0356	0.65	44.48	1265.7	18.5	222307
0.34	0.0685	0.0349	0.67	42.345	1242.3	19.8	222645
0.37	0.065	0.0342	0.7	40.183	1215.2	21.1	223004
0.39	0.0615	0.0333	0.72	37.986	1184	22.4	223386
0.41	0.0578	0.0323	0.74	35.712	1147.6	23.7	223791
0.43	0.054	0.0311	0.75	33.366	1106.1	25	224217
0.46	0.0501	0.0298	0.77	30.992	1061.1	26.3	224665
0.48	0.0463	0.0284	0.78	28.59	1011.5	27.6	225135
0.5	0.0423	0.0269	0.79	26.151	957.9	28.9	225626
0.52	0.0383	0.0252	0.79	23.646	898.3	30.2	226139
0.55	0.0341	0.0234	0.8	21.071	833.1	31.5	226674
0.57	0.03	0.0216	0.79	18.553	769.3	32.8	227229
0.59	0.0259	0.0197	0.78	16.005	700.6	34.1	227806
0.61	0.0218	0.0177	0.76	13.503	630.1	35.4	228403
0.64	0.0181	0.0159	0.72	11.173	565.9	36.7	229021
0.66	0.0147	0.0144	0.67	9.072	512.4	38	229660
0.68	0.0112	0.0127	0.6	6.941	453.6	39.3	230319
0.7	0.0083	0.0116	0.5	5.124	413.4	40.6	230999
0.73	0.0054	0.0105	0.38	3.36	373.3	41.9	231698
0.75	0.0027	0.0095	0.21	1.682	338.6	43.2	232417
0.77	0.0002	0.0087	0.01	0.097	309.6	44.5	233156
8500	RPM						
J	CT	CP	eta	Thr [N]	P [W]	v [m/s]	Re 0.7

0.05	0.1048	0.0357	0.15	73.139	1522.2	3.1	233786
0.07	0.1029	0.0361	0.21	71.797	1539.2	4.5	233854
0.1	0.1007	0.0364	0.27	70.275	1553.6	5.9	233947
0.12	0.0983	0.0367	0.32	68.592	1564.5	7.3	234065
0.14	0.0957	0.0368	0.37	66.8	1572.6	8.7	234209
0.16	0.0931	0.037	0.41	64.922	1577.6	10.1	234378
0.19	0.0903	0.037	0.46	62.974	1579.6	11.5	234572
0.21	0.0874	0.037	0.5	60.962	1578.2	12.9	234791
0.23	0.0844	0.0369	0.53	58.898	1573.9	14.3	235034
0.26	0.0814	0.0367	0.57	56.771	1566.2	15.7	235303
0.28	0.0782	0.0364	0.6	54.57	1553.4	17.1	235597
0.3	0.0749	0.036	0.63	52.243	1534.5	18.5	235915
0.32	0.0714	0.0354	0.66	49.836	1510	19.9	236258
0.35	0.0679	0.0347	0.68	47.387	1480.6	21.3	236626
0.37	0.0644	0.0339	0.7	44.905	1446.5	22.7	237018
0.39	0.0607	0.033	0.72	42.384	1407.5	24.1	237434
0.42	0.057	0.0319	0.74	39.757	1361.4	25.5	237874
0.44	0.0531	0.0307	0.76	37.057	1309.8	26.9	238338
0.46	0.0492	0.0294	0.77	34.353	1254.5	28.3	238826
0.48	0.0453	0.028	0.79	31.603	1193.2	29.7	239338
0.51	0.0413	0.0264	0.79	28.792	1125.9	31.1	239874
0.53	0.0371	0.0246	0.8	25.909	1051.6	32.5	240433
0.55	0.0331	0.0229	0.8	23.062	976.4	33.9	241015
0.58	0.0288	0.021	0.79	20.121	894.9	35.3	241620
0.6	0.0247	0.019	0.78	17.234	811.1	36.7	242248
0.62	0.0207	0.017	0.76	14.415	726.4	38.1	242899
0.65	0.017	0.0154	0.71	11.895	656.5	39.5	243572

0.67	0.0136	0.0138	0.66	9.477	589.5	40.9	244268
0.69	0.0102	0.0123	0.58	7.129	523	42.3	244986
0.71	0.0073	0.0112	0.47	5.118	477.4	43.7	245726
0.74	0.0044	0.01	0.32	3.073	426.2	45.1	246488
0.76	0.0018	0.0092	0.15	1.253	391.1	46.5	247271
9000	RPM						
J	CT	CP	eta	Thr [N]	P [W]	v [m/s]	Re 0.7
0.05	0.1048	0.0356	0.15	81.972	1802.4	3.2	247538
0.07	0.1029	0.036	0.21	80.458	1822.9	4.7	247611
0.1	0.1007	0.0363	0.27	78.738	1840.3	6.2	247711
0.12	0.0982	0.0366	0.32	76.831	1853.3	7.7	247839
0.14	0.0956	0.0368	0.37	74.798	1863	9.2	247994
0.17	0.0929	0.0369	0.42	72.662	1868.8	10.7	248176
0.19	0.0901	0.0369	0.46	70.447	1870.9	12.2	248386
0.21	0.0871	0.0369	0.5	68.165	1869	13.7	248622
0.24	0.0841	0.0368	0.54	65.818	1863.5	15.2	248886
0.26	0.081	0.0366	0.57	63.393	1853.5	16.7	249177
0.28	0.0778	0.0363	0.6	60.889	1837.6	18.2	249494
0.3	0.0744	0.0358	0.63	58.232	1813.8	19.7	249839
0.33	0.0709	0.0352	0.66	55.494	1783.4	21.2	250210
0.35	0.0674	0.0345	0.69	52.71	1747.2	22.7	250607
0.37	0.0638	0.0337	0.71	49.888	1705.1	24.2	251031
0.4	0.0601	0.0327	0.73	47.009	1656.6	25.7	251482
0.42	0.0563	0.0316	0.75	44.008	1599.8	27.2	251958
0.44	0.0523	0.0303	0.77	40.946	1537.1	28.7	252461
0.47	0.0484	0.029	0.78	37.877	1469.5	30.2	252989
0.49	0.0444	0.0275	0.79	34.764	1395.1	31.7	253543

0.51	0.0403	0.0259	0.8	31.559	1312.3	33.2	254123
0.54	0.0362	0.0241	0.8	28.277	1220.8	34.7	254727
0.56	0.032	0.0223	0.8	25.069	1131.8	36.2	255358
0.58	0.0278	0.0204	0.79	21.751	1033.1	37.7	256013
0.61	0.0236	0.0184	0.78	18.473	930.7	39.2	256692
0.63	0.0196	0.0164	0.75	15.346	831.8	40.7	257397
0.65	0.0161	0.0149	0.71	12.593	753.8	42.2	258126
0.68	0.0126	0.0132	0.64	9.831	670.5	43.7	258879
0.7	0.0094	0.0119	0.55	7.321	601.3	45.2	259656
0.72	0.0064	0.0107	0.43	5.029	543.9	46.7	260456
0.74	0.0036	0.0096	0.28	2.794	488.4	48.2	261281
0.77	0.0009	0.0088	0.08	0.736	446.4	49.7	262128
9500	RPM						
J	CT	CP	eta	Thr [N]	P [W]	v [m/s]	Re 0.7
0.05	0.1048	0.0355	0.15	91.306	2114.9	3.4	261290
0.07	0.1028	0.0359	0.21	89.612	2139.3	5	261368
0.1	0.1006	0.0363	0.27	87.683	2160.1	6.6	261475
0.12	0.0981	0.0365	0.32	85.537	2175.5	8.2	261612
0.14	0.0955	0.0367	0.37	83.248	2186.9	9.8	261779
0.17	0.0928	0.0368	0.42	80.839	2193.6	11.4	261975
0.19	0.0899	0.0369	0.46	78.339	2195.8	13	262200
0.21	0.0869	0.0368	0.5	75.765	2193.3	14.6	262454
0.24	0.0839	0.0367	0.54	73.119	2186.4	16.2	262738
0.26	0.0808	0.0365	0.58	70.39	2174	17.8	263050
0.28	0.0775	0.0362	0.61	67.554	2154.2	19.4	263392
0.31	0.0741	0.0357	0.64	64.546	2124.9	21	263763
0.33	0.0705	0.035	0.67	61.455	2087.9	22.6	264162

0.35	0.0669	0.0343	0.69	58.313	2043.8	24.2	264590
0.38	0.0633	0.0334	0.71	55.128	1992.5	25.8	265046
0.4	0.0595	0.0324	0.74	51.869	1933.1	27.4	265530
0.42	0.0556	0.0313	0.75	48.472	1864.2	29	266043
0.45	0.0517	0.03	0.77	45.031	1789.1	30.6	266584
0.47	0.0477	0.0287	0.78	41.576	1707.5	32.2	267153
0.49	0.0437	0.0272	0.8	38.066	1617.7	33.8	267749
0.52	0.0395	0.0255	0.8	34.455	1517.7	35.4	268373
0.54	0.0353	0.0236	0.81	30.769	1408.4	37	269024
0.56	0.0312	0.0219	0.81	27.15	1302	38.6	269702
0.59	0.0269	0.0199	0.8	23.428	1184.1	40.2	270407
0.61	0.0227	0.0178	0.78	19.763	1062.5	41.8	271138
0.64	0.0187	0.016	0.75	16.339	950.5	43.4	271897
0.66	0.0152	0.0144	0.7	13.27	858.4	45	272681
0.68	0.0117	0.0127	0.63	10.155	756.7	46.6	273491
0.71	0.0086	0.0115	0.53	7.491	686.2	48.2	274327
0.73	0.0056	0.0103	0.4	4.908	615.9	49.8	275189
0.75	0.0028	0.0093	0.23	2.477	557	51.4	276076
0.78	0.0002	0.0085	0.02	0.151	505.5	53	276988
10000	RPM						
J	CT	CP	eta	Thr [N]	P [W]	v [m/s]	Re 0.7
0.05	0.1047	0.0354	0.15	101.151	2461.6	3.6	275042
0.07	0.1028	0.0358	0.21	99.263	2490.3	5.3	275125
0.1	0.1006	0.0362	0.27	97.112	2514.9	7	275240
0.12	0.0981	0.0364	0.33	94.711	2533	8.7	275386
0.14	0.0954	0.0366	0.38	92.15	2546.3	10.4	275564
0.17	0.0926	0.0367	0.42	89.451	2554	12.1	275773

0.19	0.0897	0.0368	0.47	86.65	2556.3	13.8	276014
0.22	0.0867	0.0367	0.51	83.767	2553	15.5	276286
0.24	0.0837	0.0366	0.55	80.804	2544.5	17.2	276590
0.26	0.0805	0.0364	0.58	77.742	2529.1	18.9	276924
0.29	0.0772	0.036	0.61	74.563	2505.2	20.6	277290
0.31	0.0737	0.0355	0.64	71.18	2469.3	22.3	277687
0.33	0.0701	0.0349	0.67	67.715	2424.8	24	278114
0.36	0.0665	0.0341	0.7	64.194	2371.6	25.7	278572
0.38	0.0628	0.0332	0.72	60.632	2310.2	27.4	279061
0.4	0.059	0.0322	0.74	56.961	2238.4	29.1	279580
0.43	0.055	0.031	0.76	53.142	2155.8	30.8	280129
0.45	0.0511	0.0297	0.78	49.313	2067.1	32.5	280708
0.48	0.0471	0.0283	0.79	45.442	1969.5	34.2	281317
0.5	0.043	0.0268	0.8	41.511	1862.1	35.9	281956
0.52	0.0388	0.0251	0.81	37.478	1742.9	37.6	282624
0.55	0.0346	0.0233	0.81	33.4	1616.8	39.3	283321
0.57	0.0303	0.0214	0.81	29.306	1487.9	41	284047
0.59	0.026	0.0194	0.8	25.155	1348.4	42.7	284802
0.62	0.0219	0.0174	0.78	21.107	1206.3	44.4	285586
0.64	0.018	0.0156	0.74	17.398	1082	46.1	286398
0.66	0.0144	0.014	0.69	13.948	971.1	47.8	287238
0.69	0.0109	0.0123	0.61	10.507	853.1	49.5	288106
0.71	0.0079	0.0112	0.5	7.641	777.6	51.2	289001
0.74	0.0049	0.01	0.36	4.724	691.7	52.9	289924
0.76	0.0022	0.0091	0.18	2.094	629.8	54.6	290874

Chapter 11

References

1. "History of Aircraft", https://www.dkfindout.com/us/transportation/history-aircraft/
2. Walter James Boyne, "History Of Flight", https://www.britannica.com/technology/history-of-flight
3. PeterJakab, August 22, 2013, "Leonardo Da Vinci And Flight", https://airandspace.si.edu/stories/editorial/leonardo-da-vinci-and-flight
4. National Air and Space Museum in Washington, DC, "1903 Wright Flyer", https://airandspace.si.edu/collection-objects/1903-wright-flyer/nasm_A19610048000
5. 13 April, 2020, "F-35A CTOL Lightning II Multirole fighter aircraft", Defence Aviation and Aerospace Airforce Show Daily News, https://airrecognition.com/index.php/world-air-force-military-equipment-aircraft-/north-america/united-states-air-force/us-air-force-usaf-fighter-combat-aircraft/f-35-lightning-ii-variants-multirole-fighter-aircraft/137-f-35-f-35a-ctol-lightning-ii-lockheed-variants-martin-multirole-fighter-aircraft-technical-data-sheet-specifications-intelligence-description-information-identification-pictures-photos-images-video-united-states-american-us-usaf-air-force-defence-industry.html
6. August 8, 2019, "Liberty Helicopter", Liberty Helicopter News & Events, https://libertyhelicopter.com/happy-national-helicopter-day-here-is-how-we-celebrate/
7. "Zenair CH 701 STOL light aircraft" https://en.wikipedia.org/wiki/STOL
8. "A Sea Harrier launches from the flight deck of HMS Illustrious in 2001" https://en.wikipedia.org/wiki/STOVL#/media/File:FA2_Sea_Harrier_Launches_from_HMS_Illustrious_MOD_45139505.jpg
9. Skilled Flyer, "Surveillance Drone", https://skilledflyer.com/surveillance-drones-for-sale/
10. Philip Butterworth-Hayes, April 7, 2019, "Drone delivery operations underway in 27 countries", UAS traffic management news, https://www.unmannedairspace.info/latest-news-and-information/drone-delivery-operations-underway-in-26-countries/
11. "Types Of Military Drones: The Best Technology Available Today" https://www.mydronelab.com/blog/types-of-military-drones.html#:~:text=Drones%20have%20an%20array%20of,of%20interest%20to%20us%20today

12. Zacc Dukowitz, 1 November 2019, “What Types of Drones Are There? A Guide to All the Different Drone Types on the Market”, https://uavcoach.com/types-of-drones/

13. Mina Khalilzade Fathi, Prof. S. Mohammad B. Malaek, 2018-2019, “Unmanned Aerial System”, Wild Area Aerial Protective Inspector, https://www.aiaa.org/docs/default-source/uploadedfiles/education-and-careers/university-students/design-competitions/1st-place-ugrad-individual-aicraft.pdf?sfvrsn=d393867b_0

14. Huggy's Birds, S. Addarkaoui Taarabt, A. Bernier, Y. Chen, H. Compere, A. Dore, M. Fransolet, R. Jumpertz, L. Macchiaiolo, 2018-2019, “Electric Vertical Takeoff and Landing (E-VTOL) Aircraft Mistral Air Taxi”, Aiaa Graduate Team Aircraft Design Competition 2018-2019, https://www.aiaa.org/docs/default-source/uploadedfiles/education-and-careers/university-students/design-competitions/3rd-place-grad-team-aircraft.pdf?sfvrsn=5d49f2cf_0

15. J. Jensin Joshua, N. Ganesh Kumar, A. A. Aswini, 2015, “Stability Analysis of Low Reynolds Number UAV Using XFLR5”, International Journal of Engineering Research & Technology (IJERT) ISSN: 2278-0181 Published by, www.ijert.org NCRTET-2015 Conference Proceedings, https://www.ijert.org/research/stability-analysis-of-low-renolds-number-uav-using-xflr5-IJERTCONV3IS04068.pdf

16. S P Venkatesan, Beemkumar N, J. Jayaprabakar, P N Kadiresh, October 2018, “Modelling and analysis of aircraft wing with and without winglet”, International Journal of Ambient Energy 42(4):1-20, https://www.researchgate.net/publication/328210952_Modelling_and_analysis_of_aircraft_wing_with_and_without_winglet

17. Jyoti Shelar, June 2019, “Green corridors for speedy organ transport see a rise”, The Hindu,https://www.thehindu.com/news/cities/mumbai/green-corridors-for-speedy-organ-transport-see-a-rise/article28222023.ece

18. 2020-2021, “Global Observatory On Donation And Transplantation”, WHO Collaborates On Donation And Transplantation, http://www.transplant-observatory.org/

19. 2021, “Mumbai Population 2021”, World Population Review, https://worldpopulationreview.com/world-cities/mumbai-population

20. Sheela D Kadam, Satish V Kakade*, Megha A Doshi, Prakash M Durgawale, 07 May 2019, "Knowledge And Attitude Of The Rural Population Towards Organ Donation", Research Journal of Life Sciences, Bioinformatics, Pharmaceutical and Chemical Sciences (RJLBPCS), Life Science Informatics Publications, http://www.rjlbpcs.com/article-pdf-downloads/2019/28/619.pdf

21. Vaishaly K Bharambe, Vasanti U Arole, Vatsalaswamy Puranam, Preeti P Kulkarni, Prashant B Kulkarni, February 15, 2018, "Knowledge and attitude toward organ donation among people in Lanja: A rural town in India", Saudi Journal of Kidney Diseases Transplantation, https://www.sjkdt.org/article.asp?issn=1319-2442;year=2018;volume=29;issue=1;spage=160;epage=166;aulast=Bharambe

22. KL Balajee, N Ramachandran, L Subitha, September - October 2016, "Awareness and Attitudes toward Organ Donation in Rural Puducherry, India", Ann Med Health Sci Res, https://www.ncbi.nlm.nih.gov/pmc/articles/PMC5414440/

23. "Turnigy Aerodrive SK3 - 5055-280KV Brushless Outrunner Motor", https://hobbyking.com/en_us/turnigy-aerodrive-sk3-5055-280kv-brushless-outrunner-motor.html?___store=en_us

24. "TowerPro MG995 Plastic Gear Servo Motor (180° Rotation)-Standard Quality", https://robu.in/product/towerpro-mg995-metal-gear-servo-motor/

25. "YEP 100A (2~6S) SBEC Brushless Speed Controller", https://hobbyking.com/en_us/hobbyking-yep-100a-2-6s-sbec-brushless-speed-controller.html

26. "AeroStar WiFi 100A Brushless ESC with 5A BEC (2~6S)", chttps://hobbyking.com/en_us/assembly-win-dragon-esc-100a.html

27. "Radiolink SE100 GPS Module for PixHawk", https://www.robotshop.com/en/radiolink-se100-gps-module-pixhawk.html

28. "Buzzer for Pixhawk 1 / PX4", https://www.flyingtech.co.uk/electronics/pixhawk-px4-flight-controller-buzzer-status-alarm

29. "Buzzer (aka Tone Alarm)", https://ardupilot.org/copter/docs/common-buzzer.html

30. "RADIOMASTER TX16S w/Hall Sensor Gimbals 2.4GHz 16ch Multi-Protocol OpenTx Transmitter", https://hobbyking.com/en_us/radiomaster-tx16s-w-hall-sensor-gimbals-2-4ghz-16ch-multi-protocol-opentx-transmitter.html?___store=en_us

31. "Gens ace 5600mAh 80C 22.2V 6S1P Lipo Battery Pack with EC5 plug", https://www.gensace.de/gens-ace-5600mah-80c-22-2v-6s1p-lipo-battery-pack-with-ec5-plug.html

32. "Tattu 2200mah 3s 11 1v 35c lipo battery", https://flyingmachines.in/product/tattu-2200mah-3s-11-1v-35c-lipo-battery/

33. "TATTU 2200mAh 3s 35c Lipo Battery", https://www.getfpv.com/tattu-2200mah-3s-35c-lipo-battery.html

34. "Dragon Link V3 433mhz Long Range Rc Wifi & Bluetooth - Transmitter Only Dragonlink", https://hobbywireless.com/dragon-link-433mhz-c-98_110_314/dragon-link-v3-433mhz-long-range-rc-wifi-bluetooth-transmitter-only-select-your-radio-dragonlink-p-4894.html

35. "High Pressure Pixhawk PX4 Autopilot Bit Flight Controller, 115 V AC", https://www.indiamart.com/proddetail/pixhawk-px4-autopilot-bit-flight-controller-22195448488.html

36. March 12, 2020, "LED Meanings (Pixhawk Series)", PX4 Autopilot, https://docs.px4.io/master/en/getting_started/led_meanings.html

37. February 19, 2021, "3DR Pixhawk 1 Flight Controller", https://docs.px4.io/master/en/flight_controller/pixhawk.html

38. May 31, 2015, "The 10 biggest cargo aircraft", Aerospace Technology, https://www.aerospace-technology.com/features/featurethe-top-10-biggest-cargo-aircraft-4589609/

39. "Flight history for aircraft - N70VB - Smith Aerostar 600", https://www.flightradar24.com/data/aircraft/n70vb

40. "Boeing 747 8 Orders and Deliveries", Modern Airliners, https://modernairliners.com/boeing-747-8/boeing-747-8i-and-8f-orders-and-deliveries/

41. Willie Bodenstein, 2021, “The Bakeng Duce - Jerry Bakeng's Parasol Wing Beauty”, Pilot’s Post, Online Aviation Magazine, South Africa, http://www.pilotspost.com/arn0000193

42. Mohammad H Sadrey , “Aircraft Design a Systems Approach”.

43. January 19, 2021, “Ziqitza Healthcare Limited creates green corridor for ambulance carrying organ for transplant”, SNS Web, New Delhi, https://www.thestatesman.com/cities/bhubaneshwar/ziqitza-healthcare-limited-creates-green-corridor-for-ambulance-carrying-organ-for-transplant-1502947414.html?hcb=1

44. J. Roskam, 1985, “Airplane Design”.

45. D. P. RAYMER, 1989, “Aircraft design: a conceptual approach”.

46. J. Gundlach, 2012, “Designing Unmanned Aircraft Systems: A Comprehensive Approach”.

47. M. C.Y. N. Chunyun Niu, 1988, “Airframe Structural Design”.

48. N.W.R. Prasad, “Aerospace Materials and Material Technologies”.

49. DRIVE CALCULATOR by Helmut Schneck .http://www.drivecalc.de/PropCalc/

turnitin

Digital Receipt

This receipt acknowledges that Turnitin received your paper. Below you will find the receipt information regarding your submission.

The first page of your submissions is displayed below.

Submission author:	Farhan Khan
Assignment title:	17ME33
Submission title:	COLLAB
File name:	COLLAB.pdf
File size:	21.1M
Page count:	152
Word count:	23,182
Character count:	116,416
Submission date:	27-May-2021 01:22AM (UTC+0530)
Submission ID:	1594793141

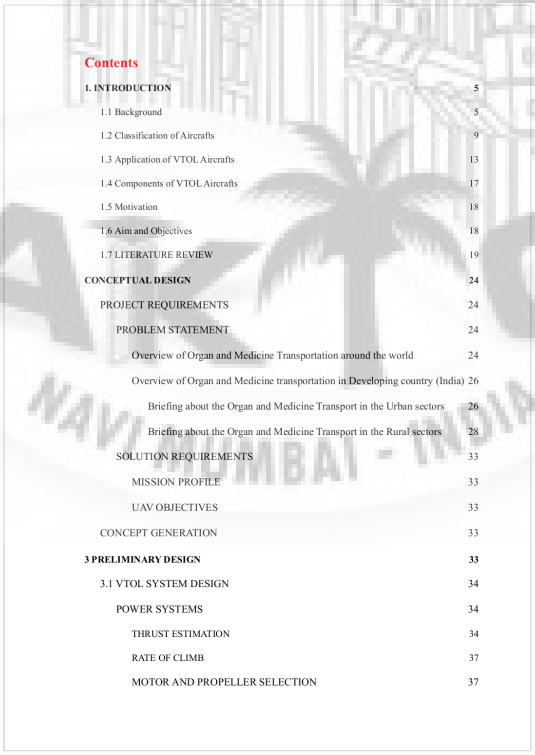

Contents

1. INTRODUCTION 5
1.1 Background 5
1.2 Classification of Aircrafts 9
1.3 Application of VTOL Aircrafts 13
1.4 Components of VTOL Aircrafts 17
1.5 Motivation 18
1.6 Aim and Objectives 18
1.7 LITERATURE REVIEW 19
CONCEPTUAL DESIGN 24
PROJECT REQUIREMENTS 24
PROBLEM STATEMENT 24
Overview of Organ and Medicine Transportation around the world 24
Overview of Organ and Medicine transportation in Developing country (India) 26
Briefing about the Organ and Medicine Transport in the Urban sectors 26
Briefing about the Organ and Medicine Transport in the Rural sectors 28
SOLUTION REQUIREMENTS 33
MISSION PROFILE 33
UAV OBJECTIVES 33
CONCEPT GENERATION 33
3 PRELIMINARY DESIGN 33
3.1 VTOL SYSTEM DESIGN 34
POWER SYSTEMS 34
THRUST ESTIMATION 34
RATE OF CLIMB 37
MOTOR AND PROPELLER SELECTION 37

COLLAB

ORIGINALITY REPORT

28%	24%	19%	19%
SIMILARITY INDEX	INTERNET SOURCES	PUBLICATIONS	STUDENT PAPERS

PRIMARY SOURCES

1	mafiadoc.com Internet Source	6%
2	faculty.dwc.edu Internet Source	3%
3	en.wikipedia.org Internet Source	1%
4	hobbyking.com Internet Source	1%
5	documents.mx Internet Source	1%
6	Submitted to Kingston University Student Paper	1%
7	onlinelibrary.wiley.com Internet Source	1%
8	Submitted to Zewail City of Science and Technology Student Paper	1%
9	Submitted to Houston Community College Student Paper	1%

10	www.scribd.com Internet Source	1 %
11	inba.info Internet Source	1 %
12	www.tandfonline.com Internet Source	1 %
13	Submitted to American College of the Middle East Student Paper	<1 %
14	Mohammad H. Sadraey. "Aircraft Design", Wiley, 2012 Publication	<1 %
15	www.123seminarsonly.com Internet Source	<1 %
16	what-when-how.com Internet Source	<1 %
17	Submitted to University of Hertfordshire Student Paper	<1 %
18	gatepathshala.com Internet Source	<1 %
19	Submitted to Emirates Aviation College, Aerospace & Academic Studies Student Paper	<1 %
20	www.sih.gov.in Internet Source	<1 %

21	Submitted to Utah Valley State College Student Paper	<1%
22	Submitted to University of Sheffield Student Paper	<1%
23	ardupilot.org Internet Source	<1%
24	surjeetyadav.wordpress.com Internet Source	<1%
25	Submitted to Sheffield Hallam University Student Paper	<1%
26	www.ijera.com Internet Source	<1%
27	Submitted to University of Adelaide Student Paper	<1%
28	Submitted to University of Petroleum and Energy Studies Student Paper	<1%
29	robu.in Internet Source	<1%
30	home.roboticlab.eu Internet Source	<1%
31	mechanicfaq.com Internet Source	<1%
32	airandspace.si.edu	

	Internet Source	<1%
33	Mohammad H. Sadraey. "Design of Unmanned Aerial Systems", Wiley, 2020 Publication	<1%
34	hyperleap.com Internet Source	<1%
35	Submitted to 7996 Student Paper	<1%
36	www.dailymail.co.uk Internet Source	<1%
37	www.slideshare.net Internet Source	<1%
38	Submitted to Nottingham Trent University Student Paper	<1%
39	"Aerodynamic Components of Aircraft at High Speeds", Walter de Gruyter GmbH, 1957 Publication	<1%
40	fancyfantasysciencelab.tistory.com Internet Source	<1%
41	Submitted to RMIT University Student Paper	<1%
42	www.readbag.com Internet Source	<1%

43	Submitted to M S Ramaiah University of Applied Sciences Student Paper	<1%
44	www.professional-multirotors.com Internet Source	<1%
45	Submitted to Los Altos High School Student Paper	<1%
46	Submitted to University of Liverpool Student Paper	<1%
47	Submitted to University of the Highlands and Islands Millennium Institute Student Paper	<1%
48	i-want-fly.com Internet Source	<1%
49	Mario Asselin. "An Introduction to Aircraft Performance", American Institute of Aeronautics and Astronautics (AIAA), 1997 Publication	<1%
50	S. P. Venkatesan, N. Beemkumar, J. Jayaprabakar, P. N. Kadiresh. "Modelling and analysis of aircraft wing with and without winglet", International Journal of Ambient Energy, 2018 Publication	<1%
51	Submitted to University of Brighton Student Paper	<1%

52	Submitted to Embry Riddle Aeronautical University Student Paper	<1%
53	N Nithyavathy, S Arun Kumar, D Rahul, B Satheesh Kumar, E R Shanthini, C. Naveen. "Detection of fire prone environment using Thermal Sensing Drone", IOP Conference Series: Materials Science and Engineering, 2021 Publication	<1%
54	hdl.handle.net Internet Source	<1%
55	Daniel H. Weinberg. "The determinants of intra-urban household mobility", Regional Science and Urban Economics, 1979 Publication	<1%
56	Submitted to Girne American University Student Paper	<1%
57	Submitted to Glyndwr University Student Paper	<1%
58	Submitted to University of Glasgow Student Paper	<1%
59	Submitted to University of Leeds Student Paper	<1%
60	www.gensace.de Internet Source	<1%

61	www.sandoz.com Internet Source	<1 %
62	doku.pub Internet Source	<1 %
63	Submitted to Massey University Student Paper	<1 %
64	Submitted to University of Witwatersrand Student Paper	<1 %
65	Submitted to University of Stellenbosch, South Africa Student Paper	<1 %
66	assets.publishing.service.gov.uk Internet Source	<1 %
67	Submitted to Central Queensland University Student Paper	<1 %
68	J. C. Wimpenny. "Stability and Control in Aircraft Design", Journal of the Royal Aeronautical Society, 2016 Publication	<1 %
69	Submitted to CSU, San Jose State University Student Paper	<1 %
70	Submitted to California State University, Fresno Student Paper	<1 %

71	Submitted to Institute of Graduate Studies, UiTM Student Paper	<1%
72	Nikolajs Glīzde. "Wing and Engine Sizing by Using the Matching Plot Technique", Transport and Aerospace Engineering, 2017 Publication	<1%
73	Submitted to University of Pretoria Student Paper	<1%
74	Submitted to Queen Mary and Westfield College Student Paper	<1%
75	Submitted to The Manchester College Student Paper	<1%
76	www.kbsec.com.vn Internet Source	<1%
77	Bilal Amin, Syed Irtiza Ali Shah, Haris Ahmad, Sidra Mehmood. "Solving for the pitching moment damping coefficient of aircraft canard surface", 2016 International Conference on Emerging Technologies (ICET), 2016 Publication	<1%
78	Submitted to Florida International University Student Paper	<1%

79	Andreas Hövelmann, Christian Breitsamter. "Leading-Edge Geometry Effects on the Vortex Formation of a Diamond-Wing Configuration", Journal of Aircraft, 2015 Publication	<1 %
80	Mohammad Sadraey, Richard Colgren. "A Systems Engineering Approach to the Design of Control Surfaces for UAVs", 45th AIAA Aerospace Sciences Meeting and Exhibit, 2007 Publication	<1 %
81	Raol, . "Aerodynamic Derivatives and Modeling", Flight Mechanics Modeling and Analysis, 2008. Publication	<1 %
82	Submitted to University of Glamorgan Student Paper	<1 %
83	Submitted to liberty Student Paper	<1 %
84	www.wikizero.com Internet Source	<1 %
85	Basudeb Bera, Ashok Kumar Das, Sahil Garg, Md. Jalil Piran, M. Shamim Hossain. "Access Control Protocol for Battlefield Surveillance in Drone-Assisted IoT Environment", IEEE Internet of Things Journal, 2021 Publication	<1 %

86	C. S. LEE, N. L. WONG, S. SRIGRAROM, N. T. NGUYEN. "DEVELOPMENT OF 3-COMPONENT FORCE-MOMENT BALANCE FOR LOW SPEED WATER TUNNEL", Modern Physics Letters B, 2011 Publication	<1 %
87	Cezary Galiński, Magdalena Gronowska, Wieńczysław Stalewski, Konrad Gumowski. "Flat-upper-surface wing for experimental high altitude unmanned aerial vehicle", Proceedings of the Institution of Mechanical Engineers, Part G: Journal of Aerospace Engineering, 2020 Publication	<1 %
88	findhistoryhere.com Internet Source	<1 %
89	pdfs.semanticscholar.org Internet Source	<1 %
90	wikivisually.com Internet Source	<1 %
91	Akira Azuma. "The Biokinetics of Flying and Swimming, Second Edition", American Institute of Aeronautics and Astronautics (AIAA), 2006 Publication	<1 %

Exclude quotes	On	Exclude matches	Off
Exclude bibliography	On		